

Preparation of octenylsuccinic anhydride modified starches and their applications in emulsion
and encapsulation

by

Zhenhua Sun

B.S., Kansas State University, 2012
M.P.S., Cornell University, 2013

AN ABSTRACT OF A DISSERTATION

submitted in partial fulfillment of the requirements for the degree

DOCTOR OF PHILOSOPHY

Department of Grain Science and Industry
College of Agriculture

KANSAS STATE UNIVERSITY
Manhattan, Kansas

2020

Abstract

Starches esterified with octenylsuccinic anhydride (OSA) are lipophilic and have been used as emulsion stabilizers in beverage, food, pharmaceutical and personal care applications. The traditional method for synthesizing octenylsuccinate (OS) starch is to react granular starch with OSA in an aqueous slurry system under mild alkaline conditions. In this dissertation, distribution of OS substituents within a single granule of modified maize and potato starches was investigated, and new technologies developed in our laboratory were used to prepare OS starches for emulsion and encapsulation applications. OS distribution predominantly occurred on the surface of the waxy maize starch granules as determined by Raman microspectroscopy, and the level of OS substitutes in the center of granules was also high and nearly equal to that on the surface. The regions between the surface and the hilum of the waxy maize starch granules had reduced OS substitution. In contrast, OS groups in OSA-modified waxy and normal potato granular starches were shown to be preferentially located on its surface. The DS of granule ghosts (the remnant of starch granule after cooking under low shear) suggested that the OS groups on the surface was about 2.5 times that of the bulk after 60% interior granule was lost and removed. In beverage application, OS waxy potato starch, which has excellent paste clarity, was hydrolyzed by α -amylase, and the products displayed good emulsion stability for orange oil.

Compared with the aqueous slurry system, the dry heating treatment for synthesizing OS starch appeared simpler, and more economical with higher yield. The OS waxy maize starch prepared by dry heating treatment was used to emulsify and encapsulate vitamin E. The stability of encapsulated vitamin E (VE) particles was excellent by OSA-modified normal maize starch prepared by dry heating method. Fresh emulsions with the high ratio of starch to VE (1:1) had a small particle size of 0.7 μm .

The conformational properties of starch granules during dextrinization (dry heating in the presence of acid) were investigated by high performance size exclusion chromatography (HPSEC) coupled with multiple detectors. The measured exponent α values in Mark-Houwink equation indicated that pyrodextrins prepared at pH 3, 170 °C and 150 °C only had one compact spherical conformation (α 0.27-0.31) during dextrinization, whereas pyrodextrins at pH 2 and 150 °C had a mixture of two shapes of molecules: compact sphere (α 0.26) and rigid coil (α 0.89) conformation. Pyrodextrins prepared at pH 3 and 150 °C for 4 h and its swollen granules recovered from glycerol/water mixtures were determined by X-ray diffraction and DSC, and the results showed that short-range crystallinity was destroyed but long-range order (birefringence) was retained. Interestingly, some intact granules could swell as much as 80% in glycerol/water 40/60 to 60/40 at 10% starch solids and still displayed Maltese cross patterns, but were not crystalline.

Preparation of octenylsuccinic anhydride modified starches and their applications in emulsion
and encapsulation

by

Zhenhua Sun

B.S., Kansas State University, 2012
M.S., Cornell University, 2013

A DISSERTATION

submitted in partial fulfillment of the requirements for the degree

DOCTOR OF PHILOSOPHY

Department of Grain Science and Industry
College of Agriculture

KANSAS STATE UNIVERSITY
Manhattan, Kansas

2020

Approved by:

Major Professor
Yong-Cheng Shi

Copyright

© Zhenhua Sun 2020.

Abstract

Starches esterified with octenylsuccinic anhydride (OSA) are lipophilic and have been used as emulsion stabilizers in beverage, food, pharmaceutical and personal care applications. The traditional method for synthesizing octenylsuccinate (OS) starch is to react granular starch with OSA in an aqueous slurry system under mild alkaline conditions. In this dissertation, distribution of OS substituents within a single granule of modified maize and potato starches was investigated, and new technologies developed in our laboratory were used to prepare OS starches for emulsion and encapsulation applications. OS distribution predominantly occurred on the surface of the waxy maize starch granules as determined by Raman microspectroscopy, and the level of OS substitutes in the center of granules was also high and nearly equal to that on the surface. The regions between the surface and the hilum of the waxy maize starch granules had reduced OS substitution. In contrast, OS groups in OSA-modified waxy and normal potato granular starches were shown to be preferentially located on its surface. The DS of granule ghosts (the remnant of starch granule after cooking under low shear) suggested that the OS groups on the surface was about 2.5 times that of the bulk after 60% interior granule was lost and removed. In beverage application, OS waxy potato starch, which has excellent paste clarity, was hydrolyzed by α -amylase, and the products displayed good emulsion stability for orange oil.

Compared with the aqueous slurry system, the dry heating treatment for synthesizing OS starch appeared simpler, and more economical with higher yield. The OS waxy maize starch prepared by dry heating treatment was used to emulsify and encapsulate vitamin E. The stability of encapsulated vitamin E (VE) particles was excellent by OSA-modified normal maize starch prepared by dry heating method. Fresh emulsions with the high ratio of starch to VE (1:1) had a small particle size of 0.7 μm .

The conformational properties of starch granules during dextrinization (dry heating in the presence of acid) were investigated by high performance size exclusion chromatography (HPSEC) coupled with multiple detectors. The measured exponent α values in Mark-Houwink equation indicated that pyrodextrins prepared at pH 3, 170 °C and 150 °C only had one compact spherical conformation (α 0.27-0.31) during dextrinization, whereas pyrodextrins at pH 2 and 150 °C had a mixture of two shapes of molecules: compact sphere (α 0.26) and rigid coil (α 0.89) conformation. Pyrodextrins prepared at pH 3 and 150 °C for 4 h and its swollen granules recovered from glycerol/water mixtures were determined by X-ray diffraction and DSC, and the results showed that short-range crystallinity was destroyed but long-range order (birefringence) was retained. Interestingly, some intact granules could swell as much as 80% in glycerol/water 40/60 to 60/40 at 10% starch solids and still displayed Maltese cross patterns, but were not crystalline.

Table of Contents

List of Figures	xvi
List of Tables	xxi
Acknowledgements.....	xxiv
Dedication.....	xxv
Chapter 1 - Overall introduction.....	1
References.....	6
Chapter 2 - Octenylsuccinic anhydride modified starches as an emulsifier in beverage, a review	8
Abstract.....	8
Introduction.....	8
Synthesis of OS starch	10
Traditional method and its variations.....	10
Alternative methods	13
Characterization of OS-starch.....	14
Application in beverages	16
Formation of flavor oil-in-water emulsions	18
Weighting agent.....	18
Hydrocolloids acting as emulsifiers.....	19
Gum Arabic vs. modified starch.....	20
OSA-modified starches as an emulsion stabilizer	21
The mechanism of emulsion stabilized by OS-starch.....	25
Mixed emulsifiers used in beverage emulsions	25
Formation of vitamin E emulsions.....	26

Characterization of emulsions.....	30
Conclusions.....	31
References.....	32
Chapter 3 - Distribution of octenylsuccinate substituents within a single granule of modified waxy maize starch determined by Raman microspectroscopy ¹	43
Abstract.....	43
Keywords	43
Introduction.....	44
Materials and Methods.....	47
Materials	47
Preparation of OS starches	47
Determination of the degree of substitution (DS).....	47
Raman microspectroscopy	48
Differential scanning calorimetry (DSC).....	48
X-ray diffraction (XRD)	49
Light microscopy	49
Statistical analysis	49
Results and discussion	49
Thermal properties and crystallinity of native and OSA-modified starches.....	49
Raman spectra of native and OSA-modified waxy maize starches	50
Distribution of OS groups within a single starch granule.....	51
Conclusions.....	52
References.....	54

Figures	57
Tables.....	61
Chapter 4 - Distribution of octenylsuccinate substituents in modified waxy and normal potato starches.....	63
Abstract.....	63
Keywords	63
Introduction.....	64
Materials and Methods.....	67
Materials	67
Preparation of OS starches.....	67
Raman microspectroscopy	68
Preparation of starch granule ghosts	68
Preparation of chemical surface gelatinization of OS starch granules.....	69
Determination of the degree of substitution (DS).....	70
Crystalline structure	71
Thermal properties of starch	71
Light microscopy	71
Scanning electron microscopy of potato starches and granule ghosts	71
Statistical analysis.....	72
Results and discussion	72
Properties of OSA-modified potato starches	72
OS substituent distribution in a single starch granule determined by Raman microspectrometry	74

OS substituent distribution in the starch revealed by granule ghosts	75
OS substituent distribution in the starch revealed by chemical surface gelatinization	77
Conclusions.....	78
References.....	80
Figures	84
Tables.....	94
Chapter 5 - Formation of orange oil-in-water emulsion stabilized by alpha-amylase-degraded octenylsuccinic anhydride waxy potato starches	97
Abstract.....	97
Keywords	97
Introduction.....	98
Materials and Methods.....	100
Materials	100
Preparation of amylase degraded OS starch	101
Approach 1 (OSA reaction + enzyme degradation).....	101
Approach 2 (enzyme degradation + OSA reaction).....	102
Characterization of OS starches	103
Determination of the degree of substitution (DS).....	103
Determination of dextrose equivalent (DE).....	103
Gel Permeation Chromatography (GPC)	104
Orange oil emulsion preparation.....	104
Droplet size	105

Particle electrical charge (ζ -potential)	105
Creaming index.....	105
Stability of emulsions	106
Results and discussion	106
Structural and physicochemical properties of α -amylase-degraded OS starch.....	106
Stability of emulsions formed using degraded OS-starch.....	108
The mechanism of emulsion stabilized by OS starch	111
Conclusions.....	112
References.....	114
Figures	118
Tables.....	122
Chapter 6 - Changes in molecular size and shape of waxy maize starch during dextrinization.	125
Abstract.....	125
Keywords	125
Introduction.....	126
Materials and methods	128
Materials	128
Preparation of pyrodextrin	128
Solubility.....	128
Gel permeation chromatography (GPC)	129
High-performance size-exclusion chromatography (HPSEC).....	129
Statistical analysis	130
Results and discussion	130

Water solubility.....	130
Molecular size distribution of pyrodextrins	131
Conformational properties of pyrodextrins.....	132
Conclusions.....	136
References.....	137
Figures	140
Tables.....	143
Chapter 7 - Swelling behavior of waxy maize pyrodextrins in glycerol and water.....	145
Abstract.....	145
Keywords	145
Introduction.....	146
Materials and methods	148
Materials	148
Preparation of pyrodextrins and swollen pyrodextrins	148
Light microscopy	149
X-ray diffraction (XRD)	149
Differential scanning calorimetry (DSC).....	149
Statistical analysis.....	150
Results and discussion	150
Microscopic observation of starch granules in glycerol/water mixtures	150
Swelling behavior of pyrodextrins prepared at pH 3 - 170 °C (P3-170) in glycerol and water.....	151

Swelling behavior of pyrodextrins prepared at pH 3 - 150 °C (P3-150) in glycerol and water	152
Swelling behavior of pyrodextrins prepared at pH 2 - 150 °C (P2-150) in glycerol and water	153
Crystallinity and birefringence of swollen pyrodextrins from P3-150	154
Conclusions	156
References	157
Figures	159
Tables	172
Chapter 8 - Encapsulation of vitamin E by octenylsuccinate starch obtained from normal maize starch by dry heating	173
Abstract	173
Keywords	173
Introduction	174
Materials and methods	176
Materials	176
Preparation of OS starch	177
Characterization of OS starches	177
Degree of substitution (DS)	177
Solubility	178
Color measurement	178
Molecular size distribution by gel permeation chromatography (GPC)	178
X-ray diffraction (XRD)	178

Scanning electron microscope (SEM)	179
Preparation of vitamin E emulsion and spray-dried encapsulates	179
Particle size determination	179
Stability study of vitamin E in microparticles by HPLC	180
Density	181
Flow properties of spray dried powders.....	181
Statistical analysis	181
Results and discussion	182
Solubility, degree of substitution, and reaction efficiency of OS starches from dry heating	182
Structure characterization of OS starches	183
Characterization of VE emulsions stabilized by OS starch	185
Encapsulation of VE by spray drying	186
Conclusions.....	187
References.....	189
Figures	192
Tables.....	196
Chapter 9 - Overall conclusions and future work	200
Conclusions.....	200
Future work.....	202
Appendix A - Copyright Permissions	204
Appendix B - Chapter 6 Supplementary Materials.....	205
Appendix C - Dry reaction of OSA reaction by ammonium hydroxide.....	206

List of Figures

Figure 2.1 Structure of OSA-modified starches [Adapted from Sweedman et al., (2013)]	9
Figure 3.1 Five positions (1, edge-left; 2, area between edge-left and center; 3, center; 4, area between center and edge-right; and 5, edge-right) within one starch granule analyzed by Raman microspectroscopy.	57
Figure 3.2 X-ray diffraction patterns of unmodified (A), OSA-modified starches with DS of 0.018 (B), and 0.041 (C).	58
Figure 3.3 Microscopic image of unmodified (A), OSA-modified starches with DS of 0.018 (B), and 0.041 (C). Scale bar in each graph represents 20 μm . Left images: normal visible light; right images: polarized light.	59
Figure 3.4 Raman image and spectra of the surface (edge-right) of one starch granule. These spectra are from unmodified (A), OSA-modified granules with DS of 0.018 (B), and 0.041 (C).	60
Figure 4.1 Five positions (a1, edge-left; a2, area between edge-left and center; a3, center; a4, area between center and edge-right; and a5, edge-right) within a speckle of 7 $\mu\text{m} \times 7 \mu\text{m}$ on one round-shaped potato starch granule, and seven positions (b1, edge-left; b2, area between edge-left and center; b3, center; b4, area between center and edge-right; b5, edge-right; b6, top edge; and b7, bottom edge) within a speckle of 10 $\mu\text{m} \times 10 \mu\text{m}$ on one long flat oval-shaped potato starch granule analyzed both by Raman microspectroscopy.	84
Figure 4.2 X-ray diffraction patterns of potato starches: unmodified normal (NP), octenylsuccinic anhydride (OSA)-modified waxy starches with degree of substitution (DS)	

of 0.0167(NP3), and 0.0400 (NP9); unmodified waxy (WP), OSA-modified normal starches with DS of 0.0174 (WP3), and 0.0383 (WP9).....	85
Figure 4.3 Microscopic image of unmodified normal potato starch (NP), octenylsuccinic anhydride (OSA)-modified normal starches with degree of substitution (DS) of 0.0167 (NP3), and 0.0400 (NP9); unmodified waxy potato starch (WP), OSA-modified waxy starches with DS of 0.0174 (WP3), and 0.0383 (WP9). Scale bar in each graph represents 20 μ m. Left images: normal visible light; right images: polarized light.	87
Figure 4.4 Scanning electron microscopy (SEM) micrographs of potato starches: unmodified normal (NP), octenylsuccinic anhydride (OSA)-modified normal starches with degree of substitution (DS) of 0.0167 (NP3), and 0.0400 (NP9); unmodified waxy (WP), OSA-modified waxy starches with DS of 0.0174 (WP3), and 0.0383 (WP9).....	88
Figure 4.5 Raman image and spectra of the surface (b1, edge-left) of one long flat oval-shaped - starch granule. These spectra are from unmodified (A), octenylsuccinic anhydride (OSA)-modified granules with degree of substitution (DS) of 0.0174 (B), and 0.0400 (C).	89
Figure 4.6 Scanning electron microscopy (SEM) micrographs of ethanol-precipitated granule ghosts of native (NP-g), 3% (NP3-g), and 9% (NP9-g) octenylsuccinic anhydride (OSA)-modified normal potato starches; native (WP-g), 3% (WP3-g), and 9% (WP9-g) OSA-modified waxy potato starches, respectively.	90
Figure 4.7 Changes on bound OS content (% OS) of 3 and 9% octenylsuccinic anhydride (OSA)-modified potato starch (A) and maize starch (B): normal potato (NP3 and NP9), waxy potato (WP3 and WP9), normal maize (NM3 and NM9), and waxy maize (WM3 and WM9), and their granule ghost and remaining granules after chemical surface gelatinization.	91

Figure 4.8 Scanning electron microscopy (SEM) micrographs of partially surface gelatinized starch granules (A) and remaining granules (B): normal potato (NP), octenylsuccinic (OS) normal potato starches (NP3, NP9), and waxy potato (WP), OS waxy potato starches (WP3, NP9).	93
Figure 5.1 Experimental design of two approaches to prepare α -amylase-degraded OSA-modified waxy potato starch	118
Figure 5.2 Molecular size distribution of waxy potato starch and granular octenylsuccinate maltodextrins obtained from approach 1 (A) and approach 2 (B).	119
Figure 5.3 Effects of selected good emulsifiers for the storage of 14 days: OSE3, EOS3, gum arabic (GA), and commercial OS starch 2 (Starch 2) on the particle size of emulsions with the ratio of oil to starch 1:1 and 2:1 after 30 days of storage at room temperature.	120
Figure 5.4 The appearance of emulsions stabilized by OSE3, EOS3, gum arabic (GA), and commercial OS starch 1 (Starch 1) and 2 (Starch 2) with diluted 1:100 by water at the same ratio of oil to starch 1:1.	121
Figure 6.1 Molecular size distribution of pyrodextrins prepared at (A) pH 3 and 170 °C, (B) pH 3 and 150 °C, and (C) pH 2 and 150 °C at different time (0.5 h to 4 h) and the pyrodextrins prepared at (D) 0.5 h, (E) 2 h, and (F) 4 h as determined by gel permeation chromatography (GPC).	140
Figure 6.2 Weight average molecular weight (M_w) (A) and intrinsic viscosity (IV) (B) of pyrodextrins prepared at (a) pH 3 and 150 °C, (b) pH 3 and 170 °C, and (c) pH 2 and 150 °C.	141
Figure 6.3 Intrinsic viscosity ($[\eta]$) vs. molecular weight (M_w) plotted on a log-log scale behavior of pyrodextrins prepared at (A) pH 3 and 150 °C, (B) pH 3 and 170 °C, and (C) pH 2 and	

150 °C from logarithmic plot of the molecular weight vs. intrinsic viscosity by HPSEC-triple detectors.....	142
Figure 7.1 Microscopic images under bright field (left) and polarized light (right) (scale bar = 20 μm) of native waxy maize starch (WMS), and pyrodextrins prepared at pH 3 and 170 °C (P3-170), pH 3 and 150 °C (P3-150), and pH 2 and 150 °C (P2-150) for 4 h, immersed in glycerol/water mixture (80/20, w/w) at 40% solid content for 180 min.....	159
Figure 7.2 Microscopic images under bright field (left) and polarized light (right) (scale bar = 20 μm) of native waxy maize starch (WMS), and pyrodextrins prepared at pH 3 and 170 °C (P3-170), pH 3 and 150 °C (P3-150), and pH 2 and 150 °C (P2-150) for 4 h, immersed in glycerol/water mixture (80/20, w/w) at 10% solid content for 180 min.....	160
Figure 7.3 Microscopic photos of native waxy maize starch (WMS) granules immersed in different ratios of glycerol/water solvents: 100/0, 80/20, 60/40, 40/60, 20/80, 0/100, (w/w) for 5, 60, and 180 min at 40% and 10% solids, respectively.....	162
Figure 7.4 Microscopic photos of pyrodextrins prepared at pH 3 and 170 °C (P3-170) for 4 h immersed in different ratios of glycerol/water solvents: 100/0, 80/20, 60/40, 40/60, 20/80, 0/100, (w/w) for 5, 60, and 180 min at 40% and 10% solids, respectively.	164
Figure 7.5 Microscopic photos of pyrodextrins prepared at pH 3 and 150 °C (P3-150) for 4 h immersed in different ratio of glycerol/water solvents: 100/0, 80/20, 60/40, 40/60, 20/80, 0/100, (w/w) for 5, 60, and 180 min at 40% and 10% solids, respectively.	166
Figure 7.6 Microscopic photos of pyrodextrins prepared at pH 2 and 150 °C (P2-150) for 4 h immersed in different ratio of glycerol/water solvents: 100/0, 80/20, 60/40, 40/60, 20/80, 0/100, (w/w) for 5, 60, and 180 min at 40% and 10% solids, respectively.	168

Figure 7.7 X-ray diffraction (XRD) pattern of (A) native waxy maize starch, (B) pyrodextrin prepared at pH 3 and 150 °C for 4 h, and its swollen pyrodextrin recovered from glycerol/water mixtures: (C) 100/0, (D) 80/20, (E) 60/40, (F) 40/60, (G) 20/80, and (H) 0/100, (w/w)..... 169

Figure 7.8 Photomicrographs viewed in pure glycerol under bright field (left) and polarized light (right) (scale bar = 20 μm) of (A) native waxy maize starch, (B) pyrodextrin prepared at pH 3 and 150 °C for 4 h, and its swollen pyrodextrin recovered from glycerol/water mixtures: (C) 100/0, (D) 80/20, (E) 60/40, (F) 40/60, (G) 20/80, and (H) 0/100, (w/w)..... 171

Figure 8.1 Process of preparing octenylsuccinate (OS) starch from dry heating [Adapted from (Shi & Bai, 2016)]..... 192

Figure 8.2 Molecular size distribution of native normal maize starch and octenylsuccinate (OS) starch prepared at 3% OSA, pH 8.02 (adjusted by 2% NH₄HCO₃), 180 °C for 2 h and 6 h; pH 8.30 (adjusted by 4% NH₄HCO₃), 180 °C for 2 h and 6 h. 193

Figure 8.3 Wide-angle X-ray diffraction patterns of unmodified maize starch (NM), octenylsuccinate (OS) starch prepared with 3% OSA, pH 8.02 (adjusted by 2% NH₄HCO₃), 180 °C for 2 h (DS of 0.0156) (A) and 6 h (DS of 0.0173) (B); pH 8.30 (adjusted by 4% NH₄HCO₃), 180 °C for 2 h (DS of 0.0170) (C) and 6 h (DS of 0.0201) (D)..... 194

Figure 8.4 Scanning electron microscope (SEM) of native normal maize starch (NM) and octenylsuccinate (OS) starch prepared at 3% OSA, pH 8.0 (adjusted by 2% NH₄HCO₃), heating at 180 °C for 2 h (OSS2-2) and 6 h (OSS2-6); pH 8.3 (adjusted by 4% NH₄HCO₃), heating at 180 °C for 2 h (OSS4-2) and 6 h (OSS4-6)..... 195

Figure B.1 Molecular size distribution of native waxy maize starch and pyrodextrins prepared at pH 3 and 170 °C, pH 3 and 150 °C, and pH 2 and 150 °C, at 4 h. 205

List of Tables

Table 2.1 Reaction conditions values most used in the recent literature in the last two years for starch esterification with OSA in aqueous slurry under mild alkaline conditions with variations.....	11
Table 2.2 Preparation of emulsion conditions of recent research articles (after 2015) on orange oil-in-water emulsion formation by OSA-modified starches using a microfluidizer and some works related to commercial OS starch (2010-2015)	24
Table 3.1 Thermal properties ^a determined by differential scanning calorimetry (DSC) on unmodified and OSA-modified waxy maize starches with degrees of substitution (DS) of 0.018 and 0.041	61
Table 3.2 The band area ratio of an OS group to starch content on five positions within one granule, calculated as $(\text{band area at } 1670 \text{ cm}^{-1} / \text{band area at } 2910 \text{ cm}^{-1}) \times 100$. Ten starch granules (n=10) of each sample were analyzed by Raman microspectroscopy ^a	62
Table 4.1 Thermal properties of unmodified and octenylsuccinic anhydride (OSA) modified normal and waxy potato starches treated with 3% and 9% OSA determined by differential scanning calorimetry (DSC) ^a	94
Table 4.2 The band area ratio of an OS group to starch content on five positions within one round-shaped granule (a1-5) and seven positions within one long flat oval-shaped potato starch granule (b1-7), calculated as $(\text{band area at } 1670 \text{ cm}^{-1} / \text{band area at } 2910 \text{ cm}^{-1}) \times 100$. Ten starch granules (n=10) of each sample were analyzed by Raman microspectroscopy ^a .	95

Table 4.3 Bound OS content (%OS), degree of substitution (DS) of octenylsuccinic anhydride (OSA) modified normal and waxy potato starch granules, starch granule ghosts, and remaining granules after chemical surface gelatinization.....	96
Table 5.1 Degree of substitution (DS), dextrose equivalent (DE) and viscosity for octenylsuccinate (OS) maltodextrins prepared from approach 1 and approach 2 in Figure 5.1	122
Table 5.2 Formulation of orange oil emulsions using degraded octenylsuccinic anhydride maltodextrin with different ratios of oil to starch	123
Table 5.3 Particle size (μm), zeta-potential (mV) and apparent viscosity (η , cp) of fresh orange oil emulsions using degraded octenylsuccinic anhydride maltodextrin in Figure 5.1 with different ratios of oil to starch, and particle size, zeta-potential and creaming index (%) were measured after the storage of 14 days	124
Table 6.1 Water solubility of pyrodextrins prepared at different pH, heating temperatures and time ^a	143
Table 6.2 Conformational properties of pyrodextrins obtained from HPSEC coupled with multiple detectors (RI, viscometer, light scattering) ^a	144
Table 7.1 Thermal properties ^a of native waxy maize starch, pyrodextrin prepared at pH 3, 150 °C (P3-150) for 4 h, and its swollen pyrodextrins recovered from glycerol/water mixture (100/0, 80/20, 60/40, 40/60, 20/80, 0/100, w/w) as determined by differential scanning calorimetry in a mixture of glycerol / water (80/20, w/w)	172
Table 8.1 Characteristics of 3% OSA-modified normal maize starches adjusted to pH by NH_4HCO_3 and heat treated at 180 °C	196

Table 8.2 Characteristics of 3% OSA-modified normal maize starches by adding 3% NH_4HCO_3 (pH 8.17) and heating for 2h.....	197
Table 8.3 Particle size of emulsions with different ratios of starch to oil	198
Table 8.4 Oil load, density, and flowability (angle of repose) of encapsulated particles.....	199
Table C.1 Degree of substitution (DS) and reaction efficiency (RE) of 3% OS waxy maize starches prepared by dry reaction at 180 °C for 0.5-4 h.....	207

Acknowledgements

First and foremost, I would like to express my sincere gratitude to my advisor Dr. Yong-Cheng Shi, for his constant support during the period of my Ph.D. study. His broad knowledge and insights into the science inspire me to grow as a researcher and scientist. It is definitely my great honor to have him as my advisor. I thank Dr. Paul Seib for reviewing my manuscripts. He has always been a role model as a scientist.

Great thanks go to Dr. Xiuzhi Susan Sun, Dr. Hulya Dogan, and Dr. Om Prakash for being my committee members, providing valuable suggestions, and Dr. Edgar Chambers IV for his time to serve as outside chairperson.

I very much appreciate all my lab mates and postdocs who worked beside me in this Carbohydrate Polymers team, for supporting me throughout the entire journey. My sincere thanks also go to all the faculty and staff in the Dept. of Grain Science and Industry. Without their precious support, it would not be possible to conduct this research.

Last but not least, a special thank goes to my devoted husband, Qiang Wang, he is a foundation and an inspiration of mine. Also to our beloved daughter, Sienna, for the unspeakable happiness she had brought to us. I want to thank my parents Gang Sun and Xiaoyan Li, who always give me trust, and endless love for my entire lifetime. I could not have gone so far without all of them. I also appreciated the help on dissertation format from my friend Miao Li.

This dissertation is completed in this special moment due to the outbreak of COVID-19. We help curb the spread of the Coronavirus under self-quarantine. I must give a shout out to the front line medical professionals all over the world, especially in China. I hope this pandemic will end soon. Stay safe and healthy. Bless 2020.

Dedication

To

All my loves in life

My parents Gang Sun and Xiaoyan Li

My husband Dr. Qiang Wang

My daughter Sienna Wang

Not just because we share blood

But because we share a bond

Built from abiding love and support

To

Myself

If you can't be a highway then just be a trail

If you can't be the sun be a star

It isn't by size that you win or you fail

The most important thing in life is to find yourself

Be the best of whatever you are

Neue Liebe, Neues Leben.

Chapter 1 - Overall introduction

Having both hydrophilic and hydrophobic groups, octenylsuccinic anhydride (OSA) modified starches are used widely as emulsifiers and stabilizers in foods, oil-in-water beverage emulsions, personal care, pharmaceuticals, and paper industries. In this dissertation, OSA-modified starch as an emulsion stabilizer in flavor beverages is reviewed (Chapter 2). Beverage emulsions are oil-in-water emulsions that are normally prepared as a concentrate and then diluted into finished products. Ring formation in beverages with emulsions during thermal processing and storage is one of the key challenges. Strategies to increase the stability of beverage emulsions generally comprise the use of homogenization, weighting agents (to raise the density of the oil phase), and emulsifiers.

Our group has been conducting research on OS starches including i) reaction mechanism and reaction uniformity (Bai et al., 2009; Bai, et al., 2014; Bai & Shi, 2013), ii) structure of OSA and OSA modified starches (Bai et al., 2011; Bai & Shi, 2011; Qiu et al., 2012), iii) new novel methods of preparing OSA-modified starches (Shi & Bai, 2016), and iv) use of OS starch in stabilizing vitamin E emulsion (Shi & Bai, 2016). Continued research on OS starch was conducted this dissertation. Distribution of OS substituents within a single granule of modified maize and potato starches was investigated, and new technologies developed in our laboratory were used to prepare OS starches for emulsion and encapsulation applications.

The number of publications in the field of OSA starch synthesis and characterization has significantly increased in the last decade (Altuna et al., 2018; Sweedman et al., 2013). Traditionally, the most widely used pathway for synthesizing OS starch is a reaction of starch in its granular form in an aqueous slurry system under mild alkaline conditions (Caldwell & Wurzburg, 1953; Sweedman et al., 2013; Trubiano, 1986). The structure of OSA modified starch

prepared by the aqueous alkaline slurry reaction was investigated in previous studies. At the granular level, after reacting with 3% (wt%, starch basis) OSA, the x-ray diffraction pattern of a starch is generally not changed, indicating that OS substitution occurs primarily in the amorphous regions of granules (Bai & Shi, 2011). Using FT-IR microspectroscopy, Bai et al. (2009) and Wetzel, Shi, & Reffner (2010) investigated the level and uniformity of OS substitution on individual waxy maize starch granules, and reported that OS concentration varied between granules. However, it should be noted that individual starch granules were flattened before measurements of FT-IR spectra due to the thickness of the whole granule and a loss of signal caused by the spherical lensing effect (Wetzel, Shi, & Schmidt, 2010). Therefore, Wetzel, Shi, & Schmidt (2010) first used confocal Raman microspectroscopy to provide greater spatial resolution and show a clear evidence for the presence of the octenyl succinate (OS) ester group at the surface of the unflattened modified starch granules at Raman band 1670 cm^{-1} . However, there is no report on the OS distribution within a single granule. Therefore, the distribution of OS substituents within a single granule of modified waxy maize starch was investigated by Raman microspectroscopy (Chapter 3).

Compared with waxy and normal cereal starches that show an A-type crystalline pattern, potato starch exhibits a B-type X-ray crystalline pattern. In contrast to maize starch, potato starch granules have no channels with smooth surface (Wang et al., 2010). No work on waxy potato starch reacted with OSA agent has been reported. In Chapter 4, the OS substituent distribution in modified waxy and normal potato starches with different degrees of substitution (DS) was also determined by Raman microspectroscopy. In addition, two approaches were used to further determine OS substituents in starch granule: 1) isolation of residual surface granule (termed granule “ghosts”) after starch is gelatinized and internal soluble starch was removed (Zhang et

al., 2014), and 2) isolation of internal starch granule after chemical surface gelatinization after the surface of starch granule was removed (Jane & Shen, 1993). The OS content in isolated starch “ghost” (surface part of the granule) and internal part of the granule was determined.

New approaches (US patent application No. 16/728,400) to prepare degraded OS starches by α -amylase were used to make OS waxy potato starch. Waxy potato starch, which contains no amylose, has a higher paste clarity than waxy maize starch (Hsieh et al., 2019). Formation of orange oil-in-water emulsion stabilized by alpha-amylase-degraded octenylsuccinic anhydride waxy potato starches was studied in Chapter 5.

Traditional method of preparation of OS starches is the alkaline slurry aqueous reaction, but this method has some drawbacks due to poor water solubility of the product, and the product requires further degradation by enzyme or acid conversion to be completely soluble in water. Compared with the aqueous system and other alternative methods, the dry heating treatment had high yield and appeared to be simpler and more economical. The dry heating treatment is an alternative way to produce dextrin, a degraded starch product prepared by a process involving heat treatment and/or acidification with high water solubility and low viscosity (Wurzburg, 1986). The dextrinization caused a decrease in molecular size of starch, gelatinization and retrogradation endotherm, and average chain length (CL) as solubility and degree of branching (DB) increased with dextrinization time from 0.5h to 4h (Bai, Cai, et al., 2014; Bai & Shi, 2016; Han et al., 2018). However, the conformational properties of the pyrodextrins have not been studied. In Chapter 6, the molecular size and shape of waxy maize starch during dextrinization were determined.

After studying of the molecular size and shape of pyrodextrins from waxy maize starch, the swelling behavior of pyrodextrins in granular structure in different ratios of glycerol/water

(100/0, 80/20, 60/40, 40/60, 20/80, and 0/100, w/w) was investigated to gain further information of structural changes in starch granules during the dry heating in the presence of acid (Chapter 7).

Shi and Bai (2016) developed a novel approach to prepare OS starch by dry heating on the mixture of OSA and granular starch. For waxy maize starch, the optimum condition to produce the best product with high solubility, degree of substitution and light color was obtained when 3% (wt% by starch weight) NH_4HCO_3 was added and heated at 180 °C for 2 h. The OS waxy maize starch had 100% solubility, a DS of 0.022 and 90% reaction efficiency with a highly branched structure. In addition to waxy maize starch, we hypothesized that normal maize starch could be used to this dry heating approach. Normal maize starch is widely available and cheaper than waxy maize starch in certain regions of the world. In Chapter 8, normal maize starch was used to prepare OS dextrin by dry heating, and the product was used to encapsulate vitamin E. The spray-dried vitamin E micro-particles have potentials to be used in feed industry.

In the final chapter, conclusions and future work are presented.

Overall, two approaches were used to prepare OS starches in this dissertation: one is slurry method and the other is dry heating method. The main objectives of this dissertation were:

1. To determine the distribution of OS groups on waxy maize starch (Chapter 3) and waxy and normal potato starches (Chapter 4).
2. To develop the optimum reaction conditions of preparing soluble OS maltodextrin from waxy potato starch in aqueous method that can be used in clear beverage application, and characterize degraded OS starches from waxy potato starch by α -amylase (Chapter 5).
3. To study the effect of dextrinization conditions on the conformation (Chapter 6) and swelling behavior of pyrodextrins (Chapter 7).

4. To further understand the structure and properties of OS starch prepared from normal maize starch by dry heating; and to investigate the effect of the molecular size of OS starch, and DS of OS starch on emulsion and encapsulation of vitamin E (Chapter 8).

References

- Altuna, L., Herrera, M. L., & Foresti, M. L. (2018). Synthesis and characterization of octenyl succinic anhydride modified starches for food applications. A review of recent literature. *Food Hydrocolloids*, *80*, 97–110.
- Bai, Y., Cai, L., Douth, J., Gilbert, E. P., & Shi, Y.-C. (2014). Structural changes from native waxy maize starch granules to cold-water-soluble pyrodextrin during thermal treatment. *Journal of Agricultural and Food Chemistry*, *62*(18), 4186–4194.
- Bai, Y., Kaufman, R. C., Wilson, J. D., & Shi, Y.-C. (2014). Position of modifying groups on starch chains of octenylsuccinic anhydride-modified waxy maize starch. *Food Chemistry*, *153*, 193–199.
- Bai, Y., & Shi, Y.-C. (2011). Structure and preparation of octenyl succinic esters of granular starch, microporous starch and soluble maltodextrin. *Carbohydrate Polymers*, *83*(2), 520–527.
- Bai, Y., & Shi, Y.-C. (2013). Reaction of octenylsuccinic anhydride with a mixture of granular starch and soluble maltodextrin. *Carbohydrate Polymers*, *98*(2), 1599–1602.
- Bai, Y., & Shi, Y.-C. (2016). Chemical structures in pyrodextrin determined by nuclear magnetic resonance spectroscopy. *Carbohydrate Polymers*, *151*, 426–433.
- Bai, Y., Shi, Y.-C., Herrera, A., & Prakash, O. (2011). Study of octenyl succinic anhydride-modified waxy maize starch by nuclear magnetic resonance spectroscopy. *Carbohydrate Polymers*, *83*(2), 407–413.
- Bai, Y., Shi, Y.-C., & Wetzel, D. L. (2009). Fourier transform infrared (FT-IR) microspectroscopic census of single starch granules for octenyl succinate ester modification. *Journal of Agricultural and Food Chemistry*, *57*(14), 6443–6448.
- Caldwell, C. G., & Wurzburg, O. B. (1953). *Polysaccharide derivatives of substituted dicarboxylic acids*, US Patent No. 2661349 A.
- Han, X., Kang, J., Bai, Y., Xue, M., & Shi, Y.-C. (2018). Structure of pyrodextrin in relation to its retrogradation properties. *Food Chemistry*, *242*, 169–173.
- Hsieh, C.-F., Liu, W., Whaley, J. K., & Shi, Y.-C. (2019). Structure and functional properties of waxy starches. *Food Hydrocolloids*, *94*, 238–254.
- Jane, J., & Shen, J. J. (1993). Internal structure of the potato starch granule revealed by chemical gelatinization. *Carbohydrate Research*, *247*, 279–290.

- Qiu, D., Bai, Y., & Shi, Y.-C. (2012). Identification of isomers and determination of octenylsuccinate in modified starch by HPLC and mass spectrometry. *Food Chemistry*, 135(2), 665–671.
- Shi, Y.-C., & Bai, Y. (2016). *Starch esters and method of preparation* (United States Patent No. US9458252B2).
- Sweedman, M. C., Tizzotti, M. J., Schäfer, C., & Gilbert, R. G. (2013). Structure and physicochemical properties of octenyl succinic anhydride modified starches: A review. *Carbohydrate Polymers*, 92(1), 905–920.
- Trubiano, P. C. (1986). Succinate and substituted succinate derivatives of starch. In *Modified starches: Properties and uses* (pp. 131–147). CRC Press.
- Wang, J., Su, L., & Wang, S. (2010). Physicochemical properties of octenyl succinic anhydride-modified potato starch with different degrees of substitution. *Journal of the Science of Food and Agriculture*, 90(3), 424–429.
- Wetzel, D. L., Shi, Y.-C., & Reffner, J. A. (2010). Synchrotron infrared confocal microspectroscopical detection of heterogeneity within chemically modified single starch granules. *Applied Spectroscopy*, 64(3), 282–285.
- Wetzel, D. L., Shi, Y.-C., & Schmidt, U. (2010). Confocal Raman and AFM imaging of individual granules of octenyl succinate modified and natural waxy maize starch. *Vibrational Spectroscopy*, 53(1), 173–177.
- Wurzberg, O. B. (1986). Converted starches. In *Modified starches-properties and uses*. CRC Press.
- Zhang, B., Dhital, S., Flanagan, B. M., & Gidley, M. J. (2014). Mechanism for starch granule ghost formation deduced from structural and enzyme digestion properties. *Journal of Agricultural and Food Chemistry*, 62(3), 760–771.

Chapter 2 - Octenylsuccinic anhydride modified starches as an emulsifier in beverage, a review

Abstract

This review focuses on the utilization of octenylsuccinic anhydride (OSA) modified starch as an emulsifier in oil-in-water emulsions for beverages. The synthesis and structural characterization of OSA-modified starch are reviewed, as well as other functional ingredients in beverage emulsions used to formulate these systems, including oil phases, surfactants, and weighting agents. Recent developments in the vitamin E emulsion are also discussed and summarized.

Introduction

Starch is a natural polysaccharide consisting of homopolymers of glucose units joined by glycosidic bonds, and comprises two types of polymers: amylose and amylopectin (BeMiller & Whistler, 2009). Starch is synthesized by plants and serves as energy storage. Starch is a readily accessible and highly versatile with a great variety of useful applications in the food industry. However, the drawbacks of unmodified starches such as insolubility in cold water, lack of pasting consistency and stability when dispersed and heated in water, loss of viscosity by acids or mechanical shear, lack of clarity, tendency to retrograde during storage, and lack of emulsification, have limited their use in many commercial applications (BeMiller, 2018). Modified starches were developed in the 1940s to achieve desirable functional properties such as solubility, texture, adhesion, texture, dispersion and heat tolerance (Philips & Williams, 2000).

To overcome the lack of emulsification properties of native starch in water, the addition of hydrophobic octenylsuccinic anhydride (OSA) was introduced (Caldwell, 1952; Caldwell & Wurzburg, 1953). A polysaccharide (such as starch, dextrans and cellulose) was esterified with a substituted cyclic dicarboxylic acid anhydride. OSA (chemical formula $C_{12}H_{18}O_3$), a cyclic dicarboxylic acid anhydride, has two active carboxyl groups which can react with the hydroxyl groups in polysaccharide under alkaline conditions in aqueous slurry systems as shown in Fig. 2.1 (Altuna et al., 2018; Bai & Shi, 2013; Sweedman et al., 2013). The long alkyl chain of octenyl groups in OSA has hydrophobicity, which converts a polysaccharide to amphiphilic molecule (Shogren et al., 2000). In the United States, only OSA among other alkenyl succinic anhydrides is approved for food use with maximum level 3% (w/w) (DS ~ 0.02) by the Food and Drug Administration (FDA). Due to a combination of OSA's hydrophilic and hydrophobic groups and starch's highly branched macromolecular structure, OSA-modified starches are used widely as emulsifiers and stabilizers in beverage, food, pharmaceutical and personal care applications and in other industries where stable emulsions are required (Altuna et al., 2018; Dokić et al., 2012; Sweedman et al., 2013; Trubiano, 1986; Zhao et al., 2017).

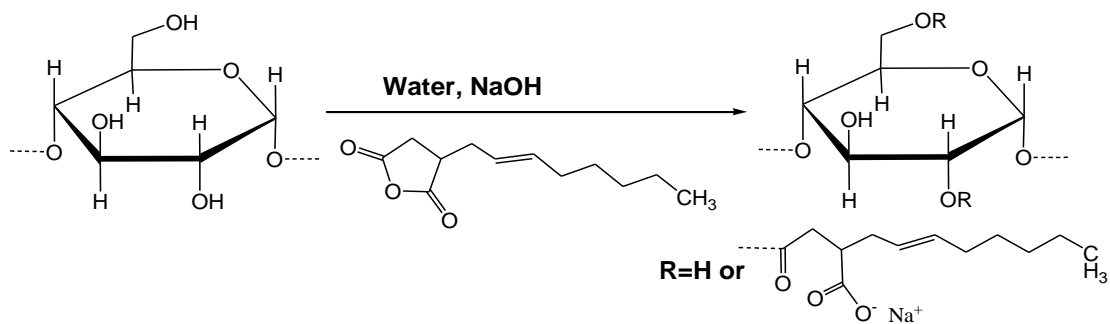


Figure 2.1 Structure of OSA-modified starches [Adapted from Sweedman et al., (2013)]

Synthesis of OS starch

Traditional method and its variations

Currently, the most widely used pathway for synthesizing OS starch is a reaction of starch in its granular form in an aqueous slurry system and adding OSA dropwise while stirring and maintaining pH under mild alkaline conditions at or near room temperature (Bai et al., 2014; Zhang et al., 2011). The number of publications in the field of OSA starch synthesis and characterization has significantly increased in the last decade (Altuna et al., 2018; Bajaj et al., 2019; Han, Zhang et al., 2019; Han, Chung et al., 2019; Jain et al., 2019; Li et al., 2018; Lin et al., 2018; Punia et al., 2019; Sun et al., 2020; Sweedman et al., 2013; Wang et al., 2020; Xu et al., 2018; Yu et al., 2019).

Acid and enzyme treatments are the most common methods to change the structure of OS-starch to make it soluble and decrease in the molecular weight and apparent viscosity. Xu et al. (2015) investigated that β -amylase which cleaves (1 \rightarrow 4)- α glycosidic bond from the non-reducing ends of starch chains could be used to hydrolyze OSA-modified waxy maize starch to obtain a better emulsion stability with orange oil, but the droplet size of emulsions was still large and the stability was weak. On the other hand, α -amylase, an endo-amylase which cuts (1 \rightarrow 4)- α bond randomly in the interior of starch chains was also used to degrade OS starch (Han, Zhang et al., 2019; Liu et al., 2008; Zhang et al., 2018). In 2019, we filed a U.S. patent application (No. 16/728,400) describing two approaches to prepare α -amylase-degraded OS starches. In the first approach, granular waxy maize starch was reacted with OSA, then cooked and hydrolyzed by α -amylase to produce maltodextrins (gOSMs). In the second approach, granular starch was cooked and hydrolyzed by α -amylase to make a maltodextrin, and the resulting soluble maltodextrin was

reacted with OSA for OS maltodextrins (sOSMs). Preparation and structure of α -amylase-degraded OS waxy maize starches with different substitution patterns were studied (Bai, 2013). The product (gOSMs) had localized OS substitution near the branching points or non-reducing ends; the other product (sOSMs) had OS groups distributed randomly throughout the starch chains, and OS substitutions were found close to the branching points as well as the non-reducing ends.

A new method for combining high hydrostatic pressure (HHP) and octenylsuccinic anhydride (OSA) esterification for starch modification in aqueous slurry was developed by Sun et al. (2020). The degree of substitution (DS) decreased after HHP treatment and OSA with combined HHP treatment destroyed the surface morphology of the starch. In previous study (Li et al., 2018), rice starch was pretreated by dynamic high-pressure microfluidization (DHPM) and subsequently modified by OSA in aqueous slurry.

These OSA modifications to the traditional synthesis methodology proposed within the last two years with reaction conditions used for starch modification with OSA in aqueous slurry under mild alkaline conditions are listed in Table 2.1. The DS achieved by esterification of starch with OSA using the aqueous slurry method depends on the botanical source of the starch used, pretreatments, and reaction conditions. The DS of OS starches generally increases when the percentage of OSA increases.

Table 2.1 Reaction conditions values most used in the recent literature in the last two years for starch esterification with OSA in aqueous slurry under mild alkaline conditions with variations.

Base starch	Starch (% w/w)	pH	T (°C)	OSA (%w/w, starch basis)	Time (h)	DS	Reference
lotus seed starch	35	8-9	35	3	3	0.015	Sun et al. (2020)
				5		0.021	
				7		0.032	
				9		0.039	
Waxy rice dextrin	20	8.5	25	1	3	0.006	Wang et al. (2020)
				2		0.011	
				3		0.019	
Taro starch	30	8.5	35	3	5	0.018	Yu et al., (2019)
				5		0.024	
				9		0.032	
Wheat starch	20	8	25	3	3	0.023	Bajaj et al. (2019)
Corn starch						0.024	
Waxy corn starch						0.018	
Potato starch						0.028	
Sweet potato starch						0.029	
Rice starch						0.027	
Kidney bean starch						0.060	
Mung bean starch	45	8	25	3	1	0.017	
Waxy corn starch	40	8.5	35	3	1	0.023	Han et al. (2019)
Corn starch	30	8.5	25	3	6	0.018	Han et al. (2019)
Waxy maize starch	35	8.5	25	3	3	0.016	Lin et al. (2018)
				5		0.025	
				7		0.034	
				9		0.042	
Rice starch	35	8.5- 9.0	25	3	6	0.018	Li et al. (2018)
Waxy maize starch	35	8.5	35	3	2	0.018	Xu et al. (2018)
Rice starch	35	8.5	35	3	2	0.014	Jain et al. (2019)
Rice starch	35	8.5	35	3	2	0.020	

Alternative methods

Apart from the traditional pathway in aqueous slurry, some studies have been conducted to increase the reaction efficiency by using acetic acid (Shogren, 2003), organic solvents (Bhandari & Singhal, 2002; Viswanathan, 1999), microwave (Biswas et al., 2006; Rivero et al., 2009), dry heating (Kim et al., 2010; Sandhu et al., 2015), dry media milling (M. Chen et al., 2014; Hu et al., 2016), ionic liquids media and lipase as catalyst (Li et al., 2016). For more details on these alternative methods, the previous reviews of Altuna et al. (2018) and Sweedman et al. (2013) are referred. In Bai et al. (2017) used supercritical carbon dioxide (ScCO₂) to synthesis of OS starch, diffusing dissolved OSA in ScCO₂ into the starch granules, which led to an even distribution of OS groups in the starch granule. Additionally, OS starch prepared in ScCO₂ had a lower gelatinization temperature and a higher peak paste viscosity indicated that this starch can be used as an effective thickener.

Shi & Bai (2016) filed a United States patent application (U.S. Patent No. 9,458,252) describing an approach to prepare OS starch by dry heating on the mixture of OSA and granular starch. Optimum reaction conditions (3% NH₄HCO₃, heating at 180 °C for 2 h) were investigated to prepare OS waxy maize starch with a high degree of substitution (DS), high reaction efficiency (RE), high solubility, and a light color. RE of ca. 90% was obtained at OSA levels from 3%. After evaluation of the structure and properties of the OS dextrans, the OSA reaction did not change the granular appearance of the starch; however, the molecular weight of starch was significantly reduced after reaction. Heat and OSA reaction resulted in significant starch hydrolysis in the amorphous and crystalline regions of starch granules. OS substitutions probably occurred at the amorphous region of starch granules. Glycosyl linkages including α -

(1→2), α -(1→6), β -(1→2), and β -(1→6) linkages were formed, and 1,6- anhydro- β -D-glucopyranose was formed at the starch chain terminals. OS starch had a degree of branching of 19.8%.

Characterization of OS-starch

The functional properties of OS starch are determined by the structure of substituted starch which can be distinguished at three levels– universal, granular, and molecular (Bai et al., 2014; Huber & BeMiller, 2009; Wang, He, Fu, Huang, & Zhang, 2016). At the universal level, the overall extent of substitution, or degree of substitution (DS) which represents the average number of modified hydroxyl groups per glucosyl unit, can be determined by titration, high performance liquid chromatography (HPLC) and nuclear magnetic resonance (NMR) spectroscopy (Bai et al., 2011; Bai & Shi, 2011; Qiu et al., 2012; Sweedman et al., 2013). At the molecular level, OS substitution, up to DS ~ 0.06, was found to occur mainly at the O-2 and O-3 positions of the anhydroglucose units (AGUs) in OSA-modified maize granular starch (Bai et al., 2011; Bai & Shi, 2011). Most OS groups were located near the branch points of amylopectin at the low DS of 0.018, whereas at the higher DS of 0.92, OS groups were located near both the branch points and on or near the non-reducing ends (Bai et al., 2014).

At the granular level, reaction patterns of modification within a granule have been examined by light microscopy, confocal laser scanning microscopy (CLSM), scanning electron microscopy (SEM), and transmission electron microscopy (TEM) (Huber & BeMiller, 2009). After reacting with 3% (wt%, starch basis) OSA, the x-ray diffraction pattern of a starch is generally not changed, indicating that OS substitution occurs primarily in the amorphous regions of granules (Bai & Shi, 2011; Liu et al., 2018; Shogren et al., 2000). When examined by

backscattered-electron imaging of osmium-stained OSA modified waxy maize starch granules (Shogren et al., 2000), the OS groups appeared to be dispersed throughout the granules. However, x-ray photoelectron spectroscopy suggested that the surface concentration of OS was higher than that of the bulk (Huang et al., 2010; Shogren et al., 2000). CLSM results also indicated that the surface of granules has more OS groups than the interior (Chen et al., 2014; Wang et al., 2013; Ye et al., 2014; Zhang et al., 2011). Using CLSM to study the effects of high-speed shear during the OSA modification reaction, Wang et al. (2015) reported increasing substitution of OS groups in the inner region of a starch granule, indicating a more even distribution of OS groups in the granules when the OSA reaction is conducted with high speed shear.

Using FT-IR microspectroscopy, Bai et al. (2009) and Wetzel, Shi, & Reffner (2010) investigated the level and uniformity of OS substitution on individual waxy maize starch granules, and reported that OS concentration varied between granules. However, it should be noted that individual starch granules were flattened before measurements of FT-IR spectra due to the thickness of the whole granule and a loss of signal caused by the spherical lensing effect (Wetzel, Shi, & Schmidt, 2010). Therefore, Wetzel, Shi, & Schmidt (2010) first used confocal Raman microspectroscopy to provide greater spatial resolution and show a clear evidence for the presence of the octenyl succinate (OS) ester group at the surface of the unflattened modified starch granules at Raman band 1670 cm^{-1} . Liu et al. (2018), using confocal 2D Raman microscopy, reported that OS groups in esterified waxy maize granules are located unevenly throughout the starch granules with an increased intensity in the center. However, it has not been reported on the OS distribution within a single granule.

Application in beverages

Recent developments in formulation, production, and applications of beverage emulsions have been reviewed (McClements et al., 2017; Piorkowski & McClements, 2014; Stounbjerg et al., 2018). Natural emulsifiers used in emulsion-based products were reviewed by McClements and Gumus (2016). Beverage products that should be either transparent or only slightly cloudy in appearance are consumed by people around the world. The main characteristics of beverage emulsions is that they are very dilute, containing as little as 20 mg/L of a dispersed oil phase in the finished product, and must remain physically stable for relatively long periods of time (4–12 months) (Given, 2009). Hydrophobic components such as flavor oils, weighting agents, clouding agents, oil-soluble vitamins, and nutraceuticals can be incorporated into a variety of different colloidal delivery systems suitable for application within beverage products (McClements, 2012; McClements & Rao, 2011), with the most common being emulsions (100 nm to 100 μ m, turbid/opaque), nanoemulsions (10-100 nm, clear/turbid), and microemulsions (2-50 nm, clear) (McClements, 2011; Piorkowski & McClements, 2014). For clear products, the majority of droplets should be less than about 50 nm in diameter so that the light scattering is very weak (Wooster et al., 2008).

Microemulsions are thermodynamically stable and typically contain very small particles and therefore tend to be optically transparent/clear, which is desirable for soft drinks that should be clear. However, the formation usually requires relatively high levels of synthetic surfactants and sometimes the use of cosurfactants/cosolvents, which can be undesirable due to toxicity, cost, taste, and labeling reasons (Piorkowski & McClements, 2014; Saari & Chua, 2020). The recent trend towards more natural (base on plant) and label friendly ingredients are considered to

replace artificial additives, as well as allergens from products of animal origin, to comply with consumer preferences (Stounbjerg et al., 2018).

Emulsions and nanoemulsions are both thermodynamically unstable systems consisting of two immiscible liquids so they will breakdown given sufficient time due to gravitational separation, flocculation, coalescence and Ostwald ripening (McClements & Rao, 2011; Vilela et al., 2018). The droplets of emulsions are larger than that of nanoemulsions and therefore they scatter light more strongly and appear more turbid or cloudy, which is an advantage for soft drinks that are required to have a cloudy appearance, but a disadvantage for products where optical clarity is required. A major advantage of emulsions and nanoemulsions is that the emulsifier-to-oil ratio required to formulate them is often much less than that required for microemulsions, and they can be formulated from all natural ingredients (such as proteins and polysaccharides) rather than synthetic surfactants (such as Tweens) (Piorkowski & McClements, 2014).

In general, nanoemulsions can be prepared using two main approaches: high-energy and low-energy (Gupta et al., 2016; McClements, 2011; McClements & Rao, 2011). High-energy approaches start with oil-in-water (O/W) emulsions and utilize mechanical devices that produce intense disruptive forces that breakup the oil and water phases, such as ultrasonication, high pressure homogenizers (HPH), microfluidizers, and ultrasound generators. In contrast, low-energy approaches mainly rely on the internal chemical energy of the system to form small droplets (Komaiko & McClements, 2015; McClements & Rao, 2011). Low energy methods start with water-in-oil (W/O) emulsions and break coarse emulsions into smaller droplets as they pass through a state of low interfacial tension during phase inversion. The emulsion inversion point (EIP) technique induces a phase inversion by water dilution whereas the phase inversion

temperature (PIT) approach induces a phase inversion on cooling of the mixture (Gupta et al., 2016). However, the emulsifiers used for low energy emulsification methods are commonly surfactant, protein or lipid, not polysaccharide, the most economical abundant and versatile material in the world.

Therefore, we focus primarily on the utilization of emulsion systems by plant-based polysaccharide using high-energy approaches in the preparation of oil-in-water emulsions for beverages. We will use the term “emulsion” to refer to both nanoemulsions and conventional emulsions.

Formation of flavor oil-in-water emulsions

The most commonly used flavor oils in the food industry are citrus oils (essential oils extracted from the orange or lemon peel) in soft drinks formulation (Molet-Rodríguez et al., 2018). Beverages are dilute oil-in-water emulsions, which are typically composed of a flavor oil blend with a polymeric emulsifier/stabilizer in continuous phase (Given, 2009). It should be noted that oil viscosity influences the efficiency of droplet disruption during high energy homogenization. When dispersed phase viscosity is close to continuous phase viscosity, droplet disruption is efficient and the emulsions with small particle size is produced (Piorkowski & McClements, 2014).

Weighting agent

In the beverage industry, weighting agents, also called density-adjusting agents, would be added into the emulsion to increase the density of oil phase to level of density of continuous phase, thereby reducing the tendency for creaming and keeping the droplets uniformly distributed throughout the beverage (Dłużewska et al., 2006; Given, 2009). The criteria for a

good weighting agent are needed to be oil soluble with no undesirable flavor, odor, or color, higher specific gravity (density) than that of flavor or essential oils, and approved by food regulatory (Tan, 2004). These are oil soluble substances with high densities. In the 1940s, brominated vegetable oil (BVO) was first used in soft drinks as the weighting agents for orange oils. Since 1970, several restrictions have been imposed on the incorporation of weighting agents in beverage emulsions. For example, in United States and Canada, the permitted level of use was restricted at 15 ppm BVO, density 1.23–1.33 g/cm³ (Stounbjerg et al., 2018; Taherian et al., 2008). Consequently, the stability of cloud or flavor emulsions for the desired period of time became a common concern in the beverage industry, and ringing or creaming has been a frequent defect in beverages containing cloud emulsions (Taherian et al., 2008). Therefore, the commonly used weighting agents have been investigated for use as weighting agent such as ester gum (EG), sucrose acetate isobutyrate (SAIB), and damar gum (DG). EG, considered as the best agent for creating cloudy emulsions when it is used in combination with other emulsifying agents and permitted for use at 0.01% in the finished beverage, is a hard, pale-amber-colored resin produced by the esterification of pale wood rosin with food-grade glycerol and purified by steam stripping (density 1.08 g/cm³) (Stounbjerg et al., 2018). SAIB is manufactured by esterification of sucrose with acetic anhydride and isobutyric anhydride in the presence of a barium hydroxide catalyst with density 1.146 g/cm³ approved by FDA for use at a maximum level of 0.03% in the finished beverage. DG is extracted from Damar plants in Malaysia, Indonesia, and the East Indies with high solubility in essential oils used as a weighting agent for edible oil to produce beverage clouds emulsion (density 1.05-1.08 g/cm³) (Tan, 2004).

Hydrocolloids acting as emulsifiers

Emulsifiers are usually selected from either high molecular weight biopolymers (such as proteins or polysaccharides) or low molecular weight surfactants (such as lecithins, saponins, Tweens, or Spans) (McClements & Jafari, 2018). Most surfactants are synthetic although these emulsifiers could be the most effective in reducing the particle size (Raikos et al., 2017). However, a great amount of surfactant and co-surfactant is not favorable due to normal membrane structure disruption and cytotoxicity (Colomer et al., 2012; Ménard et al., 2012). As natural emulsifiers, proteins are not suitable for beverages since it is sensitive to pH and ionic strength. Hydrocolloids acting as emulsifying agents was reviewed by Dickinson (2018). Hydrocolloids stabilize emulsions through steric hindrance, depletion flocculation, viscosity effects and electrostatic interactions, with some desired characteristics in high cold water solubility, low viscosity, high emulsifying capacity and no thickening and/or gelling effects with aging (Chanamai & McClements, 2001, 2002; McClements, 2010; Piorkowski & McClements, 2014). The emulsification results were independent of oil content/concentration, solid concentration, pH value, and ion valence, but the ratio of emulsifier/oil has a large influence on emulsion stability (Tesch et al., 2002).

Gum Arabic vs. modified starch

The most widely used hydrocolloids in beverage are amphiphilic polysaccharides, such as gum arabic and modified starch which has been reacted with a derivative succinic anhydride due to their colorless and tasteless in solution, good stability to droplet aggregation at a wide range of pH values, ionic strengths and temperatures (Charoen et al., 2011, 2012; Given, 2009; McClements, 2011; McClements et al., 2017; Sanchez et al., 2018; Stounbjerg et al., 2018; Williams & Phillips, 2009). The presence of hydrophilic arabinogalacton molecules conjugated to hydrophobic protein chain in gum arabic allow the macro molecule to stabilize oil and water

emulsion, creating a homogenous texture to the beverages (Al-Assaf & Phillips, 2009; McClements et al., 2017). However, gum arabic is required in high concentrations (Chanamai & McClements, 2002), and due to issues regarding availability, the fluctuating price and inconsistent quality (Harnsilawat et al., 2006), the beverage industry is exploring other alternative of emulsifiers, such as modified starch and whey protein (Chanamai & McClements, 2002). For example, 20% gum arabic was required to produce a stable 12.5 wt% oil-in water emulsion but modified starch was used as 12% (Chanamai & McClements, 2002).

Previous study has compared gum arabic and OSA-modified starches used as emulsifiers to perform in formation and stabilization of orange oil-in-water emulsions (Qian et al., 2011). At the same emulsion conditions (5% oil, three passes at 9,000 psi by microfluider), the minimum droplet diameters produced were 0.497 and 0.222 μm while the ratio of emulsifier to oil required to produce small droplets were 3:5 and 5:5, respectively. They also found that there was little effect of pH, ionic strength and temperature on emulsions stabilized by gum arabic or OSA-modified starches due to strong steric (rather than electrostatic) stabilization. The similar conclusion was also found in other studies (Chaudhari et al., 2015; Xu et al., 2018). Since the main stabilizing mechanism of OSA-modified starches is steric hindrance, the stability of emulsions is resistant to changes in pH (3-9), ionic strength (0-100 mM NaCl; 0-25 mM CaCl₂) and temperature (30-90 °C) (Chanamai & McClements, 2001, 2002; Charoen et al., 2011; Qian et al., 2011).

OSA-modified starches as emulsion stabilizers

As most of the available commercial samples of OS starch contain a high proportion of amylopectin (highly branched structure), responsible for the ingredient's interfacial functionality (Dickinson, 2018). After high-pressure homogenizer, an oil-water interfacial layer of OS starch

has been formed. Three key structural attributes of the amylopectin molecule all contribute to its steric stabilization effectiveness due to its large molecular size, its high backbone rigidity, and its extensive chain branching (Dokić et al., 2012; Sweedman et al., 2013).

Nevertheless, what factors could enhance the emulsification properties of OSA modified starch with orange oil? The most common factors affected on the stability of oil-in-water emulsion based beverage are reviewed by Meybodi et al. (2014). The importance of particle size distribution and rheological properties of water phase and emulsions on stability of beverage emulsions were highlighted.

An overview of recent research articles on oil-in-water emulsion formation by OSA-modified starches using a microfluidizer is shown in Table 2.2. Xu et al. (2015) reported that OS maltodextrin prepared from OS starch hydrolyzed by β -amylase which increased its degree of substitution (DS) and degree of branching (DB) showed better emulsification properties of orange oil. Wang et al. (2016) also found that more uniform OS group distribution would improve the stability of emulsion. The OSA reaction was performed under high shear condition from 500 rpm to 10,000 rpm, which improved the emulsion properties of modified starch with particle size from 1.76 to 1.37 μm . The effect of mineral elements (magnesium, calcium and potassium) on the stability of orange oil-in-water emulsions was studied by Krđikowska et al. (2017). They suggested that the presence of potassium ions in OSA starches resulted in a lower diameter of oil droplets and a higher stability of the emulsions. Han et al. (2019) have investigated that the emulsifying capacity of OSA-modified waxy maize starches formed by hydrolysis by α -amylase, β -amylase and HCl for various hydrolysis times and found that the degraded OSA-starches treated by α -amylase generally had the smallest average chain length and largest degree of branching, resulting in the lowest viscosity and the best droplet stability with

the smallest creaming extent. Waxy rice starch hydrolyzed by β -amylase and then modified by OSA (OSA β -limit dextrin) was evaluated by Wang et al. (2020).

Table 2.2 Preparation of emulsion conditions of recent research articles (after 2015) on orange oil-in-water emulsion formation by OSA-modified starches using a microfluidizer and some works related to commercial OS starch (2010-2015)

Base starch	DS	Starch content	Oil phase	Water phase	Condition	Particle diameter	Reference
Waxy maize starch	0.019	0.5%	4% orange oil		homogenized at 150,000 rpm	1.01 μm	(Wang et al., 2016)
Waxy maize starch	0.018	0.2%	10.0% orange oil	0.15%	homogenized at 16,000 rpm	15.60 μm	(Xu et al., 2015)
β-amylase waxy starch	0.028	0.2%	10.0% orange oil	sodium benzoate	for 3 min, then microfluidizer at 300 bar for 1 cycle	4.60 μm	
Waxy rice starch hydrolyzed by β-limit	0.006 0.011 0.019	3%	10.0% oil (not mention which oil)		homogenized at 15,000 rpm for 2.5 min, then microfluidizer at 1000 bar for 3 times	0.22 μm 0.19 μm 0.17 μm	(Wang et al., 2020)
Waxy maize starch	0.018	0.5% 1% 1.5% 3% 5%	9.5% orange oil 9% orange oil 8.5% orange oil 7% orange oil 5% orange oil	0.15% sodium azide	homogenized at 16,000 rpm for 3 min, then microfluidized at 300 bar for 1 pass	2.20 μm 1.05 μm 0.95 μm 0.78 μm 0.75 μm	(Xu et al., 2018)
Purity Gum 2000		12%	5% orange oil+5% ester gum			0.7 μm	
Purity Gum 1773		12%	5% orange oil+5% ester gum		homogenized at 6000 to 7000 rpm for 2 min, then microfluidizer at 13,000 psig	1.1 μm	(Reiner et al., 2010)
Mira Mist 662		12%	5% orange oil+5% ester gum			1.6 μm	

The mechanism of emulsion stabilized by OS-starch

Steric hindrance is the main stabilizing mechanism of OS-starch when the concentration of starch has a great influence to emulsion viscosity (Tesch et al., 2002). When the starch concentration decreased, stabilization of emulsion was mainly determined by starch structure. Macromolecule density of the OS-starch at oil-water interface decreased, the average distance between macromolecule became larger, and therefore, electrostatics may play an important role in stabilizing the emulsions (Xu et al., 2015). Smaller molecules may have a higher diffusion rate and can migrate quickly to an oil-droplet surface to form smaller droplet when homogenizing.

Mixed emulsifiers used in beverage emulsions

Improving emulsion formation, stability and performance using mixed emulsifiers are reviewed (McClements & Jafari, 2018). If the mixed emulsifiers are added prior to homogenization, then they will compete for the interface inside the homogenizer. Typically, small molecule surfactants will initially be present but may be displaced during storage due to competitive adsorption with other emulsifiers in system (McClements & Jafari, 2018). Alternatively, one emulsifier may be added before homogenization, while another one is added after homogenization. In this case, the original emulsifier may be fully or partially displaced from the droplet surfaces by the added emulsifier depending on their relatively concentrations and surface activities (McClements & Jafari, 2018). Two broad classes of emulsifying agents, small molecule surfactants (Tween 20) and macromolecular biopolymers (Hi-Cap 100, a commercial OS starch from Ingredion Inc., Bridgewater, NJ) were used together for emulsions (Jafari et al., 2007). The particle size of combination (2.5% Tween 20 and 10% Hi-Cap) was decreased from 850 nm (without adding Tween 20) to 180 nm. However, final emulsions were very unstable since a slow phase separation was observed with these emulsions during a short

time after microfluidization, especially at higher Tween concentrations (10%). This problem could arise from the influence of the combination of two emulsifiers on emulsion properties and possible interactions and competitions between both existent emulsifiers (Jafari et al., 2007). In the study of Lin et al. (2018a), 2% Tween 20 was added into 5% OSA-modified starch solution emulsified with 10% corn oil. After the treatment of Tween 20, the droplet sizes of all emulsions reduced significantly but they did not study the stability of these emulsions.

Formation of vitamin E emulsions

There is increasing interest within the food industry in incorporating various types of fat-soluble vitamins (A, D, E, and K) into food and beverage products to improve the nutritional value. Vitamin E is an essential nutrient derived from various crops (barley, wheat and soybean). The term “Vitamin E” actually refers to a group of eight closely related fat-soluble vitamins (Mayer et al., 2013; Qiu et al., 2015). Epidemiological and experimental studies have shown that DL- α -tocopherol is an effective antioxidant of VE and its acetate ester (named VE acetate) playing an important role in prevention of chronic disease and carcinogenesis (Saber et al., 2013b, 2014b). VE is not soluble in water, and it is necessary to convert it into a vitamin E emulsion before it can be used in beverage. Due to the limitation of its sensitivity to heat and oxygen, its low water-solubility, and its poor and variable bioavailability, emulsion-based delivery systems has been considerable interest to overcome these challenges (Chen & Wagner, 2004; Morais Diane & Burgess, 2014; Saber et al., 2013b, 2014b). Among the commercial VE acetate products, there are three forms: a highly concentrated oily form, encapsulated powders, and adsorbates of the oily form on selected carriers (Qiu et al., 2015). In beverages, the most challenging hurdle for VE is beverage turbidity and poor physical stability which particle size of

droplets increased and easy to form a ring around the bottleneck, so-called 'ringing (Chen & Wagner, 2004).

A recent beverages emulsion to enhance delivery of bioactive components (fat-soluble vitamins) was reviewed by Raikos and Ranawana (2017). Chen and Wagner (2004) produced a VE nanoparticle with OSA modified starch by microfluidizer. VE emulsion was prepared and stabilized with an ionic emulsifier with an average particle size of around 100 nm. The physicochemical properties of OSA modified starches ideal for good emulsification of VE were found to be high DS, low average molecular weight (Mw) and low interfacial tension (Hategekimana et al., 2014, 2015). At the latest study of Qiu et al. (2015), a VE emulsion made by OS starch with particle size of 0.1 μ m (fresh) was produced by a microfluidizer at 20,000 psi (12 passes, 5 g OS starch, 5 g oil and 50 g water). They also found that increasing the number of passes resulted in free OS content increased and the stabilizing ability of OS starch decreased during microfluidization. Otherwise, most studied on formation of VE emulsions were used other aqueous phase except modified starches. Ozturk et al. (2014) reported that formation and stabilization of VE delivery systems using gum arabic (steric repulsion), which was much more stable than protein-based emulsifier (electrostatic repulsion). A study on stability by Yang & McClements (2013a) reported that the Q-Naturale-coated VE droplets were found to be stable to droplet coalescence over a range of pH values (2-8), salt concentrations (0-500 mM NaCl), and temperatures (20-90 °C). It has been previously reported in literature that it is challenging to form nanoemulsion droplets when VE is used as the only oil because of its high viscosity (Yang & McClements, 2013a). On the other hand, small droplets could be formed when $\geq 20\%$ MCT was incorporated into the oil phase resulting at low viscosity of oil phase prior to homogenization

using a natural surfactant (Q-Naturale), which was proved to be an effective way of forming edible VE delivery systems.

Table 2.3 shows the preparation conditions of vitamin E emulsions in recent studies. The use of carrier oils has become handy in reducing the viscosity of VE. It has been previously reported in literature that it is challenging to form nanoemulsion droplets when VE is used as the only oil because of its high viscosity (Yang & McClements, 2013a). Previous studies suggest that a range of viscosity ratios (η_D/η_C) between 0.1 and 5 is the optimum to produce small droplets in homogenizers. Therefore, some studies added MCT or other oil as lipid phase to decrease the viscosity of vitamin E due to its higher viscosity (Hategekimana et al., 2014; Saberi et al., 2014b; Yang & McClements, 2013b). On the other hand, emulsion containing Tween 80 is more sensitive to viscosity changes of dispersed and continuous phases than those of Q-Naturale (Yang & McClements, 2013a). VE is a highly viscous liquid that is difficult to homogenize alone, and so low viscosity food-grade oils such as MCT and orange oil is blended to facilitate homogenization. Overall, spontaneous emulsification is normally performed by addition of an organic phase to an aqueous phase while magnetically stirring (600 rpm) the system at 25 °C to form the small droplets (Saberi et al., 2013b). The organic phase consisted of different amounts of VE, MCT and surfactant, while the aqueous phase was a buffer solution (pH 3.0, 0.8% citric acid, 0.08% sodium benzoate) that contained different amounts of glycerol (0 to 50 wt%). Yang and McClements (2013a & 2013b) examined the smaller vitamin E droplets produced by adding different amounts of glycerol to the aqueous phase, resulting higher viscosity ratio and lower interfacial tension due to glycerol is less polar than water. The influence of glycerol concentration can reduce the cloudy by preparing an emulsion from an oil phase containing either 80% VE and 20% MCT or 100% VE.

Table 2.3. Recent studies on the delivery of VE emulsion systems

Oil phase	Emulsifier	Aqueous phase	Mechanic force	Particle size	Reference
VE acetate	OSA modified starch	water	Microfluidizer ranging from 20 to 300 MPa	110-210 nm	Chen & Wagner (2004)
VE acetate MCT^a	OSA modified starch	water	Microfluidizer	250 nm	Hategekimana et al. (2014, 2015)
VE acetate	OSA modified starch	water	Microfluidizer	1.3 μm	Qiu et al., (2015)
VE acetate Orange oil	Whey protein isolate (WPI) or Gum Arabic	buffer solution (10 mM sodium phosphate, pH 7.0)	Microfluidizer	0.4 μm	Ozturk et al. (2015); Raikos, (2017)
VE acetate MCT	Tween 80 / Brij 35	water	Hydrophilic SPG membrane emulsification technique	100nm	Laouini et al. (2012)
VE acetate MCT, or MCT and corn oil	Tween 80 or Tween 80 and propylene glycol or ethanol	Acidic buffer solution that contained glycerol or ethanol (pH 3.0, 0.8% citric acid, 0.08% sodium benzoate)	Magnetic stirrer speed of 600 rpm at 25 $^{\circ}\text{C}$	50nm	Ziani et al. (2012)
VE acetate MCT	Tween 80 or Q-Naturale 200	Buffer solution (pH 7) w/o glycerol	Microfluidizer at 9000 psi	400nm	Yang & McClements, (2013a, 2013b)
VE acetate MCT	Tween 20/ 40/60/80 /85, WPI, Sucrose monopalmitate, Casein, Quillaja saponin (Q-Naturale)	Acidic buffer solution (pH 3.0, 0.8% citric acid, 0.08% sodium benzoate)	Emulsion phase inversion (EPI): aqueous phase is titrated into the oil phase with stirring at 500 rpm, and Microfluidizer at 12,000 psi	90nm (Tween 80) 25 μm (Q-Naturale, WPI, SMP) 50 μm (Casein)	Saberi et al. (2013a, 2013b, 2013c, 2014a); Mayer et al. (2013)
VE acetate Canola oil	Span80 & CremophorRH40	water	Emulsion phase inversion (EPI)	100nm	Morais Diane & Burgess, (2014) ; Morais & Burgess, (2014)
VE acetate Corn oil	Q-Naturale 200 or whey protein isolate (WPI) or gum arabic	Phosphate buffer (5 mM, pH 7.0)	Microfluidizer at 14,000 psi	1 μm	Lv et al. (2018, 2019)

^a MCT: medium chain triglyceride oil (Miglyol 812)

Characterization of emulsions

The particle size of emulsion is the sum of the radius of the oil droplet core and the thickness of the shell layer, therefore smaller size could be formed by using an emulsifier that forms a thinner layer around the oil droplets (McClements, 2011). Typically, the thickness of the film formed by emulsifiers surrounding the oil droplet: small molecule surfactants (such as Tweens and Spans) < globular proteins (such as egg, whey or soy proteins) < flexible proteins (such as caseinate or gelatin) < polysaccharides (gum Arabic or modified starch) (McClements, 2011).

It has been reported that a higher DS value of OS starch contributed to lower surface tension values at the air–water interface (Królikowska et al., 2017), which surface tension value of native and OSA modified starches (3 and 9% OSA) was 71.75, 64.69 and 61.32 mN/m, respectively. The presence of more carboxyl groups in OSA-modified starches with higher DS values may contribute to a more rigid and compact surface that resists coalescence of the droplets. The emulsions stabilized by OSA modified starches with higher DS were more stable.

The key instability mechanisms that are applied to complete emulsions' separation phase include coalescence, creaming, Ostwald ripening, and flocculation (McClements & Jafari, 2018). A simple method to measure the stability of emulsions was established by Demetriades and McClements (2000) that calculate the creaming index by ratio of the height of interface to the height of total emulsion with storage 7 days at room temperature. HPLC was used to determine the stability of vitamin E (Li et al., 2011; Qiu et al., 2015).

Conclusions

This review provided a comprehensive overview of the scientific and technological principles underlying beverage emulsion of orange oil and VE. Modification with OSA groups gives the starch amphiphilic properties to absorb to the oil droplets. The importance of particle size distribution and rheological properties of water phase and emulsions on stability of beverage emulsions were highlighted. When the steric stabilization mechanism is dominant, concentration of OS starch is responsible for rheological properties of emulsions. It is important to determine the distribution of OSA substituent in starch granules, which higher OS degree of substitution contributes to a more rigid and compact surface that resists coalescence of the droplets. The size of OS starch molecule dissolved in water is also a critical factor to form oil-in-water emulsion since the thickness of the layer around the oil droplets. There are still many challenges to overcome the instability of emulsions. Research is continuing in this area, and OSA modified starch has been identified to be suitable for stabilization of beverage emulsions.

References

- Al-Assaf, S., & Phillips, G. O. (2009). Hydrocolloids: structure-function relationships. *Food Science & Technology*, 23(3), 17–20.
- Altuna, L., Herrera, M. L., & Foresti, M. L. (2018). Synthesis and characterization of octenyl succinic anhydride modified starches for food applications. A review of recent literature. *Food Hydrocolloids*, 80, 97–110.
- Bai, J., Xie, X., Li, X., & Zhang, Y. (2017). Synthesis of octenylsuccinic-anhydride-modified cassava starch in supercritical carbon dioxide: Synthesis OSAS in supercritical CO₂. *Starch - Stärke*, 69(11–12), 1700018.
- Bai, Y. (2013). *Preparation, structure and properties of octenylsuccinic anhydride modified starch*. <https://krex.k-state.edu/dspace/handle/2097/35046>
- Bai, Y., Kaufman, R. C., Wilson, J. D., & Shi, Y.-C. (2014). Position of modifying groups on starch chains of octenylsuccinic anhydride-modified waxy maize starch. *Food Chemistry*, 153, 193–199.
- Bai, Y., & Shi, Y.-C. (2011). Structure and preparation of octenyl succinic esters of granular starch, microporous starch and soluble maltodextrin. *Carbohydrate Polymers*, 83(2), 520–527.
- Bai, Y., & Shi, Y.-C. (2013). Reaction of octenylsuccinic anhydride with a mixture of granular starch and soluble maltodextrin. *Carbohydrate Polymers*, 98(2), 1599–1602.
- Bai, Y., Shi, Y.-C., Herrera, A., & Prakash, O. (2011). Study of octenyl succinic anhydride-modified waxy maize starch by nuclear magnetic resonance spectroscopy. *Carbohydrate Polymers*, 83(2), 407–413.
- Bai, Y., Shi, Y.-C., & Wetzel, D. L. (2009). Fourier Transform Infrared (FT-IR) Microspectroscopic Census of Single Starch Granules for Octenyl Succinate Ester Modification. *Journal of Agricultural and Food Chemistry*, 57(14), 6443–6448.
- Bajaj, R., Singh, N., & Kaur, A. (2019). Properties of octenyl succinic anhydride (OSA) modified starches and their application in low fat mayonnaise. *International Journal of Biological Macromolecules*, 131, 147–157.
- BeMiller, J. N. (2018). *Carbohydrate Chemistry for Food Scientists*. Elsevier.
- BeMiller, J. N., & Whistler, R. L. (2009). *Starch: Chemistry and Technology*. Academic Press.

- Bhandari, P. N., & Singhal, R. S. (2002). Effect of succinylation on the corn and amaranth starch pastes. *Carbohydrate Polymers*, 48(3), 233–240.
- Biswas, A., Shogren, R. L., Kim, S., & Willett, J. L. (2006). Rapid preparation of starch maleate half-esters. *Carbohydrate Polymers*, 64(3), 484–487.
- Caldwell, C. G. (1952). *Free-flowing starch esters* (United States Patent No. US2613206A).
- Caldwell, C. G., & Wurzburg, O. B. (1953). *Polysaccharide derivatives of substituted dicarboxylic acids* (Patent No. US2661349 A).
- Chanamai, R., & McClements, D. J. (2001). Depletion flocculation of beverage emulsions by gum arabic and modified starch. *Journal of Food Science*, 66(3), 457–463.
- Chanamai, R., & McClements, D. J. (2002). Comparison of gum arabic, modified starch, and whey protein isolate as emulsifiers: Influence of pH, CaCl₂ and temperature. *Journal of Food Science*, 67(1), 120–125.
- Charoen, R., Jangchud, A., Jangchud, K., Harnsilawat, T., Decker, E. A., & McClements, D. J. (2012). Influence of interfacial composition on oxidative stability of oil-in-water emulsions stabilized by biopolymer emulsifiers. *Food Chemistry*, 131(4), 1340–1346.
- Charoen, R., Jangchud, A., Jangchud, K., Harnsilawat, T., Naivikul, O., & McClements, D. J. (2011). Influence of biopolymer emulsifier type on formation and stability of rice bran oil-in-water emulsions: Whey protein, gum arabic, and modified starch. *Journal of Food Science*, 76(1), E165–E172.
- Chaudhari, A., Pan, Y., & Nitin, N. (2015). Beverage emulsions: Comparison among nanoparticle stabilized emulsion with starch and surfactant stabilized emulsions. *Food Research International*, 69, 156–163.
- Chen, C.-C., & Wagner, G. (2004). Vitamin E nanoparticle for beverage applications. *Chemical Engineering Research and Design*, 82(11), 1432–1437.
- Chen, M., Yin, T., Chen, Y., Xiong, S., & Zhao, S. (2014). Preparation and characterization of octenyl succinic anhydride modified waxy rice starch by dry media milling. *Starch - Stärke*, 66(11–12), 985–991.
- Chen, X., He, X., & Huang, Q. (2014). Effects of hydrothermal pretreatment on subsequent octenylsuccinic anhydride (OSA) modification of cornstarch. *Carbohydrate Polymers*, 101, 493–498.

- Colomer, A., Pinazo, A., Garc ía, M. T., Mitjans, M., Vinardell, M. P., Infante, M. R., Mart ínez, V., & Pérez, L. (2012). pH-sensitive surfactants from lysine: Assessment of their cytotoxicity and environmental behavior. *Langmuir*, 28(14), 5900–5912.
- Demetriades, K., & Julian McClements, D. (2000). Influence of sodium dodecyl sulfate on the physicochemical properties of whey protein-stabilized emulsions. *Colloids and Surfaces A: Physicochemical and Engineering Aspects*, 161(3), 391–400.
- Dickinson, E. (2018). Hydrocolloids acting as emulsifying agents – How do they do it? *Food Hydrocolloids*, 78, 2–14.
- Dłużewska, E., Stabiecka, A., & Maszewska, M. (2006). Effect of oil phase concentration on rheological properties and stability of beverage emulsion. *Acta scientiarum polonorum technologia alimentaria*, 5(2), 147-156.
- Dokić, L., Krstonošić, V., & Nikolić, I. (2012). Physicochemical characteristics and stability of oil-in-water emulsions stabilized by OSA starch. *Food Hydrocolloids*, 29(1), 185–192.
- Given, P. S. (2009). Encapsulation of flavors in emulsions for beverages. *Current Opinion in Colloid & Interface Science*, 14(1), 43–47.
- Gupta, A., Eral, H. B., Hatton, T. A., & Doyle, P. S. (2016). Nanoemulsions: formation, properties and applications. *Soft Matter*, 12(11), 2826–2841.
- Han, H., Zhang, H., Li, E., Li, C., & Wu, P. (2019). Structural and functional properties of OSA-starches made with wide-ranging hydrolysis approaches. *Food Hydrocolloids*, 90, 132–145.
- Han, J.-A., Chung, H.-J., & Lim, S.-T. (2019). Physical and emulsifying properties of OSA-corn dextrin with various manufacturing methods. *Food Hydrocolloids*, 89, 563–569.
- Harnsilawat, T., Pongsawatmanit, R., & McClements, D. J. (2006). Stabilization of model beverage cloud emulsions using protein– polysaccharide electrostatic complexes formed at the oil– water interface. *Journal of agricultural and food chemistry*, 54(15), 5540-5547.
- Hategekimana, J., Bwengye, M. K., Masamba, K. G., Yokoyama, W., & Zhong, F. (2014). Formation and stability of vitamin E enriched nanoemulsions stabilized by octenyl succinic anhydride modified starch. *International Journal of Food Engineering*, 10(4).
- Hategekimana, J., Masamba, K. G., Ma, J., & Zhong, F. (2015). Encapsulation of vitamin E: Effect of physicochemical properties of wall material on retention and stability. *Carbohydrate Polymers*, 124, 172–179.

- Hu, H., Liu, W., Shi, J., Huang, Z., Zhang, Y., Huang, A., Yang, M., Qin, X., & Shen, F. (2016). Structure and functional properties of octenyl succinic anhydride modified starch prepared by a non-conventional technology. *Starch - Stärke*, 68(1–2), 151–159.
- Huang, Q., Fu, X., He, X., Luo, F., Yu, S., & Li, L. (2010). The effect of enzymatic pretreatments on subsequent octenyl succinic anhydride modifications of cornstarch. *Food Hydrocolloids*, 24(1), 60–65.
- Huber, K. C., & BeMiller, J. N. (2001). Location of Sites of Reaction Within Starch Granules. *Cereal Chemistry*, 78(2), 173–180.
- Jafari, S. M., He, Y., & Bhandari, B. (2007). Effectiveness of encapsulating biopolymers to produce sub-micron emulsions by high energy emulsification techniques. *Food Research International*, 40(7), 862–873.
- Jain, S., Winuprasith, T., & Suphantharika, M. (2019). Design and synthesis of modified and resistant starch-based oil-in-water emulsions. *Food Hydrocolloids*, 89, 153–162.
- Kim, H.-N., Sandhu, K. S., Lee, J. H., Lim, H. S., & Lim, S.-T. (2010). Characterisation of 2-octenylsuccinylated waxy rice amyloextrins prepared by dry-heating. *Food Chemistry*, 119(3), 1189–1194.
- Komaiko, J., & McClements, D. J. (2015). Food-grade nanoemulsion filled hydrogels formed by spontaneous emulsification and gelation: Optical properties, rheology, and stability. *Food Hydrocolloids*, 46, 67–75.
- Krđikowska, K., Fortuna, T., Pietrzyk, S., & Gryszkin, A. (2017). Effect of modification of octenyl succinate starch with mineral elements on the stability and rheological properties of oil-in-water emulsions. *Food Hydrocolloids*, 66, 118–127.
- Laouini, A., Fessi, H., & Charcosset, C. (2012). Preparation of nano-emulsions using SPG membrane emulsification -Application to vitamin E encapsulation. *Procedia Engineering*, 44, 740–742.
- Li, D., Zhang, X., & Tian, Y. (2016). Ionic liquids as novel solvents for biosynthesis of octenyl succinic anhydride-modified waxy maize starch. *International Journal of Biological Macromolecules*, 86, 119–125.
- Li, X., Anton, N., Ta, T. M. C., Zhao, M., Messaddeq, N., & Vandamme, T. F. (2011). Microencapsulation of nanoemulsions: novel Trojan particles for bioactive lipid molecule delivery. *International Journal of Nanomedicine*, 6, 1313–1325.

- Li, Y., Wang, R., Liang, R., Chen, J., He, X., Chen, R., Liu, W., & Liu, C. (2018). Dynamic high-pressure microfluidization assisting octenyl succinic anhydride modification of rice starch. *Carbohydrate Polymers*, *193*, 336–342.
- Lin, Q., Liang, R., Zhong, F., Ye, A., & Singh, H. (2018a). Interactions between octenyl-succinic-anhydride-modified starches and calcium in oil-in-water emulsions. *Food Hydrocolloids*, *77*, 30–39.
- Lin, Q., Liang, R., Zhong, F., Ye, A., & Singh, H. (2018b). Effect of degree of octenyl succinic anhydride (OSA) substitution on the digestion of emulsions and the bioaccessibility of β -carotene in OSA-modified-starch-stabilized-emulsions. *Food Hydrocolloids*, *84*, 303–312.
- Liu, W., Li, Y., Goff, H. D., Nsor-Atindana, J., & Zhong, F. (2018). Distribution of octenylsuccinic groups in modified waxy maize starch: An analysis at granular level. *Food Hydrocolloids*, *84*, 210–218.
- Liu, Z., Li, Y., Cui, F., Ping, L., Song, J., Ravee, Y., Jin, L., Xue, Y., Xu, J., Li, G., Wang, Y., & Zheng, Y. (2008). Production of octenyl succinic anhydride-modified waxy corn starch and its characterization. *Journal of Agricultural and Food Chemistry*, *56*(23), 11499–11506.
- Lv, S., Gu, J., Zhang, R., Zhang, Y., Tan, H., & McClements, D. J. (2018). Vitamin E encapsulation in plant-based nanoemulsions fabricated using dual-channel microfluidization: Formation, stability, and bioaccessibility. *Journal of agricultural and food chemistry*, *66*(40), 10532–10542.
- Lv, S., Zhang, Y., Tan, H., Zhang, R., & McClements, D. J. (2019). Vitamin E Encapsulation within Oil-in-Water Emulsions: Impact of Emulsifier Type on Physicochemical Stability and Bioaccessibility. *Journal of Agricultural and Food Chemistry*, *67*(5), 1521–1529.
- Mayer, S., Weiss, J., & McClements, D. J. (2013). Vitamin E-enriched nanoemulsions formed by emulsion phase inversion: Factors influencing droplet size and stability. *Journal of Colloid and Interface Science*, *402*, 122–130.
- McClements, D. J. (2010). Emulsion design to improve the delivery of functional lipophilic components. *Annual Review of Food Science and Technology*, *1*(1), 241–269.
- McClements, D. J. (2011). Edible nanoemulsions: fabrication, properties, and functional performance. *Soft Matter*, *7*(6), 2297–2316.
- McClements, D. J. (2012). Nanoemulsions versus microemulsions: terminology, differences, and similarities. *Soft Matter*, *8*(6), 1719–1729.

- McClements, D. J., Bai, L., & Chung, C. (2017). Recent advances in the utilization of natural emulsifiers to form and stabilize emulsions. *Annual Review of Food Science and Technology*, 8(1), 205–236.
- McClements, D. J., & Gumus, C. E. (2016). Natural emulsifiers — Biosurfactants, phospholipids, biopolymers, and colloidal particles: Molecular and physicochemical basis of functional performance. *Advances in Colloid and Interface Science*, 234, 3–26.
- McClements, D. J., & Jafari, S. M. (2018). Improving emulsion formation, stability and performance using mixed emulsifiers: A review. *Advances in Colloid and Interface Science*, 251, 55–79.
- McClements, D. J., & Rao, J. (2011). Food-grade nanoemulsions: formulation, fabrication, properties, performance, biological fate, and potential toxicity. *Critical Reviews in Food Science and Nutrition*, 51(4), 285–330.
- Ménard, N., Tsapis, N., Poirier, C., Arnauld, T., Moine, L., Lefoulon, F., Péan, J.-M., & Fattal, E. (2012). Drug solubilization and in vitro toxicity evaluation of lipoamino acid surfactants. *International Journal of Pharmaceutics*, 423(2), 312–320.
- Meybodi, N. M., Mohammadifar, M. A., & Naseri, A. R. (2014). Effective factors on the stability of oil-in-water emulsion-based beverage: A Review. *Journal of Food Quality and Hazards Control*, 1(3), 67-71.
- Molet-Rodríguez, A., Salvia-Trujillo, L., & Martín-Belloso, O. (2018). Beverage emulsions: Key aspects of their formulation and physicochemical stability. *Beverages*, 4(3), 70.
- Morais Diane, J. M., & Burgess, J. (2014). Vitamin E nanoemulsions characterization and analysis. *International Journal of Pharmaceutics*, 465(1–2), 455–463.
- Morais, J. M., & Burgess, D. J. (2014). In vitro release testing methods for vitamin E nanoemulsions. *International Journal of Pharmaceutics*, 475(1–2), 393–400.
- Ozturk, B., Argin, S., Ozilgen, M., & McClements, D. J. (2014). Formation and stabilization of nanoemulsion-based vitamin E delivery systems using natural surfactants: Quillaja saponin and lecithin. *Journal of Food Engineering*, 142, 57–63.
- Ozturk, B., Argin, S., Ozilgen, M., & McClements, D. J. (2015). Formation and stabilization of nanoemulsion-based vitamin E delivery systems using natural biopolymers: Whey protein isolate and gum arabic. *Food Chemistry*, 188, 256–263.
- Piorowski, D. T., & McClements, D. J. (2014). Beverage emulsions: Recent developments in formulation, production, and applications. *Food Hydrocolloids*, 42, 5–41.

- Punia, S., Siroha, A. K., Sandhu, K. S., & Kaur, M. (2019). Rheological and pasting behavior of OSA modified mungbean starches and its utilization in cake formulation as fat replacer. *International Journal of Biological Macromolecules*, 128, 230–236.
- Qian, C., Decker, E. A., Xiao, H., & McClements, D. J. (2011). Comparison of Biopolymer Emulsifier Performance in Formation and Stabilization of Orange Oil-in-Water Emulsions. *JAOCs, Journal of the American Oil Chemists' Society*, 88(1), 47–55.
- Qiu, D., Bai, Y., & Shi, Y.-C. (2012). Identification of isomers and determination of octenylsuccinate in modified starch by HPLC and mass spectrometry. *Food Chemistry*, 135(2), 665–671.
- Qiu, D., Yang, L., & Shi, Y.-C. (2015). Formation of vitamin E emulsion stabilized by octenylsuccinic starch: Factors affecting particle size and oil load. *Journal of Food Science*, 80(4), 680–686.
- Raikos, V. (2017). Encapsulation of vitamin E in edible orange oil-in-water emulsion beverages: Influence of heating temperature on physicochemical stability during chilled storage. *Food Hydrocolloids*, 72, 155–162.
- Raikos, V., Duthie, G., & Ranawana, V. (2017). Comparing the efficiency of different food-grade emulsifiers to form and stabilise orange oil-in-water beverage emulsions: influence of emulsifier concentration and storage time. *International Journal of Food Science & Technology*, 52(2), 348–358.
- Raikos, V., & Ranawana, V. (2017). Designing emulsion droplets of foods and beverages to enhance delivery of lipophilic bioactive components - a review of recent advances. *International Journal of Food Science & Technology*, 52(1), 68–80.
- Reiner, S. J., Reineccius, G. A., & Peppard, T. L. (2010). A comparison of the stability of beverage cloud emulsions formulated with different gum acacia- and starch-based emulsifiers. *Journal of Food Science*, 75(5), 236–246.
- Rivero, I. E., Balsamo, V., & Müller, A. J. (2009). Microwave-assisted modification of starch for compatibilizing LLDPE/starch blends. *Carbohydrate Polymers*, 75(2), 343–350.
- Saari, N. H. M., & Chua, L. S. (2020). 13 - Nano-Based Products in Beverage Industry. In A. M. Grumezescu & A. M. Holban (Eds.), *Nanoengineering in the Beverage Industry* (pp. 405–436). Academic Press.
- Saberi, A. H., Fang, Y., & McClements, D. J. (2013a). Fabrication of vitamin E-enriched nanoemulsions: Factors affecting particle size using spontaneous emulsification. *Journal of Colloid and Interface Science*, 391, 95–102.

- Saberi, A. H., Fang, Y., & McClements, D. J. (2013b). Fabrication of vitamin E-enriched nanoemulsions by spontaneous emulsification: Effect of propylene glycol and ethanol on formation, stability, and properties. *Food Research International*, *54*(1), 812–820.
- Saberi, A. H., Fang, Y., & McClements, D. J. (2013c). Effect of glycerol on formation, stability, and properties of vitamin-E enriched nanoemulsions produced using spontaneous emulsification. *Journal of Colloid and Interface Science*, *411*, 105–113.
- Saberi, A. H., Fang, Y., & McClements, D. J. (2014a). Stabilization of vitamin E-enriched nanoemulsions: Influence of post-homogenization cosurfactant addition. *Journal of Agricultural and Food Chemistry*, *62*(7), 1625–1633.
- Saberi, A. H., Fang, Y., & McClements, D. J. (2014b). Stabilization of vitamin E-enriched mini-emulsions: Influence of organic and aqueous phase compositions. *Colloids and Surfaces A: Physicochemical and Engineering Aspects*, *449*, 65–73.
- Sanchez, C., Nigen, M., Mejia Tamayo, V., Doco, T., Williams, P., Amine, C., & Renard, D. (2018). Acacia gum: History of the future. *Food Hydrocolloids*, *78*, 140–160.
- Sandhu, K. S., Sharma, L., & Kaur, M. (2015). Effect of granule size on physicochemical, morphological, thermal and pasting properties of native and 2-octenyl-1-ylsuccinylated potato starch prepared by dry heating under different pH conditions. *LWT - Food Science and Technology*, *61*(1), 224–230.
- Shi, Y.-C., & Bai, Y. (2016). *Starch esters and method of preparation* (United States Patent No. US9458252B2).
- Shogren, R. L. (2003). Rapid preparation of starch esters by high temperature/pressure reaction. *Carbohydrate Polymers*, *52*(3), 319–326.
- Shogren, Randal L., Viswanathan, A., Felker, F., & Gross, R. A. (2000). Distribution of octenyl succinate groups in octenyl succinic anhydride modified waxy maize starch. *Starch - Stärke*, *52*(6–7), 196–204.
- Stounbjerg, L., Vestergaard, C., Andreasen, B., & Ipsen, R. (2018). Beverage clouding agents: Review of principles and current manufacturing. *Food Reviews International*, *34*(7), 613–638.
- Sun, S., Lin, X., Zhao, B., Wang, B., & Guo, Z. (2020). Structural properties of lotus seed starch prepared by octenyl succinic anhydride esterification assisted by high hydrostatic pressure treatment. *LWT*, *117*, 108698.

- Sweedman, M. C., Tizzotti, M. J., Schäfer, C., & Gilbert, R. G. (2013). Structure and physicochemical properties of octenyl succinic anhydride modified starches: A review. *Carbohydrate Polymers*, 92(1), 905–920.
- Taherian, A. R., Fustier, P., Britten, M., & Ramaswamy, H. S. (2008). Rheology and stability of beverage emulsions in the presence and absence of weighting agents: A review. *Food Biophysics*, 3(3), 279–286.
- Tan, C.-T. Beverage Emulsions. In *Food Emulsions, Fourth.*; Friberg, S.E., Larsson, K., Sjöblom, J., Eds; Marcel Dekker: New York, 2004.
- Tesch, S., Gerhards, C., & Schubert, H. (2002). Stabilization of emulsions by OSA starches. *Journal of Food Engineering*, 54(2), 167–174.
- Trubiano, P. C. (1986). Succinate and substituted succinate derivatives of starch. In *Modified starches: Properties and uses* (pp. 131–147). CRC Press.
- Vilela, A., Cosme, F., & Pinto, T. (2018). Emulsions, foams, and suspensions: The microscience of the beverage industry. *Beverages*, 4(2), 25.
- Viswanathan, A. (1999). Effect of degree of substitution of octenyl succinate starch on the emulsification activity on different oil phases. *Journal of Environmental Polymer Degradation*, 7(4), 191–196.
- Wang, C., He, X., Fu, X., Huang, Q., & Zhang, B. (2016). Substituent distribution changes the pasting and emulsion properties of octenylsuccinate starch. *Carbohydrate Polymers*, 135, 64–71.
- Wang, C., He, X., Fu, X., Luo, F., & Huang, Q. (2015). High-speed shear effect on properties and octenylsuccinic anhydride modification of corn starch. *Food Hydrocolloids*, 44, 32–39.
- Wang, C., He, X., Huang, Q., Fu, X., Luo, F., & Li, L. (2013). Distribution of octenylsuccinic substituents in modified A and B polymorph starch granules. *Journal of Agricultural and Food Chemistry*, 61(51), 12492–12498.
- Wang, Y., Huang, Z., Liu, Z., Luo, S., Liu, C., & Hu, X. (2020). Preparation and characterization of octenyl succinate β -limit dextrin. *Carbohydrate Polymers*, 229, 115527.
- Wetzel, D. L., Shi, Y.-C., & Reffner, J. A. (2010). Synchrotron infrared confocal microspectroscopical detection of heterogeneity within chemically modified single starch granules. *Applied Spectroscopy*, 64(3), 282–285.

- Wetzel, D. L., Shi, Y.-C., & Schmidt, U. (2010). Confocal Raman and AFM imaging of individual granules of octenyl succinate modified and natural waxy maize starch. *Vibrational Spectroscopy*, 53(1), 173–177.
- Williams, P. A., & Phillips, G. O. (2009). 11 - Gum arabic. In G. O. Phillips & P. A. Williams (Eds.), *Handbook of Hydrocolloids (Second Edition)* (pp. 252–273). Woodhead Publishing.
- Wooster, T. J., Golding, M., & Sanguansri, P. (2008). Impact of Oil Type on Nanoemulsion Formation and Ostwald Ripening Stability. *Langmuir*, 24(22), 12758–12765.
- Xu, Y., Huang, Q., Fu, X., & Jane, J. (2015). Modification of starch octenylsuccinate by β -amylase hydrolysis in order to increase its emulsification properties. *Food Hydrocolloids*, 48, 55–61.
- Xu, Y., Wang, C., Fu, X., Huang, Q., & Zhang, B. (2018). Effect of pH and ionic strength on the emulsifying properties of two octenylsuccinate starches in comparison with gum arabic. *Food Hydrocolloids*, 76, 96–102.
- Yang, Y., & McClements, D. J. (2013a). Encapsulation of vitamin E in edible emulsions fabricated using a natural surfactant. *Food Hydrocolloids*, 30(2), 712–720.
- Yang, Y., & McClements, D. J. (2013b). Vitamin E bioaccessibility: Influence of carrier oil type on digestion and release of emulsified α -tocopherol acetate. *Food Chemistry*, 141(1), 473–481.
- Ye, F., Miao, M., Huang, C., Lu, K., Jiang, B., & Zhang, T. (2014). Elucidation of substituted ester group position in octenylsuccinic anhydride modified sugary maize soluble starch. *Journal of Agricultural and Food Chemistry*, 62(48), 11696–11705.
- Yu, Z.-Y., Jiang, S.-W., Zheng, Z., Cao, X.-M., Hou, Z.-G., Xu, J.-J., Wang, H.-L., Jiang, S.-T., & Pan, L.-J. (2019). Preparation and properties of OSA-modified taro starches and their application for stabilizing Pickering emulsions. *International Journal of Biological Macromolecules*, 137, 277–285.
- Zhang, B., Huang, Q., Luo, F., Fu, X., Jiang, H., & Jane, J. (2011). Effects of octenylsuccinylation on the structure and properties of high-amylose maize starch. *Carbohydrate Polymers*, 84(4), 1276–1281.
- Zhang, H., Schäfer, C., Wu, P., Deng, B., Yang, G., Li, E., Gilbert, R. G., & Li, C. (2018). Mechanistic understanding of the relationships between molecular structure and emulsification properties of octenyl succinic anhydride (OSA) modified starches. *Food Hydrocolloids*, 74, 168–175.

- Zhao, Y., Khalid, N., Shu, G., Neves, M. A., Kobayashi, I., & Nakajima, M. (2017). Formulation and characterization of O/W emulsions stabilized using octenyl succinic anhydride modified kudzu starch. *Carbohydrate Polymers*, 176, 91–98.
- Ziani, K., Fang, Y., & McClements, D. J. (2012). Encapsulation of functional lipophilic components in surfactant-based colloidal delivery systems: Vitamin E, vitamin D, and lemon oil. *Food Chemistry*, 134(2), 1106–1112.

Chapter 3 - Distribution of octenylsuccinate substituents within a single granule of modified waxy maize starch determined by Raman microspectroscopy¹

Abstract

Octenylsuccinic anhydride (OSA)-modified starches were prepared in granular form from waxy maize starch at two levels (3% and 9%, based on the weight of starch) of OSA reagent. The distribution of OS groups at five positions within a single starch granule was determined by Raman microspectroscopy. OSA-modified starch had one additional peak at 1670 cm^{-1} , indicative of the carbonyl group in OS group bound to starch molecules. For each Raman spectrum obtained at a given position on a starch granule, the ratio of the band areas of carbonyl (1679 cm^{-1}) to starch (2910 cm^{-1}) was calculated. The highest level of OS groups was found on the granular surface. However, the level of OS groups in the center of granules was also high and nearly equal to that on the surface. The regions between the surface and the hilum of the waxy maize starch granules had reduced OS substitution.

Keywords

Raman microspectroscopy; Waxy maize starch; Octenylsuccinic anhydride

¹This chapter was published in *Carbohydrate Polymers* (2019) 216, 282–286.

Introduction

Octenylsuccinic anhydride (OSA)-modified starches contain both hydrophilic and hydrophobic groups and they are used widely as emulsifiers and stabilizers in foods, pharmaceuticals, and other products (Altuna, Herrera, & Foresti, 2018; Sweedman, Tizzotti, Schärer, & Gilbert, 2013). Octenylsuccinated (OS) starch is commonly prepared by the esterification of granular starch, with OSA aqueous alkaline slurry at or near room temperature (Bai, Kaufman, Wilson, & Shi, 2014; Zhang et al., 2011). The functional properties of OS starch are determined by the structure of substituted starch which can be distinguished at three levels—universal, granular, and molecular (Bai et al., 2014; Huber & BeMiller, 2009; Wang, He, Fu, Huang, & Zhang, 2016).

At the universal level, the overall extent of substitution, or degree of substitution (DS) which represents the average number of modified hydroxyl groups per glucosyl unit, can be determined by titration, high performance liquid chromatography (HPLC) and nuclear magnetic resonance (NMR) spectroscopy (Bai & Shi, 2011; Bai, Shi, Herrera, & Prakash, 2011; Qiu, Bai, & Shi, 2012; Sweedman et al., 2013). At the molecular level, OS substitution, up to DS ~ 0.06, was found to occur mainly at the O-2 and O-3 positions of the anhydroglucose units (AGUs) in OSA-modified maize granular starch (Bai & Shi, 2011; Bai et al., 2011). Most OS groups were located near the branch points of amylopectin at the low DS of 0.018 (Bai et al., 2014), whereas at the higher DS of 0.92, OS groups were located near both the branch points and on or near the non-reducing ends (Bai et al., 2014).

At the granular level, reaction patterns of modification within a granule have been examined by light microscopy, confocal laser scanning microscopy (CLSM), scanning electron

microscopy (SEM), and transmission electron microscopy (TEM) (Huber and BeMiller, 2009). After reacting with 3 wt% (starch basis) OSA, the x-ray diffraction pattern of a starch is generally not changed, indicating that OS substitution occurs primarily in the amorphous regions of granules (Bai & Shi, 2011; Liu, Li, Goff, Nsor-Atindana, & Zhong, 2018; Shogren, Viswanathan, Felker, & Gross, 2000). When examined by backscattered-electron imaging of osmium-stained OSA modified waxy maize starch granules (Shogren et al., 2000), the OS groups appeared to be dispersed throughout the granules. However, x-ray photoelectron spectroscopy suggested that the surface concentration of OS was higher than that of the bulk (Huang et al., 2010; Shogren et al., 2000). CLSM results also indicated that the surface of granules has more OS groups than the interior (Chen, He, & Huang, 2014; Wang et al., 2013; Ye et al., 2014; Zhang et al., 2011). Using CLSM to study the effects of high-speed shear during the OSA modification reaction, Wang et al. (2015) reported increasing substitution of OS groups in the inner region of a starch granule, indicating a more even distribution of OS groups in the granules when the OSA reaction is conducted with high speed shear.

Using FT-IR microspectroscopy, Bai et al. (2009) and Wetzel, Shi, & Reffner (2010) investigated the level and uniformity of OS substitution on individual waxy maize starch granules, and reported that OS concentration varied between granules. However, it should be noted that in those FT-IR microspectroscopic studies, individual starch granules were flattened before measurements of FT-IR spectra. A typical maize starch granule is nearly a spherical in shape with a diameter of 10-15 μm , which means it is impossible to analyze a spherical OS-maize starch granule by infrared spectroscopy in a transmission (or absorption-reflection) mode due to the thickness of the whole granule and a loss of signal caused by the spherical lensing effect (Wetzel, Shi, & Schmidt, 2010). Therefore, Wetzel, Shi, & Schmidt (2010) first used

confocal Raman microspectroscopy to provide greater spatial resolution and analyze OS distribution on whole unflattened granules. There is another advantage of determining OS substitution patterns by Raman as opposed to infrared spectroscopy. In contrast to IR spectroscopy, which is sensitive to polar bonds, especially OH stretching in water, Raman spectroscopy is insensitive to OH-bonds, but instead is sensitive to non-polar bonds such as C-C or C-H. As a result, Raman spectroscopy eliminates the interference of moisture in starch (Wellner, 2013). Liu et al. (2018), using confocal 2D Raman microscopy, reported that OS groups in esterified waxy maize granules are located unevenly throughout the starch granules with an increased intensity in the center.

Although the structure of OSA-modified starch has been examined extensively, little work has been reported on the OS distribution within a single granule. In this study, granular waxy maize starch was reacted conventionally with two levels (3 and 9%, based on the weight of starch) of OSA. We designed experiments to determine the distribution of OS groups among 5 positions on a single granule: the edge-left, area between edge-left and center, center (hilum), area between center and edge-right, and the edge-right (Fig. 3.1).

Small openings or pores on a starch granule surface are connected with channels linking the internal cavity/hilum region of a maize starch granule (Huber & BeMiller, 1997, 2000). Those pores and channels may provide a pathway for OSA reagent to access the interior region of the starch granule (Hsieh, 2013; Huber & BeMiller, 2000, 2001). Knowledge about the distribution of OS substituents within one starch granule would be helpful in understanding the reaction patterns of starch chemical modification, as well as in designing modified starches with improved functional properties.

Materials and Methods

Materials

Waxy maize (AMOICA) starch was obtained from Ingredion Incorporated (Bridgewater, NJ, USA). Octenylsuccinic anhydride (OSA) was obtained from Gulf Bayport Chemicals L.P. (Pasadena, TX, USA). All other chemicals used were analytical grade.

Preparation of OS starches

Waxy maize starch was modified with OSA in aqueous solution as previously described (Bai et al., 2011). Briefly, a starch slurry (250 g) of 40% solids content at 25 °C was adjusted to pH 7.5 by adding 3 wt% sodium hydroxide with stirring. OSA (3% or 9% based on the dry weight of starch) was added dropwise to the starch suspension while maintaining the pH at 7.5. After the pH remained stable for 30 min, the reaction was terminated by adjusting pH to 6.0 with 1.0 M hydrochloric acid. OS starch was recovered by filtration, washed with 300 mL of methanol, and dried at 40 °C in an oven overnight.

Determination of the degree of substitution (DS)

The DS of OS starch was determined by high-performance liquid chromatography (HPLC) as reported by Qiu et al. (2012). Briefly, for free OS determination, 0.5 g (d.w.) of OS starch was stirred in 5 mL of methanol for 1 h. After centrifuge, the solution of supernatant (1 mL) and water (pH = 3) (1 mL) was analyzed by HPLC. To determine total OS, 0.5 g (d.w.) of OS starch was stirred overnight in 10 mL of 4N NaOH. The alkali solution (2 mL) was neutralized with 10 mL of 1N HCl and filled with acetonitrile to 25 mL volumetric flask. The solution was analyzed by HPLC. A mixture of acetonitrile and water containing 0.1% TFA

(45:55, v/v) was used as the mobile phase. The flow rate was 1.0 ml/min and the detection wavelength was set at 200 nm. Concentrations were determined from the peak area.

Raman microspectroscopy

A DXR™ Raman microscope (Thermo Scientific™, Waltham, MA, USA) was used for all imaging experiments. Each starch sample (~ 5 mg) was spread onto a microslide and covered by a coverslip, and excess starch was blown away. Before Raman analysis, the coverslip was removed. Five positions edge-left, area between edge-left and center, area between center and edge-right, and edge-right, were excited with a 532 nm laser line within a speckle of 7 μm × 7 μm (Fig. 3.1). Ten starch granules of each sample were analyzed one by one at the five positions within a granule. For each Raman spectrum obtained at each position on one granule, the baseline-adjusted band area ratio of carbonyl (1670 cm⁻¹) to starch (2910 cm⁻¹) was determined. The band area ratio was calculated as (band area of octenylsuccinic ester carbonyl group/band area of C-H stretching of carbohydrate) × 100.

Differential scanning calorimetry (DSC)

A differential scanning calorimeter (DSC, Perkin-Elmer, Norwalk, CT, USA) was used to analyze the thermal properties of unmodified waxy maize starch and OS waxy maize starches. The weight ratio of starch to water was 1:2 (Shi, Sweedman, & Shi, 2018). Each sample was scanned from 10 °C to 140 °C at a heating rate of 10 °C/min. An empty pan was used as a reference. The enthalpy change (ΔH), onset (T_o), peak (T_p), and conclusion (T_c) temperatures of starch gelatinization were calculated using Pyris software (Perkin Elmer, Norwalk, CT, USA).

X-ray diffraction (XRD)

X-ray diffraction patterns of unmodified and OS waxy maize starches were performed as previously described (Shi et al., 2018). Starch crystallinity was calculated as the ratio of the peak areas to the total diffractogram area (Komiya & Nara, 2006). The peak areas were calculated by OriginPro (version 8.5).

Light microscopy

The morphology of unmodified and OS waxy maize starches was observed by an Olympus BX-51 optical light microscope with a digital camera (Tokyo, Japan) under illumination by normal visible and polarized light. Starch granules (10 mg) were mixed with 1 mL of a mixture of glycerol: water (1:1, w/w) at 25 °C, and one drop of the starch suspension was placed on a microscope slide before covering with a coverslip and viewing with a 40x objective lens.

Statistical analysis

Analysis of variance was conducted using a Statistical Analysis System (SAS, version 9.3 for Windows, SAS Institute, Cary, NC, USA). Least significant differences for comparison of means were computed at $p < 0.05$.

Results and discussion

Thermal properties and crystallinity of native and OSA-modified starches

Native waxy maize, and two OSA-modified starches, DS 0.018 and 0.041, were characterized by a sharp endothermic peak at 73.4, 72.2, and 69.9 °C (T_o , T_p , T_c) and enthalpies

of 19.3, 15.1, and 12.4 J/g, respectively (Table 3.1). The XRD diffractograms of those starches are shown in Fig. 3.2. The native and OSA-modified waxy maize starches all displayed the typical A-type pattern with peaks at $2\theta = 15^\circ, 17^\circ, 18^\circ$ and 23° . Unmodified waxy maize starch had 35.8% crystallinity, whereas the OS modified starches with DS 0.018 and 0.041 had decreased crystallinity of 32.7% and 30.3%, respectively. Based on the DSC and XRD results, there was a minor reduction in the crystalline regions at these low levels of OS substitutions, suggesting that OSA reacted preferentially in the amorphous region. However, as DS increased from 0.018 to 0.041, the degree of crystallinity did decline somewhat, indicating that OS substitution slightly weakened the crystalline structure. After OSA modification, starch granules remained and appeared identical to native starch when examined under a microscope using illumination with normal and polarized light (Fig. 3.3). Under polarized light, the OS starch still showed strong birefringence indicating a radial orientation of molecules, the same in the unmodified granules.

Raman spectra of native and OSA-modified waxy maize starches

The five positions that were examined by Raman microspectroscopy on a single granule of native and OSA-modified starches are shown in Fig. 3.1. One Raman image (right edge of granule) and the Raman spectra of that edge for the unmodified and the two modified starches are shown in Fig. 3.4. Among the Raman bands, a strong band at 478 cm^{-1} is attributed to skeletal vibration modes of the pyranose ring (C-O-C). The region between 800 and 1500 cm^{-1} provided highly overlapping and complex spectra which exhibited the motions of C-H deformation (865 cm^{-1}), C-O-H bending (1082 cm^{-1}), C-O stretching and C-O-H deformation (1124 cm^{-1}), CH_2OH deformation ($1260\text{-}1280\text{ cm}^{-1}$), and CH_2 bending (1460 cm^{-1}) in the

starches (Kizil, Irudayaraj, & Seetharaman, 2002). In all the spectra, the Raman band at 940 cm^{-1} is attributed to stretching of the α -1,4-glycosidic linkages in the starches, and the bands between $2800\text{-}3000\text{ cm}^{-1}$ are assigned to C-H stretching in glucose repeat units, which exhibited vibrational modes of starches.

The Raman spectra of samples exhibited almost identical bands, except the band occurring at 1670 cm^{-1} originates from the carbonyl group as evidenced by its appearance in the spectra of the OS-esterified starches (Fig. 3.4) (Wetzel, Shi, & Schmidt, 2010). Compared with the unmodified starch, OSA-modified starch had a new peak at 1670 cm^{-1} . As the DS of OS groups increased, the band area at 1670 cm^{-1} also increased.

Distribution of OS groups within a single starch granule

In this study, 10 random starch granules of each OSA-modified starch with DS of 0.018 and 0.041 were analyzed one by one on five positions within each one granule using the Raman microspectrometer (Fig. 3.4). For each spectrum obtained from individual positions on one whole granule, the carbonyl/carbohydrate band area ratio at each position was calculated (Table 3.2). Based on those measurements, the distribution of OS groups was not uniform throughout a modified starch granule. In the case of both modified starches, the band area ratio of carbonyl/carbohydrate was reduced at positions 2 and 4 compared to surface positions 1 and 5, and to the center position 3. The level of OS groups on each modified starch was most concentrated at the surface of a granule, and was closely followed by the level at the center (Table 3.2), which included the surface and the internal central cavities/hilum region. The band area ratio at the surface (positions 1 and 5) and at the center (position 3) of starch granules was

higher than the ratio of the regions between the surface and center (positions 2 and 4), even in the low DS (0.018) of OS starch.

Based on our results of band area ratios within one granule by Raman spectroscopy, the OS groups in the OSA-modified granular starch are shown to be preferentially located on its surface as well as on the central cavity/hilum region. Huber & BeMiller (2000) have reported that the penetration of an aqueous solution of merbromin dye into a maize starch granule occurred laterally from channels and from the central cavity (hilum region) outward, rather than from the surface and inward. Hsieh (2013) reached the same conclusion for the fluorescent probe, 5-(4,6-dichlorotriazinyl) aminofluorescein (DTAF), which was observed to react from inner cavities toward the periphery of normal and waxy maize granules. Overall, it seems that OSA droplets could travel through pores and channels into the interior cavity of starch granules where esterification occurs almost as much as on the surface of the waxy maize starch granules. The central hilum region is less ordered and that may explain why it is more reactive than the regions between the surface and the hilum of the waxy maize starch granules.

Conclusions

The relative levels of OS substitution at five positions on a single starch granule were measured for the first time by the ratio of the carbonyl band and the C-H stretching bands of the starch in their Raman spectra. Waxy maize starch modified with 3% and 9% OSA gave modified granules wherein the OS groups were not uniformly distributed within an individual starch granule. The highest level of OS substitution was found on the granular surface. However, the level of OS groups in the center of a modified granule was also high and nearly equal to that on the surface, indicating that the central hilum region of a waxy maize granule was readily

accessible to OSA reagent penetration and reaction. The regions of a waxy maize starch granule between its surface and center had lower OS substitution.

References

- Altuna, L., Herrera, M. L., & Foresti, M. L. (2018). Synthesis and characterization of octenyl succinic anhydride modified starches for food applications. A review of recent literature. *Food Hydrocolloids*, *80*, 97–110.
- Bai, Y., Kaufman, R. C., Wilson, J. D., & Shi, Y.-C. (2014). Position of modifying groups on starch chains of octenylsuccinic anhydride-modified waxy maize starch. *Food Chemistry*, *153*, 193–199.
- Bai, Y., & Shi, Y.-C. (2011). Structure and preparation of octenyl succinic esters of granular starch, microporous starch and soluble maltodextrin. *Carbohydrate Polymers*, *83*(2), 520–527.
- Bai, Y., Shi, Y.-C., Herrera, A., & Prakash, O. (2011). Study of octenyl succinic anhydride-modified waxy maize starch by nuclear magnetic resonance spectroscopy. *Carbohydrate Polymers*, *83*(2), 407–413.
- Bai, Y., Shi, Y.-C., & Wetzel, D. L. (2009). Fourier transform infrared (FT-IR) microspectroscopic census of single starch granules for octenyl succinate ester modification. *Journal of Agricultural and Food Chemistry*, *57*(14), 6443–6448.
- Chen, X., He, X., & Huang, Q. (2014). Effects of hydrothermal pretreatment on subsequent octenylsuccinic anhydride (OSA) modification of cornstarch. *Carbohydrate Polymers*, *101*, 493–498.
- Hsieh, C.-F. (2013). Impact of extent of hydration and granule-associated proteins on granular and molecular reaction patterns of chemically-modified starches (Ph.D.). In *Food Science*. Moscow: University of Idaho.
- Huang, Q., Fu, X., He, X., Luo, F., Yu, S., & Li, L. (2010). The effect of enzymatic pretreatments on subsequent octenyl succinic anhydride modifications of cornstarch. *Food Hydrocolloids*, *24*(1), 60–65.
- Huber, K. C., & BeMiller, J. N. (1997). Visualization of channels and cavities of corn and sorghum starch granules. *Cereal Chemistry*, *74*(5), 537–541.
- Huber, K. C., & BeMiller, J. N. (2000). Channels of maize and sorghum starch granules. *Carbohydrate Polymers*, *41*(3), 269–276.
- Huber, K. C., & BeMiller, J. N. (2001). Location of sites of reaction within starch granules. *Cereal Chemistry*, *78*(2), 173–180.
- Huber, K. C., & BeMiller, J. N. (2009). Modified starch: Chemistry and properties. In A. Bertolini (Ed.), *Starches: Characterization, properties and applications* (pp. 145–203). Boca Raton, FL: CRC Press.

- Kizil, R., Irudayaraj, J., & Seetharaman, K. (2002). Characterization of irradiated starches by using FT-Raman and FTIR spectroscopy. *Journal of Agricultural and Food Chemistry*, *50*(14), 3912–3918.
- Komiya, T., & Nara, S. (2006). Changes in crystallinity and gelatinization phenomena of potato starch by acid treatment. *Starch - Stärke*, *38*(1), 9–13.
- Liu, W., Li, Y., Goff, H. D., Nsor-Atindana, J., & Zhong, F. (2018). Distribution of octenylsuccinic groups in modified waxy maize starch: An analysis at granular level. *Food Hydrocolloids*, *84*, 210–218.
- Qiu, D., Bai, Y., & Shi, Y.-C. (2012). Identification of isomers and determination of octenylsuccinate in modified starch by HPLC and mass spectrometry. *Food Chemistry*, *135*(2), 665–671.
- Shi, J., Sweedman, M. C., & Shi, Y.-C. (2018). Structural changes and digestibility of waxy maize starch debranched by different levels of pullulanase. *Carbohydrate Polymers*, *194*, 350–356.
- Shogren, R. L., Viswanathan, A., Felker, F., & Gross, R. A. (2000). Distribution of octenyl succinate groups in octenyl succinic anhydride modified waxy maize starch. *Starch - Stärke*, *52*(6–7), 196–204.
- Sweedman, M. C., Tizzotti, M. J., Schäfer, C., & Gilbert, R. G. (2013). Structure and physicochemical properties of octenyl succinic anhydride modified starches: A review. *Carbohydrate Polymers*, *92*(1), 905–920.
- Wang, C., He, X., Fu, X., Huang, Q., & Zhang, B. (2016). Substituent distribution changes the pasting and emulsion properties of octenylsuccinate starch. *Carbohydrate Polymers*, *135*, 64–71.
- Wang, C., He, X., Fu, X., Luo, F., & Huang, Q. (2015). High-speed shear effect on properties and octenylsuccinic anhydride modification of corn starch. *Food Hydrocolloids*, *44*, 32–39.
- Wang, C., He, X., Huang, Q., Fu, X., Luo, F., & Li, L. (2013). Distribution of octenylsuccinic substituents in modified A and B polymorph starch granules. *Journal of Agricultural and Food Chemistry*, *61*(51), 12492–12498.
- Wellner, N. (2013). Fourier transform infrared (FTIR) and Raman microscopy: principles and applications to food microstructure. In V.J. Morris & K. Groves (Eds.), *Food microstructures: Microscopy, measurement and modelling* (pp. 163-191). Cambridge: Woodhead Publishing Ltd.

- Wetzel, D. L., Shi, Y.-C., & Reffner, J. A. (2010). Synchrotron infrared confocal microspectroscopical detection of heterogeneity within chemically modified single starch granules. *Applied Spectroscopy*, *64*(3), 282–285.
- Wetzel, D. L., Shi, Y.-C., & Schmidt, U. (2010). Confocal Raman and AFM imaging of individual granules of octenyl succinate modified and natural waxy maize starch. *Vibrational Spectroscopy*, *53*(1), 173–177.
- Ye, F., Miao, M., Huang, C., Lu, K., Jiang, B., & Zhang, T. (2014). Elucidation of substituted ester group position in octenylsuccinic anhydride modified sugary maize soluble starch. *Journal of Agricultural and Food Chemistry*, *62*(48), 11696–11705.
- Zhang, B., Huang, Q., Luo, F., Fu, X., Jiang, H., & Jane, J. (2011). Effects of octenylsuccinylation on the structure and properties of high-amylose maize starch. *Carbohydrate Polymers*, *84*(4), 1276–1281.

Figures



Figure 3.1 Five positions (1, edge-left; 2, area between edge-left and center; 3, center; 4, area between center and edge-right; and 5, edge-right) within one starch granule analyzed by Raman microspectroscopy.

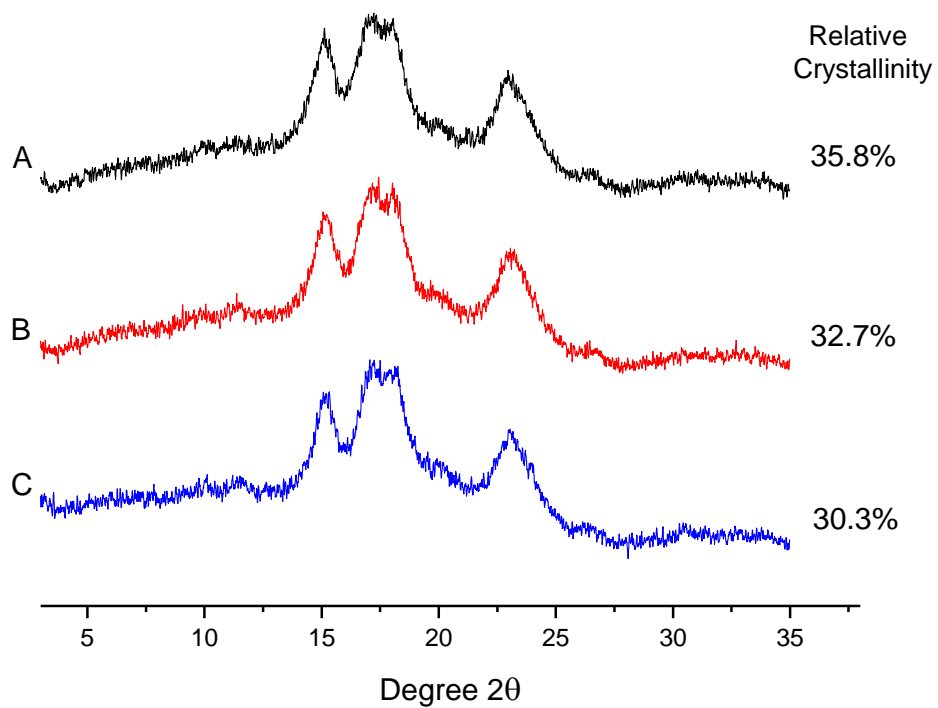


Figure 3.2 X-ray diffraction patterns of unmodified (A), OSA-modified starches with DS of 0.018 (B), and 0.041 (C).

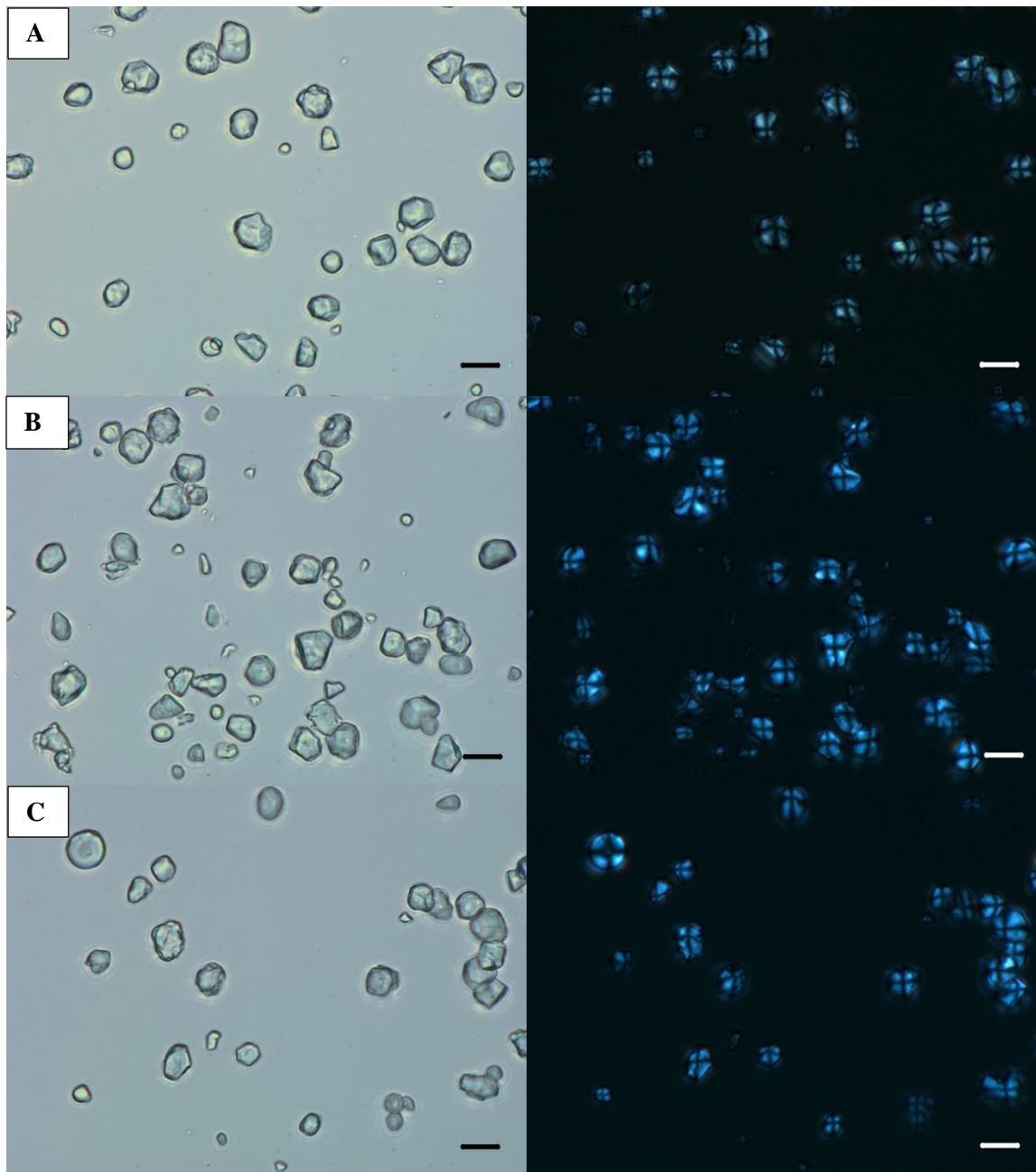


Figure 3.3 Microscopic image of unmodified (A), OSA-modified starches with DS of 0.018 (B), and 0.041 (C). Scale bar in each graph represents 20 μm . Left images: normal visible light; right images: polarized light.

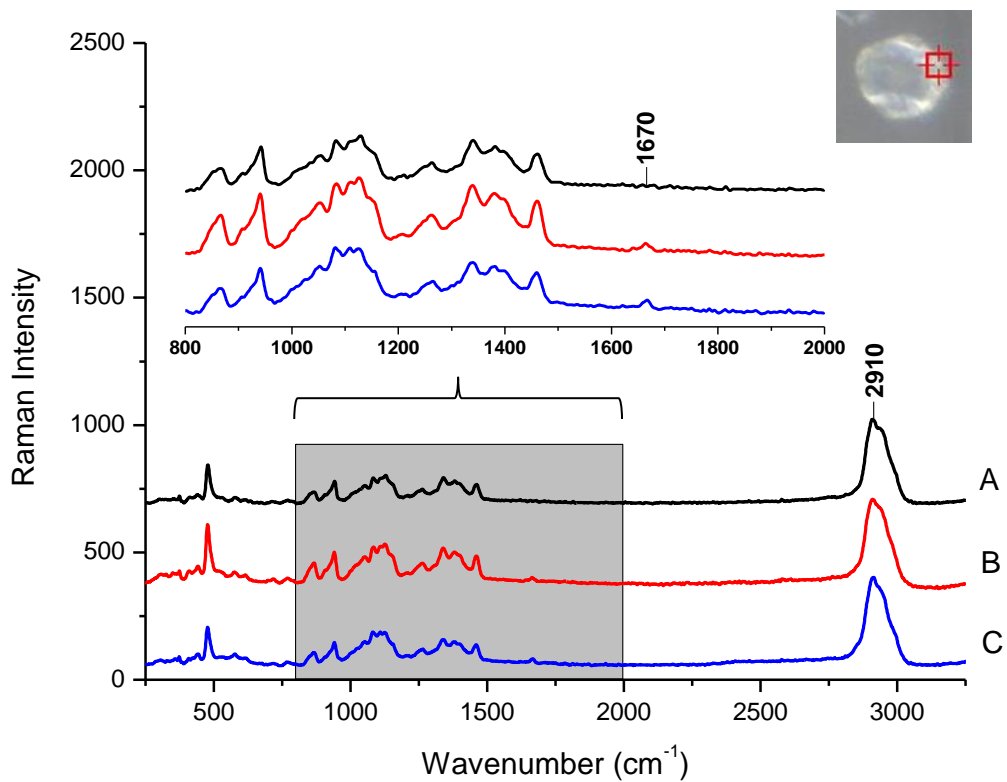


Figure 3.4 Raman image and spectra of the surface (edge-right) of one starch granule. These spectra are from unmodified (A), OSA-modified granules with DS of 0.018 (B), and 0.041 (C).

Tables

Table 3.1 Thermal properties^a determined by differential scanning calorimetry (DSC) on unmodified and OSA-modified waxy maize starches with degrees of substitution (DS) of 0.018 and 0.041

Sample	T_o (°C)	T_p (°C)	T_c (°C)	ΔH (J/g)
Native waxy maize starch	64.2±0.2 a	73.4±0.2 a	95.8±0.1 a	19.3±0.5 a
3% OSA-modified starch	63.5±0.4 a	72.2±0.6 a	96.7±0.7 a	15.1±0.3 b
9% OSA-modified starch	60.5±0.4 b	69.9±0.5 b	95.6±0.6 a	12.4±0.5 c

^a Mean ± standard deviation values are reported. Means in the same column not sharing a common letter are significantly different at $p < 0.05$.

Table 3.2 The band area ratio of an OS group to starch content on five positions within one granule, calculated as (band area at 1670 cm⁻¹ / band area at 2910 cm⁻¹) × 100. Ten starch granules (n=10) of each sample were analyzed by Raman microspectroscopy^a

Samples	Band Area Ratio $_{1670\text{cm}^{-1}} / _{2910\text{cm}^{-1}}$				
	Position 1	Position 2	Position 3	Position 4	Position 5
3% OSA-modified starch	6.42±0.38 a	4.65±0.68 c	5.58±0.32 b	4.19±0.79 c	5.98±0.44 ab
9% OSA-modified starch	9.58±1.61 a	7.95±0.84 bc	8.63±0.97 ab	7.52±1.03 c	8.91±1.13 ab

^a Mean ± standard deviation values are reported. Values followed by the same letter vertically are not significantly different ($p < 0.05$).

Chapter 4 - Distribution of octenylsuccinate substituents in modified waxy and normal potato starches

Abstract

Distribution of octenylsuccinate (OS) substituents in octenylsuccinic anhydride (OSA)-modified normal and waxy potato starches at 3% and 9% (based on the weight of starch) was studied using Raman microspectroscopy, starch gelatinization from granule ghosts (interior removed), and chemical surface gelatinization (surface removed). The distribution of OS groups at five positions for small round-shaped granules and seven positions for large oval-shaped granules within a single starch granule was determined. For each Raman spectrum obtained at a given position on a starch granule, the ratio of the band areas of ester carbonyl (1670 cm^{-1}) to starch (2910 cm^{-1}) was calculated. The OS groups in OSA-modified potato granular starches were shown to be preferentially located on its surface. As the weight of granular core loss in ca. 60%, the OS content of OSA-modified potato starch surface increased 2.5 times over that of the bulk granule. In addition, as the weight of granular surface loss in ca. 30%, the OS content of OSA-modified potato starch was 0.25 times over that of the bulk granule.

Keywords

Raman microspectroscopy; Normal potato starch; Waxy potato starch; Octenylsuccinic anhydride; Starch granule ghosts; Chemical surface gelatinization

Introduction

Octenylsuccinic anhydride (OSA, chemical formula $C_{12}H_{18}O_3$), a cyclic dicarboxylic acid anhydride, has two active carboxyl groups which can react with the hydroxyl groups in polysaccharide under alkaline conditions in aqueous slurry systems (Altuna et al., 2018; Bai & Shi, 2013; Sweedman et al., 2013). The long alkyl chain of octenyl groups in OSA has hydrophobicity, which converts a polysaccharide to amphiphilic molecule (Shogren et al., 2000). In the United States, only OSA among other alkenyl succinic anhydrides is approved for food use with maximum level 3% (w/w) (DS ~ 0.02) by the Food and Drug Administration (FDA) (Bai et al., 2009). OSA-modified starches may be used as emulsifiers, stabilizers and thickening agents in foods (Altuna et al., 2018; Bajaj et al., 2019; Ghazaei et al., 2015).

Potato is an excellent source of starch, which accounts for approximately 15–20% of its weight (Bertoft & Blennow, 2009). Starch granules from various botanical sources differ in shape, size, and morphology. In contrast to maize starch, potato starch granules have no channels with smooth surface (Wang et al., 2010). Singh et al. (2006) have shown the presence of small protuberances and fragmentation on the surface of potato starch granules. The average granule size of potato starch granules ranges from 1 to 20 μm for small spherical granules and 20 to 110 μm for large oval granules (Huber & BeMiller, 2001; Singh et al., 2003). The average length and width of large oval potato starch granules were 56.8 and 35.2 μm , respectively (Kaur et al., 2007). Compared with waxy and normal cereal starches that show an A-type crystalline pattern, potato starch exhibits a B-type X-ray crystalline pattern. Jane (2006) reported that the B-type starches have more clusters and stabilize the internal structures of granules. The A- and B-types are the polymeric forms of starch and they differ in the packing of amylopectin double helices

(Cai & Shi, 2010; Hsieh et al., 2019; Lee et al., 2012; Pérez & Bertoft, 2010). Waxy potato starch, which contains no amylose, has a lower paste viscosity and a higher paste clarity than normal potato starch (Hsieh et al., 2019). Like other starches, potato starch is often modified to improve its functional properties for food and industrial applications (Dupuis & Liu, 2019; Huber & BeMiller, 2001).

In chemically modified starches, the structure of substituted starch is characterized at three levels: universal, granular, and molecular (Huber & BeMiller, 2009). At the granular level, OSA substitution occurs primarily in the amorphous region of normal potato starch granules without change in starch crystallinity with 3% OSA (Wang et al., 2016). The granular surface can react with OSA droplets as well as with dissolved OSA molecules (Shogren et al., 2000). Wang et al. (2013) reported that OSA could only react with the granular surface of normal potato starch due to the lower fluorescence intensity in granular interior using confocal laser scanning microscopy (CLSM). It has been suggested that OSA groups reacted first on the surface of normal potato starch granules and then penetrated to the core of granules, and slight corrosion appeared on the surface with increasing DS (Hui et al., 2009; Wang et al., 2016). The scanning electron microscopy (SEM) results suggested that the morphological structure of normal potato starch granules was not altered during the esterification reaction (Wang et al., 2010).

Although some studies on OSA distribution of normal potato starches have been investigated, no work has been reported on the OS substituent distribution using Raman microspectroscopy on individual granules in waxy potato starch. In our previous study (Sun et al., 2019), we found that the level of OS groups in the center of granules was high in waxy maize starch and nearly equal to that on the surface. However, to our knowledge, no study has been done on distribution of OS groups in a single granule from either waxy or normal potato starch.

In this study, we used Raman microspectroscopy to determine the distribution of OS substituent in a single granule of OSA-modified waxy and normal potato. In addition, two more approaches were used to study the distribution of OS in waxy and normal potato starches: (i) isolation of starch ghost (mostly surface of granules remained) and (ii) surface removal by chemical surface gelatinization (inner portion remained).

Starch ghost is defined as the outmost layer surface (insoluble material) of the starch granules persist in swollen hydrated forms after gelatinization in water (Derek et al., 1992; Han & Hamaker, 2002). The gelatinization process is achieved by heating the starch suspension under gently stirring in excess water by hydration and swelling with loss of birefringence and crystallinity of starch chains (Debet & Gidley, 2007; Gómez-Lurá et al., 2017). After gelatinization, the amorphous and crystalline regions inside the starch granules were broke down. The surface structure of starch ghosts are composed mostly of amylopectin (Feng et al., 2014; Garcia-Hernandez et al., 2017). Zhang et al. (2014) reported that the potato ghost structure contains predominantly entangled amylopectin (and some amylose) molecules with the partially ordered enzyme-resistant fractions from amylopectin for B-type potato starch. Potato ghosts are more fragile and sensitive than maize ghosts due to its negatively charged phosphate monoester groups.

Chemical surface gelatinization of potato starch was first revealed to study the internal structure by Jane and Shen (1993). Aqueous calcium chloride was used to gelatinize starch granules starting at the periphery. In the study of Koch and Jane (2000), they suggested that normal and waxy potato starch surface could be gelatinized evenly by calcium chloride treatments. In addition, they mentioned that waxy potato starch granules were chemically

gelatinized faster than normal potato starch granules. The CaCl_2 solution destroyed the granules through peeling the layer by layer (Huang et al., 2014).

The objectives of this study were to determine the distribution of octenylsuccinate substituents in OSA-modified waxy and normal potato starches at two levels (3% and 9%, based on the weight of starch) using Raman microspectroscopy, starch gelatinization from granule ghosts, and chemical surface gelatinization.

Materials and Methods

Materials

Waxy potato (Eliane 100) starch was obtained from Avebe U.A. (Veendam, the Netherlands). Normal potato (PenCook 10) starch was obtained from Penford Food Ingredients Company (Centennial, Colorado, USA). Waxy maize starch (Amioca) and normal maize starch (Melojel) were obtained from Ingredion Incorporated (Westchester, Illinois, USA). Octenylsuccinic anhydride (OSA) was obtained from Gulf Bayport Chemicals L.P. (Pasadena, TX, USA). All other chemicals used were analytical grade.

Preparation of OS starches

Normal or waxy potato starches were modified with OSA in aqueous slurry as previously described (Bai et al., 2011; Sun et al., 2019). Briefly, a starch slurry (250 g) of 40% starch solids content at 25 °C was adjusted to pH 7.5 by adding 3 wt% sodium hydroxide with stirring. The OSA (3% or 9% based on the dry weight of starch) was added dropwise to the starch suspension while maintaining the pH at 7.5. After the pH remained stable for 30 min, the reaction was

terminated by adjusting pH to 6.0 with 1.0 M hydrochloric acid. OS starch was recovered by filtration, washed with 300 mL of methanol, and dried at 40 °C in an oven overnight.

Raman microspectroscopy

A DXR™ Raman microscope (Thermo Scientific™, Waltham, MA, USA) was used for all imaging experiments. Each starch sample (~ 5 mg) was spread onto a microslide and covered by a coverslip, and excess starch was blown away. Before Raman analysis, the coverslip was removed, and the sample was examined by the Raman microspectroscopy (Sun et al., 2019).

Potato starch contains two types of shapes: round and oval. For round-shaped granules, five positions: edge-left, area between edge-left and center, center, area between center and edge-right, and edge-right, were examined and excited with a 532 nm laser line within a speckle of 7 μm × 7 μm (Fig. 4.1, a1-5). For long flat oval shaped granules, seven positions (edge-left, area between edge-left and center, center, area between center and edge-right, edge-right, top edge, and bottom edge), were examined and excited with 532 nm laser line within 10 μm × 10 μm laser speckle (Fig. 4.1, b1-7). Ten starch granules of each sample were analyzed one by one. For each Raman spectrum obtained at each position on one granule, the baseline-adjusted band area ratio of carbonyl (1670 cm⁻¹) to starch (2910 cm⁻¹) was determined. The band area ratio was calculated as (band area of octenylsuccinic ester carbonyl group /band area of C-H stretching of carbohydrate) × 100.

Preparation of starch granule ghosts

Granule ghosts were prepared according to Zhang et al. (2014). Starch (200 mg) was suspended in 0.3 mL of distilled water and poured into 40 mL of hot water (90 °C). The dilute suspension (0.5% w/v starch) of normal potato starches was kept at 90 °C for 15 min at a low

stirring rate (250 rpm, “low shear cooking”). For waxy potato starches, the starch dilute suspension was kept for 30 s without cap closed using a small magnetic stir bar at 250 rpm. Then, the suspension was cooled and centrifuged (30 °C, 2,000 g for 15 min). The supernatant was discarded, and the spun ghosts were washed twice by resuspension in hot water (70 °C) with gentle manual stirring using a spatula followed by centrifugation. For scanning electron microscopy (SEM), the washed starch ghosts were suspended in ethanol and dried in an oven at 25 °C. Ghost yield was defined as the weight ratio of freeze-dried pellet to initial starch.

For maize starch, starch (200 mg) was suspended in 0.6 mL of distilled water and poured into 40 mL hot water (85 °C) at a low stirring rate (250 rpm, “low shear cooking”). Then, the suspension was cooled and centrifuged (30 °C, 2,000 g for 15 min). The supernatant was discarded, and the spun ghosts were washed twice by resuspension in hot water (75 °C) with gentle manual stirring followed by centrifugation. For scanning electron microscopy (SEM), the washed ghosts were suspended in ethanol and dried in an oven at 30 °C. Ghost yield was defined as the weight ratio of freeze-dried pellet to initial starch.

Preparation of chemical surface gelatinization of OS starch granules

The condition of chemical surface gelatinization of potato starch granules was conducted according to the method by Jane and Shen (1993) with some modifications. Each OS potato starch sample (2.5 g, dry basis) was suspended in 2 mol/L CaCl₂ (17.5 mL) with low speed, magnetic stirring at 21-23 °C for 1h. For OS maize starch, each sample (2 g, dry basis) was suspended in 4 mol/L CaCl₂ (15 mL) with low speed, magnetic stirring at 21-23 °C for 10 min (3 and 9% OSA-modified normal maize), 7min (3% OSA-modified waxy maize) and 14 min (9% OSA-modified waxy maize). The degree of surface gelatinization was monitored by using a

polarized light microscope (Olympus BX-51, Tokyo, Japan). The reaction was stopped by adding chilled water (200 mL, 4 °C). Immediately the mixture was centrifuged at 3000 g (5000 g for maize starch) for 20 min, and the starch was washed with distilled water (200 mL) to remove residual CaCl₂.

The treated starch was then re-suspended in distilled water (300 mL) and blended with a commercial blender (Oster® 14-Speed, blend, Florida, USA) for 10 min to separate the gelatinized starch from the remaining non-gelatinized starch granules. The mixture was then centrifuged at 3000 g for 10 min. The procedure was repeated one more time with distilled water. The remaining non-gelatinized starch granules were washed with ethanol and dried in an oven at 40 °C. The yield of remaining non-gelatinized starch granules was defined as below.

Degree of chemical gelatinization = (1 - the weight of remaining starch granules / the weight of initial starch) × 100

Determination of the degree of substitution (DS)

The DS of OS starch was determined by high-performance liquid chromatography (HPLC) as reported by Qiu et al. (2012) and Sun et al. (2019). Methanol washed OS starch or starch after surface gelatinization and removal (0.5 g each, d.w.) was stirred in 20 mL of 4N NaOH, whereas the starch granule ghost (0.05 g, d.w.) was stirred in 2 mL of 4N NaOH overnight. The alkali solution (2 mL) was neutralized with 10 mL of 1N HCl and diluted to 25 mL in volumetric flask with acetonitrile. The solution was filtered by nylon filter membranes (0.45 µm) and analyzed by HPLC. A mixture of acetonitrile and water containing 0.1% TFA (45:55, v/v) was used as the mobile phase. The flow rate was 1.0 mL/min and the detection wavelength was set at 210 nm. Concentrations were determined from the peak area.

Crystalline structure

X-ray diffraction (XRD) patterns of unmodified and OSA-modified waxy and normal potato starches were performed as previously described (Shi et al., 2018; Sun et al., 2019). Starch crystallinity was calculated as the ratio of the peak areas to the total diffractogram area (Komiya & Nara, 2006). The peak areas were calculated by OriginPro (version 8.5).

Thermal properties of starch

A differential scanning calorimeter (DSC, Q200, TA Instrument, New Castle, DE, USA) was used to analyze the thermal properties of unmodified and OSA-modified waxy and normal potato starches. The weight ratio of starch to water was 1:3 (Shi et al., 2018; Sun et al., 2019). Each sample was heated from 10 °C to 140 °C at a heating rate of 10 °C /min. An empty pan was used as a reference. The enthalpy change (ΔH), onset (T_o), peak (T_p), and conclusion (T_c) temperatures of starch gelatinization were calculated using Pyris software (Perkin Elmer, Norwalk, CT, USA).

Light microscopy

The morphology of unmodified and OSA-modified waxy and normal potato starches was observed by an Olympus BX-51 optical light microscope with a digital camera (Tokyo, Japan) under illumination by normal visible and polarized light viewing with a 40× objective lens (Sun et al., 2019).

Scanning electron microscopy of potato starches and granule ghosts

The morphology of potato starches, granule ghosts and starches after surface gelatinization and removal were coated with gold-palladium using a sputter coater (Denton

Vacuum, LLC, Moorestown, NJ) and examined by scanning electron microscopy (SEM, S3500N, Hitachi Science Systems, Ltd., Japan) under an accelerating voltage of 10 kV and 1000× or 450× magnification.

Statistical analysis

Analysis of variance was conducted using a Statistical Analysis System (SAS, version 9.3 for Windows, SAS Institute, Cary, NC, USA). Least significant differences for comparison of means were computed at $p < 0.05$.

Results and discussion

Properties of OSA-modified potato starches

X-ray diffraction (XRD) results showed that both native normal and waxy potato starches gave a B-type crystalline pattern with strong diffractions of peaks identified at 2θ values of 5.6° , 14.5° , 17.1° , 19.3° , 22.3° and 24.2° (Fig. 4.2) (Bajaj et al., 2018; Cai & Shi, 2010; Hsieh et al., 2019; Lee et al., 2012; McPherson & Jane, 1999), and OSA-modified normal starches (DS=0.0167, 0.0400) and waxy potato starches (DS=0.0174, and 0.0383) all displayed the same pattern. Unmodified potato normal starches had 38.3% crystallinity, whereas the OS modified starches with DS 0.0167 and 0.0400 had decreased crystallinity of 34.6% and 32.0%, respectively. For waxy potato starches, OS modified starches with DS 0.0174 and 0.0383 had decreased crystallinity of 33.9% and 29.5%, respectively compared with unmodified waxy starch (40.5%). These results suggested that esterification did not change the crystalline pattern of OSA potato starches up to DS 0.04, whereas degree of crystallinity did decline as DS increased,

indicating that OS substitution occurred primarily in the amorphous regions of granules (Bai & Shi, 2013) but OS substitution slightly weakened the crystalline structure.

The results of the thermal properties of native and OSA-modified potato starches examined by DSC are presented in Table 4.1. The unmodified waxy potato starches exhibit higher gelatinization temperatures (62.7 °C) and enthalpies (21.4 J/g) than the normal potato starch (56.7 °C and 19.8 J/g, respectively). The OSA-modified potato starches have lower T_o , T_p , and enthalpies than the native starch. With the higher degrees of substitution showed lower gelatinization temperatures. This observation can be explained as a weakening of internal hydrogen bonding by the alkenyl groups, accelerating starch swelling at relatively low temperatures and hence gradually decreasing the enthalpy of all the OSA starches with increased DS, especially affected distinctly on waxy potato starch by esterification (Bao et al., 2003). Compared with unmodified and OSA-modified maize starches, the potato starch (B-type starches) exhibits a lower gelatinization temperature than the maize starch (A-type starches) (Sun et al., 2019). The effect could be explained that potato starch has phosphate-monoester derivatives (0.09%) carrying negative charges. The negative charges of the phosphate groups repel one another and destabilize the double-helical structure of starch (Ai & Jane, 2015; Singh et al., 2006).

The polarized light micrographs of native and OSA-modified potato starches on normal and waxy are shown in Fig. 4.3. All potato starch granules are roughly spherical and oval in shapes and display a wide size distribution (most in the range of 15–80 μm). The unmodified and OSA-modified starch granules all displayed Maltese cross centered at the hilum (strong birefringence), suggesting that the granular structure of OSA potato starches was preserved, even their edges lost some definition. The morphology of the potato starches was also investigated by

SEM (Fig. 4.4). The surfaces of the granules from unmodified starches showed round or oval shapes without fissures and cavities when viewed under a scanning electron microscope at $1000\times$ (Fig. 4.4 NP and WP). SEM results showed that the OSA treatment caused some changes in the structure of starch granules compared with those of native starch. When DS increased, OSA starch granules exhibited slightly rough surfaces, which indicated that OSA modification in aqueous slurry systems moderately altered the granular structure of potato starch.

OS substituent distribution in a single starch granule determined by Raman microspectrometry

Based on the results of light microscopy (Fig. 4.3) and SEM (Fig. 4.4), potato starch contains two types of shapes: round and oval. For round-shaped granules, five positions on a single granule of native and OSA-modified normal and waxy starches were examined by Raman microspectrometry. For long flat oval shaped granules, seven positions were examined (Fig. 4.1). One Raman image (b1, left edge of granule) and the Raman spectra of that edge for the unmodified and the two OSA-modified starches (DS of 0.0174 and 0.0400) are shown in Fig. 4.5. The formation of carbonyl groups from esterification of carbonyl groups of OSA with hydroxyl groups in the starch molecules was confirmed by Raman microspectrometer (Sun et al., 2019; Wetzel et al., 2010). The Raman spectra of unmodified and OSA-modified starches showed that these have similar profiles, except the spectrum of OSA potato starches shows a new peak at 1670 cm^{-1} , which suggests the formation of ester carbonyl groups (Sun et al., 2019). As the DS of OS groups increased, the band area at 1670 cm^{-1} also increased. Compared with the Raman spectra of waxy maize starches in Sun et al. (2019), the same pattern showed between maize and potato starches, except the potato starches had a higher intensity of peak at 865 cm^{-1}

than maize starches, indicating more C-H deformation due to negatively charged phosphate ester groups in potato starch.

For each spectrum obtained from individual positions on one whole granule, the carbonyl/carbohydrate band area ratio at each position was calculated (Table 4.2). The distribution of OS groups was not uniform throughout a modified starch granule. In the case of all round-shaped starch granules, the band area ratios of carbonyl/carbohydrate at position a1 and a5 were much higher than those at position a2-a4 (Fig. 4.1). On the oval-shaped granules, the ratios of the surface positions (b1, b5, b6, and b7) were also higher than those of internal positions on a single starch granule (b2-b4). The level of OS groups on each modified starch was most concentrated at the surface of a granule. With DS increased, the band area ratios increased as well (Table 4.2). Based on our results of band area ratios within one granule by Raman spectroscopy, the OS groups in the OSA-modified potato granular starch are shown to be preferentially located on its surface. This observation agreed with the findings of Wang et al. (2013) that OSA could react with the granular surface of potato starch due to the lower fluorescence intensity in granular interior using confocal laser scanning microscopy (CLSM).

OS substituent distribution in the starch revealed by granule ghosts

In this study, fresh granule ghosts from unmodified and OSA-modified normal and waxy potato starches were isolated following the method reported by Zhang et al. (2014) with some modification. After precipitated with ethanol and dried, ghosts were examined by SEM (Fig. 4.6). Walls of the ghosts did not show much deterioration or collapse. A well-defined outer surface was formed on most granule ghosts in each sample, but some ghosts from OSA-modified potato starches showed a spongier and puckered appearance probably due to the thinner wall

formed from swollen/expanded hollow granules, especially for waxy type. Also, ethanol precipitation can reduce the roughness of surfaces of ghosts.

The OS content of granule ghosts (starch surface) was determined by HPLC (Table 4.3). Normal potato starch reacted with 3% OSA had a DS of 0.0167, whereas the ghost (yield = 39.2% of starch, d.w.) had a DS of 0.0420 (Table 4.3), indicating the ghost had about 2.5 times of OS groups ($0.0420/0.0167 = 2.51$). Normal potato starch reacted with 9% OSA had a DS of 0.0400, whereas the ghost (yield = 43.3% of starch, d.w.) had a DS of 0.0924 (Table 4.3), indicating the ghost had about 2.3 times of OS groups ($0.0924/0.0400 = 2.31$). According to the same calculation, the ghost (yield = 37.5%) from waxy potato starch reacted with 3% OSA had about 2.7 times of OS groups, and the ghost (yield = 41.6%) from waxy potato starch reacted with 9% OSA had about 2.4 times of OS groups (Table 4.3). As the weight of granular core loss in ca. 60%, the OS content of OSA-modified potato starch surface increased by a factor of 2.5 times over that of the bulk granule (Fig. 4.7), indicating that OS groups mainly concentrated on the surface area of potato starch granule.

Compared with maize starch, the ghost of waxy and normal maize starch reacted with 3% OSA (yield = 82.8% and 81.3% of starch, respectively) had about 1.2 times of OS groups on bulk granules. Similarly, the starch ghost of waxy and normal maize starch reacted with 9% OSA (yield = 88.4% and 89.1% of starch, respectively) had 1.1 times of OS groups on bulk granules (Table 4.3).

OS substituent distribution in the starch revealed by chemical surface

gelatinization

The morphology of partially surface gelatinized starch granules (Fig. 4.8, A) and the remaining granules (Fig. 4.8, B) obtained after treatment with CaCl_2 solution was also investigated by SEM. The OSA-modified normal and waxy potato starch surfaces were gelatinized evenly by CaCl_2 treatments (Fig. 4.8, A). A gradual development of a layer structure at the periphery of the granule appeared. The gelatinized layer on the potato starch looked like a ring around a circle (Fig. 4.8, A). Scanning electron micrographs of these remaining granules showed relatively rough surfaces (Fig. 4.8, B), compared with smooth granules without treatment of CaCl_2 (Fig. 4.4). The granule surfaces were rather evenly eroded and some holes were visible on some salt-treated unmodified and OSA-modified potato starch granules.

The OS content of remaining granule and the amount remained from the original non-gelatinized starches were determined in Table 4.3. Inner portion of the waxy and normal potato starch granules had a much lower DS. Normal potato starch reacted with 3% OSA had a DS of 0.0167, whereas the remaining granules (yield = 82.3% of starch, d.w.) after chemical surface gelatinization had a DS of 0.0079 (Table 4.3), indicating the remaining granules had about 0.47 times of initial OS groups ($0.0079/0.0167 = 0.47$). Normal potato starch reacted with 9% OSA had a DS of 0.0400, whereas the remaining granules after chemical surface gelatinization (yield = 70.7% of starch, d.w.) had a DS of 0.0109 (Table 4.3), indicating the remaining granules had about 0.27 times of initial OS groups ($0.0109/0.0400 = 0.27$). Similarly, the OS content of the remaining granules from 3% OSA-modified waxy potato starch (yield = 78.8%) with a DS of 0.0076 had about 0.44 times of OS groups, and the OS content of the remaining granules form

9% OSA-modified waxy potato starch (yield = 65.7%) with a DS of 0.0086 had about 0.22 times of OS groups (Table 4.3). To sum up, as the surface amount removed by ca. 20%, the OS content of OSA-modified potato starch was ca. 0.45 times over that of the bulk granule; as the surface amount removed by ca. 32%, the OS content of OSA-modified potato starch was ca. 0.25 times over that of the bulk granule (Fig. 4.6). This is also mainly attributed to the fact agreed with the findings of OS substituent distribution in the starch revealed by granule ghosts, indicating that the OS substituent was predominately distributed on the surface of potato starch.

For maize starch, the OS content of the remaining granules from 3% OSA-modified normal maize starch (yield = 80.0%) had about 0.75 times of OS groups, and the OS content of the remaining granules from 9% OSA-modified normal maize starch (yield = 56.2%) had about 0.45 times of OS groups. The OS content of the remaining granules from 3% OSA-modified waxy maize starch (yield = 51.5%) had about 0.47 times of OS groups, and the OS content of the remaining granules from 9% OSA-modified waxy maize starch (yield = 27.6%) had about 0.32 times of OS groups (Table 4.3).

Since the yield of the remaining granules was around 80%, 3% OSA-modified normal potato and maize starches were compared. The OS contents of the remaining granules were 0.47 and 0.75 times of initial OS groups, respectively, indicating that more OS substituent was distributed on potato starch; whereas more OS substituent was located in the remaining granules (interior) of maize starch.

Conclusions

To observe reaction patterns within an individual OSA-modified potato starch granule, the ratio of the carbonyl band and the C-H stretching bands of the starch was determined by

Raman microspectroscopy. The highest level of OS substitution was found on the potato granular surface. Potato starch granules do not possess channels. OSA reagent reacts with starch at the periphery first. Waxy and normal potato starch ghost (after 37.5% and 39.2% starch remained) had about 2.5 and 2.7 times of DS compared with 3% OSA modified starches. After chemical surface gelatinization, inner portion of the waxy and normal potato starch granules had a lower DS. The OS content of OSA-modified potato starch was ca. 0.45 times over that of the bulk granule after interior granule remained in 80%; the OS content of OSA-modified potato starch was ca. 0.25 times over that of the bulk granule after interior granule remained in 70%.

Both of those results showed that a greater proportion of the OS groups were distributed at the periphery than at the core of the granules, which is consistent with the result from Raman microspectroscopy. The OS groups in OSA-modified potato granular starches were shown to be preferentially located on its surface, which was different with the results of maize starches which OS substituent was distributed on both the surface and center.

References

- Ai, Y., & Jane, J. (2015). Gelatinization and rheological properties of starch. *Starch - Stärke*, 67(3–4), 213–224.
- Altuna, L., Herrera, M. L., & Foresti, M. L. (2018). Synthesis and characterization of octenyl succinic anhydride modified starches for food applications. A review of recent literature. *Food Hydrocolloids*, 80, 97–110.
- Bai, Y., & Shi, Y.-C. (2013). Reaction of octenylsuccinic anhydride with a mixture of granular starch and soluble maltodextrin. *Carbohydrate Polymers*, 98(2), 1599–1602.
- Bai, Y., Shi, Y.-C., Herrera, A., & Prakash, O. (2011). Study of octenyl succinic anhydride-modified waxy maize starch by nuclear magnetic resonance spectroscopy. *Carbohydrate Polymers*, 83(2), 407–413.
- Bai, Y., Shi, Y.-C., & Wetzel, D. L. (2009). Fourier transform infrared (FT-IR) microspectroscopic census of single starch granules for octenyl succinate ester modification. *Journal of Agricultural and Food Chemistry*, 57(14), 6443–6448.
- Bajaj, R., Singh, N., & Kaur, A. (2019). Properties of octenyl succinic anhydride (OSA) modified starches and their application in low fat mayonnaise. *International Journal of Biological Macromolecules*, 131, 147–157.
- Bajaj, R., Singh, N., Kaur, A., & Inouchi, N. (2018). Structural, morphological, functional and digestibility properties of starches from cereals, tubers and legumes: a comparative study. *Journal of Food Science and Technology*, 55(9), 3799–3808.
- Bao, J., Xing, J., Phillips, D. L., & Corke, H. (2003). Physical properties of octenyl succinic anhydride modified rice, wheat, and potato starches. *Journal of Agricultural and Food Chemistry*, 51(8), 2283–2287.
- Bertoft, E., & Blennow, A. (2009). Chapter 4 - Structure of Potato Starch. In J. Singh & L. Kaur (Eds.), *Advances in Potato Chemistry and Technology* (pp. 83–98). Academic Press.
- Cai, L., & Shi, Y.-C. (2010). Structure and digestibility of crystalline short-chain amylose from debranched waxy wheat, waxy maize, and waxy potato starches. *Carbohydrate Polymers*, 79(4), 1117–1123.
- Debet, M. R., & Gidley, M. J. (2007). Why Do Gelatinized Starch Granules Not Dissolve Completely? Roles for Amylose, Protein, and Lipid in Granule “Ghost” Integrity. *Journal of Agricultural and Food Chemistry*, 55(12), 4752–4760.
- Derek, R., Prentice, M., Stark, J. R., & Gidley, M. J. (1992). Granule residues and “ghosts” remaining after heating A-type barley-starch granules in water. *Carbohydrate Research*, 227, 121–130.

- Dupuis, J. H., & Liu, Q. (2019). Potato starch: a review of physicochemical, functional and nutritional properties. *American Journal of Potato Research*, 96(2), 127–138.
- Feng, T., Su, Q., Zhuang, H., Ye, R., Gu, Z., & Jin, Z. (2014). Ghost structures, pasting, rheological and textural properties between *Mesona Blumes* gum and various starches. *Journal of Food Quality*, 37(2), 73–82.
- Garcia-Hernandez, A., Vernon-Carter, E. J., & Alvarez-Ramirez, J. (2017). Impact of ghosts on the mechanical, optical, and barrier properties of corn starch films: Impact of ghosts on properties of corn starch films. *Starch - Stärke*, 69(1–2), 1600308.
- Ghazaei, S., Mizani, M., Piravi-Vanak, Z., & Alimi, M. (2015). Particle size and cholesterol content of a mayonnaise formulated by OSA-modified potato starch. *Food Science and Technology (Campinas)*, 35(1), 150–156.
- Gómez-Lur á, D., Vernon-Carter, E. J., & Alvarez-Ramirez, J. (2017). Films from corn, wheat, and rice starch ghost phase fractions display overall superior performance than whole starch films: Starch ghosts films performance. *Starch - Stärke*, 69(11–12), 1700059.
- Han, X.-Z., & Hamaker, B. R. (2002). Association of starch granule proteins with starch ghosts and remnants revealed by confocal laser scanning microscopy. *Cereal Chemistry Journal*, 79(6), 892–896.
- Hsieh, C.-F., Liu, W., Whaley, J. K., & Shi, Y.-C. (2019). Structure and functional properties of waxy starches. *Food Hydrocolloids*, 94, 238–254.
- Huang, J., Chen, Z., Xu, Y., Li, H., Liu, S., Yang, D., & Schols, H. A. (2014). Comparison of waxy and normal potato starch remaining granules after chemical surface gelatinization: Pasting behavior and surface morphology. *Carbohydrate Polymers*, 102, 1001–1007.
- Huber, K. C., & BeMiller, J. N. (2001). Location of Sites of Reaction Within Starch Granules. *Cereal Chemistry*, 78(2), 173–180.
- Hui, R., Chen, Q., Fu, M., Xu, Q., & He, G. (2009). Preparation and properties of octenyl succinic anhydride modified potato starch. *Food Chemistry*, 114(1), 81–86.
- Jane, J. (2006). Current understanding on starch granule structures. *Journal of Applied Glycoscience*, 53(3), 205–213.
- Jane, J., & Shen, J. J. (1993). Internal structure of the potato starch granule revealed by chemical gelatinization. *Carbohydrate Research*, 247, 279–290.
- Kaur, L., Singh, J., McCarthy, O. J., & Singh, H. (2007). Physico-chemical, rheological and structural properties of fractionated potato starches. *Journal of Food Engineering*, 82(3), 383–394.

- Koch, K., & Jane, J.-L. (2000). Morphological changes of granules of different starches by surface gelatinization with calcium chloride. *Cereal Chemistry*, 77(2), 115–120.
- Komiya, T., & Nara, S. (2006). Changes in crystallinity and gelatinization phenomena of potato starch by acid treatment. *Starch - Stärke*, 38(1), 9–13.
- Lee, C. J., Kim, Y., Choi, S. J., & Moon, T. W. (2012). Slowly digestible starch from heat-moisture treated waxy potato starch: Preparation, structural characteristics, and glucose response in mice. *Food Chemistry*, 133(4), 1222–1229.
- McPherson, A. E., & Jane, J. (1999). Comparison of waxy potato with other root and tuber starches. *Carbohydrate Polymers*, 40(1), 57–70.
- Pérez, S., & Bertoft, E. (2010). The molecular structures of starch components and their contribution to the architecture of starch granules: A comprehensive review. *Starch - Stärke*, 62(8), 389–420.
- Qiu, D., Bai, Y., & Shi, Y.-C. (2012). Identification of isomers and determination of octenylsuccinate in modified starch by HPLC and mass spectrometry. *Food Chemistry*, 135(2), 665–671.
- Shi, J., Sweedman, M. C., & Shi, Y.-C. (2018). Structural changes and digestibility of waxy maize starch debranched by different levels of pullulanase. *Carbohydrate Polymers*, 194, 350–356.
- Shogren, R. L., Viswanathan, A., Felker, F., & Gross, R. A. (2000). Distribution of Octenyl Succinate Groups in Octenyl Succinic Anhydride Modified Waxy Maize Starch. *Starch - Stärke*, 52(6–7), 196–204.
- Singh, J., McCarthy, O. J., & Singh, H. (2006). Physico-chemical and morphological characteristics of New Zealand Taewa (Maori potato) starches. *Carbohydrate Polymers*, 64(4), 569–581.
- Singh, N., Singh, J., Kaur, L., Singh Sodhi, N., & Singh Gill, B. (2003). Morphological, thermal and rheological properties of starches from different botanical sources. *Food Chemistry*, 81(2), 219–231.
- Sun, Z., Chen, Z., Xu, B., & Shi, Y.-C. (2019). Distribution of octenylsuccinate substituents within a single granule of modified waxy maize starch determined by Raman microspectroscopy. *Carbohydrate Polymers*, 216, 282–286.
- Sweedman, M. C., Tizzotti, M. J., Schäfer, C., & Gilbert, R. G. (2013). Structure and physicochemical properties of octenyl succinic anhydride modified starches: A review. *Carbohydrate Polymers*, 92(1), 905–920.

- Wang, C., He, X., Huang, Q., Fu, X., Luo, F., & Li, L. (2013). Distribution of Octenylsuccinic Substituents in Modified A and B Polymorph Starch Granules. *Journal of Agricultural and Food Chemistry*, *61*(51), 12492–12498.
- Wang, C., Tang, C.-H., Fu, X., Huang, Q., & Zhang, B. (2016). Granular size of potato starch affects structural properties, octenylsuccinic anhydride modification and flowability. *Food Chemistry*, *212*, 453–459.
- Wang, J., Su, L., & Wang, S. (2010). Physicochemical properties of octenyl succinic anhydride-modified potato starch with different degrees of substitution. *Journal of the Science of Food and Agriculture*, *90*(3), 424–429.
- Wetzel, D. L., Shi, Y.-C., & Schmidt, U. (2010). Confocal Raman and AFM imaging of individual granules of octenyl succinate modified and natural waxy maize starch. *Vibrational Spectroscopy*, *53*(1), 173–177.
- Zhang, B., Dhital, S., Flanagan, B. M., & Gidley, M. J. (2014). Mechanism for starch granule ghost formation deduced from structural and enzyme digestion properties. *Journal of Agricultural and Food Chemistry*, *62*(3), 760–771.

Figures

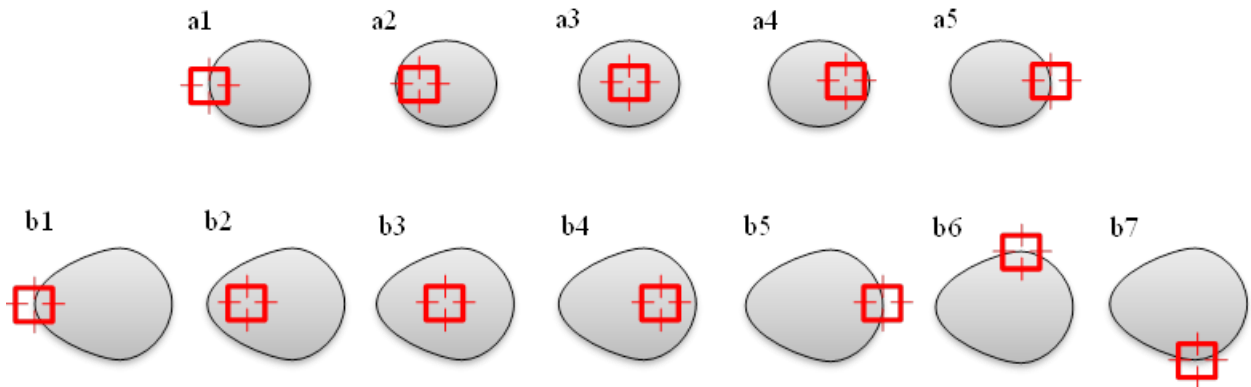


Figure 4.1 Five positions (a1, edge-left; a2, area between edge-left and center; a3, center; a4, area between center and edge-right; and a5, edge-right) within a speckle of $7\ \mu\text{m} \times 7\ \mu\text{m}$ on one round-shaped potato starch granule, and seven positions (b1, edge-left; b2, area between edge-left and center; b3, center; b4, area between center and edge-right; b5, edge-right; b6, top edge; and b7, bottom edge) within a speckle of $10\ \mu\text{m} \times 10\ \mu\text{m}$ on one long flat oval-shaped potato starch granule analyzed both by Raman microspectroscopy.

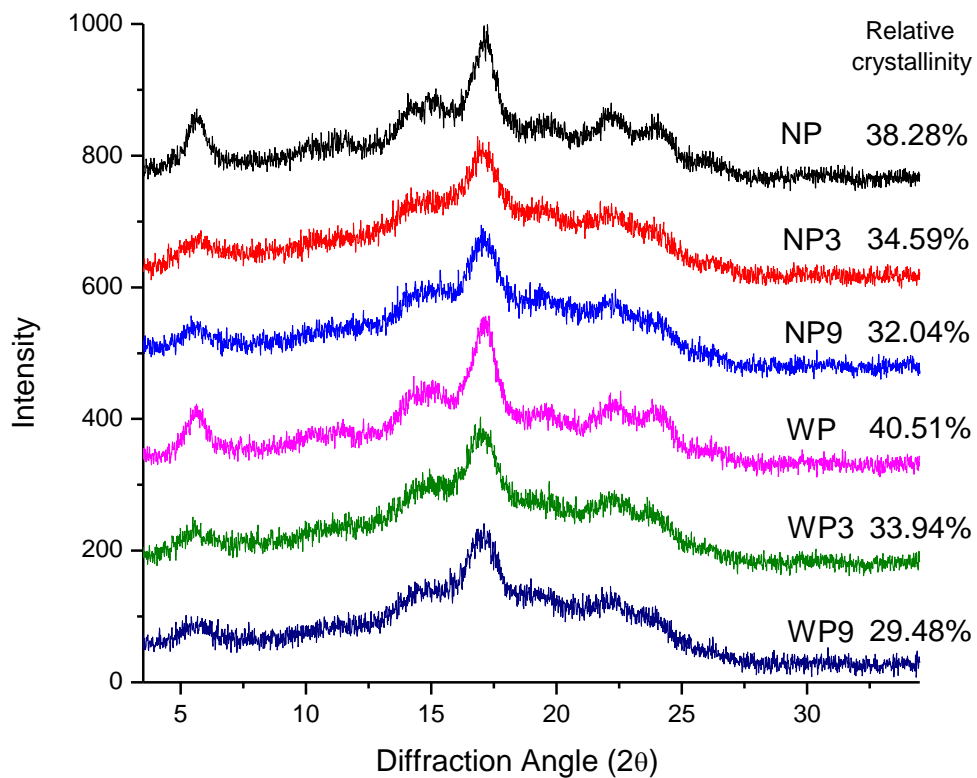
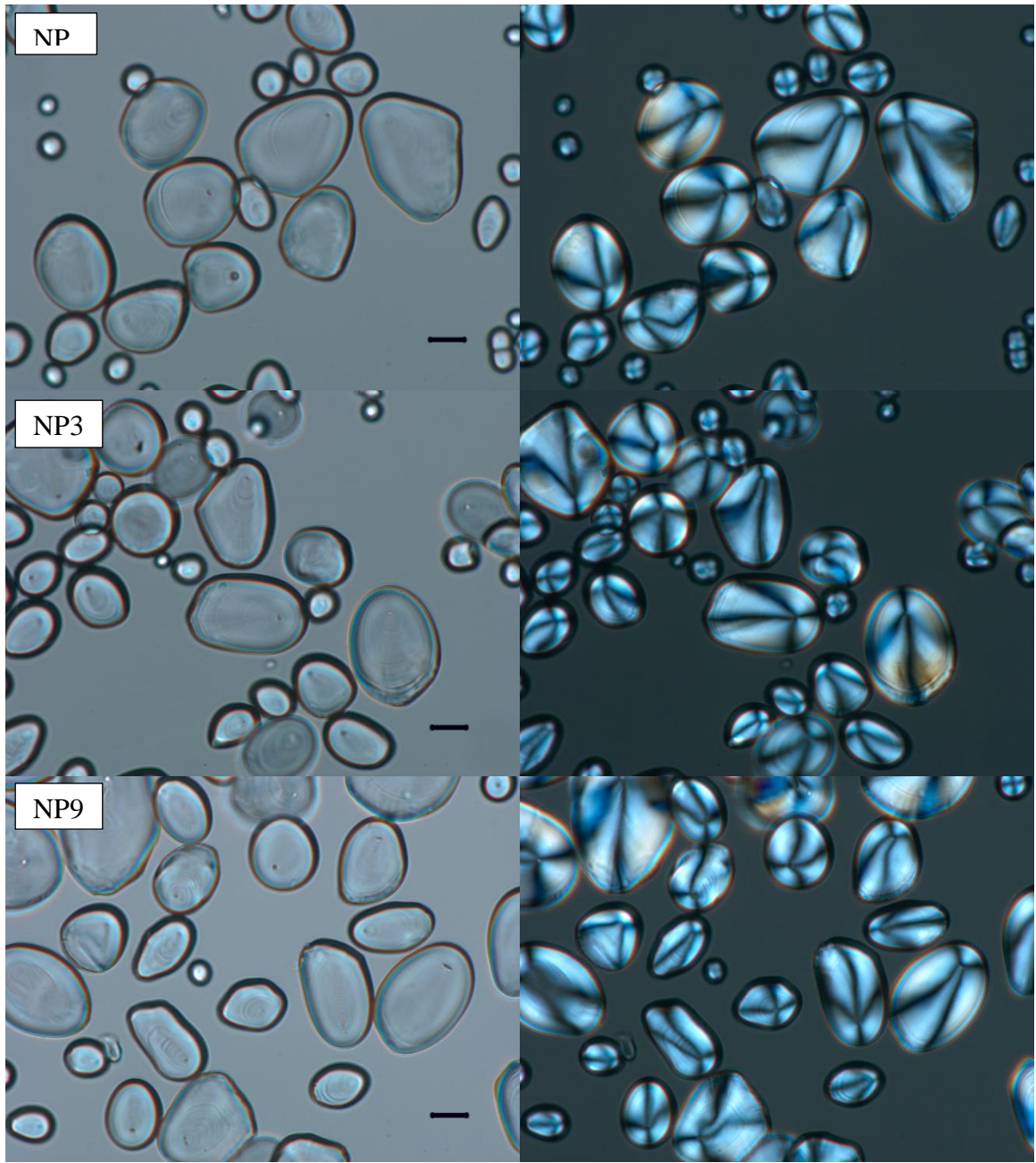


Figure 4.2 X-ray diffraction patterns of potato starches: unmodified normal (NP), octenylsuccinic anhydride (OSA)-modified waxy starches with degree of substitution (DS) of 0.0167(NP3), and 0.0400 (NP9); unmodified waxy (WP), OSA-modified normal starches with DS of 0.0174 (WP3), and 0.0383 (WP9).



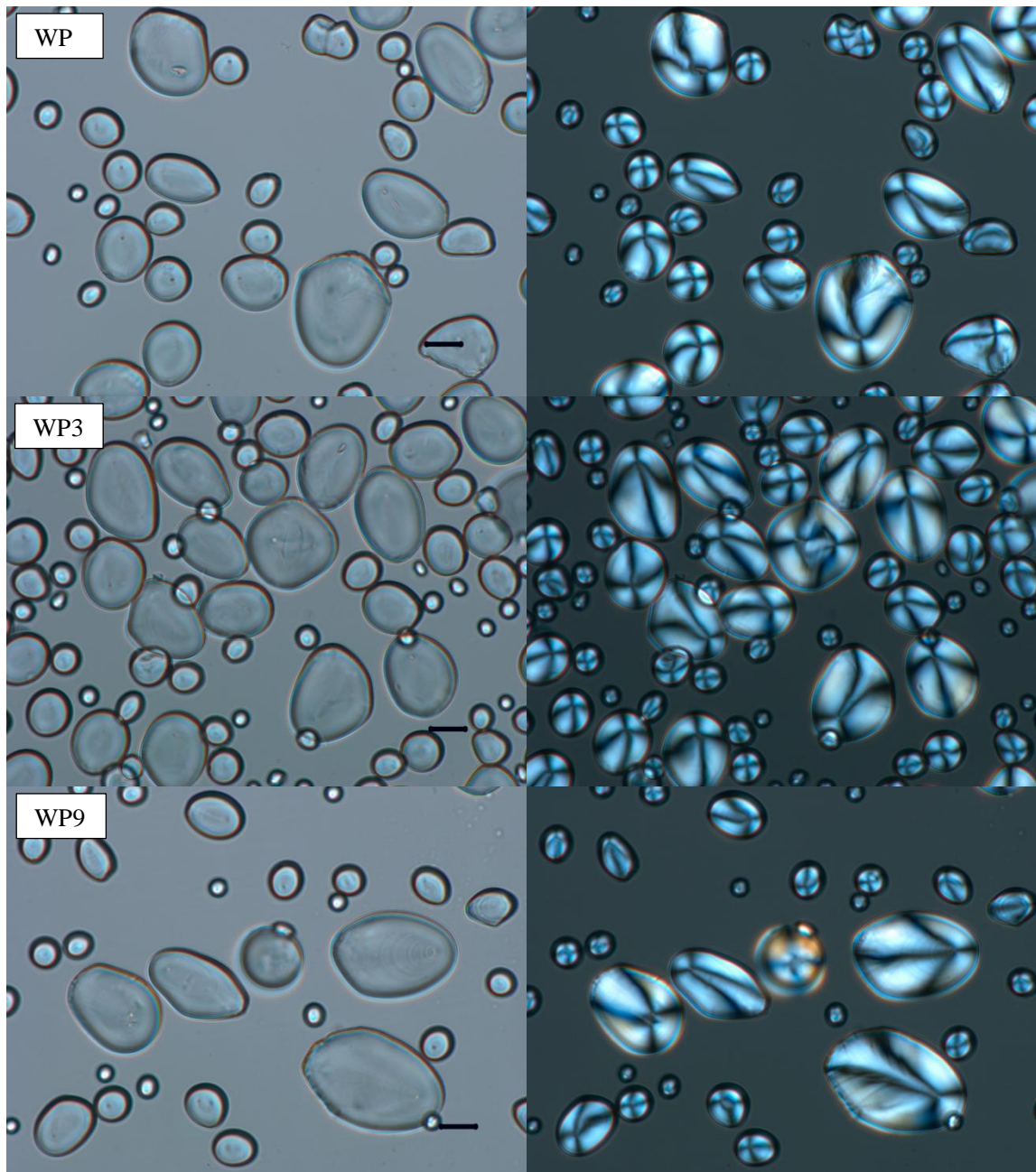


Figure 4.3 Microscopic image of unmodified normal potato starch (NP), octenylsuccinic anhydride (OSA)-modified normal starches with degree of substitution (DS) of 0.0167 (NP3), and 0.0400 (NP9); unmodified waxy potato starch (WP), OSA-modified waxy starches with DS of 0.0174 (WP3), and 0.0383 (WP9). Scale bar in each graph represents 20 μm . Left images: normal visible light; right images: polarized light.

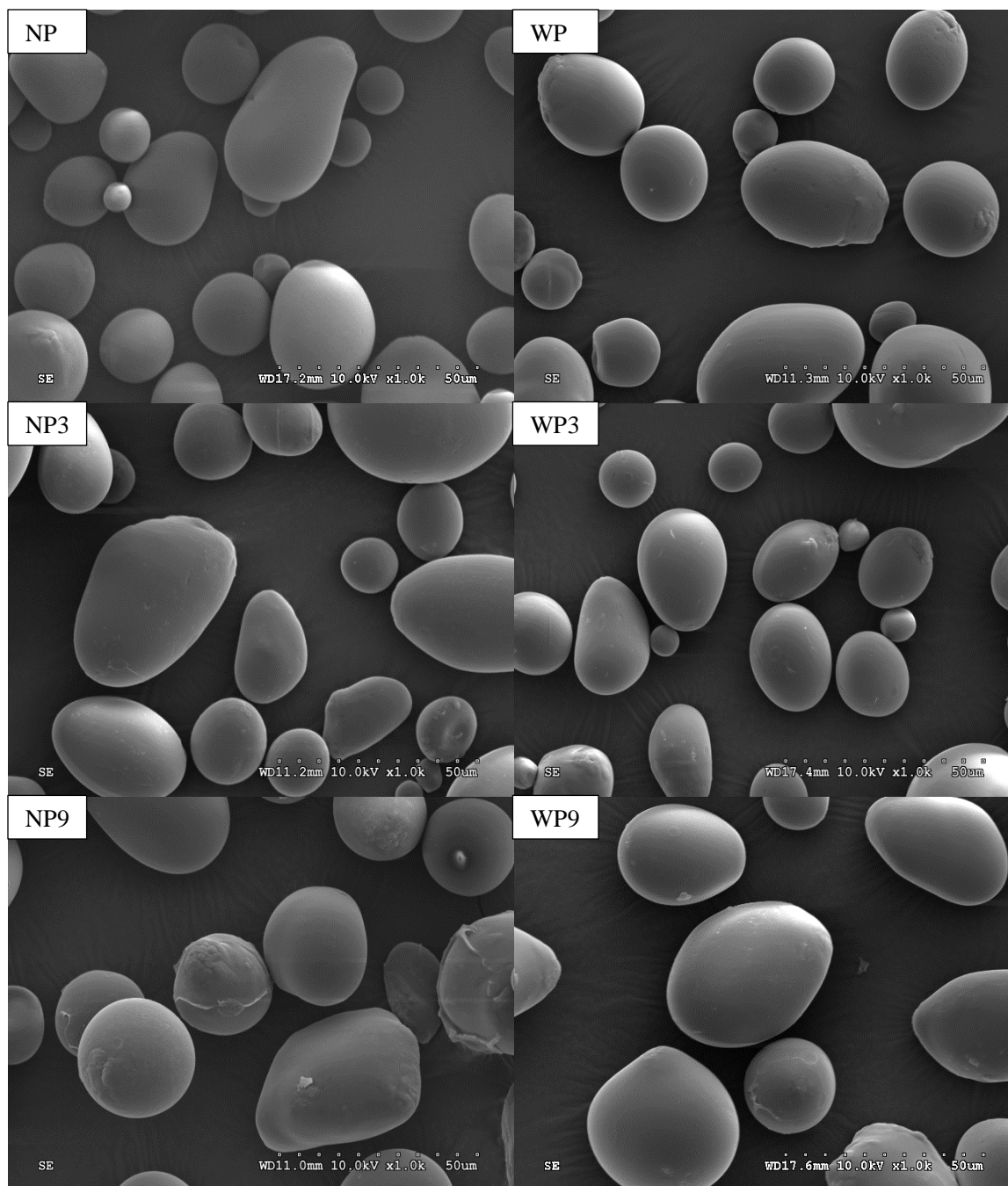


Figure 4.4 Scanning electron microscopy (SEM) micrographs of potato starches: unmodified normal (NP), octenylsuccinic anhydride (OSA)-modified normal starches with degree of substitution (DS) of 0.0167 (NP3), and 0.0400 (NP9); unmodified waxy (WP), OSA-modified waxy starches with DS of 0.0174 (WP3), and 0.0383 (WP9).

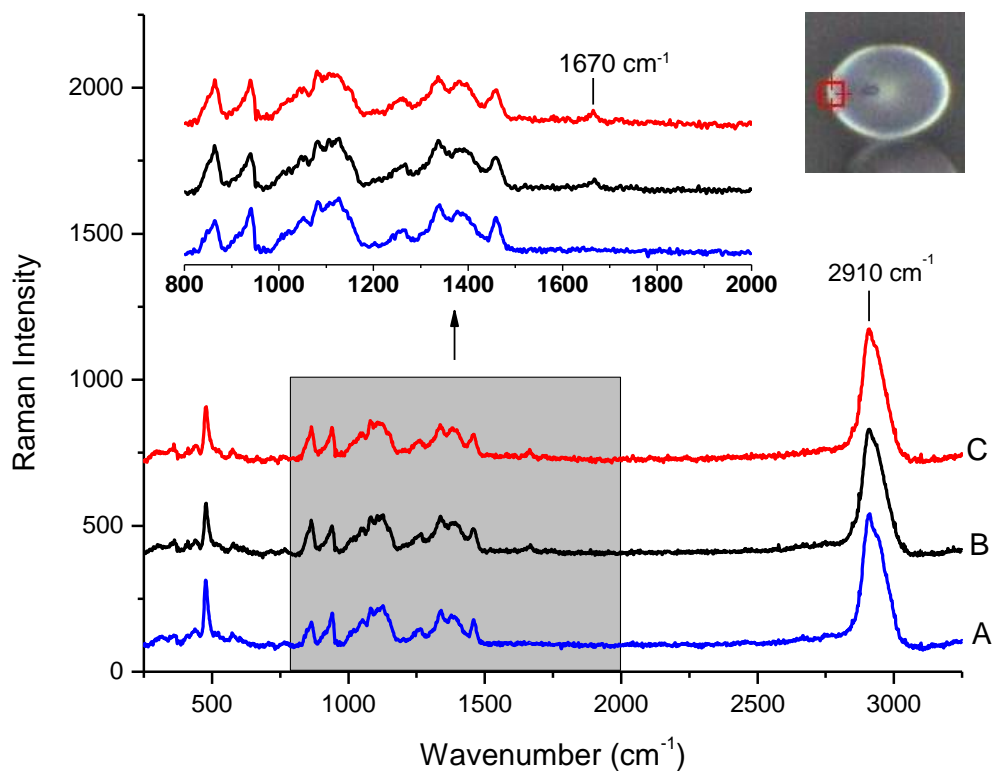


Figure 4.5 Raman image and spectra of the surface (b1, edge-left) of one long flat oval-shaped -starch granule. These spectra are from unmodified (A), octenylsuccinic anhydride (OSA)-modified granules with degree of substitution (DS) of 0.0174 (B), and 0.0400 (C).

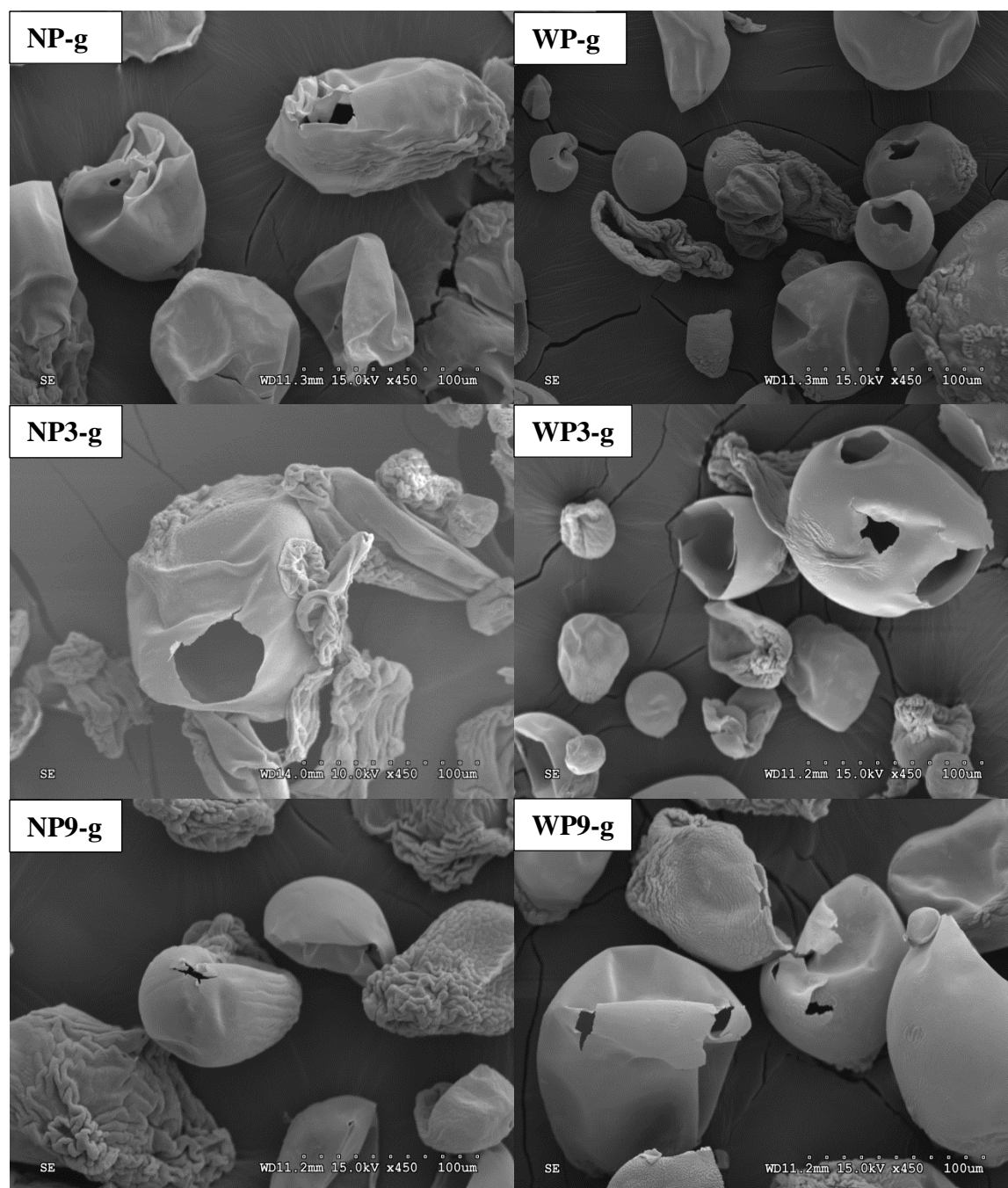


Figure 4.6 Scanning electron microscopy (SEM) micrographs of ethanol-precipitated granule ghosts of native (NP-g), 3% (NP3-g), and 9% (NP9-g) octenylsuccinic anhydride (OSA)-modified normal potato starches; native (WP-g), 3% (WP3-g), and 9% (WP9-g) OSA-modified waxy potato starches, respectively.

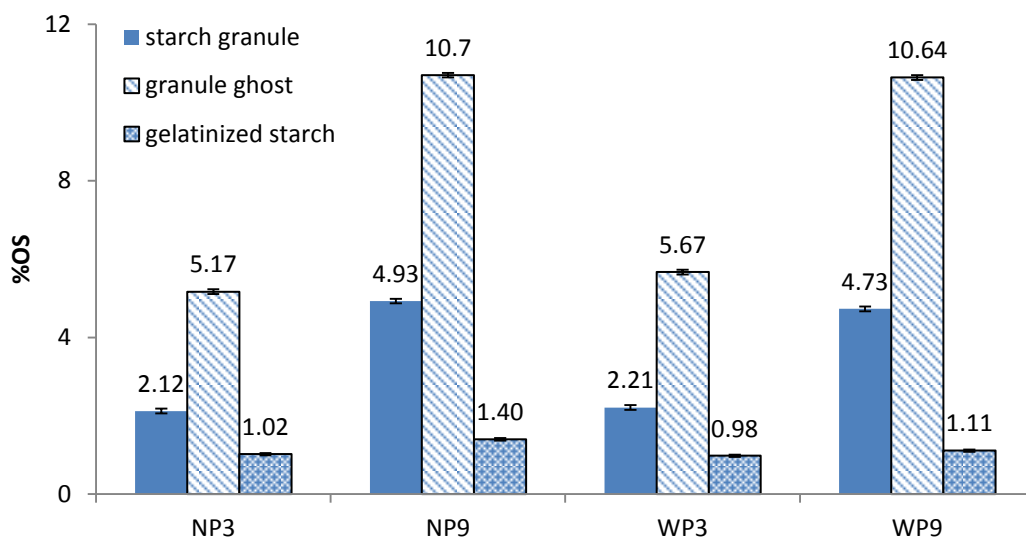
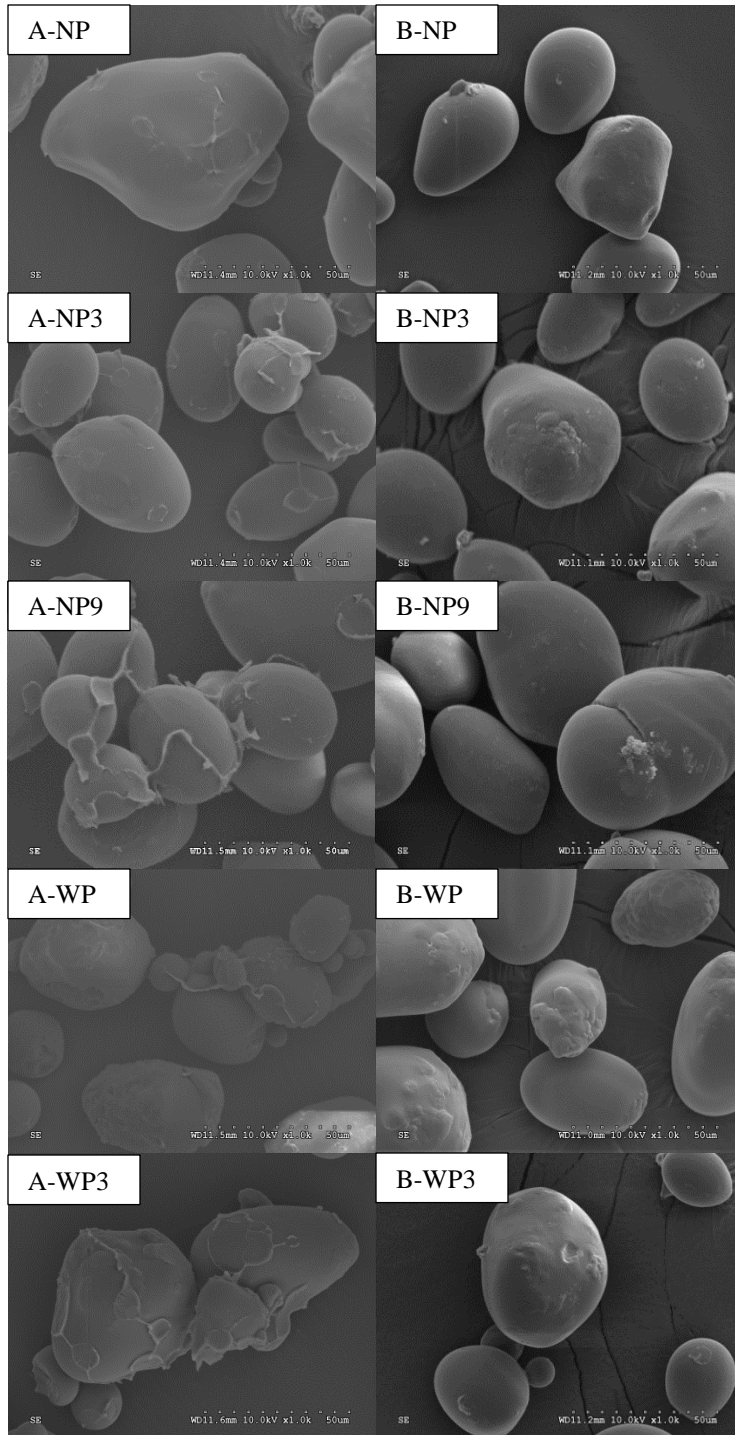


Figure 4.7 Changes on bound OS content (% OS) of 3 and 9% octenylsuccinic anhydride (OSA)-modified potato starch (A) and maize starch (B): normal potato (NP3 and NP9), waxy potato (WP3 and WP9), normal maize (NM3 and NM9), and waxy maize (WM3 and WM9), and their granule ghost and remaining granules after chemical surface gelatinization.



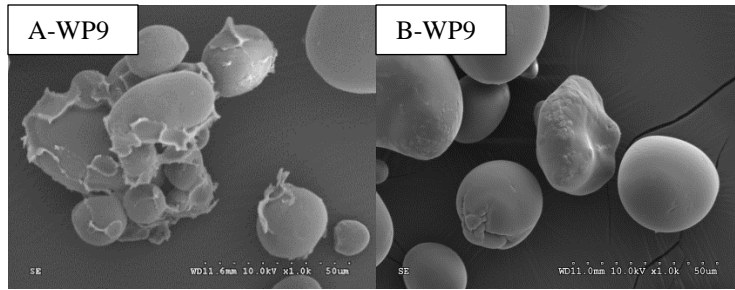


Figure 4.8 Scanning electron microscopy (SEM) micrographs of partially surface gelatinized starch granules (A) and remaining granules (B): normal potato (NP), octenylsuccinic (OS) normal potato starches (NP3, NP9), and waxy potato (WP), OS waxy potato starches (WP3, NP9).

Tables

Table 4.1 Thermal properties of unmodified and octenylsuccinic anhydride (OSA) modified normal and waxy potato starches treated with 3% and 9% OSA determined by differential scanning calorimetry (DSC)^a

Sample		DS ^b	T _o (°C)	T _p (°C)	T _c (°C)	ΔH (J/g)
Normal potato starch	Native	-	56.7 ± 0.1 a	64.0 ± 0.0 a	90.1 ± 1.3 a	19.8 ± 0.9 a
	3% OSA	0.0167	54.5 ± 0.1 ab	61.9 ± 0.1 b	90.7 ± 1.0 a	17.4 ± 0.2 b
	9% OSA	0.0400	52.2 ± 0.0 bc	60.2 ± 0.0 b	91.2 ± 0.1 a	16.7 ± 0.3 b
Waxy potato starch	Native	-	62.7 ± 0.1 a	69.7 ± 0.0 a	95.6 ± 0.9 a	21.4 ± 0.9 a
	3% OSA	0.0174	54.1 ± 0.1 b	60.2 ± 0.1 b	85.1 ± 1.1b	15.3 ± 0.5 b
	9% OSA	0.0383	50.5 ± 0.2 bc	56.8 ± 0.0 bc	80.9 ± 1.0 c	11.5 ± 0.1 c

^a Mean ± standard deviation values are reported. Means in the same column not sharing a common letter are significantly different at p < 0.05.

^b DS = degree of substitution

Table 4.2 The band area ratio of an OS group to starch content on five positions within one round-shaped granule (a1-5) and seven positions within one long flat oval-shaped potato starch granule (b1-7), calculated as (band area at 1670 cm⁻¹ / band area at 2910 cm⁻¹) × 100. Ten starch granules (n=10) of each sample were analyzed by Raman microspectroscopy^a

Position	Band area ratio 1670 cm ⁻¹ / 2910 cm ⁻¹			
	Normal potato starch		Waxy potato starch	
	3% OSA	9% OSA	3% OSA	9% OSA
a1	5.20 ±0.43 a	9.06 ±0.50 ab	6.01 ±0.32 a	7.20 ±0.54 a
a2	2.99 ±0.27 b	7.15 ±0.66 c	4.17 ±0.15 b	5.22 ±0.81 b
a3	3.06 ±0.14 b	7.99 ±1.13 bc	4.23 ±0.57 b	5.60 ±0.32 b
a4	2.98 ±0.13 b	8.15 ±0.79 bc	4.25 ±0.43 b	5.41 ±1.19 b
a5	5.02 ±0.36 a	9.72 ±0.55 a	5.61 ±0.18 a	7.03 ±0.65 a
b1	4.50 ±0.14 b	9.34 ±2.50 abc	5.39 ±0.68 ab	6.98 ±0.27 ab
b2	3.54 ±0.27 c	7.40 ±0.26 bc	4.39 ±0.23 bc	4.68 ±0.14 c
b3	3.27 ±0.03 c	7.17 ±1.22 c	3.91 ±0.35 c	4.75 ±0.40 c
b4	3.60 ±0.07 c	7.30 ±0.93 bc	4.11 ±0.29 bc	4.52 ±0.22 c
b5	4.96 ±0.16 ab	9.24 ±1.51 abc	5.18 ±0.42 abc	5.63 ±0.45 bc
b6	5.71 ±0.62 a	10.44 ±0.61 a	6.39 ±1.88 a	7.32 ±1.21 a
b7	4.88 ±0.34 ab	9.50 ±0.73 ab	5.33 ±0.44 ab	6.02 ±0.47 ab

^a Mean ± standard deviation values are reported. Values followed by the same letter vertically are not significantly different (p < 0.05).

OSA = octenylsuccinic anhydride.

Table 4.3 Bound OS content (%OS), degree of substitution (DS) of octenylsuccinic anhydride (OSA) modified normal and waxy potato starch granules, starch granule ghosts, and remaining granules after chemical surface gelatinization

Starch	OSA treatment (%)	Samples	Remaining amount (%)	%OS	DS
Normal potato	3	starch granule	100.0	2.12 ±0.04	0.0167 ±0.0001
		granule ghost	39.2	5.17 ±0.05	0.0420 ±0.0005
		remaining granule	82.3	1.02 ±0.03	0.0079 ±0.0002
	9	starch granule	100.0	4.93 ±0.03	0.0400 ±0.0003
		granule ghost	43.3	10.70 ±0.02	0.0924 ±0.0002
		remaining granule	70.7	1.40 ±0.03	0.0109 ±0.0002
Waxy potato	3	starch granule	100.0	2.21 ±0.04	0.0174 ±0.0003
		granule ghost	37.5	5.67 ±0.02	0.0463 ±0.0002
		remaining granule	78.8	0.98 ±0.00	0.0076 ±0.0000
	9	starch granule	100.0	4.73 ±0.07	0.0383 ±0.0004
		granule ghost	41.6	10.64 ±0.01	0.0918 ±0.0001
		remaining granule	65.7	1.11 ±0.02	0.0086 ±0.0001
Normal maize	3	starch granule	100.0	2.15 ±0.05	0.0169 ±0.0004
		granule ghost	81.3	2.60 ±0.02	0.0205 ±0.0001
		remaining granule	80.0	1.62 ±0.03	0.0127 ±0.0002
	9	starch granule	100.0	5.13 ±0.03	0.0418 ±0.0002
		granule ghost	89.1	5.75 ±0.03	0.0470 ±0.0002
		remaining granule	56.2	2.31 ±0.02	0.0182 ±0.0001
Waxy maize	3	starch granule	100.0	2.27 ±0.02	0.0179 ±0.0003
		granule ghost	82.8	2.56 ±0.01	0.0203 ±0.0001
		remaining granule	51.5	1.07 ±0.05	0.0084 ±0.0006
	9	starch granule	100.0	4.83 ±0.02	0.0409 ±0.0001
		granule ghost	88.4	5.45 ±0.04	0.0444 ±0.0005
		remaining granule	27.6	1.72 ±0.03	0.0135 ±0.0003

Chapter 5 - Formation of orange oil-in-water emulsion stabilized by alpha-amylase-degraded octenylsuccinic anhydride waxy potato starches

Abstract

The objectives of this study were to prepare α -amylase degraded octenylsuccinic anhydride (OSA) modified starches from waxy potato starch by two approaches and characterize their structure and emulsifying capacity and stability. In the first approach, granular waxy potato starch was reacted with 3% OSA first and then hydrolyzed by α -amylase to product OS maltodextrins (OSE) with dextrose equivalent (DE) of 4.97 and DS of 0.0175. In the other approach, granular waxy potato starch was hydrolyzed by α -amylase and then modified by 3% OSA to prepare OS maltodextrins (EOS) with DE of 4.39 and DS of 0.0209. Gel permeation chromatography (GPC) analysis confirmed that the molecular size of waxy potato starch was reduced after α -amylolysis, and the degree of decrease increased with the increase in α -amylase concentration. Emulsion stability, droplet size distribution were studied to evaluate the orange oil-in-water emulsions. With a low concentration of α -amylase, OS maltodextrin with high apparent viscosity (26 and 31 cp at 10% solid content) displayed good emulsion stability, and the product with higher molecular weight resulted more viscous emulsion and better stability.

Keywords

Octenylsuccinic anhydride; Waxy potato starch; Maltodextrin

Introduction

Octenylsuccinic anhydride (OSA) modified starch was developed by Cardwell and Wurzburg in early 1950s (Caldwell, 1952; Caldwell & Wurzburg, 1953), prepared by the esterification of granular starch with OSA aqueous alkaline slurry at or near room temperature, approved for food use at level of 3% (degree of substitution, DS <0.02) in the U.S. (Bai & Shi, 2011; Sun et al., 2019). Preparation and properties of octenylsuccinate (OS) starch was reviewed by Sweedman et al. (2013) and Altuna et al. (2018). Due to both hydrophilic and hydrophobic groups, OSA-modified starches are used widely as emulsifiers and stabilizers in foods, a variety of oil-in-water emulsions, in some water-in-oil systems, pharmaceuticals, paper industry and in any industry where stable emulsions are required (Altuna et al., 2018; Dokić et al., 2012; Sweedman et al., 2013; Trubiano, 1986; Zhao et al., 2017).

The most widely used hydrocolloids in beverage are amphiphilic polysaccharides, such as gum arabic and OSA modified starch due to their colorless and tasteless in solution, good stability to droplet aggregation at a wide range of pH values, ionic strengths and temperatures, but low interfacial surface activity compared to proteins or surfactants due to their hydrophilic glucose backbones (Charoen et al., 2011, 2012; Given, 2009; McClements, 2011; McClements et al., 2017; Sanchez et al., 2018). Less amount of modified starch is needed for stabilization of emulsions (Dickinson, 2018; McClements et al., 2017). For example, 20% gum arabic was required to produce a stable 12.5 wt% oil-in water emulsion but modified starch was used as 12% (Chanamai & McClements, 2002).

Our goal was to prepare soluble OS starch that can be used in beverage application. Also, in the area of food and beverage applications, the emulsion stabilizer with low apparent viscosity

is preferred, requiring less energy to flow during processing (Sweedman et al., 2014). Therefore, OSA-modified starch must be water soluble with low viscosity. Acid and enzyme treatments are the most common methods to hydrolyze OS-starch, decrease its molecular weight and viscosity in water. In 2019, we filed a U.S. patent application (No. 16/728,400) describing two approaches to prepare α -amylase-degraded OS starches. In the first approach, granular waxy maize starch was reacted with OSA, then cooked and hydrolyzed by α -amylase to produce maltodextrins (gOSMs). In the second approach, granular starch was cooked and hydrolyzed by α -amylase to make a maltodextrin, and the resulting soluble maltodextrin was reacted with OSA for OS maltodextrins (sOSMs). Preparation and structure of α -amylase-degraded OS waxy maize starches with different substitution patterns were studied (Bai, 2013). The product (gOSMs) had localized OS substitution near the branching points or non-reducing ends; the other product (sOSMs) had OS groups distributed randomly throughout the starch chains, and OS substitutions were found close to the branching points as well as the non-reducing ends.

There are a number of studies on OSA modified starches in the literature. Xu et al. (2015) investigated that β -amylase which cleaves (1 \rightarrow 4)- α glycosidic bond from the non-reducing ends of starch chains could be used to hydrolyze OSA-modified waxy maize starch to obtain a better emulsion stability with orange oil, but the droplet size of emulsions was still large and the stability was weak. On the other hand, α -amylase, an endo-amylase which cuts (1 \rightarrow 4)- α bond randomly in the interior of starch chains was also used to degrade OS starch (Han et al., 2019; Liu et al., 2008; Zhang et al., 2018). Han et al. (2019) investigated the emulsifying capacity of OSA-modified waxy maize starches formed by hydrolysis by α -amylase, β -amylase and acid (HCl) and found that the degraded OSA-starches treated by α -amylase generally had the smallest average chain length and largest degree of branching, resulting in the lowest viscosity and the

best droplet stability with the smallest creaming extent. Waxy rice starch hydrolyzed by β -amylase and then modified by OSA (OSA β -limit dextrin) was evaluated by Wang et al. (2020). Majority of studies in the literature of OS starch is on maize starch, especially on waxy maize. The second largest botanical origin is potato starch (Sweedman et al., 2013). Hui et al. (2009) and Won et al. (2017) reported preparation and properties of OSA-modified normal potato starch. They suggested that the crystalline pattern of OSA potato starches was not changed by esterification up to DS 0.045.

To my knowledge, there is no report on OSA modified waxy potato starch. Waxy potato starch has a B-type X ray diffraction pattern as normal potato starch (Cai et al., 2010; Hsieh et al., 2019; Lee et al., 2012). Compared with other waxy starches, waxy potato starch contains little protein and lipids, has a higher pasting viscosity and greater paste clarity. We hypothesized that α -amylase degraded OS waxy potato starch would be a colorless emulsifier with excellent emulsification performance in flavor oil beverage. The objectives of this study were to prepare OS waxy potato starches by α -amylase treatment from two approaches with the improved emulsifying properties, and to find a novel emulsifier with a minimum concentration to stabilize emulsions.

Materials and Methods

Materials

Waxy potato starch (*Eliane 100*) (phosphorus% = 0.07%) was obtained from Avebe (Veendam, the Netherlands). Octenylsuccinic anhydride (OSA) was obtained from Gulf Bayport Chemicals L.P. (Pasadena, Texas, US). Gum Arabic (pre-hydrated® Gum Arabic spray dry

powder) was from TIC Gums (Belcamp, MD, USA). Commercial OS starches (starch 1 and 2) were obtained from Ingredion Incorporated (Bridgewater, NJ, USA). An alpha-amylase (BAN® 480 L) with a standard strength of 480 KNU/g produced by submerged fermentation of a selected strain of *Bacillus amyloliquefaciens* was obtained from Novozymes North America, Inc. (Franklinton, NC, USA). One KNU is defined as the amount of enzyme that dextrinizes 5.26g of starch (Merck Amylum soluble) per hour under standard conditions (37.0 °C, 0.0003M Ca^{2+} , and pH5.6). Orange oil (1-fold and 5-fold) was obtained from Citrus and Allied Essences Ltd. (Belcamp, MD, USA). The weighting agent (Pinova® Ester Gum 8BG) was obtained from TIC Gums, Inc. (Belcamp, MD, USA). Anhydrous citric acid was obtained from J.T. Baker Chemicals (Avantor Performance Materials, Inc., PA, USA). Other chemicals were all analytical grade.

Preparation of amylase degraded OS starch

Approach 1 (OSA reaction + enzyme degradation)

Preparation of α -amylase-degraded OS starch from Approach 1 is shown in Fig. 5.1. Granular waxy potato starch was first reacted with OSA in an aqueous slurry system. Waxy potato starch (500 g) was suspended in distilled water (750 g) with agitation under an overhead stirrer. Starch suspension (1250 mL) of 40% solid content was adjusted to pH 7.5 by sodium hydroxide (3%, wt.). OSA (3% based on the dry weight of starch) was added to the starch slurry while pH was maintained at 7.5 by sodium hydroxide (3%, wt.) during the reaction. After pH stabilized for 30 min, the reaction was terminated by adjusting pH to 6 with 1 N HCl. OS starch was recovered by filtration, washed by methanol, and dried in an oven at 40 °C overnight.

The OS starches were converted to OS maltodextrins by α -amylase hydrolysis. Ban 480L (α -amylase) (0.005, 0.01, or 0.02% based on the dry weight of starch) was added to the starch slurry of 18% solids. The pH of the slurry was adjusted to 6.0-6.4 by 1 N NaOH. Starch hydrolysis was carried out at 80 °C water bath in 20 min. α -amylolysis was stopped by holding the starch solution to boiling water for 20 min, and then cooled to room temperature. The OS maltodextrin obtained was recovered by spray drying (Spray dryer, LPG-5 model; Jiangsu Fanqun Drying Equipment Factory, Jiangsu, China). The spray drying conditions were inlet temperature 180 °C and outlet temperature 100 °C.

Approach 2 (enzyme degradation + OSA reaction)

Preparation of α -amylase-degraded OS starch from Approach 2 is shown in Fig. 5.1. Granular waxy potato starch was first hydrolyzed by α -amylase as described in Approach 1. Waxy potato starch (360 g) was suspended in distilled water (1,640 g) with agitation under an overhead stirrer. The pH of starch suspension (18% solid content) was adjusted to 6.0-6.4 by 1 N NaOH. α -amylase (Ban 480L) (0.0005, 0.005, or 0.01 % based on the dry weight of starch) was added to the starch slurry. Starch hydrolysis was carried out at 80 °C water bath in 20 min. α -amylolysis was stopped by holding the starch solution to boiling water for 20 min, and then cooled to room temperature.

The starch solution was then reacted with 3% OSA (based on the dry weight of waxy potato starch) as described in Approach 1. The pH was maintained at 7.5 by sodium hydroxide (3%, wt.) during the reaction. After pH stabilized for 30 min, the reaction was terminated by adjusting pH to 6 with 1 N HCl. The OS maltodextrin was recovered by spray drying. The spray drying conditions were inlet temperature 180 °C and outlet temperature 100 °C.

Characterization of OS starches

Determination of the degree of substitution (DS)

The DS of OS maltodextrin was determined by high-performance liquid chromatography (HPLC) as reported by Qiu et al. (2012). Briefly, for free OS determination, 0.5 g (d.w.) of OS maltodextrin was stirred in 5 mL of methanol for 1 h. After centrifuge, 1 ml of supernatant was mixed with 1 ml of water (pH = 3, prepared by adding 1 ml of 1 N hydrochloric acid into 1 L water). The solution was analyzed by HPLC. To determine total OS, 0.5 g (d.w.) of OS maltodextrin was stirred overnight in 10 mL of 4 N NaOH. The alkali solution (2 mL) was neutralized with 10 mL of 1 N HCl and filled with acetonitrile to 25 mL volumetric flask. The solution was analyzed by HPLC. A mixture of acetonitrile and water containing 0.1% TFA (45:55, v/v) was used as the mobile phase. The flow rate was 1.0 ml/min and the detection wavelength was set at 210 nm. Concentrations were determined from the peak area.

Determination of dextrose equivalent (DE)

DE of the α -amylase hydrolyzed products was determined by the Nelson-Somogyi method (Somogyi, 1952). Glucose standards in distilled water were prepared ranging from 0-0.5 $\mu\text{mol/mL}$. The OS maltodextrin sample was prepared in an appropriate dilution (0.1 $\mu\text{mol/mL}$). Each standard or OS maltodextrin sample (1 ml) was placed in separate tubes and 1 mL of distilled water was used as the blank. To each tube, 1 mL of the copper reagent was added and placed in boiling water for 10 min. The tubes were cooled to room temperature and 1 mL of arsenomolybolic acid reagent – Nelson Reagent was added. The absorbance was measure at 520 nm.

Gel Permeation Chromatography (GPC)

GPC analysis was performed as previously described (Shi et al., 2018). Each sample (4 mg) were dissolved in dimethyl sulfoxide (DMSO) (4 mL) containing lithium bromide (0.5% w/w), and stirred at room temperature for 12 h. The mixture was filtered through a 2 μm filter and then injected into a PL-GPC 220 instrument (Polymer Laboratories, Inc., Amherst, MA, USA). The eluent was DMSO containing 0.5% (w/w) LiBr, and the flow rate was 0.8 mL/min. The molecular size (hydrodynamic radius, R_h) distribution was determined as described by Vilaplana & Gilbert (2010).

Orange oil emulsion preparation

Orange oil emulsion stabilized by solubilized OS starch was prepared by the method of Trksak and Makariou (2010) with some modifications. To prepare the oil phase, 48% (w/w) 1 \times orange oil and 12% (w/w) 5 \times orange oil were mixed with 40% (w/w) weighting agent (Ester Gum 8BG) under constant stirring using a magnetic stirrer for 3 hours at room temperature. To prepare the water phase, 0.3% citric acid and 0.15% sodium benzoate were added in distilled water under constant stirring for 1 hour.

To study the effects of the ratio of oil to starch on emulsion properties, the total amount of starch and oil, and water phase was maintained at 24 g, and 76 g, respectively. The ratio of oil:starch was designed as 12:12 (1:1), 16:8 (2:1), and 18:6 (3:1), respectively. Different amounts of OS starch (12, 8, or 6 g, dry basis) were weighed into water phase containing 0.3% citric acid and 0.15% sodium benzoate in a 200-mL glass bottle using a magnetic stirrer to continuously disperse starch slurry in a water bath at 70 $^{\circ}\text{C}$ and 500 rpm for 2 hours. Starch slurry was cooled to room temperature. Then orange oil mixture (oil phase) (12, 16, or 18 g) was

added into starch slurry, and pre-homogenized by a bench-top homogenizer (PRO 350, PRO Scientific Inc., Oxford, CT) at 8,000 rpm for 3 min. The crude emulsion was homogenized by an M-110P microfluidizer (Microfluidics, Newton, MA, US) for 3 passes at a pressure of 30,000 psi. The middle part of fresh emulsion was collected for analysis immediately.

Droplet size

Droplet size of orange oil emulsions was determined using the laser scattering particle size distribution analyzer (LA-910, Horiba, Japan). Emulsions were shaken, brought into a stirring tank filled with distilled water. The reported d_{43} value is the mean volume-weighted particle sizes. All samples were performed in duplicate. The OS starch after dissolution in water phase was measure but had no signal.

Particle electrical charge (ζ -potential)

The oil droplets ζ -potential was measured based on the principle of electrophoretic mobility and dynamic light scattering using a zeta potential analyzer (ZetaPALS, Brookhaven Instruments Corporation, Holtsville, NY). Emulsions were diluted 1:100 (v/v) with demineralized water and transferred into a cuvette having two electrodes. An electrical voltage was applied over the electrodes, resulting in particle movement which was influenced by the particle charge. The ζ -potential obtained describes the charge of the measured oil droplet.

Creaming index

The creaming index of the emulsions was measured at 14 days after preparation. Capped, glass tubes were filled with 5 mL of emulsion and the total height was measured. The height of the upper cream layer was measured, allowing to calculate the creaming index. The creaming index (%) is expressed as the ratio of the height of the upper, cream layer (mm) to the height of

the total emulsion (mm). Tubes used for determination of the creaming index were not shaken during the storage experiment.

Stability of emulsions

All emulsions were stored at room temperature for 14 and 30 days. The droplet size and particle electrical charge of emulsions were determined.

Results and discussion

Structural and physicochemical properties of α -amylase-degraded OS starch

The action of α -amylase on starch was altered after OS substitution. When α -amylase was performed under 0.02, 0.01, and 0.005% at 80 °C for 20 min, the products prepared by approach 1 (OSE) from 3% OSA-modified waxy potato starch with DS of ca. 0.0175 had DE of 7.42, 5.33, and 4.97, respectively (Table 5.1). The viscosity at 10% solid content of each sample was 6.5, 13.0, and 26.0 cp respectively (Table 5.1). Similarly, When α -amylase was performed under 0.01, 0.005, and 0.0005% at 80 °C for 20 min, the products by approach 2 (EOS 1) from native waxy potato starch with DS of c.a. 0.0209 had DE of 6.57, 5.25, and 4.39, respectively (Table 5.1). After enzyme treatment, maltodextrin directly reacted with 3% OSA. The DS of each sample was c.a. 0.0210. The viscosity at 10% solid content of each sample was 8.0, 15.5, and 30.5 cp respectively (Table 5.1). All the hydrolyzed OSA maltodextrin samples for all treatments showed a decreasing tendency of apparent viscosity with increase of enzyme concentration. With lower enzyme concentration, α -amylase hydrolysates had a lower DE with higher viscosity. The viscosities of the OSA maltodextrins are closely related with their molecular sizes.

The molecular size distribution profiles of α -amylase-degraded OS waxy potato starch (OS maltodextrin) prepared from approaches 1 and 2 are shown in Fig. 5.2. For all degraded OS starch samples after the α -amylase hydrolysis, the molecular size was significantly reduced compared with the unmodified waxy potato starch. The α -amylase hydrolyzed OSA starch with the lowest concentration of enzyme (OSE 3) had two peaks at $R_h = 15$ nm and 40 nm, whereas the other degraded starch sample with the highest concentration of enzyme (OSE1) had only one size peak at 1.5 nm. Similarly, the molecular size distribution of degraded OS waxy potato starch prepared from approach 2 (EOS) reduced with an increasing of enzyme concentration from 0.0005 to 0.01% (Fig. 5.2B). These results suggest that the molecular size decreased with the increased of enzyme concentration.

Alpha-amylase is an endo-acting amylase that hydrolyze α -1,4 bonds and bypass α -1,6 linkages. OSA-modification has been suggested to occur preferentially at amorphous region (Bai & Shi, 2013). OS groups were distributed close to the branching points and non-reducing ends of amylopectin for degraded OS maltodextrin from approach 1 and localized randomly throughout the starch chains for degraded OS maltodextrin from approach 2 (Bai, 2013). This explained the differences of molecular size with and without OS-modification (compared to unmodified waxy potato starch). OS maltodextrins from approach 1 (OSE2) required higher enzyme concentration than OS maltodextrins from approach 2 (EOS2) to achieve the similar DE (~5.3) and molecular size distribution (Fig. 5.2). It was probably due to the starch molecules containing OS substitution groups that were resistant to α -amylases hydrolysis.

Stability of emulsions formed using degraded OS-starch

The orange-oil-in-water emulsion was formulated as in Table 5.2. The physicochemical stability of all emulsions was evaluated by determination of the particle size, particle charge (ζ -potential) and creaming index, in combination with visual observation. The results from these analyses are shown in Table 5.3 and Fig 5.3.

The influence of emulsifier type on the formation of emulsion-based delivery systems for α -amylase-degraded OS waxy potato starches (OSE 1, 2, 3 and EOS 1, 2, 3), natural biopolymers gum arabic and two types of commercial OS starches is shown in Table 5.3. The results for particle size measurement of fresh emulsions with the highest ratio of oil to starch (1:1) showed that all emulsions had a small particle size below 1.5 μm except for emulsifier EOS1 and EOS2. During 14 days stored at room temperature, the creamy separated oil layer appeared on the top of emulsions from EOS1 and EOS2. Droplet coalescence induced by the creaming may be formed resulting in the instability of the emulsions. The separation phenomena also occurred on the α -amylase hydrolyzed OSA-starch sample OSE1, even though its fresh emulsion had a particle size ranging from 1.3-1.8 μm with an increase of oil ratio. These may due to low molecular size/weight and viscosity of these three highly enzyme converted OS starches by α -amylase. OSA-starches with lower molecular weight tend to have higher encapsulation efficiency and capacity (Hategekimana et al., 2015), while OSA modified starch samples containing larger molecules have better emulsion stability (Sweedman et al., 2013).

The emulsion stability of the emulsion is expressed by the change (%) in the droplet size of the emulsions over storage with respect to the droplet size of the fresh emulsion (immediately after preparation) (Han et al., 2019). On the observation of particle size after storage of 14 days,

droplet size of the emulsions made by OSE2 showed a shift to larger size above 5 μm without creaming layer at the higher ratio of oil and starch (3:1), indicating that OSE2 had a poor emulsifying capacity at high oil load. At the lower ratio of oil to starch (1:1 and 2:1), the particle size of emulsion made by OSE2 was increased by 80% compared to the corresponding particle size at the initial stage of storage, where the largest particle size (2.8-3.4 μm) among other un-creamed emulsions. The emulsion droplet size of commercial starch 1 also increased at a significantly faster rate by up to 76% at the ratio of oil to starch (1:1), > 5 μm at the ratio of 2:1, and separated creamy layer on the top of emulsion with creaming index 32.4% at the ratio of 3:1 after 14 days. The emulsions made by gum arabic at ratio of 1:1 and 2:1 were stable after 14 days, but gum arabic was not suitable for high oil load at the ratio of oil to gum arabic 3:1.

For the α -amylase degraded OSA-starch samples (OSE3 and EOS3), there was an increase in the droplet size of the emulsion after 14 days of storage (increased by up to 40%, correspondingly to up to 3% per day), but still with small droplet size ranging from 0.90-0.93 μm at the ratio of oil to starch (3:1). There was also no creaming layer occurred on the emulsions by commercial starch 2 with the particle size below 3 μm . Compared with the emulsion stability (%), the particle size increased by up to 70% after 14 days with an average particle size of 2.8 μm , which much larger than that of emulsions by degraded OSA-starch samples (OSE3 and EOS3). Among all the emulsions, the emulsions of the α -amylase degraded OSA-starch samples (OSE3 and EOS3) presented a relatively steady particle size with the increasing storage time indicating a better emulsion stability. The viscosity of OSA starch solutions was related to starch molecular size and the relative amounts of small molecules. Studies have reported that apparent viscosity of emulsion plays an important role in determining storage stability of emulsion, and a large M_w of OS-starch can lead to a more viscous solution and better stabilization of emulsion

when the addition of starch has a great influence on emulsion viscosity (Dokić et al., 2012; Xu et al., 2015). In Table 5.3, apparent viscosity of fresh emulsions stabilized by OSE3 and EOS3 was much higher than other emulsions at the corresponding ratio of oil to starch. The high viscosity of the emulsion could retard free motion of the oil droplets delaying creaming, flocculation, and coalescence. Therefore, higher viscosity of emulsion is influenced by larger Mw of OS starch and higher emulsifier concentration.

Because of their good emulsion performance at 14 days, OSE3, EOS3, gum arabic (GA), and commercial OS starch 2 (Starch 2) were selected to check the particle size distribution of emulsions with the ratio of oil to starch 1:1 and 2:1 after 30 days storage at room temperature (Fig. 5.3). At the ratio of oil to starch (1:1), all emulsions were stable with one peak of a narrow particle size distribution. OSE3 and EOS3 had a smaller volume diameter 0.578 and 0.656 μm , respectively. Gum arabic and commercial OS starch 2 had a larger volume diameter 1.350 and 1.283 μm , respectively. Those emulsifiers showed good emulsify properties when the ratio of oil to starch was 1:1 after 30 days storage. The particle size distributions of selected emulsions with the ratio of oil to starch (2:1) increased after storage for 30 days. The wide particle size distribution after 30 days storage suggested the formation of free oil, and the emulsions were unstable. Oil was observed on the surface of those emulsions although obvious cream was not noted. The clarity of emulsions at the same ratio of oil to starch (1:1) diluted in 1:100 was shown in Fig. 5.4. Obviously, the emulsions made by OSE3 and EOS3 were much more clarity than that by gum arabic, commercial starch 1 and 2, indicating OS waxy potato starches by two approaches is suitable for clear beverage emulsions.

The zeta-potential of the orange-oil-n-water emulsions made by α -amylase degraded OSA-starch samples was determined, and the results are presented in Table 5.3. The zeta-

potential reflects the surface characteristic of the tested particles and is often applied to determine the stability of charged colloids (McClements et al., 2007). The charge of all the OS maltodextrins-coated oil droplets was highly negative. It can be attributed the presence of negatively charged carboxyl groups ($-\text{COO}^-$) on the acidic polysaccharide (Chanamai & McClements, 2002). EOS2 and EOS3 exhibited the highest absolute potential (-12 mV) among OSA starches, and associated with the largest DS (Miao et al., 2014). When the oil to starch ratio decreased (emulsifier concentration increased), the potentials of EOS2- and 3-stabilized emulsions fell from -12.94 and -12.95 mV to -12.09 and -11.93 mV, respectively. The higher DS was related with a lower zeta-potential, revealing that there were more OSA groups at the surface of the modified starch. The zeta-potential could not be measured for the separated emulsions (shown as 'separation' in Table 5.3), indicating a zeta-potential reading is representative of the stable emulsion.

The mechanism of emulsion stabilized by OS starch

OS starches with large molecular size and long branches tend to form stable emulsions. OSA maltodextrins adsorb at interfaces and retard separation of oil and water phases, stabilizing oil droplets against coalescence (Nilsson & Bergenstahl, 2007). Steric stabilization is expected to increase with many branches and especially many long branches (Tesch et al., 2002). In general, steric hindrance is the main stabilizing mechanism of OS starch. At low apparent viscosity of emulsions with high oil loading (low starch content), the increase of DS and degree of branching of the OS starch would form more stable emulsion (Xu et al., 2015). Under the similar DS values, the chemical structure of OS starches was only one factor which influenced the emulsion stability (Wang et al., 2016). For approach 1 (OSA modification first and then enzyme

degradation), the OS groups are bound to starch first and have an action-blocking effect on α -amylolysis of gelatinized starch. Substitution occurred near the branching points as well as at the non-reducing ends. Therefore, after hydrolysis, the OS groups were exposed outside and easy to reach the interface between oil and water. Starch molecular with more branching was preferred to stabilize emulsion by steric hindrance. For approach 2 (enzyme degradation first and then OSA modification), higher DS led to a stronger hydrophobic interaction with the surface of oil droplet to stabilize oil droplets. OS groups distributed randomly throughout the starch chains. Emulsion droplet size is mainly determined by the whole molecular size of the OSA maltodextrins. Our results showed the OSE3 and EOS3 were excellent emulsifiers, whereas the viscosity of emulsion had great effect on its stability. Therefore, both structure of emulsifier and viscosity of emulsion play important role in oil-water emulsion stabilization.

Conclusions

The structural and emulsifying properties of OSA-modified waxy potato maltodextrins produced by two different approaches have been evaluated. With the increase of enzyme concentration, the molecular size and apparent viscosity for all the OSA maltodextrin samples with varying treatments were significantly decreased indicating the molecular degradation due to the enzyme hydrolysis. The α -amylase hydrolyzed products with relatively large molecular sizes and high apparent viscosities presented the best emulsion stability with the lowest creaming extent. Both of OSA-modified waxy potato starch hydrolyzed by α -amylase and waxy potato maltodextrin modified by OSA showed good emulsifying property with small droplets of orange oil when the ratio of oil to starch was 1:1 after 30 days storage. However, at the ratio of 2:1, OS

maltodextrin from approach 1 had better emulsion stability than that from approach 2, but OS maltodextrin from approach 2 had better clarity.

References

- Altuna, L., Herrera, M. L., & Foresti, M. L. (2018). Synthesis and characterization of octenyl succinic anhydride modified starches for food applications. A review of recent literature. *Food Hydrocolloids*, *80*, 97–110.
- Bai, Y. (2013). *Preparation, structure and properties of octenylsuccinic anhydride modified starch*. <https://krex.k-state.edu/dspace/handle/2097/35046>
- Bai, Y., & Shi, Y.-C. (2011). Structure and preparation of octenyl succinic esters of granular starch, microporous starch and soluble maltodextrin. *Carbohydrate Polymers*, *83*(2), 520–527.
- Bai, Y., & Shi, Y.-C. (2013). Reaction of octenylsuccinic anhydride with a mixture of granular starch and soluble maltodextrin. *Carbohydrate Polymers*, *98*(2), 1599–1602.
- Cai, L., Shi, Y.-C., Rong, L., & Hsiao, B. S. (2010). Debranching and crystallization of waxy maize starch in relation to enzyme digestibility. *Carbohydrate Polymers*, *81*(2), 385–393.
- Caldwell, C. G. (1952). *Free-flowing starch esters* (United States Patent No. US2613206A).
- Caldwell, C. G., & Wurzburg, O. B. (1953). *Polysaccharide derivatives of substituted dicarboxylic acids* (Patent No. US2661349 A).
- Chanamai, R., & McClements, D. J. (2002). Comparison of gum arabic, modified starch, and whey protein isolate as emulsifiers: Influence of pH, CaCl₂ and temperature. *Journal of Food Science*, *67*(1), 120–125.
- Charoen, R., Jangchud, A., Jangchud, K., Harnsilawat, T., Decker, E. A., & McClements, D. J. (2012). Influence of interfacial composition on oxidative stability of oil-in-water emulsions stabilized by biopolymer emulsifiers. *Food Chemistry*, *131*(4), 1340–1346.
- Charoen, R., Jangchud, A., Jangchud, K., Harnsilawat, T., Naivikul, O., & McClements, D. J. (2011). Influence of biopolymer emulsifier type on formation and stability of rice bran oil-in-water emulsions: Whey protein, gum arabic, and modified starch. *Journal of Food Science*, *76*(1), E165–E172.
- Dickinson, E. (2018). Hydrocolloids acting as emulsifying agents – How do they do it? *Food Hydrocolloids*, *78*, 2–14.
- Dokić, L., Krstonošić, V., & Nikolić, I. (2012). Physicochemical characteristics and stability of oil-in-water emulsions stabilized by OSA starch. *Food Hydrocolloids*, *29*(1), 185–192.
- Given, P. S. (2009). Encapsulation of flavors in emulsions for beverages. *Current Opinion in Colloid & Interface Science*, *14*(1), 43–47.

- Han, H., Zhang, H., Li, E., Li, C., & Wu, P. (2019). Structural and functional properties of OSA-starches made with wide-ranging hydrolysis approaches. *Food Hydrocolloids*, *90*, 132–145.
- Hategekimana, J., Masamba, K. G., Ma, J., & Zhong, F. (2015). Encapsulation of vitamin E: Effect of physicochemical properties of wall material on retention and stability. *Carbohydrate Polymers*, *124*, 172–179.
- Hsieh, C.-F., Liu, W., Whaley, J. K., & Shi, Y.-C. (2019). Structure and functional properties of waxy starches. *Food Hydrocolloids*, *94*, 238–254.
- Lee, C. J., Kim, Y., Choi, S. J., & Moon, T. W. (2012). Slowly digestible starch from heat-moisture treated waxy potato starch: Preparation, structural characteristics, and glucose response in mice. *Food Chemistry*, *133*(4), 1222–1229.
- Liu, Z., Li, Y., Cui, F., Ping, L., Song, J., Ravee, Y., Jin, L., Xue, Y., Xu, J., Li, G., Wang, Y., & Zheng, Y. (2008). Production of octenyl succinic anhydride-modified waxy corn starch and its characterization. *Journal of Agricultural and Food Chemistry*, *56*(23), 11499–11506.
- McClements, D. J., Decker, E. A., & Weiss, J. (2007). Emulsion-based delivery systems for lipophilic bioactive components. *Journal of Food Science*, *72*(8), R109–R124.
- McClements, David Julian. (2011). Edible nanoemulsions: fabrication, properties, and functional performance. *Soft Matter*, *7*(6), 2297–2316.
- McClements, David Julian, Bai, L., & Chung, C. (2017). Recent advances in the utilization of natural emulsifiers to form and stabilize emulsions. *Annual Review of Food Science and Technology*, *8*(1), 205–236.
- Miao, M., Li, R., Jiang, B., Cui, S. W., Zhang, T., & Jin, Z. (2014). Structure and physicochemical properties of octenyl succinic esters of sugary maize soluble starch and waxy maize starch. *Food Chemistry*, *151*, 154–160.
- Nilsson, L., & Bergenst hl, B. (2007). Adsorption of hydrophobically modified anionic starch at oppositely charged oil/water interfaces. *Journal of Colloid and Interface Science*, *308*(2), 508–513.
- Qiu, D., Bai, Y., & Shi, Y.-C. (2012). Identification of isomers and determination of octenylsuccinate in modified starch by HPLC and mass spectrometry. *Food Chemistry*, *135*(2), 665–671.
- Sanchez, C., Nigen, M., Mejia Tamayo, V., Doco, T., Williams, P., Amine, C., & Renard, D. (2018). Acacia gum: History of the future. *Food Hydrocolloids*, *78*, 140–160.

- Shi, J., Sweedman, M. C., & Shi, Y.-C. (2018). Structural changes and digestibility of waxy maize starch debranched by different levels of pullulanase. *Carbohydrate Polymers*, *194*, 350–356.
- Sun, Z., Chen, Z., Xu, B., & Shi, Y.-C. (2019). Distribution of octenylsuccinate substituents within a single granule of modified waxy maize starch determined by Raman microspectroscopy. *Carbohydrate Polymers*, *216*, 282–286.
- Sweedman, M. C., Schäfer, C., & Gilbert, R. G. (2014). Aggregate and emulsion properties of enzymatically-modified octenylsuccinylated waxy starches. *Carbohydrate Polymers*, *111*, 918–927.
- Sweedman, M. C., Tizzotti, M. J., Schäfer, C., & Gilbert, R. G. (2013). Structure and physicochemical properties of octenyl succinic anhydride modified starches: A review. *Carbohydrate Polymers*, *92*(1), 905–920.
- Tesch, S., Gerhards, C., & Schubert, H. (2002). Stabilization of emulsions by OSA starches. *Journal of Food Engineering*, *54*(2), 167–174.
- Trksak, R., & Makariou, A. (2010). *Alkenyl succinic acid anhydride half ester emulsifier* (United States Patent No. US7829600B1).
- Trubiano, P. C. (1986). Succinate and substituted succinate derivatives of starch. In *Modified starches: Properties and uses* (pp. 131–147). CRC Press.
- Vilaplana, F., & Gilbert, R. G. (2010). Characterization of branched polysaccharides using multiple-detection size separation techniques. *Journal of Separation Science*, *33*(22), 3537–3554.
- Wang, C., He, X., Fu, X., Huang, Q., & Zhang, B. (2016). Substituent distribution changes the pasting and emulsion properties of octenylsuccinate starch. *Carbohydrate Polymers*, *135*, 64–71.
- Wang, Y., Huang, Z., Liu, Z., Luo, S., Liu, C., & Hu, X. (2020). Preparation and characterization of octenyl succinate β -limit dextrin. *Carbohydrate Polymers*, *229*, 115527.
- Won, C., Jin, Y., Kim, M., Lee, Y., & Chang, Y. H. (2017). Structural and rheological properties of potato starch affected by degree of substitution by octenyl succinic anhydride. *International Journal of Food Properties*, *20*(12), 3076–3089.
- Xu, Y., Huang, Q., Fu, X., & Jane, J. (2015). Modification of starch octenylsuccinate by β -amylase hydrolysis in order to increase its emulsification properties. *Food Hydrocolloids*, *48*, 55–61.
- Zhang, H., Schäfer, C., Wu, P., Deng, B., Yang, G., Li, E., Gilbert, R. G., & Li, C. (2018). Mechanistic understanding of the relationships between molecular structure and

emulsification properties of octenyl succinic anhydride (OSA) modified starches. *Food Hydrocolloids*, 74, 168–175.

Zhao, Y., Khalid, N., Shu, G., Neves, M. A., Kobayashi, I., & Nakajima, M. (2017). Formulation and characterization of O/W emulsions stabilized using octenyl succinic anhydride modified kudzu starch. *Carbohydrate Polymers*, 176, 91–98.

Figures

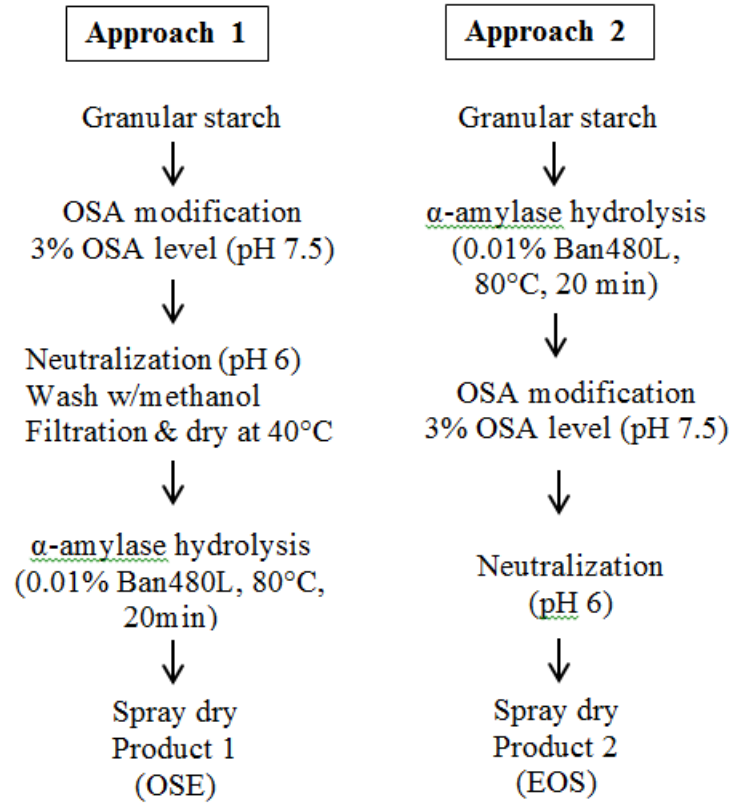


Figure 5.1 Experimental design of two approaches to prepare α -amylase-degraded OSA-modified waxy potato starch

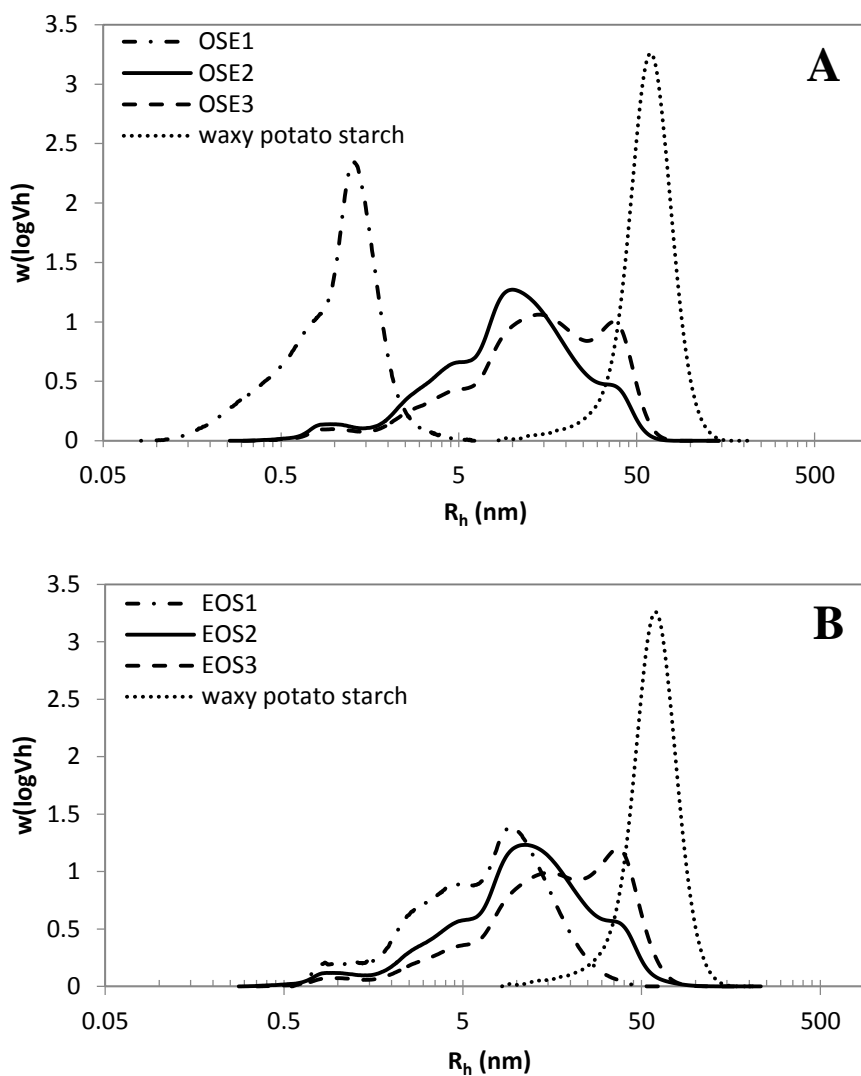


Figure 5.2 Molecular size distribution of waxy potato starch and granular octenylsuccinate maltodextrins obtained from approach 1 (A) and approach 2 (B).

OSE1: OS maltodextrin from Approach 1 of degree of substitution (DS) of 0.0174

OSE2: OS maltodextrin from Approach 1 of DS of 0.0176

OSE3: OS maltodextrin from Approach 1 of DS of 0.0175

EOS1: OS maltodextrin from Approach 2 of DS of 0.0209

EOS2: OS maltodextrin from Approach 2 of DS of 0.0210

EOS3: OS maltodextrin from Approach 2 of DS of 0.0210

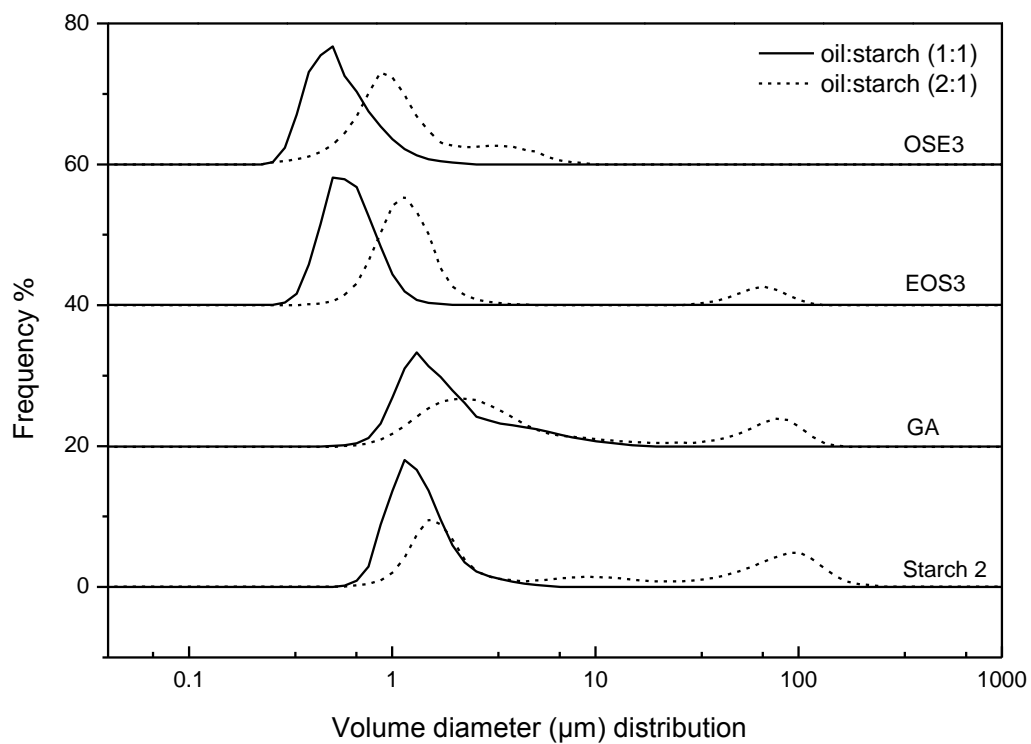


Figure 5.3 Effects of selected good emulsifiers for the storage of 14 days: OSE3, EOS3, gum arabic (GA), and commercial OS starch 2 (Starch 2) on the particle size of emulsions with the ratio of oil to starch 1:1 and 2:1 after 30 days of storage at room temperature.

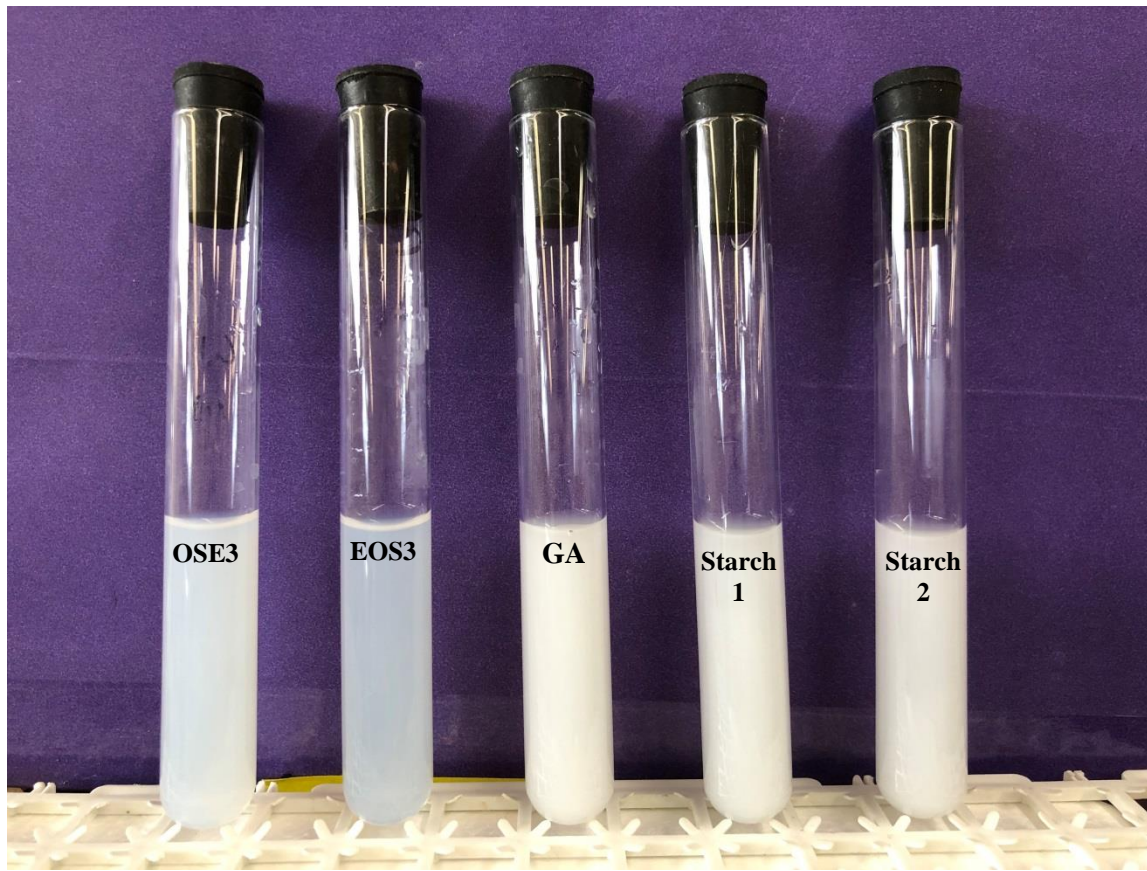


Figure 5.4 The appearance of emulsions stabilized by OSE3, EOS3, gum arabic (GA), and commercial OS starch 1 (Starch 1) and 2 (Starch 2) with diluted 1:100 by water at the same ratio of oil to starch 1:1.

Tables

Table 5.1 Degree of substitution (DS), dextrose equivalent (DE) and viscosity for octenylsuccinate (OS) maltodextrins prepared from approach 1 and approach 2 in Figure 5.1

Sample	Treatments	Enzyme concentration	DS	DE	Viscosity (cp)*
OSE1	OSA (3%) + α -amylase	0.02%	0.0174 \pm 0.0002	7.42	6.5
OSE2		0.01%	0.0176 \pm 0.0004	5.34	13.0
OSE3		0.005%	0.0175 \pm 0.0005	4.97	26.0
EOS1	α -amylase + OSA (3%)	0.01%	0.0209 \pm 0.0008	6.57	8.0
EOS2		0.005%	0.0210 \pm 0.0003	5.25	15.5
EOS3		0.0005%	0.0210 \pm 0.0006	4.39	30.5

* Viscosity was measured using Brookfield spindle #21 running at 100 rpm at 10% solid content.

Table 5.2 Formulation of orange oil emulsions using degraded octenylsuccinic anhydride maltodextrin with different ratios of oil to starch

Designed ratio	Amount (g)			
	Oil (g) :Starch (g)	Orange oil^a	OS starch	Water^b
1:1		12	12	76
2:1		16	8	76
3:1		18	6	76

^a Composition of orange oil mix: 48% orange oil (1X), 12% orange oil (5X), and 40% ester gum 8BG.

^b Water contains 0.3% citric acid, and 0.15% sodium benzoate.

Table 5.3 Particle size (μm), zeta-potential (mV) and apparent viscosity (η , cp) of fresh orange oil emulsions using degraded octenylsuccinic anhydride maltodextrin in Figure 5.1 with different ratios of oil to starch, and particle size, zeta-potential and creaming index (%) were measured after the storage of 14 days

Sample	oil: starch	Fresh emulsion (1 h)			Storage of 14 d		
		η (cp)	Droplet size (μm)	ζ -potential (mV)	Droplet size (μm)	ζ -potential (mV)	Creaming index (%)
OSE1	1:1	11.0	1.346 ± 0.016	N/A ^a	separation	N/A	18.5 ± 0.9
	2:1	9.5	1.566 ± 0.018	N/A ^a	separation	N/A	20.1 ± 1.8
	3:1	6.5	1.767 ± 0.018	N/A ^a	separation	N/A	21.7 ± 1.4
OSE2	1:1	19.5	0.526 ± 0.021	-9.90 ± 0.67	2.320 ± 0.013	-10.38 ± 0.66	N/A
	2:1	16.5	0.666 ± 0.017	-10.60 ± 0.75	3.810 ± 0.086	-10.94 ± 0.26	N/A
	3:1	12.0	1.295 ± 0.014	-11.19 ± 0.32	separation	N/A	N/A
OSE3	1:1	24.5	0.313 ± 0.010	-10.00 ± 0.88	0.506 ± 0.010	-10.45 ± 1.07	N/A
	2:1	18.0	0.318 ± 0.021	-11.53 ± 0.50	0.731 ± 0.015	-11.10 ± 0.53	N/A
	3:1	15.5	0.520 ± 0.004	-11.59 ± 0.74	0.927 ± 0.016	-12.09 ± 0.52	N/A
EOS1	1:1	14.0	2.185 ± 0.123	N/A ^a	separation	N/A	30.9 ± 0.8
	2:1	10.5	3.560 ± 0.081	N/A ^a	separation	N/A	33.7 ± 1.2
	3:1	8.5	3.973 ± 0.090	N/A ^a	separation	N/A	35.1 ± 1.9
EOS2	1:1	16.5	1.673 ± 0.122	-12.09 ± 0.43	separation	N/A	28.6 ± 1.8
	2:1	13.0	2.544 ± 0.020	-12.18 ± 0.43	separation	N/A	31.3 ± 0.9
	3:1	11.0	2.648 ± 0.124	-12.94 ± 0.52	separation	N/A	32.4 ± 1.1
EOS3	1:1	26.0	0.326 ± 0.021	-11.93 ± 0.69	0.593 ± 0.037	-13.10 ± 0.53	N/A
	2:1	20.5	0.428 ± 0.014	-12.67 ± 0.02	0.773 ± 0.029	-13.25 ± 0.14	N/A
	3:1	18.5	0.632 ± 0.012	-12.95 ± 0.58	0.903 ± 0.045	-14.65 ± 1.23	N/A
Gum Arabic	1:1	29.0	0.811 ± 0.014	-21.82 ± 0.50	1.268 ± 0.058	-21.32 ± 0.98	N/A
	2:1	23.5	0.949 ± 0.021	-23.44 ± 1.04	1.698 ± 0.162	-22.02 ± 1.07	N/A
	3:1	16.5	1.609 ± 0.013	-23.85 ± 1.01	separation	N/A	N/A
Starch 1	1:1	12.5	0.359 ± 0.004	-8.25 ± 0.36	1.488 ± 0.067	-11.01 ± 0.89	N/A
	2:1	6.5	0.865 ± 0.022	-8.33 ± 0.56	separation	N/A	N/A
	3:1	4.0	0.958 ± 0.026	-8.41 ± 0.49	separation	N/A	N/A
Starch 2	1:1	22.5	0.524 ± 0.008	-8.10 ± 0.15	1.214 ± 0.098	-10.57 ± 1.02	N/A
	2:1	16.5	0.759 ± 0.011	-8.18 ± 0.13	1.495 ± 0.093	-10.95 ± 0.58	N/A
	3:1	12.5	0.882 ± 0.016	-8.35 ± 0.81	2.804 ± 0.083	-11.09 ± 1.43	N/A

^aData was not determined.

Chapter 6 - Changes in molecular size and shape of waxy maize starch during dextrinization

Abstract

The conformational properties of pyrodextrins from waxy maize starch were investigated by high performance size exclusion chromatography with multiple detectors, and the relationships (Mark-Houwink equations) between molecular weights and intrinsic viscosities of pyrodextrins in water were established. Pyrodextrin was prepared by adjusting waxy maize starch to pH 3 or 2, heating at 170 °C or 150 °C. As heating time increased from 0.5 to 4 h, the molecular size was decreased in the order of pH 2 and 150 °C > pH 3 and 170 °C > pH 3 and 150 °C. The measured exponent α values in Mark-Houwink equation indicated that pyrodextrins prepared at pH 3, 170 °C and 150 °C only had one compact spherical conformation (α 0.27-0.31) during dextrinization, whereas pyrodextrins at pH 2 and 150 °C had a mixture of two shapes of molecules: compact sphere (α 0.26) and rigid coil (α 0.89) conformation.

Keywords

Pyrodextrin; Thermal treatment; Conformation; Size exclusion chromatography; Starch

Introduction

Pyrodextrins are degraded starch products prepared by a process involving heat treatment and/or acidification of granular starch and widely used as adhesives, coatings, binders, and encapsulating agents in foods, pharmaceuticals, paper, and textile industries (Bai et al., 2014; Bai & Shi, 2016; Han et al., 2018; Wurzburg, 1986, 2006). Pyrodextrins could also be a source of soluble dietary fiber due to their resistance to α -amylase (Ashwar et al., 2016; Cao et al., 2018; Kwon et al., 2005; Laurentin & Edwards, 2004; Sajilata et al., 2006).

The structural changes during pyroconversion from native waxy maize starch granules to pyrodextrin has been investigated in our laboratory (Bai et al., 2014; Bai & Shi, 2016; Han et al., 2018). Hydrolysis of the starch molecules in both amorphous and crystalline regions occurred but the radial arrangement of the starch molecules remained during dextrinization (Bai et al., 2014). New chemical bonds formed during dextrinization were determined by nuclear magnetic resonance spectroscopy (NMR) (Bai & Shi, 2016), and the retrogradation properties of pyrodextrins were examined by differential scanning calorimetry (DSC) (Han et al., 2018; Weil et al., 2020). The dextrinization caused a decrease in pyrodextrin molecular size and average molecular weight, gelatinization and retrogradation endotherm, and average chain length (CL) as solubility and degree of branching (DB) increased with dextrinization time. However, the conformational properties of the pyrodextrins have not been studied.

High performance size exclusion chromatography (HPSEC) with multi angle light scattering (MALS), intrinsic viscosity and refractive index (RI) detectors has been employed to determine molecular structure and conformational properties (dimensions and shape characterization) via parameters such as absolute molecular weight (MW), MW distribution,

polydispersity index (M_w/M_n), intrinsic viscosity $[\eta]$, hydrodynamic radius (R_h), radius of gyration (R_g), and the exponent (α) in Mark-Houwink equation (Kang et al., 2015, 2018; Lee et al., 2009; Millard et al., 1997; Vilaplana & Gilbert, 2010; Yokoyama et al., 1998). Intrinsic viscosity $[\eta]$ is useful to characterize the conformation, as function of average molecular weight, M_w , and represented by Mark-Houwink equation:

$$[\eta] = kM_w^\alpha \quad (1)$$

where k is a constant for a given polysaccharide-solvent-temperature system, and the exponent α can be determined by evaluating a plot of $\log [\eta]$ vs. logarithmic molecular weight by HPSEC-triple detectors (Kang et al., 2015). Both k and α values are related to the stiffness of the polymer and depend on the particular polymer-solvent pair and on the temperature. The parameter k is dependent mainly on the geometry of the inter-residue linkages with the polymer chain (Lapasin, 2012). The logarithmic slope α values reveals three dimensional chain conformation: sphere, random coil, and rod shapes (Wyatt, 1993). The α values are 0.0–0.5 for compact sphere in branched polymers, 0.5–0.8 for random coil in flexible macromolecules, and as high to 2.0 for rigid rods in more extended polymer (Lapasin, 2012).

The molecular weight, dimensions, and shape of starch are important in determining its functional properties such as viscosity, stability, pasting, and digestibility (Fishman et al., 1996; Jane et al., 1999; Terpstra et al., 2010; Wurzburg, 1986, 2006). The stability of the solution of pyrodextrins differs widely depending upon the degree of pyroconversion. Branched structures give more stable solution than linear ones. Waxy maize starch contains essentially 100% amylopectin (branched polymers). We hypothesize that conformation of waxy maize starch changes during dextrinization and pyrodextrins have a mixture of compact sphere and rigid coil conformation. The objective of this study was to characterize the molecular size and shape

changes in waxy maize starch during dextrinization as well as its fractions by obtaining relationships between weight-average molecular weights (M_w), intrinsic viscosities ($[\eta]$), and hydrodynamic radius (R_h) in water. The information gained would be useful in understanding rheological properties particularly solution and paste viscosity and stability of pyrodextrins and guiding the use of pyrodextrins in food, beverage, and industrial applications such as adhesives.

Materials and methods

Materials

Waxy maize starch (Amoica) was obtained from Ingredion Incorporated (Bridgewater, NJ, USA). All other chemicals used were analytical grade.

Preparation of pyrodextrin

Pyrodextrins were prepared as described by Bai et al., (2014) and Bai & Shi, (2016). Briefly, waxy maize starch slurry of 40% solid content was adjusted to pH 3.0 by adding HCl solution (0.5 M). After filtration and drying, the starch was heated in an oven at 150 °C or 170 °C for 0.5, 1, 2, 3, and 4 h. The experiments were also prepared the samples described as above by pH adjustment of 2.0 and at 150 °C.

Solubility

Solubility of pyrodextrin was determined by a hand-held refractometer (Fisher Scientific, Pittsburgh, PA, USA). Pyrodextrin (0.100 g) was dissolved in distilled water (0.9 mL) and mixed by vortex. The slurry was centrifuged at 6708 g for 3 min. Pyrodextrin concentration in the supernatant was determined.

Gel permeation chromatography (GPC)

GPC analysis was performed as previously described by Shi et al. (2018). Each pyrodextrin sample (4 mg) were dissolved in 4 mL dimethyl sulfoxide (DMSO) containing lithium bromide (0.5% w/w) and stirred at room temperature for 12 h. The mixture was filtered through a 2 μm filter and then injected into a PL-GPC 220 instrument (Polymer Laboratories, Inc., Amherst, MA, USA) equipped with three Phenogel columns (00H-0642-K0; 00H-0644-K0; 00H-0646-K0) and one guard column (03B-0290-K0) (Phenomenex Inc., Torrance, CA, USA), and a differential refractive index detector. The eluent was DMSO containing 0.5% (w/w) LiBr, and the flow rate was 0.8 mL/min. The molecular size (hydrodynamic radius, R_h) distribution was determined as described by Vilaplana & Gilbert (2010).

High-performance size-exclusion chromatography (HPSEC)

The molecular characterization was determined using a HPSEC (1100 Series, Agilent Technologies, Waldbronn, Germany) equipped with multiple detectors: a combined light scattering and viscometric detector (Viscotek 270 Dual Detector, Malvern Instruments, Westborough, MA) for molecular weight and intrinsic viscosity determination and a refractive index (RI) detector (Viscotek VE3580 RI Detector, Malvern Instruments, Westborough, MA) for concentration determination. Two columns PSS SUPREMA 3000 \AA (10 μm , 8 \times 300 mm and 100 μm , 8 \times 300 mm) with a guard column (10 μm , 8 \times 50 mm) were used for the water-based eluent (0.1 M sodium nitrate (NaNO_3) containing 0.03% (w/w) sodium azide (NaN_3)) at a flow rate of 1.0 mL/min and injection volume was 100 μL .

Each sample (1 mg) was dissolved in 1 mL distilled water at room temperature for 2h. For some samples that were not 100% soluble in water at 25 $^\circ\text{C}$, they were neutralized by 0.001

N NaOH to pH 6.5 and heated at 60 °C in a water bath for 10–20 min until the samples were completely dissolved. All samples were cooled to room temperature and filtered through a 0.45 µm nylon syringe filter directly into small vials, and then analyzed. All the calculations regarding polydispersity index, molecular weight averages, intrinsic viscosities, hydrodynamic radius, and the Mark-Houwink α value were processed and analyzed with the OmniSEC 4.7 software (Malvern, TX, USA).

Statistical analysis

Each experiment was performed in duplicate. The statistical analysis was conducted using a Statistical Analysis System (SAS, version 9.3 for Windows, SAS Institute, Cary, NC, USA). Least significant difference for comparison of means was computed at $P < 0.05$.

Results and discussion

Water solubility

The water solubility of pyrodextrins at different thermal treatments is shown in Table 6.1. The solubility of the pyrodextrins prepared at pH 3, 150 °C and 170 °C increased from 64.7% to 100% and 78.7% to 100% by heating from 0.5 h to 4 h, respectively. Starch became 100% soluble after heating for 3 h. At pH 3, the solubility of starch increased rapidly during conversion at the beginning (0.5 h) and reached to 100% at 3 h. In contrast, at pH 2 and 150 °C, starch became 100% soluble after heating for 0.5 h, indicating that lower pH affected starch degradation at a faster rate.

Molecular size distribution of pyrodextrins

The molecular size distribution of the pyrodextrins is shown in Fig. 6.1. Compared with the unmodified waxy maize starch, the molecular size of the pyrodextrins was significantly reduced (Figure B.1, Appendix B); a similar pattern using relative molecular weight ($\log M_w$) was reported by Bai et al. (2014) but in this study, the molecular size distribution profile using hydrodynamic radius (R_h) as described by Vilaplana & Gilbert (2010) was reported. Acid hydrolyzed the glucosidic linkages in the starch and decreased the molecular weight and size (Bai et al., 2014; Wang & Wang, 2001; Wang et al., 2003; Wurzburg, 1986, 2006). Pyrodextrins treated at pH 3 and 170 °C for different periods of time 0.5–4.0 h was compared in Fig. 6.1A. The profiles of each pyrodextrin showed two peaks of different groups of molecular sizes at first 2 h, where the first peak appearing at $R_h = 4\text{--}6$ nm and the second peak at $R_h = 8\text{--}10$ nm. As heating time increased, the proportion of the larger molecular size peak decreased rapidly at the beginning (0.5–2 h) and had relatively little change after 3 h of heating. At the latter stage of dextrinization, starch molecular size mainly retained one broad smaller molecular size peak. Pyrodextrins prepared at pH 3 and 150 °C also exhibited two peaks of different groups of molecular sizes (first peak $R_h = 5$ nm and second peak $R_h = 10$ nm) at 0.5–4 h in Fig. 6.1B. Increasing the heating time, the proportion of the larger molecular size peak had little change at the first 2 hours, and dramatically decreased after 3 h of heating. At the same time, the proportion of the smaller molecular size peak increased. After 3 h, at pH 3 and 150 °C, there was no shift in molecular size distribution profile. At pH 2 and 150 °C, there was no change in molecular size (peak $R_h = 3$ nm) during dextrinization between 0.5 and 4 h, indicating that starch was degraded in granular form by the acid at lower pH (pH = 2) in the first 0.5 h (Fig. 6.1C). The

results on those three different pyrodextrins suggest that for the first 0.5 h, pH is a more critical factor on the pyrodextrin structure compared with temperature. After heating for 0.5 h, temperature has greater effect on starch molecular scission.

Pyrodextrins prepared with the same processing time but different temperatures and pHs were compared in Fig. 6.2D, 6.2E, and 6.2F. After heating for 0.5 h, molecular size of pyrodextrin at pH 3, 150 °C and 170 °C had the similar molecular size range with two peak R_h s of 5 and 10 nm, respectively (Fig. 6.1D). However, pyrodextrin prepared at pH 2, 150 °C already had a much smaller molecular size at 0.5 h compared with pyrodextrins prepared at pH 3, 150 °C and pH 3, 170 °C in this study (Fig. 6.1D). As heating time increased to 2h (Fig. 6.1E) and 4 h (Fig. 6.1F), the proportion of the larger molecular size peak (peak 2) of pyrodextrin prepared at pH 3, 170 °C decreased more than that of pyrodextrin prepared at pH 3, 150 °C, indicating that more conversion occurred at higher temperature. These results suggest that starch molecular scission was promoted by higher temperature at the same pH value. At the end of dextrinization (4 h), the molecular size of pyrodextrins prepared at different conditions were in the order of pH 2 and 150 °C < pH 3 and 170 °C < pH 3 and 150 °C.

Conformational properties of pyrodextrins

Conformational parameters such as weight-average molecular weight (M_w), intrinsic viscosity $[\eta]$, hydrodynamic radius (R_h), and exponent (α) in Mark-Houwink equation were determined by HPSEC coupled with multiple detectors: refractive index, low/right angle light scattering and viscometer, and reported in Table 6.2.

After heating at 150 °C and 170 °C, pH 3 for 0.5 h, pyrodextrins had a similar average molecular weight (~142 kDa) (Fig. 6.2A, a and b). However, as the time increased to 4 h, the

pyrodextrins prepared at 170 °C had a rapidly decrease in average molecular weight, decreasing from ~142 kDa (0.5 h) to 46.7 kDa (4.0 h). After 4 h of dextrinization, the largest average molecular weight (~80 kDa) was obtained from pyrodextrin at pH 3 and 150 °C. The molecular weight of pyrodextrin at pH 3, 150 °C had a dramatically decrease from 2 to 3 h, but little changes after 3h. Pyrodextrin prepared at pH 2 and 150 °C had similar average molecular weight (~21 kDa) between 0.5 and 4 h, which was consistent with molecular size data in Fig. 6.1C obtained from GPC. Compared to other two sets of pyrodextrins prepared at pH 3, pyrodextrins at pH 2 had lowest absolute Mw with the highest retention volume (Fig. 6.2A, c), indicating that the level of acid used played a major role in degrading the starch during dextrinization.

In Table 6.2, hydrodynamic radius (R_h) of pyrodextrins prepared at pH 3, 170 °C and 150 °C, and pH 2 and 150 °C from 0.5 to 4 h decreased from 5.59 to 3.50 nm, 5.61 to 4.46 nm, and 2.62 to 2.46, respectively. Pyrodextrins were separated in solution by their size or hydrodynamic volume (V_h), which is proportional to the average molecular weight (M_w) and intrinsic viscosity $[\eta]$ (Vilaplana & Gilbert, 2010). This size parameter, hydrodynamic volume V_h can be equivalent to the hydrodynamic radius (R_h) with equation: $V_h = 4/3\pi R_h^3$ (Eq. 3).

Intrinsic viscosity (IV, $[\eta]$) is related to polysaccharide conformation (Kang et al., 2015). IV of pyrodextrins prepared at pH 3, 170 °C and 150 °C decreased from 0.106 to 0.078 dL/g, and 0.109 to 0.094 dL/g, respectively from 0.5 to 4 h (Table 6.2). The pyrodextrins prepared at pH 2 had the lowest value of $[\eta]$ at 0.06 dL/g, indicating that lower molecular weight was related to lower value of intrinsic viscosity (Fig. 6.2 A and B), and the level of acid used played a major role in degrading the starch during dextrinization.

The average of Mark-Houwink α value for each pyrodextrin in different conditions was also shown in Table 6.2. The average α values of all pyrodextrins was in the range of 0.22–0.39.

However, the average α values may not reflect molecular shape changes for the whole molecular weight distribution (Fig. 6.3), and detailed analysis is needed. Based on Mark-Houwink equation (Eq. 6.1), the exponent α can be determined by evaluating a plot of $\log [\eta]$ vs. logarithmic molecular weight, as

$$\log[\eta] = \log k + \alpha \log M_w \quad (2)$$

According to quadratic equation, α is the slope and $\log k$ is the y-intercept. Fig. 6.3 showed the relationship between logarithmic plots of the molecular weight vs. intrinsic viscosity determined by HPSEC-triple detectors. When the M_w and $[\eta]$ data were plotted on a log-log scale (Eq. 2) as in Fig. 6.3 and fitted to a straight line by regression, a Mark-Houwink relation was obtained. These figures help us to understand the changes of molecular shape of pyrodextrins during dextrinization. A linear relationship between $\log M_w$ and $\log [\eta]$ was observed in pyrodextrins prepared at pH 3, 150 °C and 170 °C for 4 h, where the slope (exponent α) was less than 0.5 (0.277 and 0.269, respectively) (Fig. 6.3, A and B), indicating a compact sphere conformation. In contrast, the logarithmic plot of pyrodextrins prepared at lower pH (pH = 2, heating at 150 °C for 4 h) (Fig. 6.3C) was very different from others. At lower molecular weight range ($M_w 10^{3.0} - 10^{4.1}$ Da), α value was 0.8855, in the range of 0.8–1.8 for rigid coil conformation; however, at higher molecular weight range ($M_w 10^{4.1} - 10^{5.1}$ Da), α value decreased to 0.2557 for compact sphere conformation. At pH 2, acid-catalyzed degradation in starch probably has a strong pyroconversion, and as a result, shorter side chains form a less flexible structure.

The parameter k equals 10 to the power of the y-intercept in Fig. 6.3 (Eq. 2). For pyrodextrins prepared at pH 3, 150 °C and 170 °C for 4 h, one Mark-Houwink equation, $[\eta] = 0.002 M_w^{0.27}$, may be used to represent the relationship between weight-average molecular weights (M_w) and intrinsic viscosities ($[\eta]$) for compact sphere conformation. In contrast, two

Mark-Houwink equations are needed for pyrodextrins prepared at pH 2 and 150 °C: $[\eta] = 0.133 \times 10^{-4} M_w^{0.89}$ for rigid coil ($M_w 10^{3.0} - 10^{4.1}$ Da), and $[\eta] = 0.005 M_w^{0.26}$ for compact sphere ($M_w 10^{4.1} - 10^{5.1}$ Da).

The pyrodextrin prepared at pH 2 and 150 °C had a lower M_w and intrinsic viscosity than the pyrodextrins prepared at pH 3 and 150 °C and pH 3 and 170 °C (Table 6.2). We would expect that a higher solids concentration is needed for the pyrodextrin prepared at pH 2 and 150 °C to reach the critical concentration at which overlapping of the domains of pyrodextrin molecules in solution first occurs. It would be interesting to establish the relationship between viscosity and pyrodextrin concentration for pyrodextrins prepared at different conditions in the future work. The magnitude in viscosity increase with increasing in solids concentration would be different among pyrodextrins because the results from this study demonstrate that pyrodextrins have different conformational properties depending on processing conditions (pH and temperature). Solution and paste stability may also be affected by the conformation of the pyrodextrins in water although chain length of the pyrodextrins plays a critical role (Han et al., 2018).

We should note that in this study, the size and shape of the amylopectin in waxy maize starch was not measured in water by HPSEC because of its tendency to aggregate. Waxy maize starch was composed of essentially 100% amylopectin. It has been a challenge to determine the exact size and shape of amylopectin because for an accurate analysis, a complete dissolution of the starch in solvent is required; yet amylopectin has a very large molecular weight and tends to aggregate in aqueous solutions (Lee et al., 2014). Microwave heating in a high-pressure vessel has been used to dissolve starch in water (Bello-Perez et al., 1998; Fishman & Hoagland, 1994). Using analytical ultracentrifugation, Lelievre et al. (1986) reported that the amylopectin from

wheat starch in DMSO had a flat-sheet or disc-like, oblate ellipsoid structure with semi-major and semi-minor axes of 45 and 1.2 nm, respectively. Callaghan and Lelievre (1985) suggested that amylopectin from wheat starch aggregated in water to form a large spherical shape that had a volume about 400 times larger than the single molecule.

Conclusions

The molecular size decreased in the order of pyrodextrins prepared at pH 2 and 150 °C > pH 3 and 170 °C > pH 3 and 150 °C. The relationship between molecular weight and intrinsic viscosity (Mark-Houwink equation) was established for the pyrodextrins. The measured Mark-Houwink α values indicated that pyrodextrins prepared at pH 3, 170 °C and 150 °C only had one compact spherical conformation (α 0.27 - 0.31) with average R_h 5.59 to 3.50 nm, and 5.61 to 4.46 nm during dextrinization, respectively, whereas pyrodextrins at pH 2 and 150 °C had a mixture of two shapes of molecules: compact sphere (α 0.26) and rigid coil (0.89) conformation.

References

- Ashwar, B. A., Gani, A., Shah, A., Wani, I. A., & Masoodi, F. A. (2016). Preparation, health benefits and applications of resistant starch—a review. *Starch - Stärke*, 68(3–4), 287–301.
- Bai, Y., Cai, L., Douth, J., Gilbert, E. P., & Shi, Y.-C. (2014). Structural changes from native waxy maize starch granules to cold-water-soluble pyrodextrin during thermal treatment. *Journal of Agricultural and Food Chemistry*, 62(18), 4186–4194.
- Bai, Y., & Shi, Y.-C. (2016). Chemical structures in pyrodextrin determined by nuclear magnetic resonance spectroscopy. *Carbohydrate Polymers*, 151, 426–433.
- Bello-Pérez, L. A., Colonna, P., Roger, P., & Parees-López, O. (1998). Laser light scattering of high amylose and high amylopectin materials in aqueous solution, effect of storage time. *Carbohydrate Polymers*, 37(4), 383–394.
- Callaghan, P. T., & Lelievre, J. (1985). The size and shape of amylopectin: A study using pulsed-field gradient nuclear magnetic resonance. *Biopolymers*, 24(3), 441–460.
- Cao, Y., Chen, X., Sun, Y., Shi, J., Xu, X., & Shi, Y.-C. (2018). Hypoglycemic effects of pyrodextrins with different molecular weights and digestibilities in mice with diet-induced obesity. *Journal of Agricultural and Food Chemistry*.
- Fishman, M., & Hoagland, P. (1994). Characterization of starches dissolved in water by microwave heating in a high pressure vessel. *Carbohydrate Polymers*, 23(3), 175–183.
- Fishman, M. L., Rodriguez, L., & Chau, H. K. (1996). Molar masses and sizes of starches by high-performance size-exclusion chromatography with on-line multi-angle laser light scattering detection. *Journal of Agricultural and Food Chemistry*, 44(10), 3182–3188.
- Han, X., Kang, J., Bai, Y., Xue, M., & Shi, Y.-C. (2018). Structure of pyrodextrin in relation to its retrogradation properties. *Food Chemistry*, 242, 169–173.
- Jane, J., Chen, Y. Y., Lee, L. F., McPherson, A. E., Wong, K. S., Radosavljevic, M., & Kasemsuwan, T. (1999). Effects of amylopectin branch chain length and amylose content on the gelatinization and pasting properties of starch. *Cereal Chemistry*, 76(5), 629–637.
- Kang, J., Guo, Q., & Shi, Y.-C. (2018). Molecular and conformational properties of hemicellulose fiber gum from dried distillers grains with solubles. *Food Hydrocolloids*, 80, 53–59.
- Kang, J., Guo, Q., Wang, Q., Phillips, G. O., & Cui, S. W. (2015). New studies on gum ghatti (*Anogeissus latifolia*) part 5: The conformational properties of gum ghatti. *Food Hydrocolloids*, 43, 25–30.

- Kwon, S., Koo, M. C., Shin, S. I., & Moon, T. W. (2005). Contents of indigestible fraction, water solubility, and color of pyrodextrins made from waxy sorghum Starch. *Cereal Chemistry; St. Paul*, 82(1), 101–104.
- Lapasin, R. (2012). *Rheology of Industrial Polysaccharides: Theory and Applications*. Springer Science & Business Media.
- Laurentin, A., & Edwards, C. A. (2004). Differential fermentation of glucose-based carbohydrates in vitro by human faecal bacteria: A study of pyrodextrinised starches from different sources*. *European Journal of Nutrition; Heidelberg*, 43(3), 183–189.
- Lee, J. H., Han, J.-A., & Lim, S.-T. (2009). Effect of pH on aqueous structure of maize starches analyzed by HPSEC-MALLS-RI system. *Food Hydrocolloids*, 23(7), 1935–1939.
- Lelievre, J., Lewis, J. A., & Marsden, K. (1986). The size and shape of amylopectin: a study using analytical ultracentrifugation. *Carbohydrate Research*, 153(2), 195–203.
- Millard, M. M., Dintzis, F. R., Willett, J. L., & Klavons, J. A. (1997). Light-scattering molecular weights and intrinsic viscosities of processed waxy maize starches in 90% dimethyl sulfoxide and H₂O. *Cereal Chemistry*, 74(5), 687–691.
- Sajilata, M. G., Singhal, R. S., & Kulkarni, P. R. (2006). Resistant Starch—A Review. *Comprehensive Reviews in Food Science and Food Safety*, 5(1), 1–17.
- Shi, J., Sweedman, M. C., & Shi, Y.-C. (2018). Structural changes and digestibility of waxy maize starch debranched by different levels of pullulanase. *Carbohydrate Polymers*, 194, 350–356.
- Terpstra, K. R., Woortman, A. J. J., & Hopman, J. C. P. (2010). Yellow dextrins: Evaluating changes in structure and colour during processing. *Starch - Stärke*, 62(9), 449–457.
- Vilaplana, F., & Gilbert, R. G. (2010). Characterization of branched polysaccharides using multiple-detection size separation techniques. *Journal of Separation Science*, 33(22), 3537–3554.
- Wang, L., & Wang, Y.-J. (2001). Structures and Physicochemical Properties of Acid-Thinned Corn, Potato and Rice Starches. *Starch - Stärke*, 53(11), 570–576.
- Wang, Y.-J., Truong, V.-D., & Wang, L. (2003). Structures and rheological properties of corn starch as affected by acid hydrolysis. *Carbohydrate Polymers*, 52(3), 327–333.
- Weil, W., Weil, R. C., Keawsompong, S., Sriroth, K., Seib, P. A., & Shi, Y.-C. (2020). Pyrodextrin from waxy and normal tapioca starches: Physicochemical properties. *Food Hydrocolloids*, 104, 105745.

Wurzburg, O. B. (1986). Converted starches. In *Modified starches-properties and uses*. CRC Press.

Wurzburg, O. B. (2006). *Food polysaccharides and their applications: Vol. pp. 87-118* (6th ed.). CRC Press.

Wyatt, P. J. (1993). Light scattering and the absolute characterization of macromolecules. *Analytica Chimica Acta*, 272(1), 1–40.

Yokoyama, W., Renner-Nantz, J. J., & Shoemaker, C. F. (1998). Starch molecular mass and size by size-exclusion chromatography in DMSO-LiBr coupled with multiple angle laser light scattering. *Cereal Chemistry*, 75(4), 530–535.

Figures

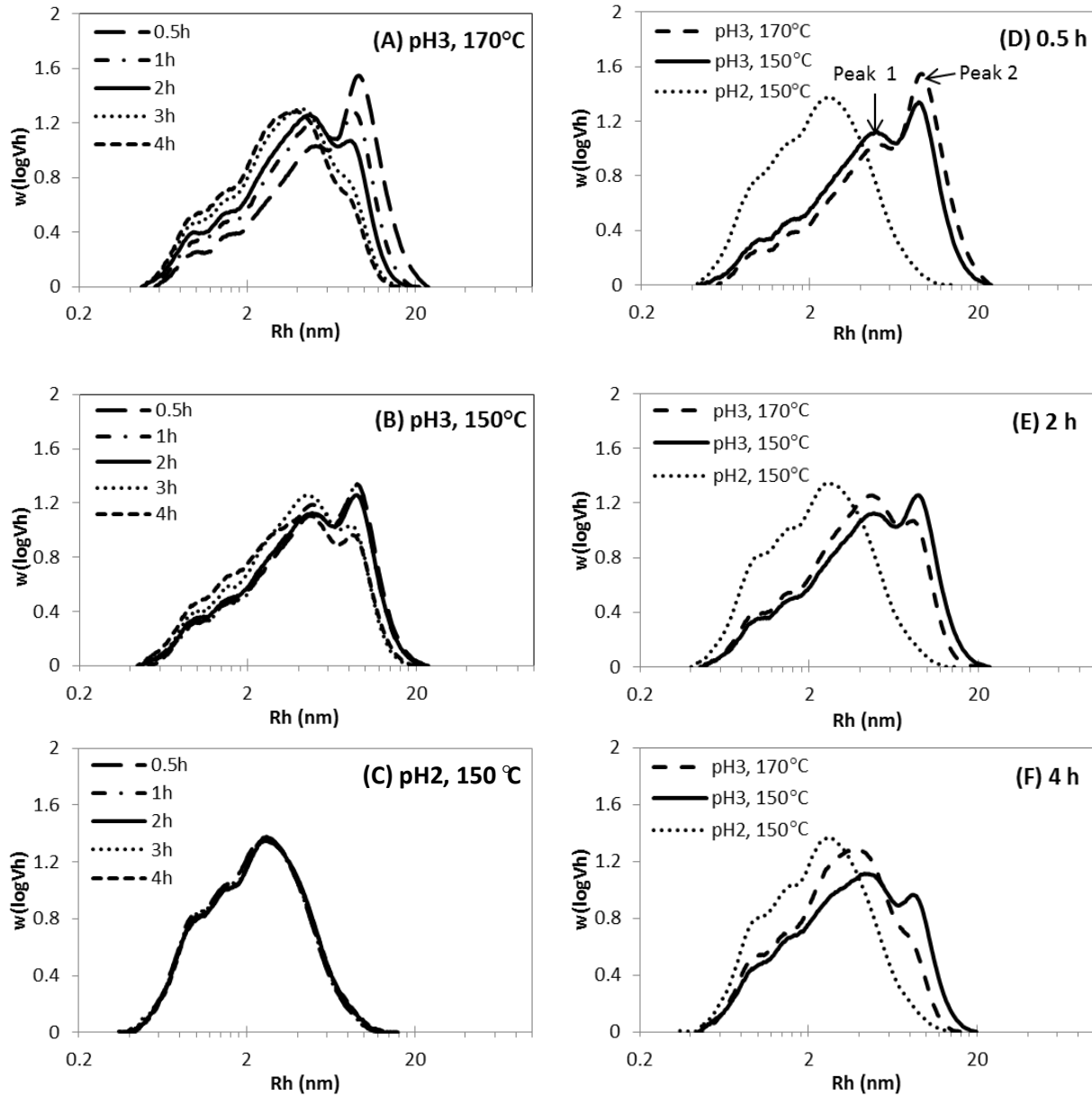


Figure 6.1 Molecular size distribution of pyrodextrins prepared at (A) pH 3 and 170 °C, (B) pH 3 and 150 °C, and (C) pH 2 and 150 °C at different time (0.5 h to 4 h) and the pyrodextrins prepared at (D) 0.5 h, (E) 2 h, and (F) 4 h as determined by gel permeation chromatography (GPC).

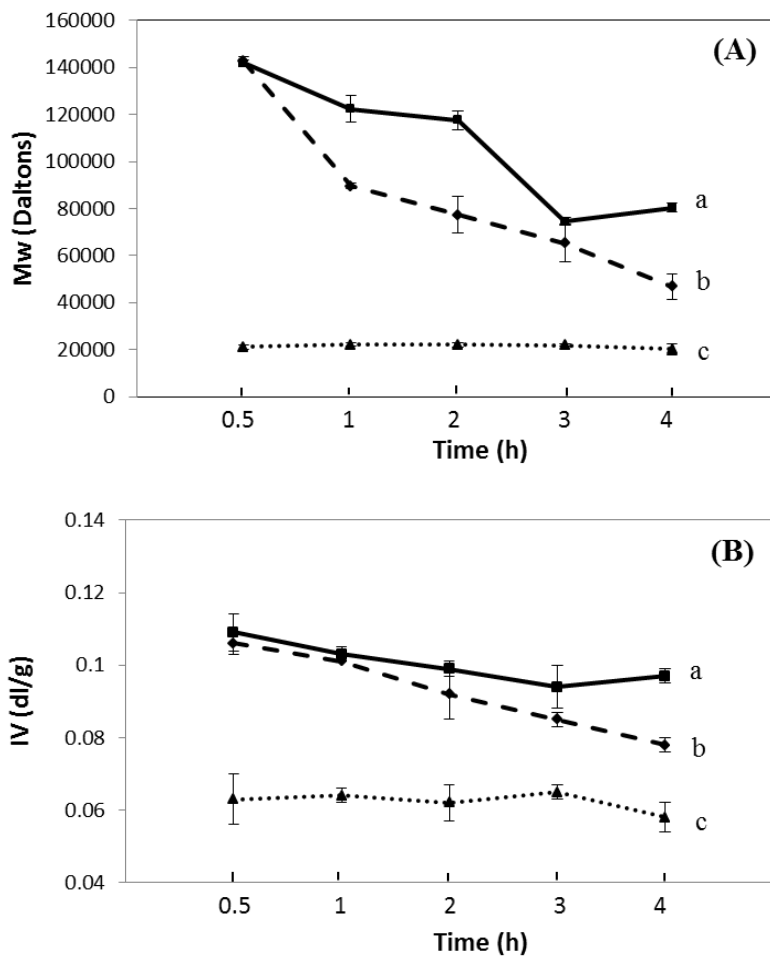


Figure 6.2 Weight average molecular weight (Mw) (A) and intrinsic viscosity (IV) (B) of pyrodextrins prepared at (a) pH 3 and 150 °C, (b) pH 3 and 170 °C, and (c) pH 2 and 150 °C.

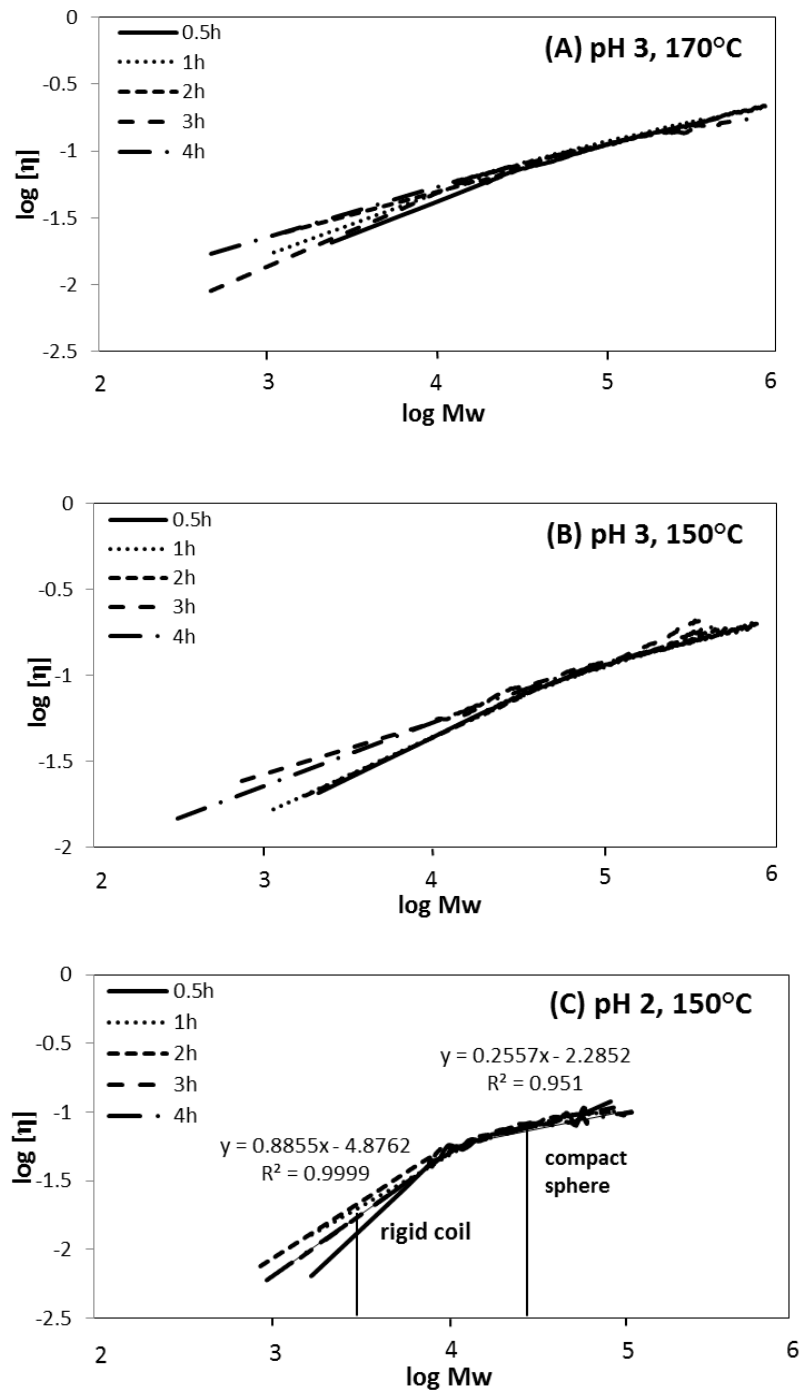


Figure 6.3 Intrinsic viscosity ($[\eta]$) vs. molecular weight (Mw) plotted on a log-log scale behavior of pyrodextrins prepared at (A) pH 3 and 150 °C, (B) pH 3 and 170 °C, and (C) pH 2 and 150 °C from logarithmic plot of the molecular weight vs. intrinsic viscosity by HPSEC-triple detectors.

Tables

Table 6.1 Water solubility of pyrodextrins prepared at different pH, heating temperatures and time ^a.

pH	Temp (°C)	Time (h)	Solubility (%)
3	170	0.5	78.7 ± 0.5 d
		1	88.5 ± 0.4 c
		2	97.1 ± 0.3 b
		3	100.0 ± 0.1 a
		4	100.0 ± 0.0 a
3	150	0.5	64.7 ± 0.6 c
		1	84.7 ± 0.5 b
		2	86.6 ± 0.6 b
		3	100.0 ± 0.2 a
		4	100.0 ± 0.0 a
2	150	0.5	100.0 ± 0.0 a
		1	100.0 ± 0.0 a
		2	100.0 ± 0.0 a
		3	100.0 ± 0.0 a
		4	100.0 ± 0.0 a

^a Mean ± standard deviation values are reported. Means in the same column not sharing a common letter are significantly different at $P \leq 0.05$.

Table 6.2 Conformational properties of pyrodextrins obtained from HPSEC coupled with multiple detectors (RI, viscometer, light scattering) ^a.

pH	Temp (°C)	Time (h)	Peak RV (mL) ¹	Mw (Daltons) ²	IV (dl/g) ³	R _h (w) (nm) ⁴	Mark-Houwink α ⁵
3	170	0.5	18.237±0.037 d	141,823±1,605 a	0.106±0.003 a	5.592±0.088 a	0.299±0.034 a
		1	18.314±0.023 c	89,628±1,135 b	0.101±0.000 a	4.775±0.061 b	0.308±0.003 a
		2	18.432±0.007 b	77,349±7,831 bc	0.092±0.007 b	4.359±0.230 c	0.305±0.007 a
		3	18.560±0.014 a	65,307±8,069 c	0.085±0.002 b	3.964±0.167 d	0.294±0.004 a
		4	18.597±0.004 a	46,736±5,570 d	0.078±0.002 c	3.504±0.126 e	0.269±0.020 a
3	150	0.5	18.240±0.015 c	142,541±2,205 a	0.109±0.005 a	5.606±0.092 a	0.278±0.006 a
		1	18.282±0.024 bc	122,388±5,616 b	0.103±0.002 ab	5.234±0.095 b	0.293±0.014 a
		2	18.295±0.026 b	117,533±3,990 b	0.099±0.002 b	5.128±0.083 b	0.297±0.041 a
		3	18.417±0.037 a	74,478±1,725 c	0.094±0.006 b	4.338±0.144 c	0.324±0.039 a
		4	18.399±0.036 a	80,448±1,950 c	0.097±0.002 b	4.458±0.062 c	0.277±0.033 a
2	150	0.5	18.779±0.010 a	21,045±815 a	0.063±0.007 a	2.619±0.084 a	0.292±0.062 ab
		1	18.762±0.005 a	22,088±743 a	0.064±0.002 a	2.580±0.022 a	0.394±0.025 a
		2	18.764±0.017 a	22,030±790 a	0.062±0.005 a	2.485±0.120 a	0.222±0.026 b
		3	18.773±0.017 a	21,900±349 a	0.065±0.002 a	2.562±0.026 a	0.346±0.027 a
		4	18.791±0.012 a	20,293±2,363 a	0.058±0.004 a	2.463±0.075 a	0.298±0.006 ab

^a Mean ± standard deviation values are reported. Means in the same column not sharing a common letter are significantly different at $p \leq 0.05$.

¹ Peak RV = peak with retention volume.

² Mw = weight-average molecular weight.

³ IV = intrinsic viscosity.

⁴ R_h = hydrodynamic radius.

⁵ Mark-Houwink α = exponent (α) in Mark-Houwink equation.

Chapter 7 - Swelling behavior of waxy maize pyrodextrins in glycerol and water

Abstract

Pyrodextrins were prepared by heating waxy maize starch for 4 h at pH 3 - 150 °C, pH 3 - 170 °C, and pH 2 - 150 °C. Those pyrodextrins were soluble in water, but insoluble in glycerol, and displayed a granular shape and a Maltese cross pattern of birefringence in glycerol by light microscopy. The objectives of this study were to investigate the swelling behavior of the pyrodextrins in mixtures of glycerol/water and determine the crystalline structure of the swollen pyrodextrins. Pyrodextrins prepared at pH 3 - 170 °C (high temperature) and pH 2 - 150 °C (high acid) dissolved at 25 °C when the level of water was greater than 60%, and they swelled marginally in glycerol/water mixtures of 80/20 and 60/40. In contrast, the pyrodextrin prepared at pH 3 - 150 °C (P3-150) with less molecular degradation, swelled in the glycerol/water mixtures. The diameter of the granules increased as much as ~ 80% in glycerol/water 40/60 to 60/40 at 10% solids. Despite that swelling, P3-150 still displayed birefringence (Maltese cross). However, x-ray crystallography showed that those swollen granules of P3-150 were amorphous, which was confirmed by differential scanning calorimetry.

Keywords

Pyrodextrin; Swelling behavior; Maltese cross; Birefringence; Starch

Introduction

Starch is a glucose polymer linked by α -1, 4 and α -1, 6 linkages. It is biosynthesized in plants as insoluble, compact, and partially crystalline granules of dimensions ranging in diameter from 0.1–200 μm (Pérez et al., 2009; Wurzburg, 1986). Starch granules vary in size and shape depending on their botanical origin. Common maize starch has polygonal-shaped granules with some spherical granules, and with an average diameter of 15 μm (Wurzburg, 1986). The crystallinity of starches varies from 15% to 45%, including the whole granule, the growth rings, the semicrystalline lamellae, and the crystallites (Bulón et al., 1998; Pérez & Bertoft, 2010). Under a microscopy, starch granules illuminated with polarized light are birefringent and show a “Maltese cross” pattern. The positive birefringence indicates that the organized molecular segments are densely packed in starch granules and confined to a radial orientation of the principle axis of the crystallites (Bertoft, 2017; Pérez & Bertoft, 2010; Zobel, 1988). Therefore, a loss of birefringence is a good indicator of the destruction of the ordered structure of molecules in starch granules.

Pyrodextrin is a degraded starch product which is made by heat or a combination of heat and acid. The dextrinization process involves heating a dry starch powder having intact granules to give products that generate a low viscosity and high cold-water solubility (Bai et al., 2014; Wurzburg, 1986). The changes from insoluble granular starch to soluble pyrodextrin during the dextrinization process have been examined by multiple techniques, including small-angle and wide-angle X-ray scattering, differential scanning calorimetry (DSC), and gel permeation chromatography (GPC) (Bai et al., 2014). Pyrodextrin molecular weight and size, crystallinity, crystal size, its associated melting enthalpy, the degree of retrogradation, and average chain

length (CL) decreased, and the degree of branching (DB) increased as pyrodextrin solubility increased (Bai et al., 2014; Han et al., 2018). No small-angle X-ray scattering (SAXS) characteristic peak was observed in native waxy maize and pyrodextrins in glycerol, but a peak at ca. 0.6 nm^{-1} appeared for native starch in a mixture of water and glycerol (20/80, w/w), reflecting the alternating crystalline and amorphous lamellars in the starch granules (Bai et al., 2014). The intensity of the peak decreased as pyrodextrin solubility increased and the peak disappeared as pyrodextrin solubility reached 100%. Based on NMR spectroscopic identification, new glycosyl linkages including α -1,6, β -1,6, α -1,2, and β -1,2, as well as 1,6-anhydro- β -D-glucopyranosyl end groups were found in the pyrodextrin (Bai & Shi, 2016). Pyrodextrins exhibited hypoglycemic bioactivities in mice with high-fat-diets induced obesity, probably due to its highly branched structure and non-digestible bonds (Cao et al., 2018).

When examined under a microscope, pyrodextrins in glycerol appear as granules identical to the native starch under illumination by a normal and polarized light. Pyrodextrins show strong birefringence with a Maltese cross pattern, indicating a radial orientation of molecules in the granules (Bai et al., 2014; Sjostrom, 1936; Wurzburg, 1986). However, granules of pyrodextrins lose birefringence when placed in water at room temperature. We hypothesize that pyrodextrins would swell in a mixture of glycerol and water. The objectives of this study were to prepare pyrodextrins from waxy maize starch, and to investigate the swelling behavior of those pyrodextrins over a period of 5 min in mixtures of glycerol/water (100/0, 80/20, 60/40, 40/60, 20/80, 0/100, w/w) at room temperature. In addition, two levels of the solids content (10 and 40%) were used to study the effects of solids content on the swelling of the pyrodextrins. Pre-swollen pyrodextrins were isolated after holding in various mixtures of glycerol and water

and subjected to DSC and X-ray diffraction (XRD) measurements. The data on the pre-swollen pyrodextrins was used to explain the swelling behavior of the pyrodextrins in glycerol/water.

Materials and methods

Materials

Waxy maize starch (WMS) was Amioca starch obtained from Ingredion Incorporated (Bridgewater, NJ, USA). All other chemicals were analytical grade.

Preparation of pyrodextrins and swollen pyrodextrins

Pyrodextrin was prepared as described by Bai et al. (2014). Briefly, an aqueous slurry (40 wt% starch) of waxy maize starch (150 g, dry weight) was adjusted to pH 3.0 by adding hydrochloric acid (0.5 M). After filtration and drying at 40 °C in a forced-draft oven overnight, the starch was heated in an open ceramic dish at 170 °C or 150 °C for 4 h. Those two waxy maize pyrodextrins were labeled as P3-150 and P3-170. Another pyrodextrin (P2-150) was prepared by adjustment to pH 2.0 and heating at 150 °C for 4 h.

Pyrodextrin (1.0 g, dry weight) was suspended in 9.0 g of glycerol/water (100/0, 80/20, 60/40, 40/60, 20/80, 0/100, w/w) at room temperature (25 °C). After 3 h the paste or slurry was added portion-wise into ethanol (50 mL) with mild stirring using a magnetic stir bar. The starch was collected and placed in a desiccator, and vacuum dried using a solvent trap cooled in dry ice/acetone. A treated pyrodextrin was sealed in a screw-cap bottle and saved for microscopic, XRD and DSC analysis.

Light microscopy

Waxy maize starch or pyrodextrin (0.4 or 0.1 mg, dry weight) was placed in 0.6 or 0.9 g of glycerol/water (100/0, 80/20, 60/40, 40/60, 20/80, 0/100, w/w) at 40 or 10% solids for 5, 60, and 180 min at 25 °C. A drop of each mixture was placed on a glass slide and covered with a cover slip. All samples were viewed with a 40× objective lens under bright-field and polarized-light illumination using an Olympus BX51 optical microscope with a digital camera (Olympus America Inc., Melville, NY, USA). Images were captured by a SPOT Insight camera, and each selected diameter of granule was measured using SPOT ADVANCE software (Diagnostic Instruments Inc., Sterling Heights, MI, USA).

X-ray diffraction (XRD)

Wide-angle x-ray diffraction was conducted with an x-ray diffractometer (PANalytical, Almelo, The Netherlands) at 35 kV and 20 mA with a theta-compensating slit and a diffracted beam monochromator. The diffractograms were recorded between 3° and 35° (2θ). The degree of crystallinity was estimated by the ratio of the total areas of the crystalline peaks to the total diffractogram area. The peak areas were calculated by OriginPro (version 8.5).

Differential scanning calorimetry (DSC)

Thermal properties of native starch, pyrodextrin and swollen pyrodextrins were determined by DSC (Q200, TA Instruments, New Castle, DE, USA). Samples (~ 15 mg, dry weight) were mixed with ~ 45 mg of glycerol/water mixture (80/20, w/w) at a ratio of 1:3 (starch: solvent, w/w) and a mixture was lightly stirred with a spatula. Pyrodextrins that formed a paste were mixed with the liquids in a centrifuge vial and each mixture was allowed to stand for 6 h at room temperature (25 °C). A pyrodextrin paste (45–55 mg) was accurately weighed with a

microbalance and placed into a large DSC stainless steel pan. DSC pans were held at 10 °C for 1 min, then heated up to 160 °C at 10 °C/min. The onset, peak, conclusion temperatures (T_o , T_p , and T_c , respectively) and enthalpy energy (ΔH) were calculated using Universal Analysis (TA Instruments). An empty pan was used as a reference.

Statistical analysis

Data were analyzed by analysis of variance (ANOVA) using Minitab 17 Statistical Software Program (Minitab Inc. State College PA, USA) with a significant level of $p < 0.05$. Experiments were run in duplicate. Mean values and standard deviation of replications were reported.

Results and discussion

Microscopic observation of starch granules in glycerol/water mixtures

Figure 7.1 and 7.2 show that microscopic photos of native WMS, and pyrodextrins prepared at pH 3 and 170 °C (P3-170), pH 3 and 150 °C (P3-150), and pH 2 and 150 °C (P2-150) for 4 h, immersed in glycerol/water mixture (80/20, w/w) at room temperature (25 °C) for 180 min, at 40 and 10% solids, respectively. Under a light microscopy, when examined at 40% solid content, the pyrodextrins prepared at pH 3 - 170 °C and pH 2 - 150 °C (P3-170 and P2-150) showed evidence of weakened structure of granules compared with native WMS and the pyrodextrin prepared at pH 3 - 150 °C (P3-150). At 10% solid content, all pyrodextrins showed weakened structure compared with the WMS.

At high solid content (40%) (Fig. 7.1 WMS), WMS granules were aggregated. At 10% solid content (Fig. 7.2 WMS), the granules were better dispersed, and the size was similar to

what was observed at 40% solid content. Under polarized light, native WMS in a glycerol/water mixture (80/20, w/w) showed Maltese cross with strong birefringence at both 40% and 10% solid contents at room temperature (Fig. 7.1 and 7.2, WMS). Native WMS had mainly polygonal shaped with some spherical granules ranging from 5–25 μm in accordance with the results previously reported (Muñoz et al., 2015; Pérez & Bertoft, 2010). Native WMS granules were insoluble in either glycerol or water at room temperature, and no obvious difference in size was observed when the starch was placed in glycerol and water (100/0, 80/20, 60/40, 40/60, 20/80, 0/100, w/w) (Fig. 7.3).

Pyrodextrins (P3-170, P3-150, and P2-150) in different ratios of glycerol to water at room temperature are shown in Figs. 7.4, 7.5, and 7.6, respectively. When examined under a microscope, the shape and size of all pyrodextrins in glycerol appeared identical to the native WMS and showed Maltese cross with strong birefringence under polarized light (Figs. 7.4–6, glycerol/water = 100/0, w/w), indicating they were insoluble in glycerol. The granules of P3-170, P3-150, and P2-150 were dissolved in water after suspended 180 min (Fig. 7.4–6, solvent: glycerol/water = 0/100, w/w). Glycerol is not an effective solvent for starch compared with water as a plasticizer because it has a larger molecular weight (Donald, 2001; Perry & Donald, 2000).

Microscopic investigation of pyrodextrins in other ratios of glycerol/water solvents (80/20, 60/40, 40/60, 20/80, w/w) revealed that pyrodextrin granules had a decreased intensity of birefringence as the level of water increased. Detailed examination revealed that the pyrodextrins prepared at difference conditions behaved differently in the mixture of glycerol and water systems and is discussed in the three sections below.

Swelling behavior of pyrodextrins prepared at pH 3 - 170 °C (P3-170) in glycerol and water

At 40% solid content, starch granules of P3-170 did not swell in glycerol/water of 80/20 (w/w) and 60/40 (w/w) mixtures but partial cracks through the central hilum region were observed when the immersion time increased to 180 min (Fig. 7.4). When the water level increased to 60%, birefringence was completely lost in 5 min (Fig. 7.4, 40% solid content at 5 min immersion time, glycerol/water = 40/60, 20/80). As immersion time increased to 180 min, all starch granules disappeared (Fig. 7.4, glycerol/water = 40/60 and 20/80).

At 10% solid content, P3-170 in glycerol/water (80/20, w/w) mixture (Fig. 7.2, P3-170) retained a similar feature as that at 40% solid content ((Fig. 7.1, P3-170). However, at 10% solid content in glycerol/water of 60/40 and 40/60 (w/w) mixtures, some granules swelled to 29 μm and lost the birefringence (Fig. 7.4, 10% solid content at 5 min immersion time, glycerol/water = 60/40 and 40/60), indicating that granules swelled more at 10% solids than that at 40% solids, and those long-range order was destroyed.

The granules of P3-170 were dissolved in water (Fig. 7.4, glycerol/water = 0/100, w/w), reflecting that P3-170 was a highly converted pyrodextrin and the granules immediately disappeared when the samples came in contact with water. When examined in water, the more highly converted pyrodextrins showed evidence of structural weakening and exfoliation of the outer layers (Sjostrom, 1936).

Swelling behavior of pyrodextrins prepared at pH 3 - 150 °C (P3-150) in glycerol and water

At 40% solid content, with increasing immersed time to 180 min, P3-150 granules swelled slightly at glycerol/water (80/20 and 60/40, w/w) mixture (Fig. 7.5). The greatest granule swelling with the maximum diameter of swollen granule ($\sim 31 \mu\text{m}$) was observed when the water level increased to 60%; yet the Maltese cross patterns were still maintained in these granules

when viewed under polarized light (Fig. 7.5, 40% solid content at 180 min immersion time, glycerol/water = 40/60). Therefore, the granules of P3-150 swelled in the mixtures of glycerol and water but the swelling at 40% solid content was limited due to insufficient swelling space.

With the solid content decreased to 10%, the starch granules (P3-150) swelled dramatically in glycerol/water (60/40, w/w) in the longer immersion time (180 min), and similar swelling occurred in glycerol/water (20/80, w/w) in the shorter immersion time (5 min) (Fig. 7.5, 10% solid content). At 60% glycerol and 180 min immersion time, granules could swell to 36 μm , an increasing $\sim 80\%$ of average initial size in 100% glycerol ($\sim 20 \mu\text{m}$) (Fig. 7.5, glycerol/water = 100/0). At 20% glycerol and 5 min immersion time, granules swelled to 35 μm , increasing $\sim 75\%$ of average initial size in 100% glycerol ($\sim 20 \mu\text{m}$) (Fig. 7.5, glycerol/water = 100/0). The swelling was evident but birefringence was still observed under polarized light, indicating that solvents were not strong enough to destroy the long range order of starch granules of P3-150 until extra water was used. For P3-150 (10%) in water alone, the granules partially swelled, and the Maltese crosses disappeared.

In studying granular cold-water swelling starch prepared by aqueous ethanol treatments at elevated temperatures (Dries et al., 2014), Dries et al reported that those cold-water swelling starch granules swelled to several times their initial size in water but birefringence was completely lost. In our study, we found that Maltese cross was observed when the starch granules (P3-150) swelled in the mixture glycerol and water but long-range order (birefringence) was not lost.

Swelling behavior of pyrodextrins prepared at pH 2 - 150 °C (P2-150) in glycerol and water

For the pyrodextrin prepared at pH 2 - 150 °C (P2-150), its swelling behavior (Fig. 7.6) was different from P3-150 (Fig. 7.5) but similar to P3-170 (Fig. 7.4) in the glycerol and water mixtures. At 40% solid content, radial cracks were found in glycerol/water mixture (80/20 and 60/40, w/w) immersed for 60 and 180 min (Fig. 7.6). At 100% water, the outside of the granules dissolved first and then whole granules dissolved and disappeared. At 10% solid content, P2-150 granules appeared weaken structure at 40% water, and disappeared when water content was 60% and higher (glycerol/water, and 20/80, 0/100, w/w). There was no swelling of the granules. Instead a granule was broken into pieces, and dissolved gradually as water content and immersion time increased. P2-150, which was more degraded by acid, appeared to be solubilized in water without swelling of the granules.

It is interesting to note that the swelling behavior of the pyrodextrin prepared at pH 3 and 150 °C (P3-150) (Fig. 7.5) differed from the other two pyrodextrins (P3-170 and P2-150) (Fig. 7.4 and 7.6). Both P3-170 (high temperature) and P2-150 (high acid) were more converted than P3-150. The average molecular weight of P3-170, P3-150, and P2-150 was 46.7, 80.5, and 20.3 kDa, respectively (Sun et al., 2020). P3-170 could swell slightly but Maltese cross pattern was totally lost, and P2-150 did not swell at all. In contrast, P3-150 granules, which had a higher molecular weight, could swell ~ 80% in glycerol and water mixture to break down the ordered structures yet still displayed Maltese cross patterns. To further understand the unique swelling behavior of P3-150, we isolated and examined its swollen pyrodextrins by XRD and DSC.

Crystallinity and birefringence of swollen pyrodextrins from P3-150

Both native WMS and the pyrodextrin (P3-150) exhibited the typical A-type diffraction pattern with strong peaks at 2θ values at 15 °, 17 °, 18 ° and 23 ° (Fig. 7.7, A and B). Crystallinity of

the native WMS was approximately 35.8%, which is close to previous literature values (Dries et al., 2014; Lopez-Rubio et al., 2008). Pyrodextrin (P3-150) had a reduced crystallinity of 19.4%. Acid and heat treatment impacted the intensity of the peaks and the relative crystallinity of the WMS granules (Bai et al., 2014). Swollen pyrodextrins recovered from 100/0 and 80/20 glycerol/water mixtures (Fig. 7.7, C and D) still showed an A-type pattern but with broadened peaks and reduced intensity at 15 °, 17.5 °, and 23 °. As the water content in the solvent increased to more than 40%, the swollen pyrodextrins recovered were amorphous (Fig. 7.7, E-H).

The thermal properties of native waxy maize starch, pyrodextrin and its swollen pyrodextrins recovered from different glycerol/water mixtures were analyzed by DSC. A reduction in the crystallinity of pyrodextrins was also reflected in the DSC data (Table 7.1). The onset (T_o), peak (T_p), and conclusion (T_c) gelatinization temperatures of WMS in 80% glycerol were 92.3, 100.6, and 133.8 °C, respectively, which were higher than the gelatinization temperatures of the WMS in water (Bai et al., 2014; Liu et al., 2011). The gelatinization temperature is elevated due to glycerol by reducing the volume fraction of water within the system (Perry & Donald, 2000). For the pyrodextrin (P3-150) in 80% glycerol, the gelatinization peak was shifted to lower temperature and much broader than the native starch. The enthalpy values (ΔH) of the pyrodextrin decreased from 20.2 to 10.3 J/g, suggesting a lower crystallinity. Table 7.1 shows the DSC results of swollen pyrodextrins (100/0, 80/20, 60/40, 40/60, 20/80, 0/100) recovered from glycerol/water mixtures. The swollen pyrodextrin recovered from 100% glycerol had a similar gelatinization peak compared with the pyrodextrin (P3-150). As water content increased in glycerol/water mixture, swollen pyrodextrins did not show any endothermic peak, indicating that the crystallinity of swollen pyrodextrins recovered from 0–80% glycerol was lost. These DSC results suggested loss of the crystallinity during granules swelling. X-ray

crystallography showed that those swollen granules of P3-150 were amorphous, in agreement with the DSC results.

To confirm if the recovered swollen pyrodextrins from P3-150 were still birefringent, we re-examined them by light microscopy. Figure 7.8, C-H shows bright field and polarized light micrographs of swollen pyrodextrins. The shape and size of the pyrodextrin granules (P3-150) recovered from 100% glycerol (Fig. 7.8, C) appeared identical to the native WMS (Fig. 7.8, A) and the P3-150 (Fig. 7.8, B) and showed Maltese cross with strong birefringence under polarized light. Majority of the granules recovered from the mixtures of glycerol/water 80/20, 60/40, and 40/60 (Fig. 7.8, D-F) still had Maltese cross patterns although some soluble materials might be lost during the recovery process. The swollen pyrodextrin recovered from 80 and 100% water had few starch granules (Fig. 7.8, G and H). In the study of Sittipod and Shi (Sittipod & Shi, 2016), intact starch granules from parboiled rice still displayed Maltese cross patterns, but were not crystalline; some granules from the parboiled rice were able to swell in glycerol to 4-5 times of their original size. In this study, the pyrodextrin prepared at pH 3 and 150 °C was able to swell in the mixture of glycerol and water and still retain its birefringence.

Conclusions

Pyrodextrins prepared at pH 3 - 170 °C and pH 2 - 150 °C (P3-170 and P2-150) were highly converted by heat or acid and did not swell much when placed in water. In contrast, granules in the pyrodextrin prepared at pH 3 and 150 °C (P3-150) could swell in glycerol/water ~ 80% of their original size and still displayed Maltese cross patterns, but were not crystalline. The applications of this unique swelling property of P3-150 in a mixture of glycerol and water need to be further investigated.

References

- Bai, Y., Cai, L., Douth, J., Gilbert, E. P., & Shi, Y.-C. (2014). Structural changes from native waxy maize starch granules to cold-water-soluble pyrodextrin during thermal treatment. *Journal of Agricultural and Food Chemistry*, 62(18), 4186–4194.
- Bai, Y., & Shi, Y.-C. (2016). Chemical structures in pyrodextrin determined by nuclear magnetic resonance spectroscopy. *Carbohydrate Polymers*, 151, 426–433.
- Bertoft, E. (2017). Understanding Starch Structure: Recent Progress. *Agronomy*, 7(3), 56.
- Bulón, A., Colonna, P., Planchot, V., & Ball, S. (1998). Starch granules: structure and biosynthesis. *International Journal of Biological Macromolecules*, 23(2), 85–112.
- Cao, Y., Chen, X., Sun, Y., Shi, J., Xu, X., & Shi, Y.-C. (2018). Hypoglycemic effects of pyrodextrins with different molecular weights and digestibilities in mice with diet-induced obesity. *Journal of Agricultural and Food Chemistry*.
- Donald, A. M. (2001). Plasticization and Self Assembly in the Starch Granule. *Cereal Chemistry*, 78(3), 307–314.
- Dries, D. M., Gomand, S. V., Goderis, B., & Delcour, J. A. (2014). Structural and thermal transitions during the conversion from native to granular cold-water swelling maize starch. *Carbohydrate Polymers*, 114, 196–205.
- Han, X., Kang, J., Bai, Y., Xue, M., & Shi, Y.-C. (2018). Structure of pyrodextrin in relation to its retrogradation properties. *Food Chemistry*, 242, 169–173.
- Liu, P., Xie, F., Li, M., Liu, X., Yu, L., Halley, P. J., & Chen, L. (2011). Phase transitions of maize starches with different amylose contents in glycerol–water systems. *Carbohydrate Polymers*, 85(1), 180–187.
- Lopez-Rubio, A., Flanagan, B. M., Gilbert, E. P., & Gidley, M. J. (2008). A novel approach for calculating starch crystallinity and its correlation with double helix content: A combined XRD and NMR study. *Biopolymers*, 89(9), 761–768.
- Muñoz, L. A., Pedreschi, F., Leiva, A., & Aguilera, J. M. (2015). Loss of birefringence and swelling behavior in native starch granules: Microstructural and thermal properties. *Journal of Food Engineering*, 152, 65–71.
- Pérez, S., Baldwin, P. M., & Gallant, D. J. (2009). Chapter 5 - Structural Features of Starch Granules I. In J. BeMiller & R. Whistler (Eds.), *Starch (Third Edition)* (pp. 149–192). Academic Press.

- Pérez, S., & Bertoft, E. (2010). The molecular structures of starch components and their contribution to the architecture of starch granules: A comprehensive review. *Starch - Stärke*, 62(8), 389–420.
- Perry, P. A., & Donald, A. M. (2000). The role of plasticization in starch granule assembly. *Biomacromolecules*, 1(3), 424–432.
- Sittipod, S., & Shi, Y.-C. (2016). Changes of starch during parboiling of rice kernels. *Journal of Cereal Science*, 69, 238–244.
- Sjostrom, O. A. (1936). Microscopy of starches and their modifications. *Industrial & Engineering Chemistry*, 28(1), 63–74.
- Sun, Z., Kang, J., & Shi, Y.-C. (2020). Changes in molecular size and shape of waxy maize starch during dextrinization. *Food Chemistry*. (submitted)
- Wurzburg, O. B. (1986). Converted starches. In *Modified starches-properties and uses*. CRC Press.
- Zobel, H. F. (1988). Molecules to granules: A comprehensive starch review. *Starch - Stärke*, 40(2), 44–50.

Figures

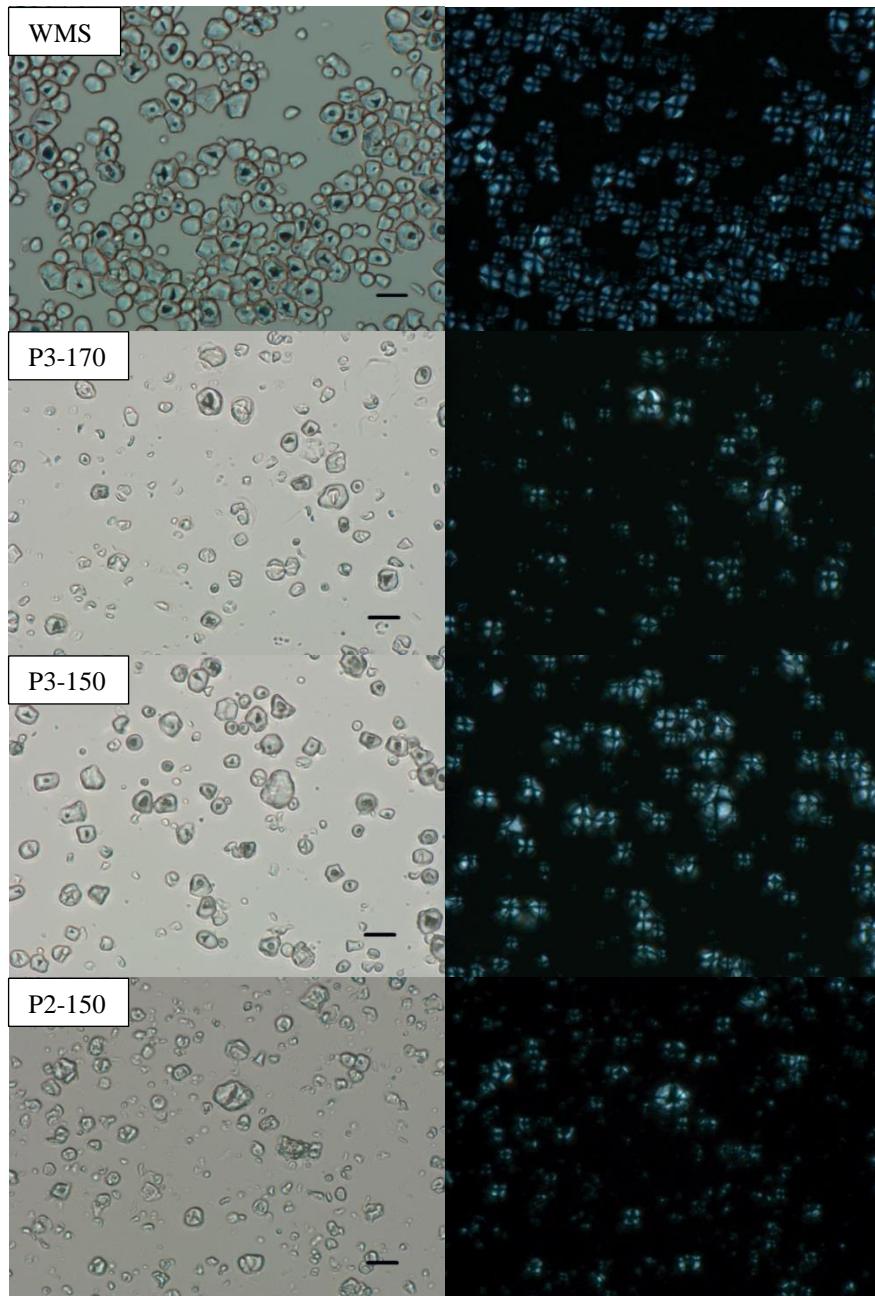


Figure 7.1 Microscopic images under bright field (left) and polarized light (right) (scale bar = 20 μm) of native waxy maize starch (WMS), and pyrodextrins prepared at pH 3 and 170 °C (P3-170), pH 3 and 150 °C (P3-150), and pH 2 and 150 °C (P2-150) for 4 h, immersed in glycerol/water mixture (80/20, w/w) at 40% solid content for 180 min.

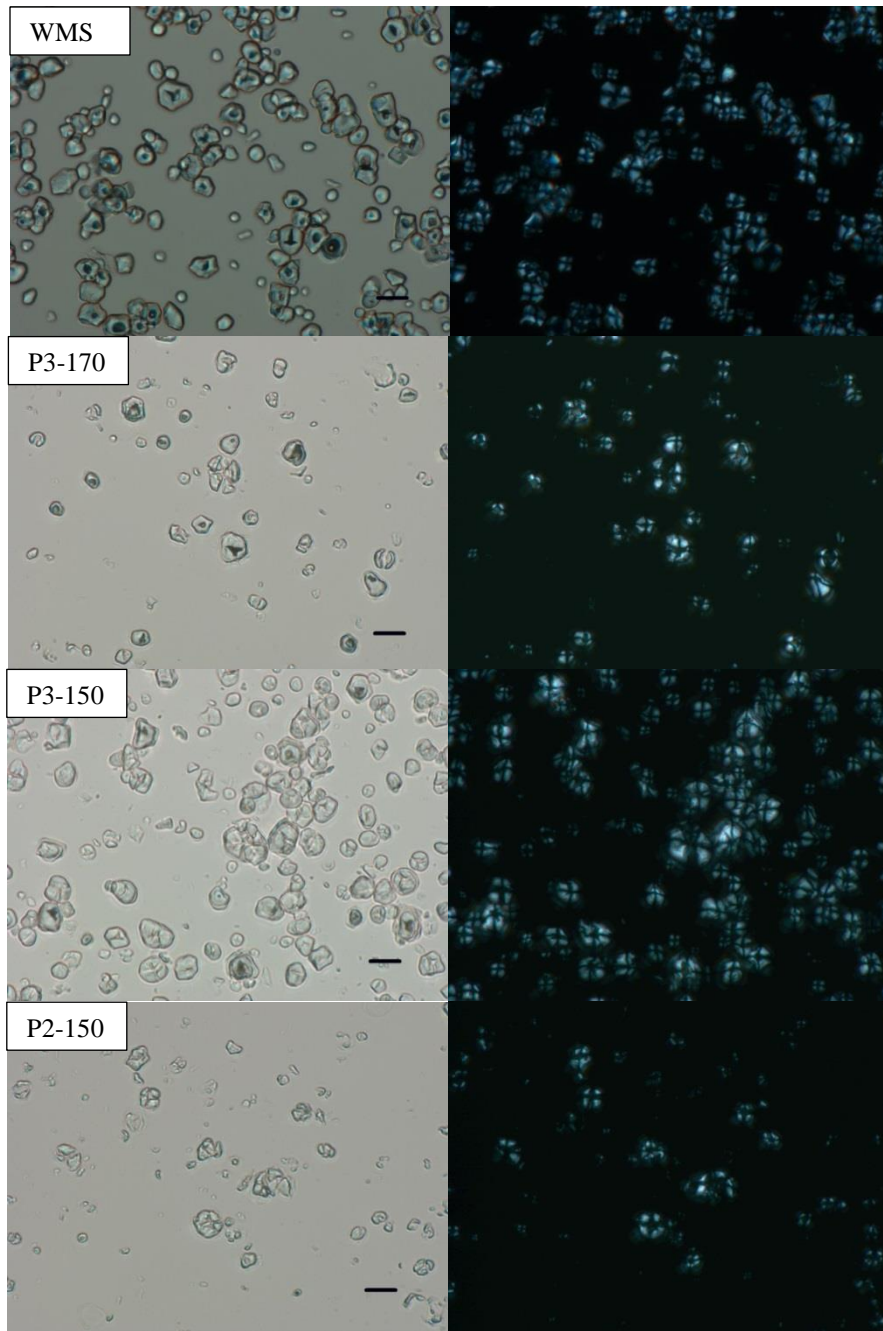


Figure 7.2 Microscopic images under bright field (left) and polarized light (right) (scale bar = 20 μm) of native waxy maize starch (WMS), and pyrodextrins prepared at pH 3 and 170 $^{\circ}\text{C}$ (P3-170), pH 3 and 150 $^{\circ}\text{C}$ (P3-150), and pH 2 and 150 $^{\circ}\text{C}$ (P2-150) for 4 h, immersed in glycerol/water mixture (80/20, w/w) at 10% solid content for 180 min.



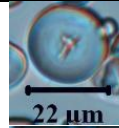
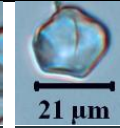
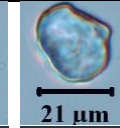
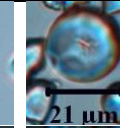

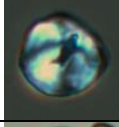

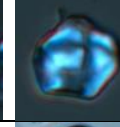
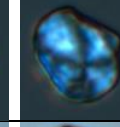

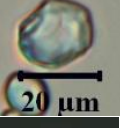


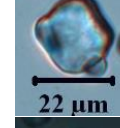
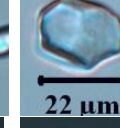
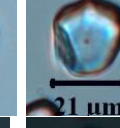
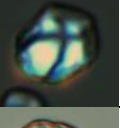
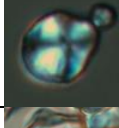


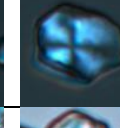

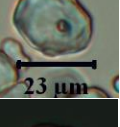
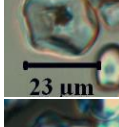
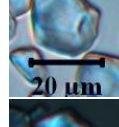
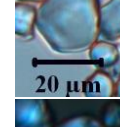
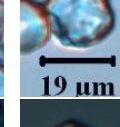
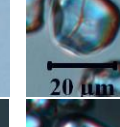
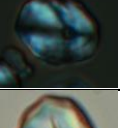
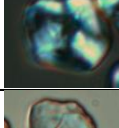
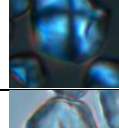
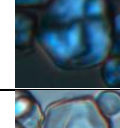
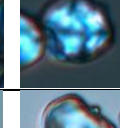

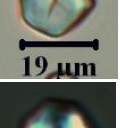
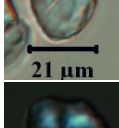
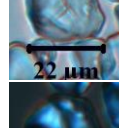
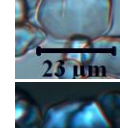
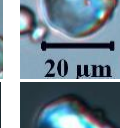
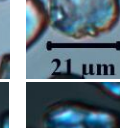
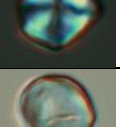
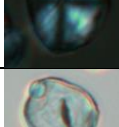
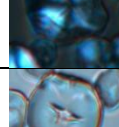

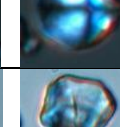

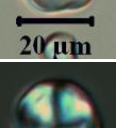
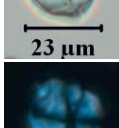
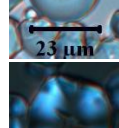

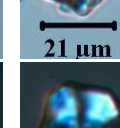
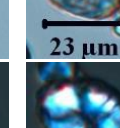
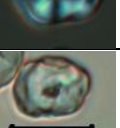
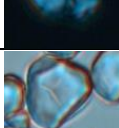
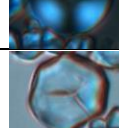
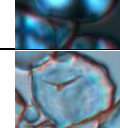
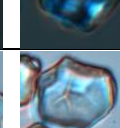
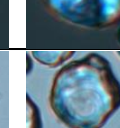

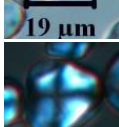
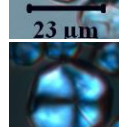
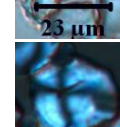
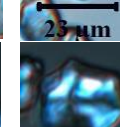
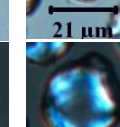
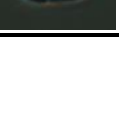
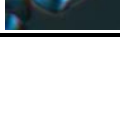
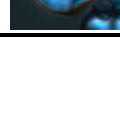
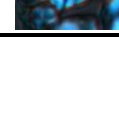
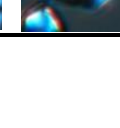

Solid content	Immersion time (min)	Microscopy light	glycerol/water (w/w)					
			100/0	80/20	60/40	40/60	20/80	0/100
40%	5	Normal						
		Polarized						
	60	Normal						
		Polarized						
	180	Normal						
		Polarized						
10%	5	Normal						
		Polarized						
	60	Normal						
		Polarized						
	180	Normal						
		Polarized						

Figure 7.3 Microscopic photos of native waxy maize starch (WMS) granules immersed in different ratios of glycerol/water solvents: 100/0, 80/20, 60/40, 40/60, 20/80, 0/100, (w/w) for 5, 60, and 180 min at 40% and 10% solids, respectively.

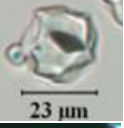
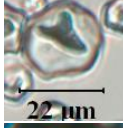
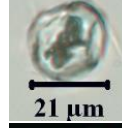
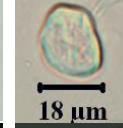
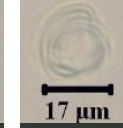
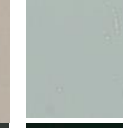

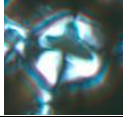
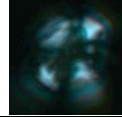
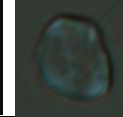


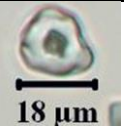
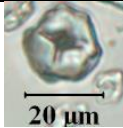




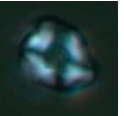
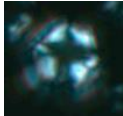
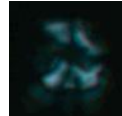
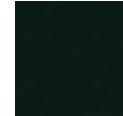



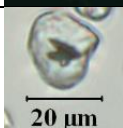
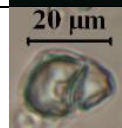
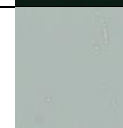
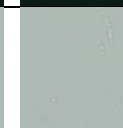

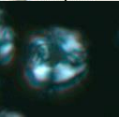
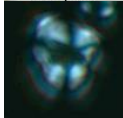

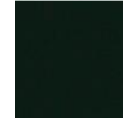


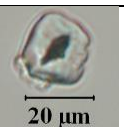
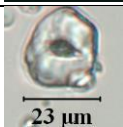
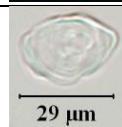

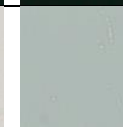
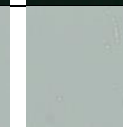

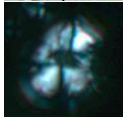
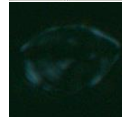

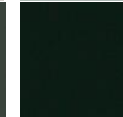

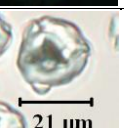



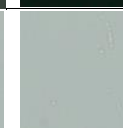
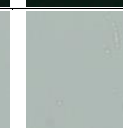

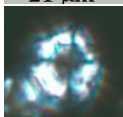

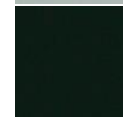
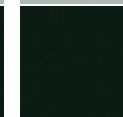
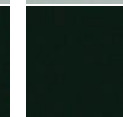


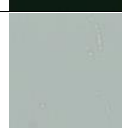
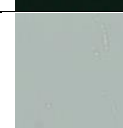
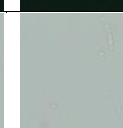
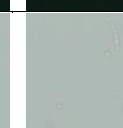
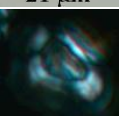
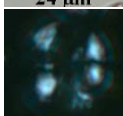
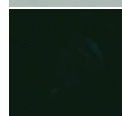
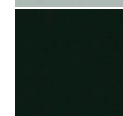
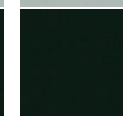
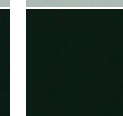
Solid content	Immersion time (min)	Microscopy light	glycerol/water (w/w)					
			100/0	80/20	60/40	40/60	20/80	0/100
40%	5	Normal						
		Polarized						
	60	Normal						
		Polarized						
	180	Normal						
		Polarized						
10%	5	Normal						
		Polarized						
	60	Normal						
		Polarized						
	180	Normal						
		Polarized						

Figure 7.4 Microscopic photos of pyrodextrins prepared at pH 3 and 170 °C (P3-170) for 4 h immersed in different ratios of glycerol/water solvents: 100/0, 80/20, 60/40, 40/60, 20/80, 0/100, (w/w) for 5, 60, and 180 min at 40% and 10% solids, respectively.

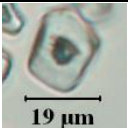
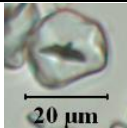




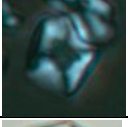
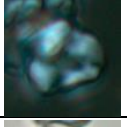
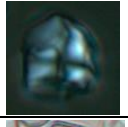
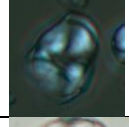
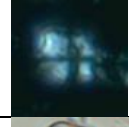
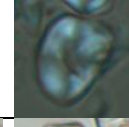
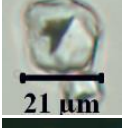
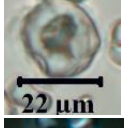
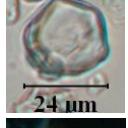


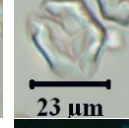

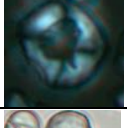
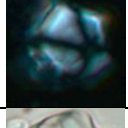
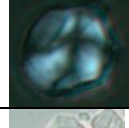
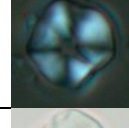
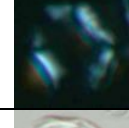
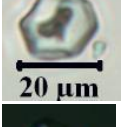


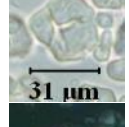

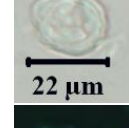

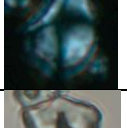
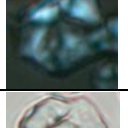


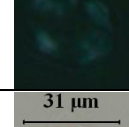
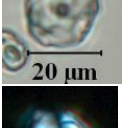
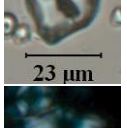
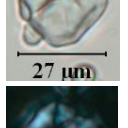
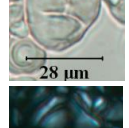
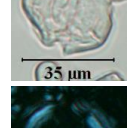

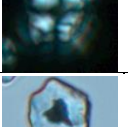
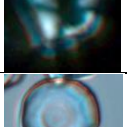

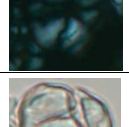
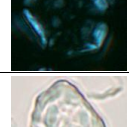
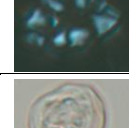
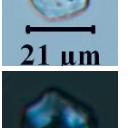
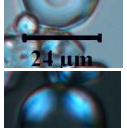
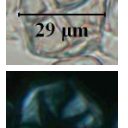
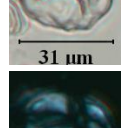
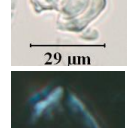
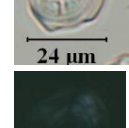
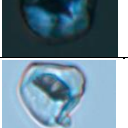
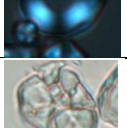
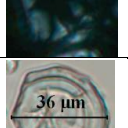
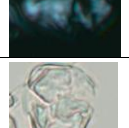
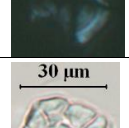
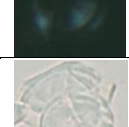
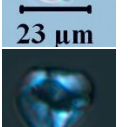
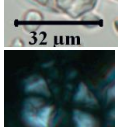
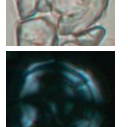
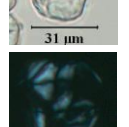
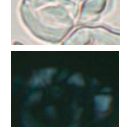
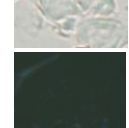
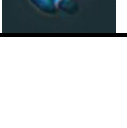




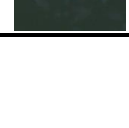
Solid content	Immersion time (min)	Microscopy light	glycerol/water (w/w)					
			100/0	80/20	60/40	40/60	20/80	0/100
40%	5	Normal						
		Polarized						
	60	Normal						
		Polarized						
	180	Normal						
		Polarized						
10%	5	Normal						
		Polarized						
	60	Normal						
		Polarized						
	180	Normal						
		Polarized						

Figure 7.5 Microscopic photos of pyrodextrins prepared at pH 3 and 150 °C (P3-150) for 4 h immersed in different ratio of glycerol/water solvents: 100/0, 80/20, 60/40, 40/60, 20/80, 0/100, (w/w) for 5, 60, and 180 min at 40% and 10% solids, respectively.

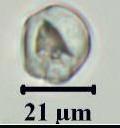

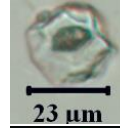
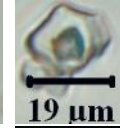
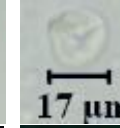
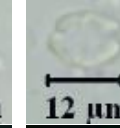


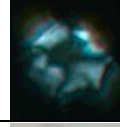
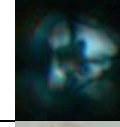


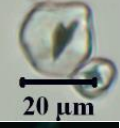
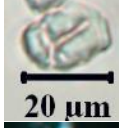
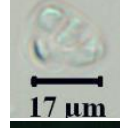
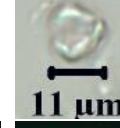


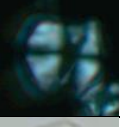

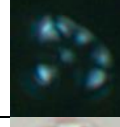
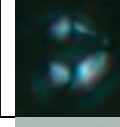

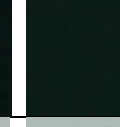


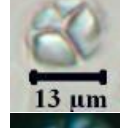



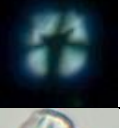
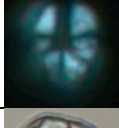
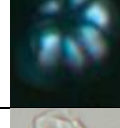



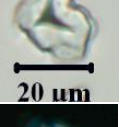
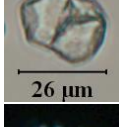
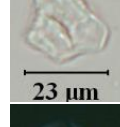



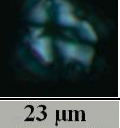





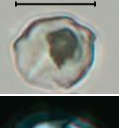
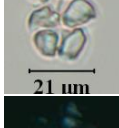
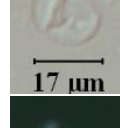




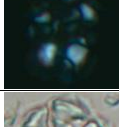
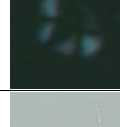

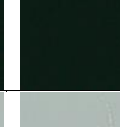

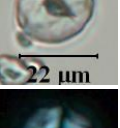
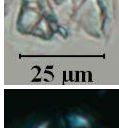
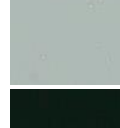

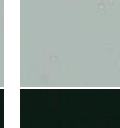







Solid content	Immersion time (min)	Microscopy light	glycerol/water (w/w)					
			100/0	80/20	60/40	40/60	20/80	0/100
40%	5	Normal						
		Polarized						
	60	Normal						
		Polarized						
	180	Normal						
		Polarized						
10%	5	Normal						
		Polarized						
	60	Normal						
		Polarized						
	180	Normal						
		Polarized						

Figure 7.6 Microscopic photos of pyrodextrins prepared at pH 2 and 150 °C (P2-150) for 4 h immersed in different ratio of glycerol/water solvents: 100/0, 80/20, 60/40, 40/60, 20/80, 0/100, (w/w) for 5, 60, and 180 min at 40% and 10% solids, respectively.

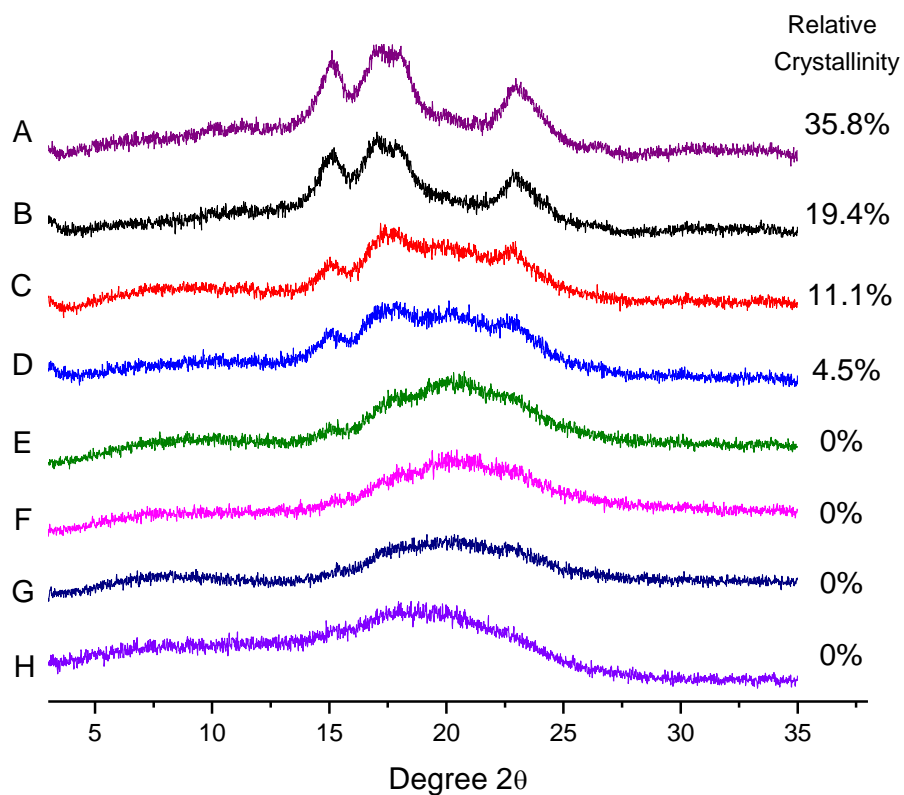
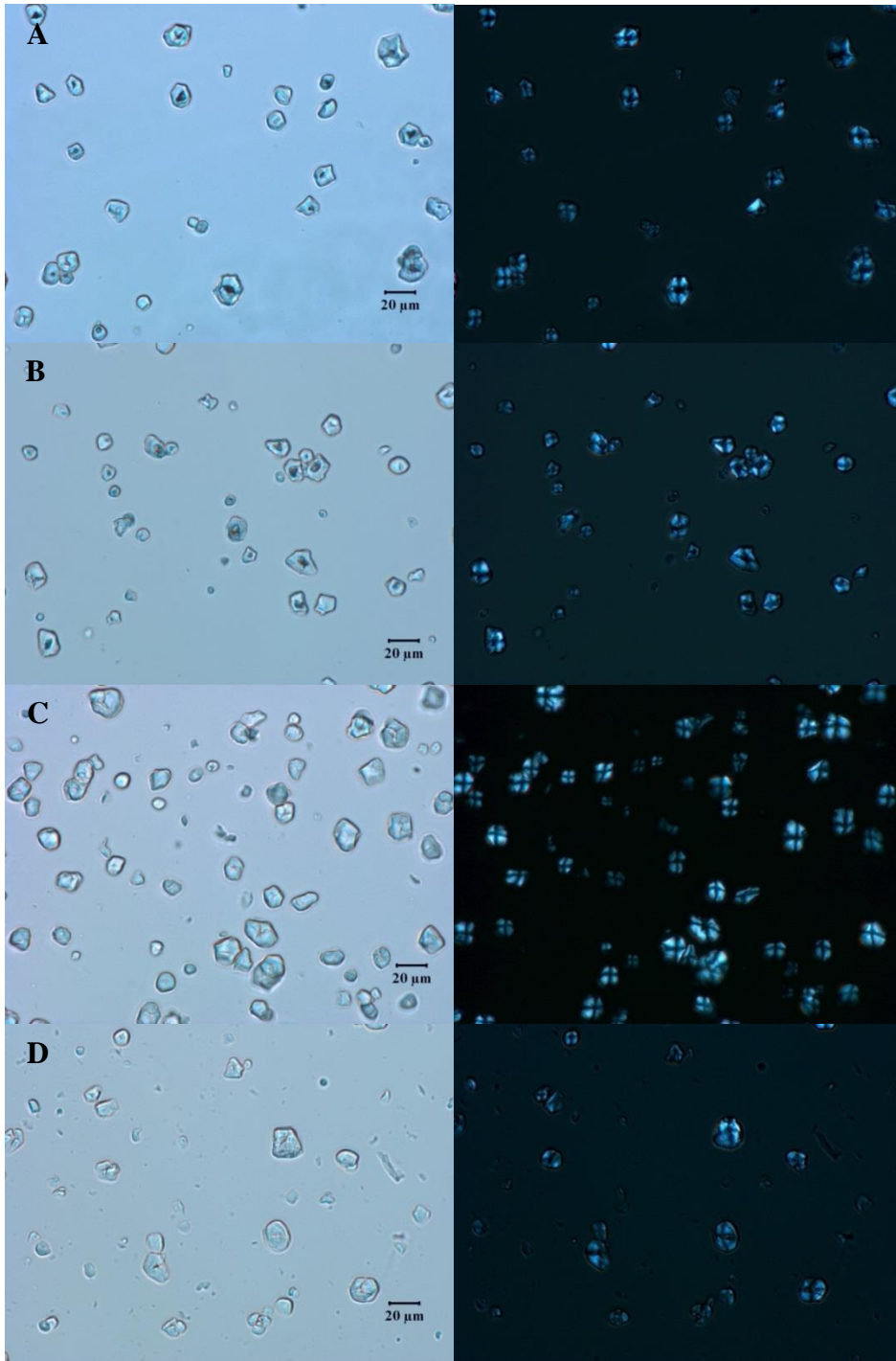


Figure 7.7 X-ray diffraction (XRD) pattern of (A) native waxy maize starch, (B) pyrodextrin prepared at pH 3 and 150 °C for 4 h, and its swollen pyrodextrin recovered from glycerol/water mixtures: (C) 100/0, (D) 80/20, (E) 60/40, (F) 40/60, (G) 20/80, and (H) 0/100, (w/w).



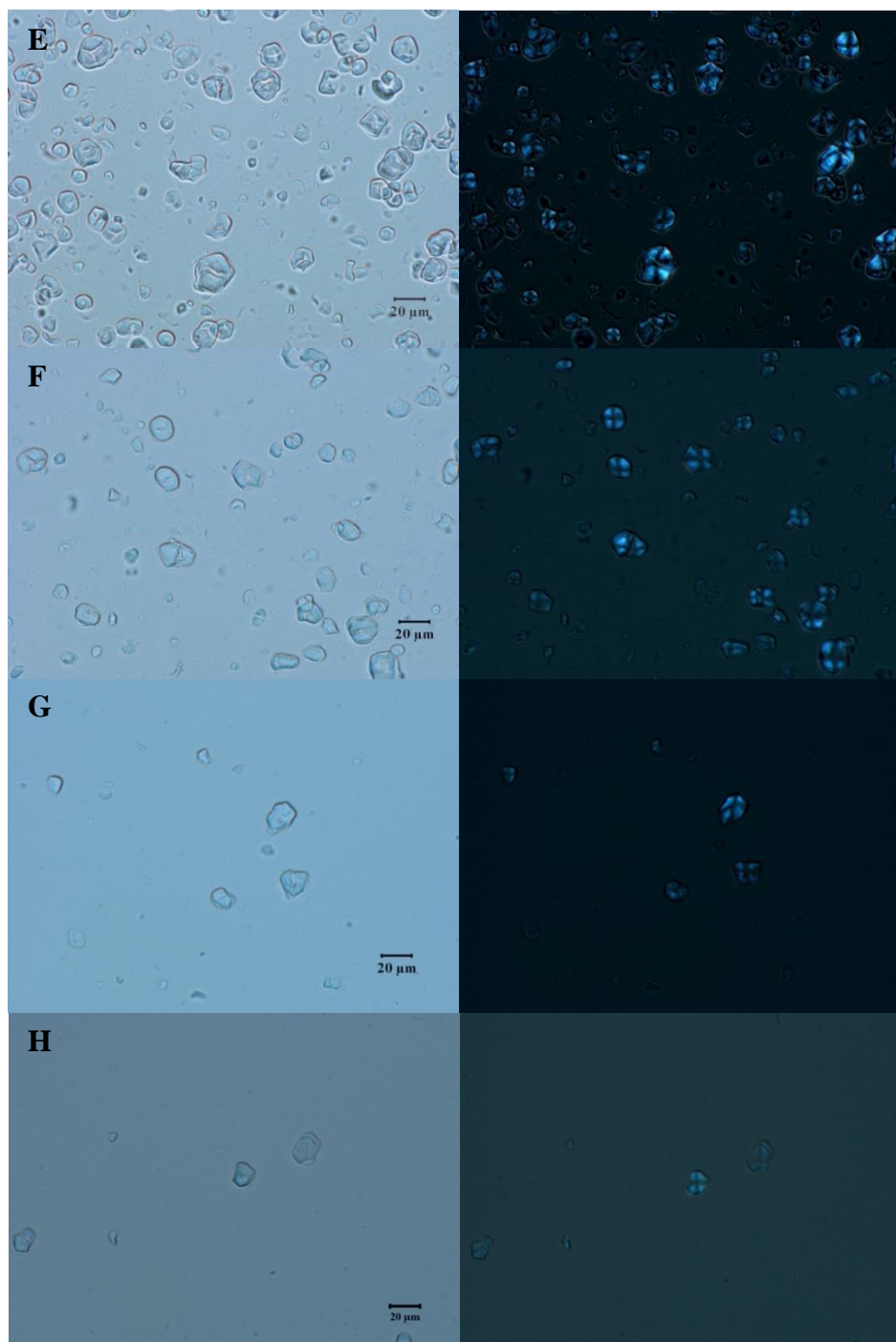


Figure 7.8 Photomicrographs viewed in pure glycerol under bright field (left) and polarized light (right) (scale bar = 20 μm) of (A) native waxy maize starch, (B) pyrodextrin prepared at pH 3 and 150 $^{\circ}\text{C}$ for 4 h, and its swollen pyrodextrin recovered from glycerol/water mixtures: (C) 100/0, (D) 80/20, (E) 60/40, (F) 40/60, (G) 20/80, and (H) 0/100, (w/w).

Tables

Table 7.1 Thermal properties^a of native waxy maize starch, pyrodextrin prepared at pH 3, 150 °C (P3-150) for 4 h, and its swollen pyrodextrins recovered from glycerol/water mixture (100/0, 80/20, 60/40, 40/60, 20/80, 0/100, w/w) as determined by differential scanning calorimetry in a mixture of glycerol / water (80/20, w/w)

Sample	T_o (°C)	T_p (°C)	T_c (°C)	ΔH (J/g)
Waxy maize starch	92.3 a	100.6 a	133.8 a	20.2 a
Pyrodextrin (P3-150)	63.3 b	74.0 b	102.3 b	10.3 b
P3-150 recovered from 100% glycerol	63.2 b	73.2 c	101.8 c	7.8 c
P3-150 recovered from glycerol/water mixtures (80/20, 60/40, 40/60, 20/80, 0/100, w/w)	No endothermic peak			

^a Means in the same column not sharing a common letter are significantly different at $p < 0.05$.

Chapter 8 - Encapsulation of vitamin E by octenylsuccinate starch obtained from normal maize starch by dry heating

Abstract

The aim of the present study was to investigate the application of octenylsuccinic anhydride (OSA) starch from normal maize starch to form emulsions in the spray-drying microencapsulation of Vitamin E oil. OS starch was prepared by dry heating a mixture of normal maize starch and octenylsuccinic anhydride (OSA). The effects of the heating conditions (reaction pH, temperature and heating time) on the degrees of substitution (DS), water solubility, and the physical properties of the OS dextrans were evaluated. Heat and OSA reaction resulted in starch hydrolysis in the amorphous and crystalline regions of starch granules with the reduced molecular size. The effect of ratio of starch to oil on emulsion properties was studied. The emulsion with high VE loaded (7.5%) at ratio of starch to oil (1:1) had a small particle size of 0.704 μm . The spray-dried microencapsulated particles were characterized by oil load efficiency (97.4%) and density (1.082 g/cm^3) with fair flowability. The stability of encapsulated VE particles was excellent for OSA starch prepared at pH 8.0 attained by the addition of 2% NH_4HCO_3 and heating at 180 $^\circ\text{C}$ for 2 h. These results indicated that OS starch prepared by dry heating as both emulsifier and wall materials was effective for encapsulation of functional additives by spray drying.

Keywords

OSA modified starches; Normal maize; Dextrin; Dry heating; Vitamin E; Emulsion; Encapsulation; Spray drying

Introduction

Preparation of octenylsuccinic anhydride (OSA) modified starch was first patented by Caldwell and Wurzburg (1953). Conventionally, the most widely used pathway for synthesizing OS starch is a reaction of starch in its granular form in an aqueous slurry system under mild alkaline conditions (Altuna et al., 2018; Caldwell & Wurzburg, 1953; Sweedman et al., 2013). This pathway for starch esterification with OSA has been investigated extensively and reaction conditions have been optimized (Altuna et al., 2018). However, the aqueous reaction has some disadvantages due to poor water solubility, and the reaction requires further degradation of OS starch undergo enzyme or acid conversion to be completely soluble in water. Apart from the traditional pathway in aqueous slurry, some studies have been conducted to increase the reaction efficiency by using acetic acid (Shogren, 2003), organic solvents (Bhandari & Singhal, 2002; Viswanathan, 1999), microwave assisted (Biswas et al., 2006; Rivero et al., 2009), dry heating (Kim et al., 2010; Sandhu et al., 2015), dry media milling (Chen et al., 2014; Hu et al., 2016), ionic liquids media and lipase as catalyst (Li et al., 2016). For more details on these alternative methods, the previous reviews of Altuna et al. (2018) and Sweedman et al. (2013) are referred. In the latest study of novel preparation, Bai et al. (2017) used supercritical carbon dioxide (ScCO₂) to synthesis of OS starch, diffusing dissolved OSA in ScCO₂ into the starch granules. Their chemical surface gelatinization results indicated that substituent groups of OS starch prepared in ScCO₂ were more evenly distributed.

The using of carbohydrates as wall material should take into consideration of their properties and cost, such as solubility, emulsifying activity, and bioactivity. Compared with the aqueous reaction and other alternative methods, the dry heating treatment appeared simpler,

higher yield and more economical, which results a significant degradation of starch during the process. The dry heating treatment is an alternative way to produce dextrin, a degraded starch product prepared by a process involving heating starch granules at higher than 100 °C and/or acidification with high water solubility and low viscosity (Wurzburg, 1986, 2006). Dextrin could be used together with OSA to enhance its emulsifying capacity. The OS substitution could allow the starch dextrin to be used as an emulsifier due to esters containing both hydrophilic and hydrophobic groups. The OS dextrin produced from this approach was suggested as an effective substitute for the fat in dairy cream and muffins (Chung et al., 2010) and cake (Punia et al., 2019), and as a stabilizer for pickering emulsions (Marku et al., 2012; Rayner et al., 2012; Timgren et al., 2013).

In 2016, we filed a United States patent (U.S. Patent No. 9,458,252) describing an approach to prepare OS starch by dry heating on the mixture of OSA and granular starch (Y.-C. Shi & Bai, 2016). Optimum reaction conditions (3% NH_4HCO_3 , heating at 180 °C for 2 h) were investigated to prepare OS waxy maize starch with a high degree of substitution (DS), high reaction efficiency (RE), high solubility, and a light color. RE of ca. 90% was obtained at OSA levels from 1 to 6%. After evaluation of the structure and properties of the OS dextrans, we knew that the OSA reaction did not change the granular appearance of the starch; however, the molecular weight of starch was significantly reduced after reaction. Heat and OSA reaction resulted in significant starch hydrolysis in the amorphous and crystalline regions of starch granules. OS substitutions probably occurred at the amorphous region of starch granules. Glycosyl linkages including α -(1→2), α -(1→6), β -(1→2), and β -(1→6) linkages were formed, and 1,6- anhydro- β -D-glucopyranose was formed at the starch chain terminals. OS starch had a degree of branching of 19.8%. Our previous goal was to prepare soluble OS dextrin that can be

used in beverage applications. Therefore, Shi and Bai (2016) used this highly branched OS starch by dry heating for vitamin E emulsion that showed excellent emulsification property.

Instead of waxy maize starch, we investigated normal maize starch in the dry reaction. We hypothesized that normal maize starch with 28% amylose would have different properties. Normal maize starch is widely available, and OS starch made by dry heating method offer a low-cost product. The use of OSA esterified intact starch granules as a novel powder material stabilizing oil in water emulsions was studied. Particle size plays an important role in the stability of emulsion systems and the decrease in particle diameter has also been reported to increase bioavailability of encapsulated compounds (Chen & Wagner, 2004; Ozturk et al., 2014, 2015). Spray drying technique was successfully used to form VE loaded encapsulates using OSA- modified starches as emulsifiers and wall materials (Hategekimana et al., 2015). The objectives of this study were to prepare OS dextrin by dry heating, use OS dextrin to emulsify vitamin E, and determine the stability of vitamin E in spray dried products.

Materials and methods

Materials

Octenylsuccinic acid anhydride (OSA) was obtained from Gulf Bayport Chemicals L.P. (Pasadena, TX). Normal maize starch was provided by Tate & Lyle (Decatur, IL). Vitamin E acetate (purity >98%) was obtained from Zhejiang NVB Co. Ltd (Xin Chang, Zhejiang, China). All other chemicals were analytical grade.

Preparation of OS starch

The process of preparing OS starch was followed by preparation of OSA-modified waxy maize starch in Shi and Bai (2016). Normal maize starch (100 g) was suspended in distilled water (150 g) with agitation. The pH of the starch slurry was adjusted by adding NH_4HCO_3 . The starch suspension was filtered and the starch cake was mixed with 1–3% OSA (wt% based on the dry weight of starch) by a mixer (Model K45SSWH, KitchenAid, St. Joseph, MI) at 2nd speed for 15 min. The mixture was dried in an air-forced oven at 40 °C overnight. Starch mixture was ground by an analytical mill (A-10, Tekmar, Staufen, Germany) followed by sieving through a 110-mesh sifter. The powdered starch was thinly spread over an oven pan and heated at 140–180 °C for 0.5–6 h.

Characterization of OS starches

Degree of substitution (DS)

The degree of substitution (DS) of OS starch was determined by high-performance liquid chromatography (HPLC) as reported by (Qiu et al., 2012). Briefly, for free OS determination, 0.5 g (d.w.) of OS starch was stirred in 5 mL of methanol for 1 h. After centrifuge, the solution of supernatant (1 mL) and water (pH = 3) (1 mL) was analyzed by HPLC. To determine total OS, 0.5 g (d.w.) of OS starch was stirred overnight in 10 mL of 4 N NaOH. The alkali solution (2 mL) was neutralized with 10 mL of 1 N HCl and filled with acetonitrile to 25 mL volumetric flask. The solution was analyzed by HPLC. A mixture of acetonitrile and water containing 0.1% TFA (45:55, v/v) was used as the mobile phase. The flow rate was 1.0 ml/min and the detection wavelength was set at 200 nm. Concentrations were determined from the peak area.

Solubility

Solubility was measured according the methods of Bai et al. (2014). Starch (0.1 g) was dissolved in distilled water (0.9 mL) using a stir bar, and centrifuged at 6708 x g for 3 min. After centrifugation, starch concentration in the supernatant was determined using a hand-held refractometer (Fisher Scientific, Pittsburgh, PA) under direct lighting.

Color measurement

Colors of starches were measured using a digital colorimeter (Minolta CR-310 Chroma Meter, Konica Minolta Sensing Americas, Inc., Ramsey, NJ). The starch samples were packed in the granular-materials attachment CR- A50 and the parameters were expressed in the CIE L*a*b color system as L* (lightness; 0 = black, 100 = white), a* (+a = redness, -a = greenness), and b* (+b = yellowness, -b = blueness) values.

Molecular size distribution by gel permeation chromatography (GPC)

GPC analysis was performed as previously described (J. Shi et al., 2018). OS starches (4 mg) were dissolved in DMSO (4 mL) and stirred at room temperature for 12 h. The mixture was filtered through a 2 μ m filter and then injected into a PL-GPC 220 instrument (Polymer Laboratories, Inc., Amherst, MA, USA). The eluent was DMSO containing 0.5% (w/w) LiBr, and the flow rate was 0.8 ml/min. The results of GPC were presented with the terms of hydrodynamic radius (R_h).

X-ray diffraction (XRD)

X-ray diffraction patterns of unmodified and OS waxy maize starches were performed as previously described (Shi et al., 2018). Starch crystallinity was calculated as the ratio of the peak areas to the total diffractogram area (Komiya & Nara, 2006). The peak areas were calculated by OriginPro (version 8.5).

Scanning electron microscope (SEM)

The starch samples were coated with 18nmAu/Pt and examined by a scanning electron microscope (LEO1530VP, Zeiss, German) with the field emission gun operating at 3kV.

Preparation of vitamin E emulsion and spray-dried encapsulates

The OS starch sample (7.5 or 10 g) was dispersed in distilled water at room temperature for 2 h and heated in a boiling water bath with stirring for 30 min to completely dissolve the OS starch. Sodium benzoate (0.04 g) was added to the starch solution as a preservative. Vitamin E acetate (7.5 or 5 g) was added and mixed with a portable homogenizer (Bamix, Mettlen, Switzerland) for 3 min. The starch and vitamin E mixture were pre-homogenized by a bench-top homogenizer (PRO 350, PRO Scientific Inc., Oxford, CT) at 8,000 rpm for 10 min. The crude emulsion was homogenized by a microfluidizer (M-110P, Microfluidics, Newton, MA) for 6 passes at 30,000 psi. The fresh emulsion was collected for analysis on particle size, apparent viscosity and HPLC (Qiu et al., 2015).

After measurement, the rest of the emulsion was spray dried (Mini Spray Dryer B-290, BUCHI Corporation, New Castle, DE USA) at an inlet temperature of 160 °C and outlet temperature of 100 °C, and feed rate 15 mL/min. Each spray dried powder was packed in a sealed glass bottle and stored at room temperature for further analysis after one month.

Droplet size determination

Emulsion droplet size distribution was measured 1 h after preparation of the emulsion by a laser diffraction particle size distribution analyzer (LA-910, HORIBA, Ltd., Tokyo, Japan) at ambient temperature. The volume mean diameter (d_{43}) was recorded. Emulsions were stored in

the dark at room temperature. The OS starch solution after homogenization was also measured but no particle size was observed.

Stability study of vitamin E in microparticles by HPLC

HPLC was used to study the stability and integrity of VE encapsulated in the spray-dried microparticles. HPLC system Agilent 1100 Series (Agilent, Waldbronn, Germany) equipped with a Phenomenex Kinetex C18 column (2.6 μm , 100 \times 4.6 mm; Torrance, Calif., U.S.A.). For measurement of VE acetate, methanol was used as the mobile phase, the flow rate was 1.0 mL/min, and the detection wavelength was set at 285 nm.

To determine the surface/free oil, spray dried encapsulates (0.1 g) were extracted with 9 mL of methanol with magnetic stirring for 30 min. The mixture was stood and 1 mL of supernatant was collected and mixed with 9 mL of methanol. The solution was filtered by nylon filter membranes (0.45 μm) and then analyzed by HPLC. For total oil determination, spray-dried encapsulates (0.1 g) were re-suspended in 0.9 mL of distilled water, 10 μL of α -amylase (Ban480L) was added and placed into water bath at 60 $^{\circ}\text{C}$ for 20 min. After the mixture was cooled to 25 $^{\circ}\text{C}$, and it was transferred into a 10-mL volumetric flask, and filled with methanol for extraction of VE. The mixture was centrifuged at 3000 g for 15 min, and the supernatant (1 mL) was transferred to another 10-mL volumetric flask and filled with methanol. The solution was filtered by a nylon filter membrane (0.45 μm) and analyzed by HPLC. The standard curves for VE acetate was established as previously described (Qiu et al., 2015). The amount of vitamin E in the emulsion was calculated from a vitamin E standard curve. Oil load (g), free oil (W_{free} , g) and oil load efficiency (%) were calculated from the equations below:

$$\text{Oil load (g)} = W_{\text{total}} - W_{\text{free}}$$

$$\text{Oil load efficiency (\%)} = \frac{\text{oil load}}{W_{\text{total}}} \times 100\%$$

The amount of vitamin E acetate was determined immediately and at the storage of one month after the spray-drying process.

Density

The density of the encapsulated powder samples was measured using a helium gas pycnometer (AccuPyc II 1340, Micromeritics, Norcross, GA, USA), and was calculated from the weight and particle volume. The averages of three measurements were calculated and reported.

Flow properties of spray dried powders

Angle of repose is one of flow indicators that are commonly used. Higher angle of repose could indicate poor flow of bulk material (Ambrose et al., 2016; Bian et al., 2015). The angle of repose was measured by a Hosokawa powder tester (Micron powder systems, Summit, NJ). The sample was poured into the funnel at a stable feeding by vertical vibration. After pouring the samples, the height of the cone was measured and the angle of repose was calculated using the following relationship:

$$\theta = \arctan(2H/D) \tag{1}$$

Statistical analysis

Analysis of variance was conducted using a Statistical Analysis System (SAS, version 9.3 for Windows, SAS Institute, Cary, NC, USA). Least significant differences for comparison of means were computed at $p < 0.05$.

Results and discussion

Solubility, degree of substitution, and reaction efficiency of OS starches from dry heating

Process of preparing octenylsuccinate (OS) starch from dry heating is shown in Fig. 8.1. NH_4HCO_3 was used because it decomposed to NH_3 and CO_2 at high temperature. The pH of the starch changed during the process (Table 8.1). First, pH of the starch slurry was adjusted to 7.6, 8.0, 8.2 and 8.3 (pH I) by 0.3, 2.0, 3.0. and 4.0% NH_4HCO_3 (wt% based on the dry weight of starch), respectively. Different concentration of NH_4HCO_3 resulted in differences in pH. Second, pH of the pre-dried starch decreased to ca. 5 (pH II) after pre-drying, which was attributed to some hydrolysis of OSA from anhydride form to acid form. Finally, after heating at 180 °C, pH of the starch decreased to ca. 4 (pH III, not shown), resulting from the decomposition of NH_4HCO_3 and reaction of OSA with the starch.

At 2 h heating time, DS and RE of OS starch were significantly increased with the increase in the level of NH_4HCO_3 (Table 8.1). As the level of NH_4HCO_3 increased from 0.3 to 2.0%, solubility increased from 61.3 to 64.9%. However, future increasing the level of NH_4HCO_3 resulted in decreased solubility from 64.9 to 47.8%. At 4 h heating time, DS and RE increased as the level of NH_4HCO_3 increased 0.3 to 2.0%, but further increase to 4% did not change DS and RE, but decreased solubility from 75.9 to 57.5%. At 6 h heating time, future increase in NH_4HCO_3 did not change the solubility, and DS and RE were ca.0.017 and ca.73%, respectively. NH_4HCO_3 probably played an important role in ionizing starch as well as hydrolyzing OSA, because DS and RE were low with low NH_4HCO_3 (0.3%). Adding a small amount of NH_4HCO_3 probably limited starch ionization and OSA hydrolysis, but at a high

concentration of NH_4HCO_3 , the reduced solubility and increased DS and RE was probably due to the reaction between OSA and NH_4HCO_3 during pre-drying. Compared with OS starch from waxy maize starch, OS starch from normal maize starch had low solubility and high molecular size due to amylose content. The reaction was optimum when 2% NH_4HCO_3 was added to adjust pH I to 8.0.

Properties of OS starch at different substitution levels are shown in Table 8.2. Solubility and DS of OS starch increased with the OSA concentration. Also, DS increased as temperature increased from 140 to 180 °C. The solubility of OS starch was 5.7% when OSA and the starch mixture were heated at 140 °C for 2h and increased to 51.1% when heated at 180 °C. The highest solubility was obtained when the reaction was carried out at 180 °C. The color of OS starch became yellowish when 180 °C was used. High temperature and long reaction time resulted in products with higher b value and lower L value, reflecting a yellowish color, and the starch darkened. Because longer reaction time resulted in starch with a darker color, the optimum reaction time was 2 h.

To sum up, OS starches (OSS) prepared at pH 8.3 (4% NH_4HCO_3), 180 °C for 2 and 6 h (OSS4-2 and OSS4-6) were selected due to their high DS and RE. OS starches prepared at pH 8.0 (2% NH_4HCO_3), 180 °C for 2 and 6 h (OSS2-2 and OSS2-6) were selected due to their high solubility among those samples. These two sets of OS normal maize starch were used to analysis their structure and evaluated as emulsifiers to encapsulate vitamin E in application.

Structure characterization of OS starches

OS starches reacted with 3% OSA were characterized by GPC, XRD and SEM. Molecular size distribution of OS starch prepared at pH 8.02 (adjusted by 2% NH_4HCO_3) heated at 180 °C for 2 h and 6 h, and pH 8.30 (adjusted by 4% NH_4HCO_3) heated at 180 °C for 2 h and

6 h are shown in Fig. 8.2. Each OS starch showed two peaks. OS starches prepared at 2 h had a high proportion of the larger molecular size peak (8.0 nm). As reaction time increased to 6 h, the proportion of larger molecular size peak (8.0 nm) decreased and the smaller molecular size (1.8 nm) increased. Starch molecules were significantly hydrolyzed during the dry heating reaction, and starch hydrolysis increased with reaction time. As the concentration of NH_4HCO_3 increased from 2.0 (pH 8.02) to 4.0% (pH 8.30), the molecular size distribution had slightly shifted. More OSA hydrolyzed to its acid form due to more concentration of NH_4HCO_3 in starch granule. Therefore, starch with 4% NH_4HCO_3 was degraded in granular form by the acid and heat.

The native and OSA-modified waxy maize starches all displayed a typical A-type x-ray diffraction pattern with peaks at 2θ of 15° , 17° , 18° and 23° (Fig. 8.3). Native normal maize starch had a crystallinity of 34.4%. After OSA reaction, crystallinity decreased to 33.1 and 27.2% for starch prepared at pH 8.0 at 2 and 6 h, respectively. OS starch at elevated pH (8.3) showed a decreasing trend for peak broadening and peak intensity 32.3 and 26.8% for 2 and 6 h respectively. Based on the XRD results, there was a minor reduction in the crystalline regions at these low levels of OS substitutions, suggesting that OSA reacted preferentially in the amorphous region in the starch granules. However, as heating time from 2 to 6 h, the degree of crystallinity of the thermal degradation of the starch during the dry heat treatment did decline, indicating that heat for long time slightly weakened the crystalline structure. Compared with OSA reaction in an aqueous slurry system, which did not affect the crystalline region of starch granules (Bai & Shi, 2011), the OSA reaction in this study significantly hydrolyzed the crystalline regions of starch granules. The process affected the starch granules in a manner similar to dextrinization (Bai et al., 2014).

After OSA modification, starch granules remained and appeared identical to the unmodified normal maize starch when examined under SEM (Fig. 8.4). OS starch appeared to have the same granular shape and surface morphology as native starch, indicating that OSA modification by dry heating did not change the appearance of the starch granules.

Characterization of VE emulsions stabilized by OS starch

The use of OSA esterified intact starch granules (OSS2-2, OSS2-6, OSS4-2, and OSS 4-6) as a novel powder material stabilizing oil in water emulsions was studied. Table 8.3 shows the formulation, viscosity after microfluidizer, particle size of emulsions with different ratios of starch to oil (their total concentrations of starch and oil were 15.0%). All OS starches resulted in stable emulsions with fine particle size. The viscosity of all emulsions was in the range of 4.0-6.0 cp. At the ratio of starch to oil (2:1), the smallest mean particle size of 0.485 μm was obtained by OS starch prepared at pH 8.0 (adjusted by 2% NH_4HCO_3), and 180 $^\circ\text{C}$ for 2 h with (OSS2-2). The smallest mean diameter was 0.704 μm when the ratio of starch to oil was 1:1 (Table 8.3). The mean particle diameter (d_{43}) decreased with decreasing oil phase concentration or increasing emulsifier concentration for OS starch-stabilized emulsions. The amount of emulsifier needed to create small droplets was considerably higher for OSS2-6 than for OSS2-2. For example, about 10.5% OSS2-6 was needed to achieve $d_{43} = 0.816 \mu\text{m}$, but only 8.1% OSS2-2 was needed to achieve $d_{43} = 0.704 \mu\text{m}$. The mean particle size of emulsions made by OSS4-2, and OSS4-6 was higher than the emulsion made by OSS2-2, and OSS2-6, respectively. OSS2-2 displayed good emulsification properties implying that it was rapidly adsorbed to the surface of the oil droplets during homogenization due to its relatively large molecular size with a high solubility.

In this study, we monitored the emulsions during storage at room temperature for 4 and 20 h after preparation. Our result showed that the diameter of droplets for all emulsions increased during storage (Table 8.3, 1, 4, and 20 h), but the mean particle size was still less than 1.3 μm , indicating the good stability of emulsions 20 h after preparation. Tesch et al. (2002) suggested that steric hindrance was the main stabilizing mechanism of OS starch. This mechanism of emulsion stabilized by OS starch agreed well with the conclusions of other studies (Hategekimana et al., 2014; Simsek et al., 2015; Xu et al., 2015).

Encapsulation of VE by spray drying

In this study, the emulsion was spray-dried after it showed stability after stored at 25 $^{\circ}\text{C}$ for 20 h. Oil load, density, and flowability (angle of repose) of encapsulated powders are shown in Table 8.4. The spray-dried powder (P2-2) made by OSS2-2 had a higher oil load efficiency than encapsulates (P2-6) made by OSS2-6 at the same ratio of starch to oil, indicating that OSS2-2 was adsorbed more VE acetate oil. Similarly, P4-2 had a better emulsifying capacity than P4-6. Through measuring reconstructed emulsions by HPLC, oil load efficiency was as high as 98.1%, and low free oil (0.10 g) was found when the ratio of starch to oil was 2:1 (Table 8.4) by the OS starch prepared at pH 8.0 (adjusted by 2% NH_4HCO_3) heating at 180 $^{\circ}\text{C}$ for 2 h (OSA2-2). The same spray-dried powder had the highest oil load efficiency (95.4%) after one month's storage. In addition, oil load efficiency was as high as 97.4% and low free oil (0.19 g) was found when the ratio of starch to oil was 1:1 (Table 8.4) prepared by the same OS starch (OSS2-2). Also, the same formulated spray-dried powder had the highest oil load efficiency (94.1%) after one month's storage. The oil load efficiency of P4-2 and P4-6 decreased to c.a. 65% after one month's storage at room temperature, indicating P4-2 and P4-6 had bad encapsulation capacity

due to its low solubility and high DS (Table 8.1). These results suggested that OSA2-2 displayed the best emulsification and encapsulation properties, and the high ratio of starch to oil was beneficial to encapsulation stability.

Through observation on density, the spray-dried powder made by OSS2-2 and OSS4-2 had a higher density than powder made by OSS2-6 and OSS4-6, respectively. Starch reacts with OSA by dry heat treatment at longer heating time caused lower molecular weight and density. The density of P2-2 and -6 had little changes after one month's storage, whereas the density of P4-2 and -6 decreased to 1.061 g/cm^3 which was close to the density of VE acetate (0.95 g/cm^3), indicating more free oil on the surface of spray-dried powder. For fresh encapsulates, P2-2 a and b, P2-6 a and b, P4-6 a and b had an angle of repose value below 45° , indicating that those spray dried powder had acceptable flow property, whereas P4-2 a and b had poor flow property due to its angle of repose greater than 45° (Ambrose et al., 2016). After one month's storage, all spray-dried powders of P2-2 and -6 had little changes on flow property, but angle of repose on powders of P4-2 and -6 increased, indicating poor flow property due to higher free oil in the powder. The results were in a good agreement with free oil (g), oil load efficiency (%) and density g/cm^3 (Table 8.4). These results confirmed that OSS2-2 displayed the best emulsification and encapsulation properties.

Conclusions

VE can be successfully encapsulated using OS starch from normal maize starch as emulsifiers and wall materials by spray drying technique. Dry-heating with starch premixed with OSA produces dextrans by simultaneous substitution and thermal degradation. OSA modification by dry heating did not change the appearance of the granular starch, but the molecular weight of

starch was significantly reduced. OSA modification and heat resulted in significant starch hydrolysis in amorphous and crystalline region. The best product with high solubility and DS with light color was obtained when 2% (wt% by starch weight) NH_4HCO_3 was added and the starch was heated at 180 °C for 2 h. The OS starch was 65% soluble in water with a DS of 0.016.

For the same concentration of starch and oil (15%), emulsions with high VE loaded (7.5%) at ratio of starch to oil (1:1) had a small particle size of 0.704 μm . After spray drying, the microencapsulated particles had high oil load efficiency (97.4%) with passable flow property as fresh samples. These results showed that OS starch prepared by dry heating as wall material was effective in delivering and encapsulating VE by spray drying. OS-stabilized VE may be suitable for incorporation in many functional feed systems.

References

- Altuna, L., Herrera, M. L., & Foresti, M. L. (2018). Synthesis and characterization of octenyl succinic anhydride modified starches for food applications. A review of recent literature. *Food Hydrocolloids*, *80*, 97–110.
- Ambrose, R. K., Jan, S., & Siliveru, K. (2016). A review on flow characterization methods for cereal grain-based powders. *Journal of the Science of Food and Agriculture*, *96*(2), 359–364.
- Bai, J., Xie, X., Li, X., & Zhang, Y. (2017). Synthesis of octenylsuccinic-anhydride-modified cassava starch in supercritical carbon dioxide: Synthesis OSAS in supercritical CO₂. *Starch - Stärke*, *69*(11–12), 1700018.
- Bai, Y., Cai, L., Douth, J., Gilbert, E. P., & Shi, Y.-C. (2014). Structural changes from native waxy maize starch granules to cold-water-soluble pyrodextrin during thermal treatment. *Journal of Agricultural and Food Chemistry*, *62*(18), 4186–4194.
- Bai, Y., & Shi, Y.-C. (2011). Structure and preparation of octenyl succinic esters of granular starch, microporous starch and soluble maltodextrin. *Carbohydrate Polymers*, *83*(2), 520–527.
- Bhandari, P. N., & Singhal, R. S. (2002). Effect of succinylation on the corn and amaranth starch pastes. *Carbohydrate Polymers*, *48*(3), 233–240.
- Bian, Q., Ambrose, R. P. K., & Subramanyam, B. (2015). Effect of chaff on bulk flow properties of wheat. *Journal of Stored Products Research*, *64*, 21–26.
- Biswas, A., Shogren, R. L., Kim, S., & Willett, J. L. (2006). Rapid preparation of starch maleate half-esters. *Carbohydrate Polymers*, *64*(3), 484–487.
- Caldwell, C. G., & Wurzburg, O. B. (1953). *Polysaccharide derivatives of substituted dicarboxylic acids* (Patent No. US2661349 A).
- Chen, C.-C., & Wagner, G. (2004). Vitamin E nanoparticle for beverage applications. *Chemical Engineering Research and Design*, *82*(11), 1432–1437.
- Chen, M., Yin, T., Chen, Y., Xiong, S., & Zhao, S. (2014). Preparation and characterization of octenyl succinic anhydride modified waxy rice starch by dry media milling. *Starch - Stärke*, *66*(11–12), 985–991. <https://doi.org/10.1002/star.201400015>
- Chung, H.-J., Lee, S.-E., Han, J.-A., & Lim, S.-T. (2010). Physical properties of dry-heated octenyl succinylated waxy corn starches and its application in fat-reduced muffin. *Journal of Cereal Science*, *52*(3), 496–501.

- Hategekimana, J., Bwengye, M. K., Masamba, K. G., Yokoyama, W., & Zhong, F. (2014). Formation and stability of vitamin E enriched nanoemulsions stabilized by octenyl succinic anhydride modified starch. *International Journal of Food Engineering*, 10(4).
- Hategekimana, J., Masamba, K. G., Ma, J., & Zhong, F. (2015). Encapsulation of vitamin E: Effect of physicochemical properties of wall material on retention and stability. *Carbohydrate Polymers*, 124, 172–179.
- Hu, H., Liu, W., Shi, J., Huang, Z., Zhang, Y., Huang, A., Yang, M., Qin, X., & Shen, F. (2016). Structure and functional properties of octenyl succinic anhydride modified starch prepared by a non-conventional technology. *Starch - Stärke*, 68(1–2), 151–159.
- Kim, H.-N., Sandhu, K. S., Lee, J. H., Lim, H. S., & Lim, S.-T. (2010). Characterisation of 2-octen-1-ylsuccinylated waxy rice amyloextrins prepared by dry-heating. *Food Chemistry*, 119(3), 1189–1194.
- Li, D., Zhang, X., & Tian, Y. (2016). Ionic liquids as novel solvents for biosynthesis of octenyl succinic anhydride-modified waxy maize starch. *International Journal of Biological Macromolecules*, 86, 119–125.
- Marku, D., Wahlgren, M., Rayner, M., Sjö M., & Timgren, A. (2012). Characterization of starch Pickering emulsions for potential applications in topical formulations. *International Journal of Pharmaceutics*, 428(1–2), 1–7.
- Ozturk, B., Argin, S., Ozilgen, M., & McClements, D. J. (2014). Formation and stabilization of nanoemulsion-based vitamin E delivery systems using natural surfactants: Quillaja saponin and lecithin. *Journal of Food Engineering*, 142, 57–63.
- Ozturk, B., Argin, S., Ozilgen, M., & McClements, D. J. (2015). Formation and stabilization of nanoemulsion-based vitamin E delivery systems using natural biopolymers: Whey protein isolate and gum arabic. *Food Chemistry*, 188, 256–263.
- Punia, S., Siroha, A. K., Sandhu, K. S., & Kaur, M. (2019). Rheological and pasting behavior of OSA modified mungbean starches and its utilization in cake formulation as fat replacer. *International Journal of Biological Macromolecules*, 128, 230–236.
- Qiu, D., Bai, Y., & Shi, Y.-C. (2012). Identification of isomers and determination of octenylsuccinate in modified starch by HPLC and mass spectrometry. *Food Chemistry*, 135(2), 665–671.
- Qiu, D., Yang, L., & Shi, Y.-C. (2015). Formation of vitamin E emulsion stabilized by octenylsuccinic starch: Factors affecting particle size and oil load. *Journal of Food Science*, 80(4), C680–C686.
- Rayner, M., Sjö M., Timgren, A., & Dejmek, P. (2012). Quinoa starch granules as stabilizing particles for production of Pickering emulsions. *Faraday Discussions*, 158, 139.

- Rivero, I. E., Balsamo, V., & Müller, A. J. (2009). Microwave-assisted modification of starch for compatibilizing LLDPE/starch blends. *Carbohydrate Polymers*, *75*(2), 343–350.
- Sandhu, K. S., Sharma, L., & Kaur, M. (2015). Effect of granule size on physicochemical, morphological, thermal and pasting properties of native and 2-octenyl-1-ylsuccinylated potato starch prepared by dry heating under different pH conditions. *LWT - Food Science and Technology*, *61*(1), 224–230.
- Shi, J., Sweedman, M. C., & Shi, Y.-C. (2018). Structural changes and digestibility of waxy maize starch debranched by different levels of pullulanase. *Carbohydrate Polymers*, *194*, 350–356.
- Shi, Y.-C., & Bai, Y. (2016). *Starch esters and method of preparation* (United States Patent No. US9458252B2).
- Shogren, R. L. (2003). Rapid preparation of starch esters by high temperature/pressure reaction. *Carbohydrate Polymers*, *52*(3), 319–326.
- Simsek, S., Ovando-Martinez, M., Marefati, A., Sjöö, M., & Rayner, M. (2015). Chemical composition, digestibility and emulsification properties of octenyl succinic esters of various starches. *Food Research International*, *75*, 41–49.
- Sweedman, M. C., Tizzotti, M. J., Schäfer, C., & Gilbert, R. G. (2013). Structure and physicochemical properties of octenyl succinic anhydride modified starches: A review. *Carbohydrate Polymers*, *92*(1), 905–920.
- Tesch, S., Gerhards, C., & Schubert, H. (2002). Stabilization of emulsions by OSA starches. *Journal of Food Engineering*, *54*(2), 167–174.
- Timgren, A., Rayner, M., Dejmek, P., Marku, D., & Sjöö, M. (2013). Emulsion stabilizing capacity of intact starch granules modified by heat treatment or octenyl succinic anhydride. *Food Science & Nutrition*, *1*(2), 157–171.
- Viswanathan, A. (1999). Effect of degree of substitution of octenyl succinate starch on the emulsification activity on different oil phases. *Journal of Environmental Polymer Degradation*, *7*(4), 191–196.
- Wurzburg, O. B. (1986). Converted starches. In *Modified starches-properties and uses*. CRC Press.
- Wurzburg, O. B. (2006). *Food polysaccharides and their applications: Vol. pp. 87-118* (6th ed.). CRC Press.
- Xu, Y., Huang, Q., Fu, X., & Jane, J. (2015). Modification of starch octenylsuccinate by β -amylase hydrolysis in order to increase its emulsification properties. *Food Hydrocolloids*, *48*, 55–61.

Figures

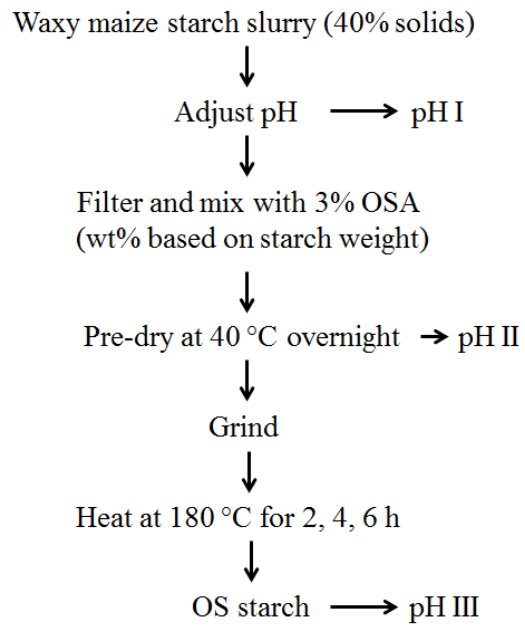


Figure 8.1 Process of preparing octenylsuccinate (OS) starch from dry heating [Adapted from (Shi & Bai, 2016)].

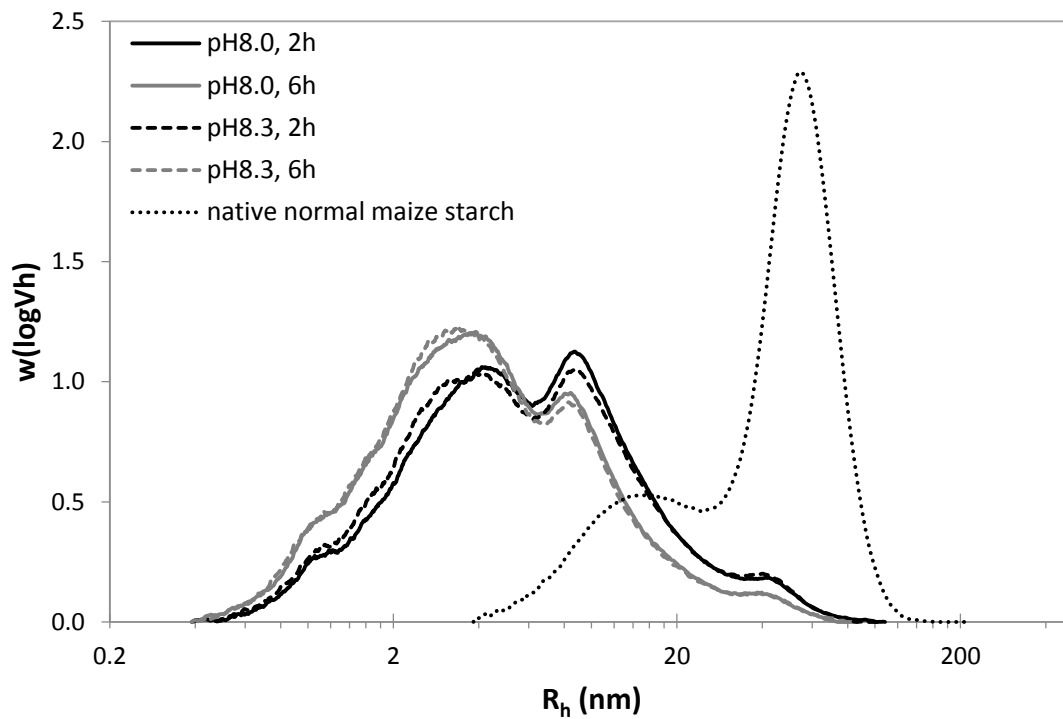


Figure 8.2 Molecular size distribution of native normal maize starch and octenylsuccinate (OS) starch prepared at 3% OSA, pH 8.02 (adjusted by 2% NH_4HCO_3), 180 °C for 2 h and 6 h; pH 8.30 (adjusted by 4% NH_4HCO_3), 180 °C for 2 h and 6 h.

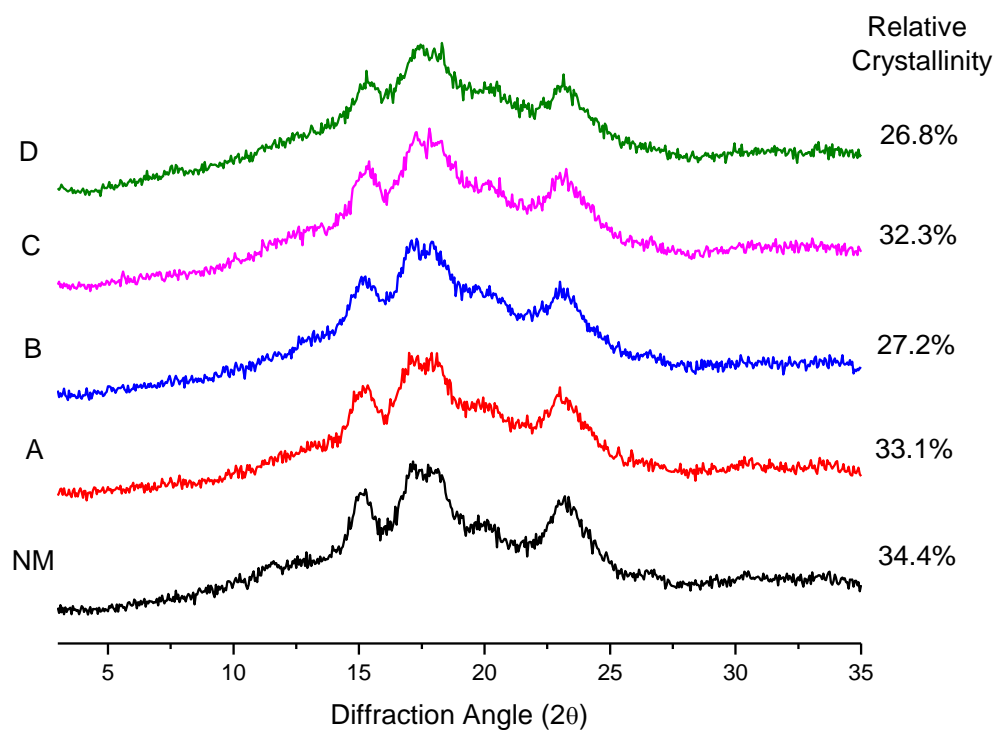


Figure 8.3 Wide-angle X-ray diffraction patterns of unmodified maize starch (NM), octenylsuccinate (OS) starch prepared with 3% OSA, pH 8.02 (adjusted by 2% NH_4HCO_3), 180 °C for 2 h (DS of 0.0156) (A) and 6 h (DS of 0.0173) (B); pH 8.30 (adjusted by 4% NH_4HCO_3), 180 °C for 2 h (DS of 0.0170) (C) and 6 h (DS of 0.0201) (D).

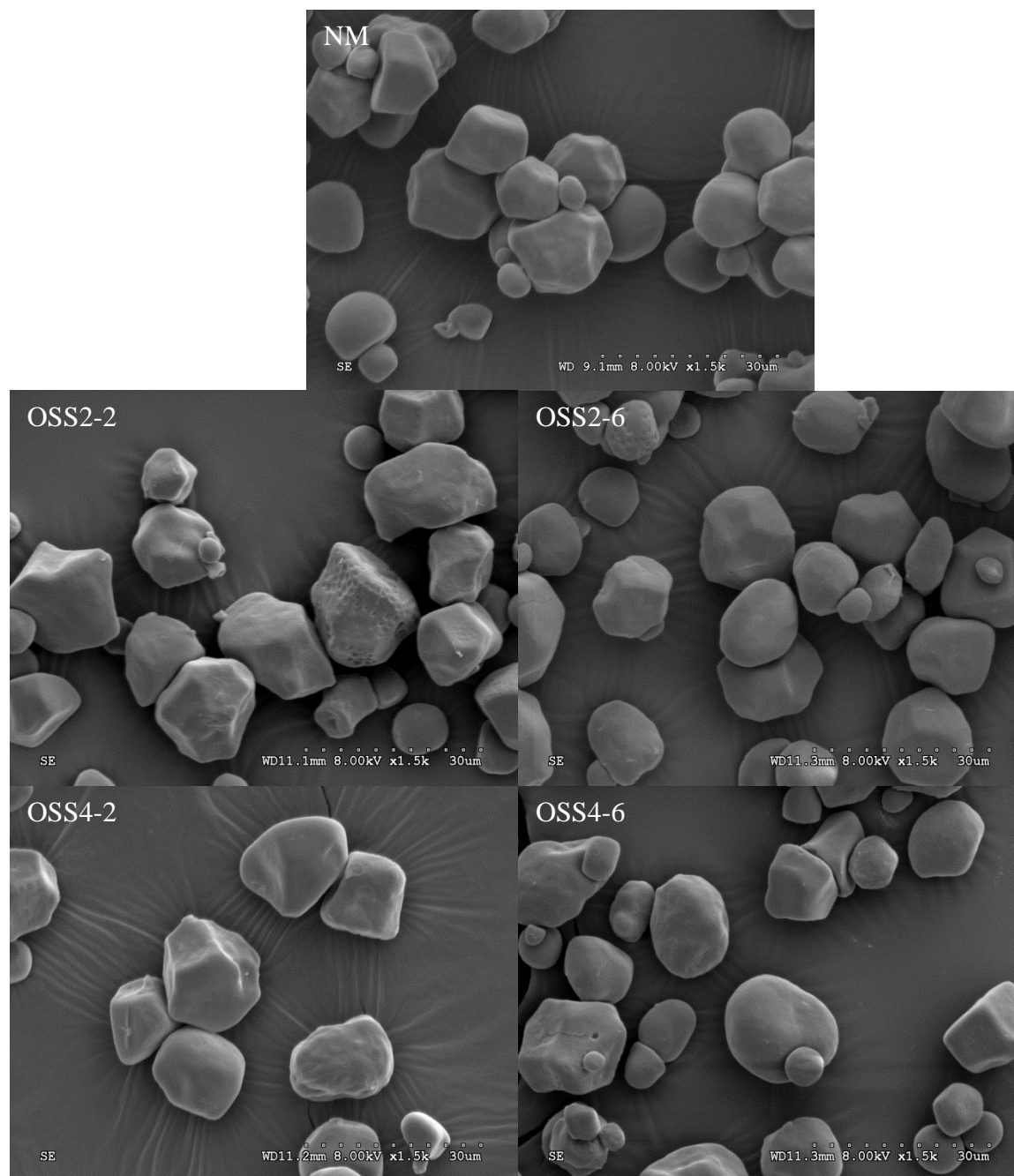


Figure 8.4 Scanning electron microscope (SEM) of native normal maize starch (NM) and octenylsuccinate (OS) starch prepared at 3% OSA, pH 8.0 (adjusted by 2% NH_4HCO_3), heating at 180 °C for 2 h (OSS2-2) and 6 h (OSS2-6); pH 8.3 (adjusted by 4% NH_4HCO_3), heating at 180 °C for 2 h (OSS4-2) and 6 h (OSS4-6).

Tables

Table 8.1 Characteristics of 3% OSA-modified normal maize starches adjusted to pH by NH_4HCO_3 and heat treated at 180 °C

NH_4HCO_3 added (%)	pH		Time (h)	DS ^a	RE (%) ^a	Solubility (%) ^a	Color ^a		
	I	II					L	a	b
0.3	7.63	4.58	2	0.0129 ± 0.0003 c	54.97 b	61.3 c	94.95 a	-1.64 c	10.47 c
			4	0.0135 ± 0.0001 b	57.19 a	75.9 b	93.99 b	-1.30 b	11.65 b
			6	0.0140 ± 0.0002 a	59.51 a	77.2 a	91.75 c	-0.41 a	12.42 a
2.0	8.02	5.51	2	0.0156 ± 0.0004 c	66.15 b	64.9 c	94.77 a	-1.60 c	10.15 c
			4	0.0167 ± 0.0004 b	70.80 b	73.5 b	93.34 b	-1.12 b	12.11 ab
			6	0.0173 ± 0.0002 a	73.01 a	80.9 a	91.58 c	-0.40 a	12.70 a
3.0	8.17	5.05	2	0.0165 ± 0.0002 b	69.61 b	51.1 c	94.33 a	-1.72 c	10.27 c
			4	0.0169 ± 0.0004 b	71.47 ab	72.0 b	92.93 b	-0.47 b	11.90 b
			6	0.0173 ± 0.0001 a	73.11 a	80.7 a	91.20 c	-0.05 a	12.64 a
4.0	8.30	5.34	2	0.0170 ± 0.0004 b	72.06 b	47.8 c	94.02 a	-1.26 c	10.68 c
			4	0.0173 ± 0.0006 a	73.06 a	57.5 b	92.64 b	-0.44 b	12.02 b
			6	0.0171 ± 0.0005 b	72.65 b	79.7 a	90.06 c	0.79 a	13.11 a

^a Means with the same letter (a, b, c) in each column within each treatments indicate significant differences ($p < 0.05$) between treatments.

Table 8.2 Characteristics of 3% OSA-modified normal maize starches by adding 3% NH₄HCO₃ (pH 8.17) and heating for 2h

OSA (%)	Temp (°C)	Solubility (%) ^a	DS ^a	RE (%) ^a	Color ^a		
					L	a	b
1	180	6.7±0.6 c	0.0065±0.0003 d	82.94 a	96.85 a	-0.99 c	8.96 d
2	180	12.8±0.9 b	0.0130±0.0002 c	82.61 a	93.99 c	-0.84 b	10.65 c
3	180	51.1±3.4 a	0.0165±0.0002 a	69.61 c	92.93 d	-0.47 a	11.36 a
3	140	5.7±0.3 d	0.0153±0.0004 b	65.02 b	95.02 b	-1.30 d	11.20 b

^a Values with the same letter are not significantly different (p < 0.05). The statistical analysis is done only for the data of same column

Table 8.3 Droplet size of emulsions with different ratios of starch to oil

Starch sample ^a	Starch:Oil ^b	Designed amount (g)		Added VE oil (g) ^c	Viscosity (cp) after micro-fluidizer ^d	Droplet size (µm) ^e		
		Starch	Oil			Fresh (1h)	4h	20h
OSS2-2	2:1	10.0	5.0	4.97	5.5	0.485 ± 0.013 e	0.553 ± 0.016 d	0.648 ± 0.027 d
	1:1	7.5	7.5	7.46	4.0	0.704 ± 0.022 d	0.767 ± 0.001 c	0.883 ± 0.032 c
OSS2-6	2:1	10.0	5.0	5.02	4.5	0.816 ± 0.018 c	0.849 ± 0.004 b	0.974 ± 0.018 bc
	1:1	7.5	7.5	7.50	4.0	0.919 ± 0.008 b	1.077 ± 0.057 a	1.054 ± 0.089 b
OSS4-2	2:1	10.0	5.0	5.05	6.0	0.835 ± 0.021 c	0.898 ± 0.036 b	0.925 ± 0.046 c
	1:1	7.5	7.5	7.56	4.0	0.855 ± 0.011 c	1.087 ± 0.028 a	1.239 ± 0.078 a
OSS4-6	2:1	10.0	5.0	5.03	5.0	0.824 ± 0.017 c	0.900 ± 0.025 b	0.912 ± 0.037 c
	1:1	7.5	7.5	7.52	4.0	1.025 ± 0.022 a	1.051 ± 0.016 a	1.087 ± 0.019 b

^a OSS2-2: OS starches prepared at pH 8.0 (2% NH₄HCO₃), 180 °C for 2 h

OSS2-6: OS starches prepared at pH 8.0 (2% NH₄HCO₃), 180 °C for 6 h

OSS4-2: OS starches prepared at pH 8.3 (4% NH₄HCO₃), 180 °C for 2 h

OSS4-6: OS starches prepared at pH 8.3 (4% NH₄HCO₃), 180 °C for 6 h

^b The designed solid concentration (wt%) is 15.0%. The starch concentrations (wt%) are 10.5% at ratio of 2:1, and 8.1% at ratio of 1:1.

^c The actual weight of VE acetate oil added when emulsion was prepared.

^d Viscosity was measured using Brookfield spindle #21 running at 100 rpm

^e Values with the same letter are not significantly different (p < 0.05). The statistical analysis is done only for the data of same column.

Table 8.4 Oil load, density, and flowability (angle of repose) of encapsulated particles

Sample	Fresh encapsulates					Storage of 1 month				
	Oil load (g) ^a	Free oil (g)	Oil load efficiency ^b	Density (g/cm ³) ^b	Angle of repose (°) ^b	Oil load (g) ^a	Free oil (g)	Oil load efficiency ^b	Density (g/cm ³) ^b	Angle of repose (°) ^b
P2-2a^I	4.87 ±0.03	0.10	98.1% a	1.125 ± 0.007 d	36.2 e	4.79 ±0.01	0.23	95.4% a	1.132 ± 0.005 a	36.1 d
P2-2b^{II}	7.27 ±0.06	0.19	97.4% a	1.082 ± 0.012 g	42.3 c	6.98 ±0.03	0.52	94.1% b	1.066 ± 0.009 d	42.8 b
P2-6a	4.86 ±0.01	0.16	96.9% a	1.144 ± 0.005 c	31.7 f	4.59 ±0.01	0.38	92.3% b	1.138 ± 0.002 a	33.5 e
P2-6b	7.04 ±0.06	0.46	93.9% bc	1.078 ± 0.003 g	40.3 d	6.83 ±0.03	0.63	91.6% b	1.109 ± 0.007 b	40.7 c
P4-2a	4.85 ±0.01	0.18	96.4% a	1.275 ± 0.005 a	48.6 b	3.39 ±0.04	1.66	67.1% c	1.108 ± 0.009 bc	53.1 a
P4-2b	6.98 ±0.04	0.58	94.3% c	1.217 ± 0.012 b	49.9 a	4.72 ±0.02	2.84	62.4% d	1.087 ± 0.008 c	52.9 a
P4-6a	4.74 ±0.03	0.32	94.4% b	1.113 ± 0.009 e	32.3 f	3.27 ±0.05	1.76	65.0% c	1.064 ± 0.012 d	41.5 c
P4-6b	6.99 ±0.02	0.53	92.9% bc	1.094 ± 0.009 f	36.2 e	4.59 ±0.00	2.93	61.0% d	1.061 ± 0.002 d	43.3 b

^a The calculated weight of VE acetate oil in emulsion based on HPLC analysis and calculation.

^b Values with the same letter are not significantly different (p < 0.05). The statistical analysis is done only for the data of same column.

^I a represents the designed ratio of starch:oil of 2:1 in Table 8.3.

^{II} b represents the designed ratio of starch:oil of 1:1 in Table 8.3.

Chapter 9 - Overall conclusions and future work

Conclusions

Octenylsuccinate (OS) starches could be prepared by two different approaches – slurry reaction and dry heating reaction. When octenylsuccinic anhydride (OSA) modified starch was prepared in an aqueous slurry system from granular waxy maize starch, OSA droplets could penetrate through pores and channels into the interior cavity of starch granules where esterification occurs almost as much as on the surface of the waxy maize starch granules as determined by Raman microspectroscopy analysis on individual granules. The OS groups in the OSA-modified granular starch are preferentially located on its surface as well as on the central cavity/hilum region. The regions between the surface and the hilum of the waxy maize starch granules had reduced OS substitution.

Compared with the Raman spectra of maize starches, potato starches had a similar pattern but a higher intensity of peak at 865 cm^{-1} , indicating more C-H deformation due to negatively charged phosphate ester groups in potato starches. OS groups in OSA-modified potato granular starches were preferentially located on granular surface. After the interior part of the granules (ca. 60%) was removed after gelatinization, the residual OSA-modified potato starch surface had ca. 2.5 times OS content as the whole granules. After chemical surface gelatinization, as the exterior surface of granules was removed by ca. 20%, the OS content of OSA-modified potato starch decreased by a factor of ca. 0.45 times over that of the bulk granule; as the surface amount removed by ca. 30%, the OS content of OSA-modified potato starch decreased by a factor of ca. 0.25 times over that of the bulk granule.

Alpha-amylase-degraded OSA starches from waxy potato starch were obtained through two approaches. Granular waxy potato starch was reacted with 3% OSA first and then hydrolyzed by α -amylase to product OS maltodextrins (OSE) with dextrose equivalent (DE) of 4.97 and DS of 0.0175. Granular waxy potato starch was hydrolyzed by α -amylase and then modified by 3% OSA to prepare OS maltodextrins (EOS) with DE of 4.39 and DS of 0.0209. At the ratio of oil to starch (1:1), the emulsions by OSE and EOS had a smaller volume diameter 0.578 and 0.656 μm , respectively with one peak of a narrow particle size distribution after 30 days storage. These two products with high apparent viscosity (26 and 31 cp at 10% solid content) displayed good emulsion stability for orange oil.

The conformational properties of starch granules during dextrinization were investigated by high performance size exclusion chromatography (HPSEC) coupled with multiple detectors. At the end of dextrinization, the molecular size was altered in the order of pyrodextrins at pH 3 and 150 $^{\circ}\text{C}$ > pH 3 and 170 $^{\circ}\text{C}$ > pH 2 and 150 $^{\circ}\text{C}$, indicating that the level of acid used played a major role in degrading the starch during dextrinization. The measured α values indicated that pyrodextrins prepared at pH 3, 170 $^{\circ}\text{C}$ and 150 $^{\circ}\text{C}$ only had one compact spherical conformation (α 0.27-0.31) during dextrinization, whereas pyrodextrins at pH 2 and 150 $^{\circ}\text{C}$ had a mixture of two shapes of molecules: compact sphere (α 0.26) and rigid coil (α 0.89) conformation.

Pyrodextrins prepared at pH 3 and 150 $^{\circ}\text{C}$ for 4 h and its swollen granules recovered from glycerol/water mixtures were determined by X-ray diffraction differential scanning calorimetry, and microscopy, and showed that short-range crystallinity was destroyed but long-range order (birefringence) was retained. Interestingly, some intact granules could swell in glycerol/water to ~ 80% of its original size and still displayed Maltese cross patterns, but were not crystalline.

The stability of encapsulated vitamin E particles was excellent by OSA-modified normal maize starch prepared at pH 8.0 attained by the addition of 2% NH_4HCO_3 and heating at 180 °C for 2 h. The spray-dried microencapsulated particles were characterized by oil load efficiency (97.4%) and density (1.082 g/cm^3) with good flowability. These results indicated that low molecular weights OSA modified starches were effective for the spray-drying encapsulation of functional additives with OSA starch as both emulsifier and wall materials.

Future work

Based on the results and conclusions from this dissertation, future research on the following subjects should be considered. For slurry reaction, the conditions of two approaches (lower enzyme concentration) in Chapter 4 could be optimized with higher viscosity obtained. In addition, α -amylase degraded OSA-modified starch from waxy potato starch obtained through first approach (first OSA modification and then enzyme degradation) could be designed to obtain the same DS with the degraded OS starch obtained through second approach (first enzyme degradation and then OSA modification). For the same DS, the emulsion performance between two approaches could be compared. In addition, the degraded OS starches from waxy maize starch by two approaches could be also obtained to compare with the emulsion capacity of that from waxy potato starch.

For dry heating system, OS starch prepared from waxy potato starch should be explored since the clarity of waxy potato starch is better than waxy maize starch. To further explore on clear vitamin E emulsion, Tween 20 or 80 as small-molecular emulsifier could be used with OS waxy potato starch together since the particle size is decreased obviously by surfactants, investigating the effect of OS starch with other surfactants.

Pyrodextrin prepared at pH 3 and 150 °C could swell in glycerol/water and still displayed Maltese cross patterns, but was not crystalline. The applications of this unique swelling property in a mixture of glycerol and water need to be further investigated.

Appendix A - Copyright Permissions

Published work – Chapter 3 (Sun et al., 2019)

Elsevier Copyright Policy: as the author of this Elsevier article, you retain the right to include it in a thesis or dissertation, provided it is not published commercially. Permission is not required, but please ensure that you reference the journal as the original source. Non-commercial Creative Commons user license (CC-BY-NC-ND) is attached as below.

© 2019. This manuscript version is made available under the CC-BY-NC-ND 4.0 license

<https://doi.org/10.1016/j.carbpol.2019.04.034>



RightsLink®



Home



Help



Email Support



Sign In



Create Account



Distribution of octenylsuccinate substituents within a single granule of modified waxy maize starch determined by Raman microspectroscopy

Author: Zhenhua Sun,Zhongwei Chen,Bin Xu,Yong-Cheng Shi

Publication: Carbohydrate Polymers

Publisher: Elsevier

Date: 15 July 2019

© 2019 Elsevier Ltd. All rights reserved.

Appendix B - Chapter 6 Supplementary Materials

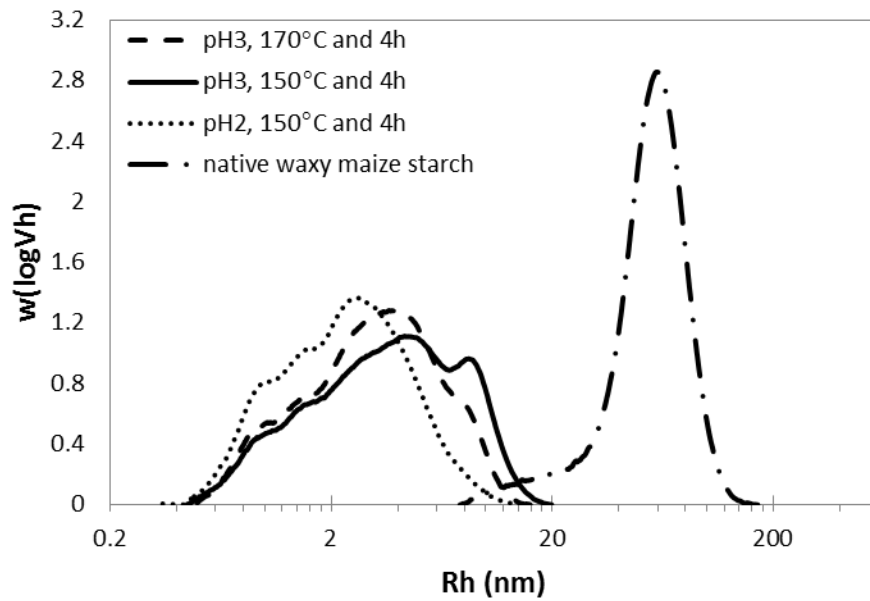


Figure B.1 Molecular size distribution of native waxy maize starch and pyrodextrins prepared at pH 3 and 170 °C, pH 3 and 150 °C, and pH 2 and 150 °C, at 4 h.

Appendix C - Dry reaction of OSA reaction by ammonium hydroxide

Waxy maize starch (100 g) was suspended in distilled water (150 g) with agitation. The pH of the starch slurry (pH 8, 9, and 10) was adjusted by adding NH_4OH . The starch suspension was filtered and the starch cake was mixed with 3% OSA (wt% based on the dry weight of starch) by a mixer (Model K45SSWH, KitchenAid, St. Joseph, MI) at 2nd speed for 15 min. The mixture was dried in an air-forced oven at 40 °C overnight. Starch mixture was ground by an analytical mill (A-10, Tekmar, Staufen, Germany) followed by sieving through a 110-mesh sifter. The powdered starch was thinly spread over an oven pan and heated at 180 °C for 0.5–4 h. Degree of substitution (DS) was measured by high-performance liquid chromatography (HPLC).

Table C.1 Degree of substitution (DS) and reaction efficiency (RE) of 3% OS waxy maize starches prepared by dry reaction at 180 °C for 0.5-4 h.

Adjusted pH	Properties (DS and RE)	Reaction time (h)				
		0.5	1	2	3	4
pH 8	OS _{free}	0.977	0.817	0.618	0.488	0.386
	OS _{total}	2.159	2.133	2.120	2.401	2.527
	OS _{bound}	1.183	1.316	1.502	1.913	2.141
	DS	0.009	0.010	0.012	0.015	0.017
	RE (%)	39.4	43.9	50.1	63.8	71.4
pH 9	OS _{free}	0.840	0.681	0.564	0.353	0.300
	OS _{total}	2.034	2.117	2.116	2.112	2.198
	OS _{bound}	1.194	1.437	1.552	1.759	1.897
	DS	0.009	0.011	0.012	0.014	0.015
	RE (%)	39.8	47.9	51.7	58.6	63.2
pH 10	OS _{free}	0.673	0.500	0.359	0.379	0.296
	OS _{total}	2.234	2.231	2.284	2.228	2.172
	OS _{bound}	1.560	1.731	1.926	1.849	1.876
	DS	0.012	0.014	0.015	0.015	0.015
	RE (%)	52.0	57.7	64.2	61.6	62.5